Sources, Sinks and Subsidies: Carbon in Scotland's Coastal Environment

Craig Smeaton

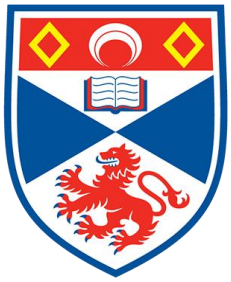

University of
St Andrews

This thesis is submitted in partial fulfilment for the degree of

Doctor of Philosophy (PhD)

at the University of St Andrews

November 2017

Declaration

Candidate's declaration

I, Craig Smeaton, do hereby certify that this thesis, submitted for the degree of PhD, which is approximately 45,000 words in length, has been written by me, and that it is the record of work carried out by me, or principally by myself in collaboration with others as acknowledged, and that it has not been submitted in any previous application for any degree.

I was admitted as a research student at the University of St Andrews in September 2013.

I received funding from an organisation or institution and have acknowledged the funder(s) in the full text of my thesis.

Date Signature of candidate

Supervisor's declaration

I hereby certify that the candidate has fulfilled the conditions of the Resolution and Regulations appropriate for the degree of PhD in the University of St Andrews and that the candidate is qualified to submit this thesis in application for that degree.

Date Signature of supervisor

Permission for publication

In submitting this thesis to the University of St Andrews we understand that we are giving permission for it to be made available for use in accordance with the regulations of the University Library for the time being in force, subject to any copyright vested in the work not being affected thereby. We also understand, unless exempt by an award of an embargo as requested below, that the title and the abstract will be published, and that a copy of the work may be made and supplied to any bona fide library or research worker, that this thesis will be electronically accessible for personal or research use and that the library has the right to migrate this thesis into new electronic forms as required to ensure continued access to the thesis.

I, Craig Smeaton, confirm that my thesis does not contain any third-party material that requires copyright clearance.

The following is an agreed request by candidate and supervisor regarding the publication of this thesis:

Printed copy

Embargo on all of print copy for a period of 2 years on the following ground(s):

- Publication would preclude future publication

Supporting statement for printed embargo request

Publication of thesis would hamper further publication in the future

Electronic copy

Embargo on all of electronic copy for a period of 2 years on the following ground(s):

- Publication would preclude future publication

Supporting statement for electronic embargo request

Publication would hamper further publication

Title and Abstract

- I agree to the title and abstract being published.

Date Signature of candidate

Date Signature of supervisor

Underpinning Research Data or Digital Outputs

Candidate's declaration

I, Craig Smeaton, understand that by declaring that I have original research data or digital outputs, I should make every effort in meeting the University's and research funders' requirements on the deposit and sharing of research data or research digital outputs.

Date Signature of candidate

Permission for publication of underpinning research data or digital outputs

We understand that for any original research data or digital outputs which are deposited, we are giving permission for them to be made available for use in accordance with the requirements of the University and research funders, for the time being in force.

We also understand that the title and the description will be published, and that the underpinning research data or digital outputs will be electronically accessible for use in accordance with the license specified at the point of deposit, unless exempt by award of an embargo as requested below.

The following is an agreed request by candidate and supervisor regarding the publication of underpinning research data or digital outputs:

Embargo on all of electronic files for a period of 2 years on the following ground(s):

- Publication would preclude future publication

Supporting statement for embargo request

Publication would preclude further publication

Date Signature of candidate

Date Signature of supervisor

Abstract

The rise of anthropogenic carbon dioxide concentrations in the atmosphere has forced a revaluation of our current understanding of the magnitude and mechanisms which govern natural carbon pools around the world. A largely overlooked carbon pool is held within the sediments of the world's oceans with the coastal oceans potentially playing a globally significant role in climate regulation. These marine sedimentary environments and fjords in particular are recognised as hotspots for the burial of carbon, yet little is known about the quantity of carbon held within such environments. In this study, we use the mid-latitude fjords of Scotland as a natural laboratory to develop new methodologies to quantify marine sedimentary C stores and better understand how these stores develop through time with a specific focus on the long-term linkages with the terrestrial environment.

The newly developed methodology has allowed for the first time the quantification of a national marine sedimentary carbon stock. The sediments within these mid-latitude fjords hold a quantity of carbon comparable in magnitude to most terrestrial environments in Scotland. However, when area-normalised comparisons are made, these mid-latitude fjords are significantly more effective as C stores than their terrestrial counterparts, including Scottish peatlands. Additionally; our understanding of the long-term role of the terrestrial environment in the development of these systems has been significantly improved with it being estimate that approximately half the carbon held within Scottish fjords is terrestrial in origin. Through the Holocene fjordic sediments have been shown too adapted to increased carbon input through increasing the rate at which carbon in buried, going forward this will be highly significant in mitigating the impact of predicated climatic and human induced environmental change.

This project has highlighted the importance of understanding carbon held within marine and coastal sediments. By increasing our understanding of such coastal sedimentary carbon stores we will be better able to estimate the global carbon burial rates and storage further constraining the their role in the global carbon cycle.

Acknowledgments

I would like to thank my supervisors, William Austin, Althea Davies and John Howe for support and encouragement throughout this project, and for always making time to for discussions. Additionally; I would like to thank my many collaborators especially Agnes Baltzer for providing geophysical data key for this project and Thomas Bianchi and Xingquin Cui for providing supervision on my brief foray in to the world of molecular biomarkers.

Thanks should also go to NERC and the University of St Andrews for their financial support for this project as well as the MASTS and SAGES for providing additionally finical support to facilitate extra travel, fieldwork and laboratory analysis.

Thanks to Richard Abell, Colin Cameron and Angus Calder for his technical help in and out of the lab with useful advice and ideas. I would like to thank my fellow PhD students especially Steve, Colin Batzi, Emily and Fiona for making the last four years an enjoyable and truly unique experience. Last but not least, thanks to my family for their support.

Table of Contents

Chapter 2 *Materials and Methods*

Chapter 3 ***A Sedimentary Carbon Inventory for a Scottish Fjord: An Integrated Geochemical and Geophysical Approach***

Table of Figures

Chapter 1 *Introduction and Background*

Chapter 2 *Materials and Methods*

List of Tables

Chapter 1 *Introduction and Background*

Chapter 2 *Materials and Methods*

Chapter 4 *Source to Sink: Tracing the Origin of Organic Carbon in a Mid-Latitude Fjord*

Chapter 5 *A National Assessment of Mid-Latitude Fjord Sedimentary C Stocks*

Standard Units

Distance

Micrometre	μm
Millimetre	mm
Centimetre	cm
Metre	m
Kilometre	km

Area

Centimetre squared	cm^2
Metre squared	m^2
Kilometre squared	km^2
Hectare	ha

Volume

Centimetre cubed	cm^3
Metre cubed	m^3

Mass

Milligram	mg
Gram	g
Kilogram	kg
Tonne	t
Megatonne	Mt
Gigatonne	Gt
Teragram	Tg
Petagram	Pg

Time

Millisecond	ms
Second	s
Year	yr

Specialised Units

Density

Grams per centimetre cubed	g cm^{-3}
Kilograms per centimetre cubed	kg m^{-3}

Concentration

Parts per million	ppm
Parts per billion	ppb
Micrograms per gram	µg g^{-1}
Milligram per gram	mg g^{-1}
Milligram per milligram	mg kg^{-1}

Rates

Centimetre per year	cm yr^{-1}
Grams per year	g yr^{-1}
Tonnes per year	t yr^{-1}
Megatonnes per year	Mt yr^{-1}
Grams per metre squared per year	g m^{-2} yr^{-1}
Tonnes per kilometre per year	t km^{-2} yr^{-1}

Other

Percentage	%
Per mille	‰
Counts per second/minute	cps
Kilowatt	kw
Kilohertz	kHz
Calibrated before present	Cal Bp
Tonnes per hectare	t ha^{-1}
Tonne per kilometre squared	t km^{-2}
Megatonnes per kilometre squared	Mt km^{-2}

Chapter 1

Introduction and Background

1.1 Project Rational

One of the biggest threats to human populations globally is climatic change induced largely by the anthropogenic release of carbon (C) to the atmosphere in the form of carbon dioxide (CO_2) and methane (CH_4) (Solomon et al., 2009; Diaz and Moore, 2017; Silva et al.,2017). Natural ecosystems such as forest are widely recognised to have the ability to collect and lock away C over significant time periods providing a valuable climate regulation service. The importance of the terrestrial environments (forests, peatlands etc.) in the global C cycle is well recognised but in comparison, the role the oceans and in particular the coastal seas play has largely been overlooked.

In the last decade, the intertidal ecosystems have been the focus of significant research with saltmarshes, mangroves and shallow subtidal seagrass meadows being shown to be globally significant sites for the burial of C (Duarte et al., 2005). The term "Blue Carbon" was coined to highlight the important role these habitats play in C capture and storage (Nellemann et al., 2009). In comparison, subtidal sedimentary environments have largely been overlooked as sites of C accumulation and storage. Marine sedimentary environments globally occupy an area of 396,155,000 km^2 (Hedges et al., 1997; Smith et al., 2014) which is over 500 times more than their intertidal equivalents. The vast areal extent of these environments means that they may play a potentially significant role in global climate regulation through the burial and storage of C which is likely to be greater than the intertidal ecosystems and potentially equivalent to the service the terrestrial environment provides.

In fact, marine sedimentary environments have been highlighted as globally important areas for the burial and long-term storage of C (Hedges et al. 1997; Duarte et al., 2005; Smith et al., 2014) but not all sediments are equal. It is recognised that the C burial rates and storage duration differ significantly between different types of sedimentary environments (pelagic, shelf, biogenic etc.). Coastal sediments at the land-ocean interface have the potential to be sites of high C burial and storage due to their geomorphology and direct links to terrestrial environments (Bianchi, 2011). Yet different coastal geomorphologies (estuary, deltas, continental shelf, etc.) can have significant impact on C burial rates and storage capacity of a given environment (Bauer et al., 2013).

Within the coastal zones the over-deepened submarine glacial geomorphology of fjords (McIntyre and Howe. 2010) makes them excellent natural sediment traps, this combined with their vicinity to the terrestrial environment results in them being areas of high C burial

and potential long-term C stores. Work by Smith et al. (2014) has confirmed that fjords are globally significant “hotspots” for C burial. Fjordic sediments are also crucial in capturing lost C from the terrestrial environment, it has been estimated that between 55-62% of the C held in fjordic sediments is terrestrial in origin (Cui et al., 2016a). Though we now recognise the importance of fjords to C burial at the global scale, the question of how much C is stored within these sediments remains unanswered. Further our understanding of regional differences in burial rates and the source of the C held within the sediment remains poor.

There is a growing policy interest to better understand the role of marine sediments in the burial and storage of C. The rising anthropogenic C input to the atmosphere (Jones, 2013) combined with the realisation that these sedimentary environments play an important role in climate regulation has seen calls for their inclusion in national greenhouse gas (GHG) budgets (Avelar et al., 2017) and for their use in C offsetting schemes. In addition, C is seen by many as an important tool for the management and protection of environments. Despite these goals, it is clear that our current understanding of C burial and storage in sedimentary environments needs improving to provide a strong scientific foundation for to guide policy ambitions.

At this moment in time with rising atmospheric CO_2 concentrations it is more important than ever to develop a better scientific understanding of the C sources, sinks and subsidies in our natural environment.

1.2 The Global Carbon Cycle

Carbon is present in the Earth's atmosphere, soils, biosphere, oceans, and crust. When viewing the Earth as a system, these components are referred to as C pools, stocks and reservoirs as they act as storage for large quantities of C. Any movement of carbon between these reservoirs is called a flux. In any integrated system, fluxes connect pools together to create cycles and feedbacks (Fig.1.1). Viewing the Earth as a whole, individual cycle's link the C pools on a range of spatial and temporal scales to form an integrated global C cycle (Fig 1.1).

On the shortest time scales, of seconds to minutes, plants take C out of the atmosphere through photosynthesis and release it back into the atmosphere via respiration. On longer time scales, carbon from dead plant material can be incorporated into soils and sediments, where it might reside for years, decades or centuries before being broken down by soil microbes and released back to the atmosphere. On longer time-scales, organic matter becomes buried in deep marine sediments which largely protect the C from decay allowing storage over millennia. Over geological time these marine sediment C stores can be slowly transformed into deposits of coal, oil and natural gas. When burnt C that has been stored for millions of years is released once again to the atmosphere as CO_2.

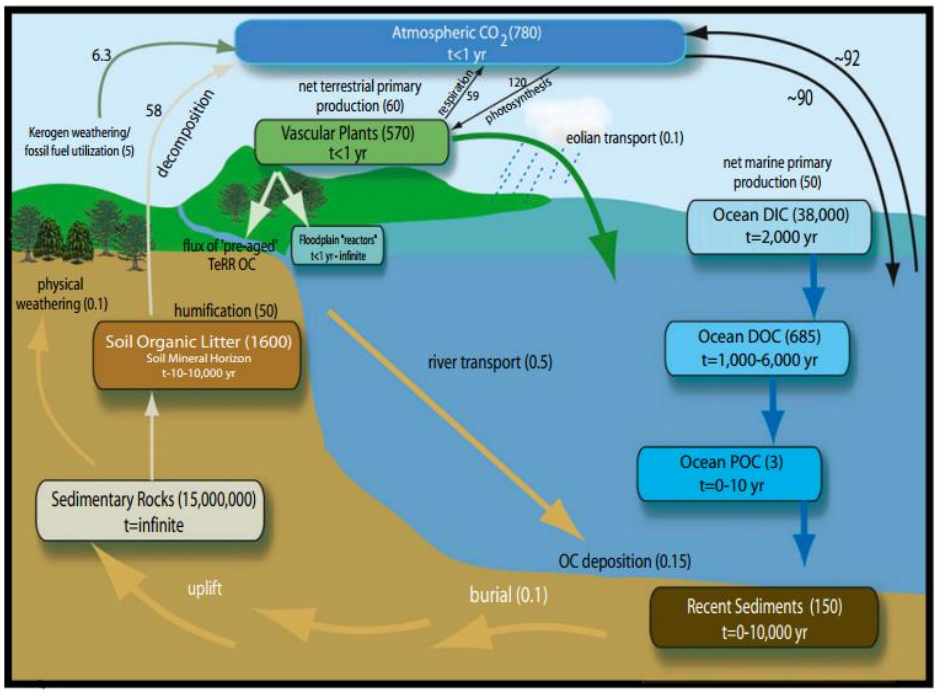

Figure 1.1 The global carbon cycle (units are in PgC or Pg C y^{-1}) (Bianchi, 2011)

Globally, the C cycle plays a key role in regulating the Earth's climate by controlling the concentration of CO_2 in the atmosphere. CO_2 contributes to the greenhouse effect, in which heat generated from sunlight at the Earth's surface is trapped by certain gasses and prevented from escaping through the atmosphere. The greenhouse effect itself is a perfectly natural phenomenon and, without it, the Earth would be much colder. In recent years CO_2 has received much attention because its concentration in the atmosphere has risen to approximately 30% above natural background levels and is continuing to rise (Fig.1.2), recently reaching a concentration of 400ppm (Jones, 2013).

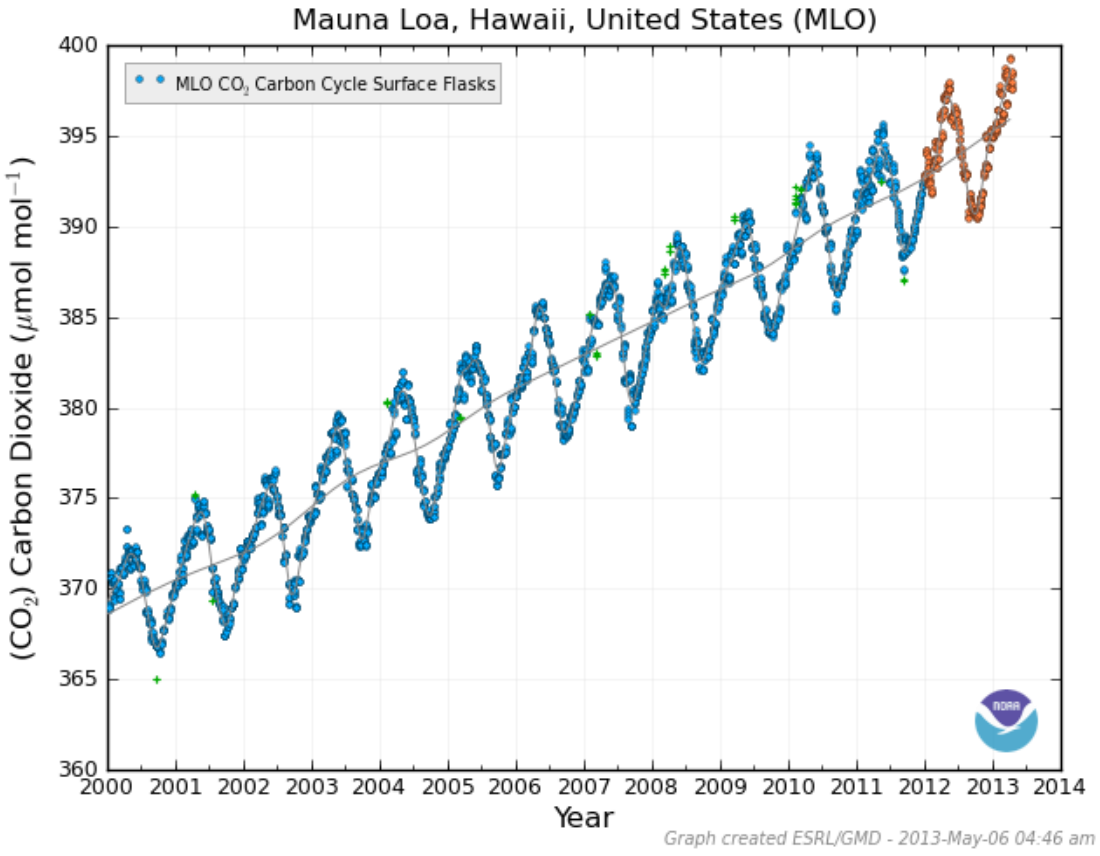

Figure 1.2. Atmospheric CO_2 concentration (2000-2014) from the Mauna Loa atmospheric observatory (Source: *NOAA*)

The Earth's C pools naturally act as both sources, adding C to the atmosphere, and sinks, removing C from the atmosphere. If all sources are equal to all sinks, the carbon cycle can be said to be in equilibrium (or in balance) and there is no change in the size of the pools over time. Maintaining a steady amount of CO_2 in the atmosphere helps maintain

stable average temperatures at the global scale. The increase in atmospheric CO_2 concentrations is a result of human activities that have occurred over the last 150 years, largely due the extraction and burning of ancient C in the form of fossil fuels. Fossil fuel combustion has increased CO_2 inputs to the atmosphere at the same time natural sinks that draw CO_2 out of the atmosphere (oceans, forests, etc.) have been reduced, these activities have caused the size of the atmospheric carbon pool to increase. This is the primary cause of climate change and is the main reason for increasing interest in the carbon cycle.

1.2.1 Global Carbon Pools

In order to understand how carbon is cycled and how atmospheric CO_2 will change in the future, an improved understanding of the places in which carbon is stored (pools), how long the C resides there, and processes that transfer it from one pool to another (fluxes) is required. The global C cycle is immensely complex and as we can't deal with that level of complexity currently, the C cycle is often described by lumping similar mechanisms or environments into simpler groups (i.e. forest, soils, atmosphere, ocean) and focusing only on the processes that are most important at the global scale.

The earth's C pools can be grouped into any number of different categories. Here, we will consider the major categories (Earth's crust, atmosphere, terrestrial vegetation, soils and oceans) that have the greatest relevance to the overall C cycle.

The largest pool of C on Earth is stored in the form sedimentary rocks within the planet's crust. These are rocks produced either by the hardening of mud containing organic matter over geological time, or by the collection of calcium carbonate particles, from the shells and skeletons of marine organisms. Together all sedimentary rocks on Earth store 15,000,000 Pg C (Hedges, 1992, Drenzek et al. 2009). Another 4,000 Pg C is stored in the Earth's crust as hydrocarbons formed over millions of years from ancient living organisms under intense temperature and pressure (Drenzek et al. 2009).

The atmosphere contains approximately 780 Pg C, most of which is in the form of CO_2, with much smaller amounts of CH_4 and various other compounds (Hedges, 1997; Houghton, 2007). Although this is considerably less carbon than that contained in the oceans or crust, C in the atmosphere is of vital importance because of its influence on the greenhouse effect and climate. The relatively small size of the atmospheric C pool

also makes it more sensitive to disruptions caused by an increase in CO_2 from the Earth's other pools.

Terrestrial ecosystems contain C in the form of plants, animals, soils and microorganisms (bacteria and fungi). Of these, plants and soils are by far the largest pool. Unlike the Earth's crust and oceans, most of the C in terrestrial ecosystems exists in short lived organic forms. Plants exchange C with the atmosphere relatively rapidly through photosynthesis, in which CO_2 is absorbed and converted into new plant tissues, and respiration, where some fraction of the previously captured CO_2 is released back to the atmosphere as a product of metabolism. Of the various kinds of tissues produced by plants, woody stems such as those produced by trees have the greatest ability to store large amounts of C. Collectively, the Earth's plants store approximately 570 Pg C, with the wood in trees being the largest fraction (Bellassen and Luyssaert, 2014).

The total amount of C in the world's soils is estimated to be 1600 Pg C (Scharlemann et al., 2017). Measuring soil C can be challenging, but a few basic assumptions are used to estimate total stocks. First, the most common form of carbon in the soil is organic carbon derived from dead plant materials and microorganisms. Second, as soil depth increases the abundance of organic carbon decreases. Standard soil measurements are typically only taken to 1m in depth in line with IPPC reporting (IPCC, 2013). In most cases, this captures the dominant fraction of carbon in soils, although some environments have very deep soils where this rule doesn't apply (i.e. peatlands). Most of the C in soils enters in the form of dead plant matter that is broken down by microorganisms. The decay process also releases C back to the atmosphere because the metabolism of these microorganisms eventually breaks most of the organic matter down to CO_2.

1.3 Carbon in the World's Oceans

The world's oceans are estimated to contain 38,000 Pg C, in the form of dissolved inorganic carbon (DIC) and 685 Pg C in the form of dissolved organic carbon (DOC) (Houghton, 2007; Hansell et al., 2009) which is stored at great depths with long residence times (Fig.1.1). A much smaller amount of C, approximately 1,000 Pg C, is located near the ocean surface. This carbon is exchanged rapidly with the atmosphere through both physical processes, such as CO_2 degassing into the water, and biological processes, such as the growth, death and decay of plankton. Although most of this surface carbon cycles rapidly, some of it can also be transferred by sinking particles to the deep ocean pool where it can be stored for a much longer time in sediments (Burdige, 2005; Hedges, 1997).

1.3.1 Marine Carbon Stores

The main long-term C stores in the global marine system are the sediments. Sedimentary stores can be found in all subtidal ecosystems where they have the ability to lock both organic carbon (OC) and inorganic carbon (IC) away for significant periods of time (>10^3 years). The environments and mechanisms that govern the storage of C in sediments differ significantly around the world from oxygen minimum zones at the equator to fjords and permafrost at high latitudes (Fig.1.3). Each of these environments has unique characteristics (Table 1.1) which are conducive to the storage of C in their sediments. These different characterises result in large differences in the quantity of C buried within these systems (Fig.1.4).

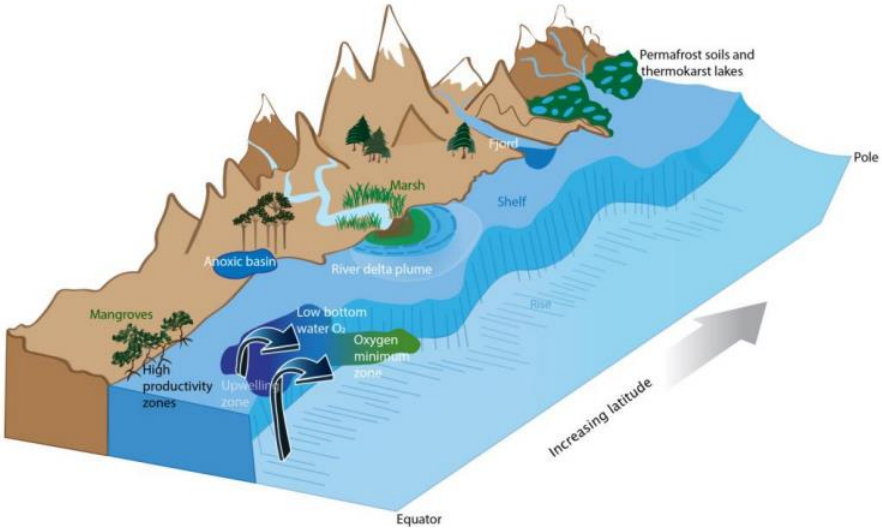

Figure 1.3 The distribution and general characteristics of the C storing systems. These systems represent potential hot spots and hot moments of carbon burial and oxidation at land-ocean interfaces (Bianchi et al. 2017).

Environment	C Burial Characteristics	Example	References
Wide energetic shelves (tropical/temperate)	Low burial efficiency/high aerobic and suboxic oxidation rates. Carbon burial oxidation dominated by marine processes.	Amazon Shelf	Aller and Blair, 2006; Feng et al., 2016; Kastner and Goñi, 2003; Keil et al., 1997; Kuehl et al., 1986; Showers and Angle, 1986; Sun et al., 2017; Williams et al., 2015.
		Northern Gulf of Mexico	Bianchi et al., 2002; Goñi et al., 1998; Gordon and Goñi, 2003, 2004; Gordon et al., 2001; Sampere et al., 2011a; Sampere et al., 2011b; Sampere et al., 2008; Wakeham et al., 2009; Waterson and Canuel, 2008
		Pan-China Sea	Bao et al., 2016; Li et al., 2012; Tao et al., 2015, 2016; Wang et al., 2015; Wang and Li, 2007; Wu et al., 2013; Yao et al., 2015
Subaqueous delta foreset beds (tropical/temperate)	High specific burial rates but small global volume. Carbon burial influenced by riverine sediment flux and marine processes.	Amazon	Aller and Blair, 2006; Feng et al., 2016; Kastner and Goñi, 2003; Keil et al., 1997; Kuehl et al., 1986; Showers and Angle, 1986; Sun et al., 2017; Williams et al., 2015
		Papua New Guinea	Aller and Blair, 2004; Goni et al., 2008
		Bengal Fan	Galy et al., 2007; Galy et al., 2008
Small mountainous river shelves (temperate)	High specific and global carbon burial rates.	US West Coast	Blair et al., 2003; Coppola et al., 2007; Dickens et al., 2006; Feng et al., 2013; Hastings et al., 2012; Hwang et al., 2005; Komada et al., 2016b; Komada et al., 2005; Mollenhauer and Eglinton, 2007; Wakeham et al., 2009; White, 2006
		NZ Margin	Kniskern et al., 2010; Kniskern et al., 2014; Miller and Kuehl, 2010; Sikes et al., 2009
		Papua New Guinea	Aller and Blair, 2004; Goni et al., 2008
Semi-closed coasts/ estuaries	High specific carbon burial rates and high rates of anaerobic diagenesis.	Fjords	Cui et al., 2016a; Cui et al., 2017; Cui et al., 2016b; Louchouarn et al., 1997; Nuwer and Keil, 2005; Smith et al., 2015; Smittenberg et al., 2004
		Chesapeake Bay	Zimmerman and Canuel, 2001, Hinojosa et al. 2014
		Baltic Sea	Leipe et al., 2011; Miltner and Emeis, 2000; Miltner and Emeis, 2001; Struck et al., 2000
High latitude coastal	High rates of organic carbon burial.	Arctic	Drenzek et al., 2007; Feng et al., 2015a; Feng et al., 2015b; Goni et al., 2005; Goñi et al., 2000; Karlsson et al., 2011; Karlsson et al., 2016; Bröder et al., 2016; Tesi et al., 2014; Vonk et al., 2012; White, 2006; Yunker et al., 2005
		Antarctica	Wakeham and McNichol, 2014; White, 2006
Upwelling systems	High rates of organic carbon burial. Marine dominated	Peru Margins	Bergamaschi et al., 1997; White, 2006
		Mexico Margins	Arnarson and Keil, 2007; Dickens et al., 2006; Wakeham et al., 2009
Intertidal Systems	High rates of carbon burial and in-situ carbon production. Vulnerable to environmental and anthropogenic changes.	Salt Marsh	Bridgham et al., 2006; Chumura et al., 2003; Duarte et al. 2005; Duarte et al. 2010; McLeod et al., 2011
		Mangrove	Alongi et al. 2002; Duarte et al. 2005; Kristensen et al., 2013; McLeod et al., 2011; Smoak et al., 2013
		Seagrass	Duarte et al. 2005; Fourqurean et al. 2012; Kennedy et al., 2010; McLeod et al., 2011

Table 1.1. Characteristics of different environments which are conducive to C storage (Adapted from Bianchi et al. 2017)

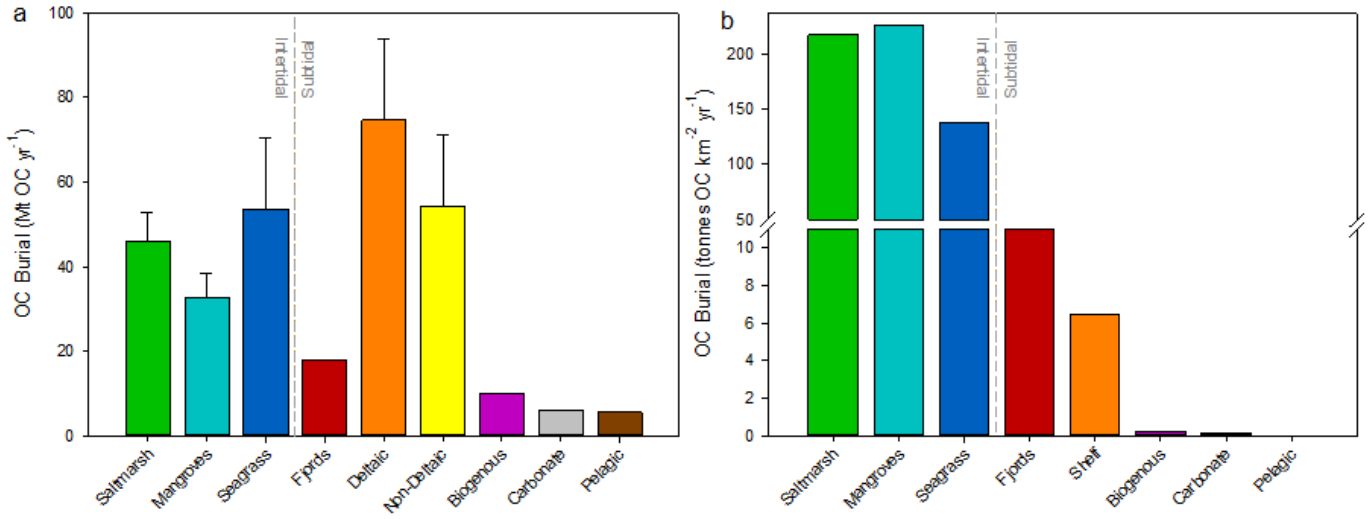

Figure 1.4 Annual OC burial in global intertidal and subtidal sedimentary environments. (**a**) Annual OC burial. (**b**) Area normalised OC burial (Hedges et al., 1997, Smith et al., 2014)

1.3.2 Subtidal Sedimentary C Stores

Subtidal sedimentary environments occupy a vast area of the earth's surface (Table 1.2) and are estimated to bury 171.1 ± 38 Mt OC yr^{-1}, making them an integral component of the global climate regulation system. The deltaic and non-deltaic shelf sediments bury the largest quantity of C each year, locking away an estimated 129 Mt of CO_2. Annually fjords store a further 18 Mt of OC (Smith et al., 2014) which is significant when you consider the areal extent of these environments. Finally the biogenous, carbonate and pelagic sediments which cover large areas of the world's oceans only slightly contribute to the global burial and storage of C.

Ecosystem	**Area** (km^2)	**Global Carbon Burial** (Mt OC yr^{-1})	**CO_2 Sequestration** (Mt CO_2 yr^{-1})
Fjords	455000	18	66.1
Deltaic	19900000	74.6 ± 19.4	273.8 ± 71.3
Non-Deltaic		54.4 ± 16.7	199.6 ± 61.2
Biogenous	45900000	10	36.7
Carbonate	45900000	6	22.0
Pelagic	284000000	5.5	20.2
Global Sedimentary Environments		**171.1 ± 38.0**	**627.8 ± 139.5**

Table 1.2 Global carbon burial, areal extent subtidal sedimentary environments (Hedges et al. 1997; Smith et al., 2014).

At the global scale the rates at which OC is buried in sediments is broadly understood (Table 1.2). These estimates (Hedges et al.1997, Smith et al., 2014) were calculated using very limited data sets and significant assumptions were made to simplify the calculations. The calculations assume that the different sedimentary environments are homogenous and the OC burial rates of different environments are the same (i.e. OC is buried in all shelf sediments at the same rate). This assumption likely results in a vast over estimation of OC burial; therefore to better constrain these estimates more regional studies are required. For example, it is estimated that globally fjords bury 18 Mt of OC each year (Smith et al. 2014), this estimate was made using only 44 different fjords. Scotland along has over 111 large fjords. The Smith et al. (2014) global estimate of C burial was calculate using one sediment core in Scotland (Loh et al., 2010). This highlights that if we want to better understand the global burial of C in sediments, as well as the global climate regulation service these environments provide, these data gaps must be filled through local and regional studies.

If the global understanding of C burial in sediments remains fairly rudimental, by comparison our knowledge about the location and magnitude of C stocks in these environments is very limited. Unlike the terrestrial environments where C stock estimates are made routinely for forests, soils, peatlands (Wilson et al. 2013, Draper et al., 2014, Dargie et al., 2017), the same is not true for marine sediments. Current sedimentary OC stock estimates are limited (Table 1.3) but what has been done shows that there are large quantities of C stored in coastal and shelf sediments.

	OC Stock (Mt)	**Max Sediment Depth of Used to Calculate Stock (m)**	**Reference**
Namibia (EEZ)	811	0.1	Avelar et al., 2017
Pakistan (EEZ)	385	0.1	Avelar et al., 2017
UK (EEZ)	661	0.1	Avelar et al., 2017
NW European Shelf	250	0.1	Diesing et al., 2017
Scotland (EEZ)	592	0.1	Burrows et al. 2017

Table 1.3 Sedimentary C stock estimates for national Exclusive Economic Zone (EEZ) and the wider shelf.

While it is clear that a significant quantity of OC is stored in these sediments it is also clear that the total quantity of OC has been vastly underestimated. All the sedimentary C stock estimates listed in Table 1.3 are based on estimates down to a depth of 10 cm

only, yet it is known that fjord sediments can extend beyond 70m in depth (Baltzer et al., 2010) and shelf sediment can extent even further. A secondary issue is that these estimates vary significantly. For example, the UK EEZ is estimated to hold 661 Mt OC (Avelar et al., 2017) while the Scottish EEZ alone is believed to store 592 Mt OC (Burrows et al., 2014). However and finally the NW European shelf which includes the majority of the UK EEZ and as well as other European nations EEZ's has been estimated to store 250 Mt OC (Diesing et al. 2017). The significant differences in the estimated OC stocks of the same area largely come down to methodological approaches. Diesing et al. (2017) employed a model, Burrow et al. (2014) uses spatial interpolation combined with data produced from historic sampling campaigns and Avelar et al. (2017) used existing data and simply extrapolates out for the area of the EEZ. The current quality of sedimentary C stock estimation highlights the need for a new methodological approach which is able to estimate the full sedimentary C stocks (i.e. beyond 10cm) and can be applied by the community to a wide range of environments.

1.3.3 Blue Carbon

Intertidal habitats bury C at a greater rate and store more C per unit area than their subtidal and terrestrial counterparts (Fig.1.4). Occupying only 0.2% of the ocean surface area (Fig.1.5) coastal vegetated habitats such as saltmarsh, mangroves and seagrass contribute 50% of global OC burial in marine sediments (Duarte et al. 2005)(Fig.1.4).

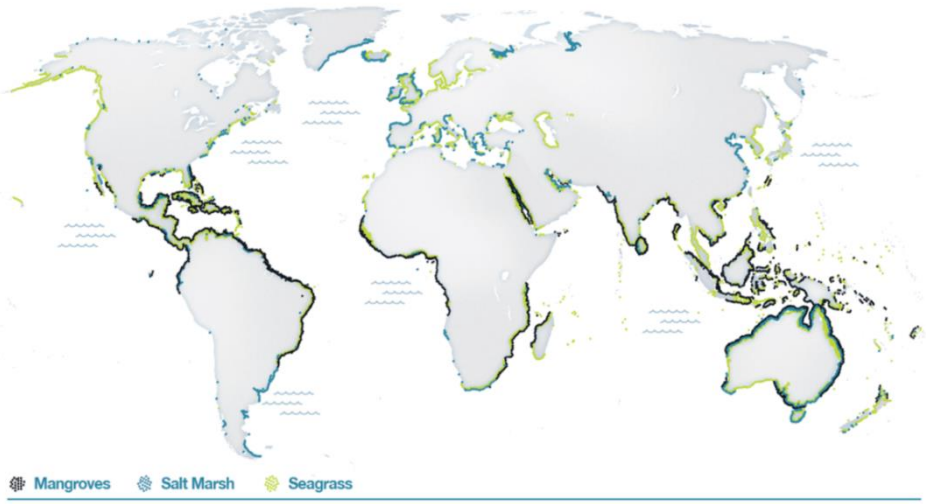

Figure 1.5 Global extent of coastal vegetated environments (Source: *Blue Carbon Initiative*)

The C sequestered and stored by these vegetated intertidal ecosystems is better known as Blue carbon (BC) (Nellemann et al., 2009). Globally the intertidal BC environments

provide an important climate regulation service through the burial and storage of C in sediments and soils. Currently there are a number of global estimates of OC burial rates (Table.1.4), globally these BC ecosystem are estimated to bury 132.4 ± 10.9 Mt OC yr^{-1} (Mcleod et al. 2011).

Ecosystem	**Area** (km^2)	**Carbon Burial Rate** (g OC m^{-2} yr^{-1})	**Global Carbon Burial** (Mt OC yr^{-1})	**CO_2 Sequestration** (Mt CO_2 yr^{-1})	**Rate of Global Loss** (% yr^{-1})
Saltmarsh	211000 (Range: 22000-400000)	218 ± 24	46.0 ± 6.8	168.8 ± 24.9	1 – 2 (1.5)
Mangroves	145061 (Range: 137760-152361)	226 ± 39	32.8 ± 5.7	120.3 ± 20.9	~ 0.7 – 3 (1.85)
Seagrass	388500 (Range: 177000-600000)	138 ± 38	53.6 ± 16.8	196.7 ± 61.7	~ 7 (7)
Global Intertidal Environments			**132.4 ± 10.9**	**485.8 ± 40.3**	

Table 1.4 Global carbon burial, areal extent and habitat loss rates for intertidal vegetated environments (Mcleod et al., 2011).

Intertidal ecosystems and the C held within has had much more attention in recent decades in comparison to their subtidal equivalents this is largely due to their vulnerability. Since the early 1800's it is estimated that 25% of global saltmarsh habitat has been lost, with assessments predicting that a further 50% of the world's saltmarshes may permanently disappear by the end of this century from erosion and coastal squeeze (Kirwan et al., 2016, Spencer et al., 2016). Mangroves and seagrass meadows are under similar pressure with predicted habitat loss rates ranging between 0.7 and 7 % yr^{-1} (Table 1.4). The quantity of the intertidal BC stocks lost due to this widespread habitat disturbance is unknown but global C sequestration has undoubtedly been diminished with the loss of intertidal habitats.

These intertidal ecosystems (Duarte, 2017) are now reconginsed as globally important sites for C sequestration and crucial to global climate regulation. Yet this has not always been the case with saltmarsh and seagrass ecosystems being overlooked for years in favour of the more "charismatic" habitats (i.e. coral reefs)(Duarte et al., 2008). It took a concerted effort (Donato et al., 2011; Duarte et al., 2005; Fourqurean et al., 2012;

Macreadie et al., 2017) overs years to get intertidal BC research to where it is today. There are current calls for sedimentary environments to be included under the defintion of BC and in a similar vane to BC habitats, for sedimentary enviroments themselves to be included in national GHG reporting (Avelar et al., 2017). It is important to reconginise there are distict difference between the C held with subtidal sedimentary stores and BC ecosystems; so this ambtion may be a step too far at present.

1.3.3.1 Sedimentary vs Blue Carbon

At first glance BC intertidal and sedimentary subtidal environments seem to store C in a similar way (i.e. burial of C in soil/sedimentary stores) so it would seem reasonable to argue for the term "Blue Carbon" should include subtidal sedimentary environments (Burrows et al., 2014). The original definition of BC is C captured by living organisms which is stored in the form of biomass and sediments (Nellemann et al., 2009). This definition sets out two key criteria for ecosystems to be considered as BC habitats:

1. Vegetation in these ecosystems must directly sequester CO_2 from the atmosphere.
2. The ecosystem must have the ability to store the captured C normally locking it away temporally in plant biomass and long-term in soils and sediments.

Sedimentary environments do not directly sequester C, as a direct link to atmospheric CO_2 does not exist. Rather they rely on other ecosystems to sequester C which is eventually transport and stored in the sediments (Fig.1.6). In terrestrial environments this role is largely undertaken by vascular plants which take CO_2 from the atmosphere locking it away in living biomass or within the soil. Over time the plants die and soil erodes, so that the the C held within these stores are eventually transported and deposited in coastal and shelf sediments. Phytoplankton and macro algae serve a similar function in marine ecosystems. The original definition of BC listed algae as a potential BC ecosystem as these organisms are capable of sequestering CO_2 from the atmosphere but they fail to meet the second criteria to be defined as BC (i.e. C storage). As algae cannot store C over the long-term (>10^3 yrs) they cannot be considered BC ecosystems even though they are regularly referred to as such (Chung et al., 2011; Hill et al., 2015). Therefore phytoplankton and macro algae must be considered C donors (Krause-Jensen and Duarte, 2016) to the sediment in a similar way that the terrestrial environment provides a terrestrial OC subsidy to the marine environment. An important point when discussing C donors is that could be easily overlooked is that the definition of BC

(Nellemann et al., 2009) does not mention C subsidies from other environments, so the terrestrial and marine derived C held in intertidal and subtidal soils and sediments cannot be considered BC.

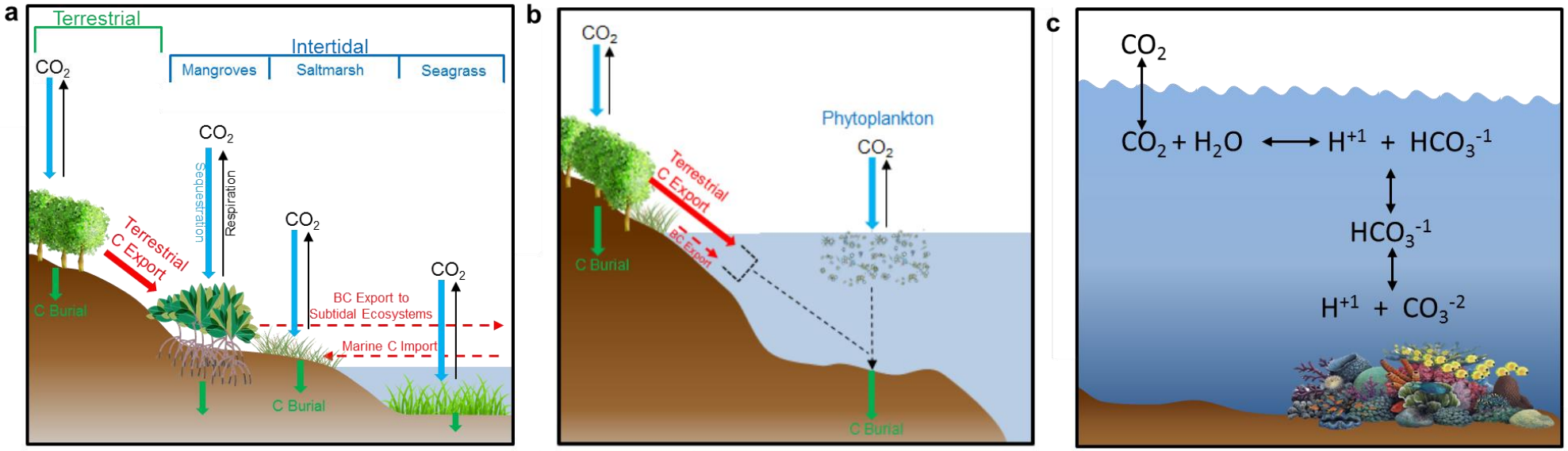

Figure 1.6 Mechanisms governing the burial and storage of C in the marine environments (**a**) Intertidal blue carbon ecosystems (**b**) subtidal sedimentary environments (**c**) carbonate systems (i.e. coral)

1.3.4 Interconnected environments

These ecosystems do not exist in isolation within the C cycle, rather they are linked, with the intertidal BC environments providing C to the marine sediments (Chen et al., 2017; Duarte and Krause-Jensen, 2017; Hyndes et al., 2015; Krause-Jensen and Duarte, 2016). It has been suggested that up to 30% of the C lost from intertidal BC ecosystems could be buried in sedimentary environments (Duarte and Krause-Jensen, 2017; Krause-Jensen and Duarte, 2016). If the current rates of intertidal habitat loss (Table 1.3) continue to rise the quantity of material entering coastal and shelf seas will increase, further interlinking these environments. BC ecosystems themselves can also be closely coupled, with mangroves and saltmarshes providing C to seagrass ecosystems (Hyndes et al., 2015); in Indonesian systems it has been estimated that mangroves provided 34 to 84% of the OC held within neighbouring seagrass meadows (Chen et al., 2017).

Taking a wider overview it is clear that the terrestrial environment also plays a crucial role as a C donor to both the sedimentary subtidal and the BC intertidal environments. The subsidy of terrestrial C to the subtidal sedimentary environments is widely recognised (Bröder et al., 2016; Cui et al., 2016a; Galy et al., 2015), for example it is estimated that between 55% to 62% of the OC buried in fjords globally is terrestrial in origin (Cui et al., 2016a). Intertidal environments are clearly also recipients of terrestrial OC (Kristensen et al., 2008; Smoak et al., 2013). An example from the Florida everglades estimated that approximately 30% of the C held within mangroves sediments is terrestrial in origin (Smoak et al., 2013).

The linkages between environments and especially to the terrestrial environment is clearly a significant factor governing the quantity of C buried and stored in both subtidal and intertidal ecosystems. Yet our understanding of the sources of the C held within both types of environment remains limited.

1.3.5 Inorganic Carbon (Carbonate)

Both the subtidal and intertidal environments are significant stores of IC (Mazarrasa et al., 2015; Wang et al., 2016, Koziorowska et al., 2017), largely formed from calcifying marine organisms (e.g. foraminifera) or from the erosion of sedimentary rocks (Galy et al., 2007,2008). The mechanisms governing C capture in calcifying environments and organisms differ significantly from that of OC trapping environments. It is true they have the ability to sequester CO_2 directly from the atmosphere/water column and have a mechanism to facilitate storage (i.e. Carbonate). However the complexities of carbonate production means that even though large quantities of IC are stored in sediments and corals over geological timescales the original production of that carbonate caused the release of C to the atmosphere. In the simplest terms the calcification process increases pCO_2 reducing alkalinity, which allows the return of CO_2 to the atmosphere (Frankignoulle et al., 1994), for every mole of $CaCO_3$ precipitated as carbonate 1 mole of CO_2 is released:

$$Ca^{2+} + 2HCO_3^{-1} \underset{CaCO_3 \text{ dissolution}}{\overset{\text{Calcification}}{\rightleftharpoons}} CaCO_3 + H_2O + CO_2$$

Seawater has the ability to buffer this process resulting in only ~0.63 moles of CO_2 reaching the atmosphere (under current atmospheric CO_2 concentrations) (Frankignoulle et al., 1995), even so this means that these carbonate systems are net sources of CO_2. Certain coral and coralline algae (Heijden and Kamenos, 2015) ecosystems can act as traps of OC from adjacent ecosystems (Briand et al., 2015) similar to the subtidal sediments and like these systems C stored within is not BC. It is therefore crucial to better understand the burial and storage of IC alongside that of OC, within the sedimentary C literature this understanding is incomplete.

1.4 Scotland's Carbon Resource

Scotland's terrestrial environment is dominated by C (Fig.1.7) with 66% of its land mass covered with peat which accounts for 50% of the UK total soil C stock (Cummins et al., 2011). In total, the Scottish peatlands hold an estimated 1600 Mt of OC (Chapman et al. 2009) with the other soils storing a further 1252 Mt C (Bradley et al., 2005). In addition, Scotland's vegetated environment is estimated to hold 106 Mt C in living biomass with a further 21 Mt held in forest litter (Henry et al., 2016, Vanguelova et al., 2013). Scotland's terrestrial carbon resource is well characterised and quantified but the same is not true for the marine environment.

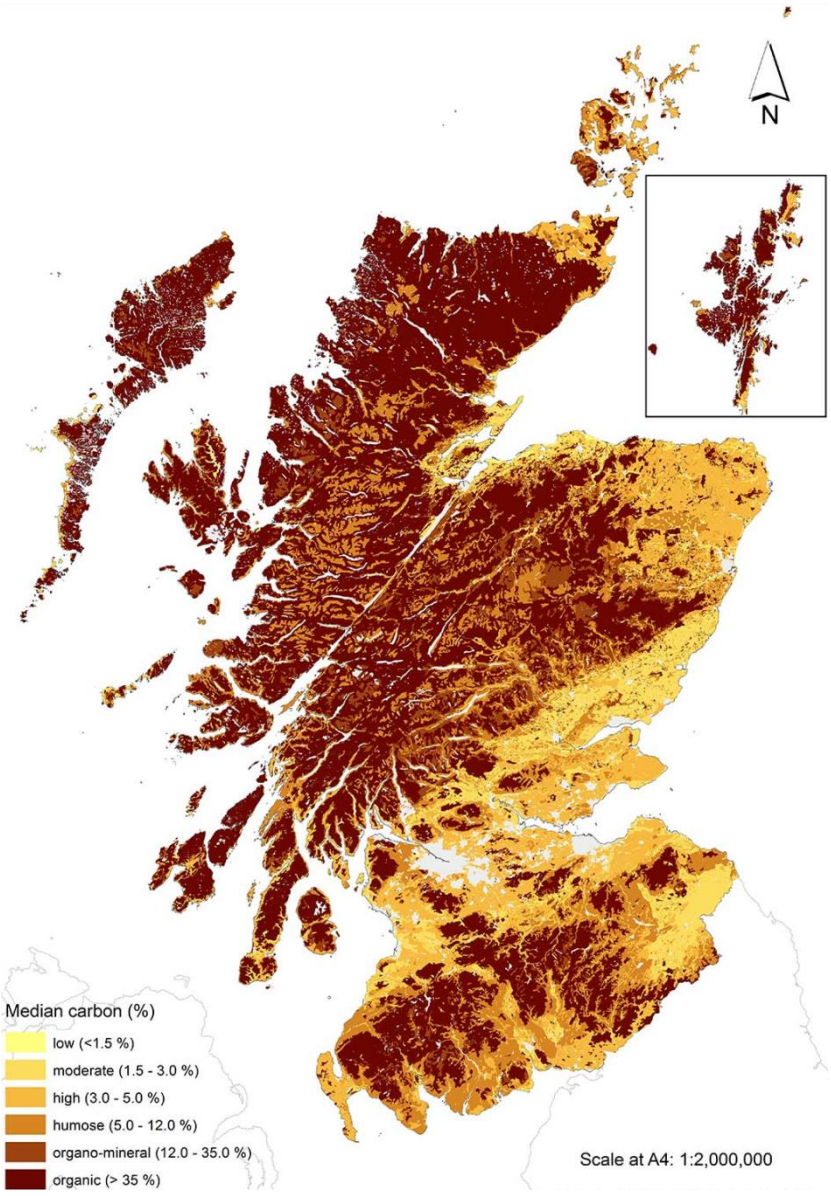

Figure 1.7 Scotland soil and peatland C resource (Source: *James Hutton Institute*)

1.4.1 Scotland's Marine Carbon Resource

Similar to the global outlook, our understanding of where C is stored in Scotland's marine and coastal environment is very limited in comparison to terrestrial ecosystems. The bulk of the available information comes from Burrows et al. (2014) a Scottish Natural Heritage commissioned report. This desk based study used existing data sources to make first order estimates of Scotland's marine and coastal C resource. The Burrows et al. (2014) report focused on sedimentary, intertidal and calcifying environments.

Habitat	Extent (km^2)	OC Stock (Mt)	OC Sequestration Rate ($g\ C\ m^{-2}\ yr^{-1}$)	IC Stock (Mt)	IC Sequestration Rate ($g\ C\ m^{-2}\ yr^{-1}$)
Biogenic Habitats	2283	0.4		0.58	109
Kelp Beds	2155	404			
Intertidal Macroalgae	24.1	11.8			
Mearl	7.1			440.6	74
Seagrass	15.9		83		
Saltmarh	67.5	8.6	210		
Biogenic Reefs	13.4			142	582

Table 1.5 C stock estimates of Scotland BC and biogenic ecosystems (Burrows et al., 2014).

Unlike many other global attempts to estimate marine and coastal C stocks Burrows et al. (2014) made an effort to include both OC and IC in the estimates (Table 1.5, 1.6). The report found (if the sediments are excluded) that the main stock of OC is held in the kelp and microalgae but as previously discussed (Section 1.3.3.1) these are short lived stores of OC. Mearl beds constitute a significant store of IC (Table 1.5) which is equivalent to that stored in the sediments (Table 1.6). The issue with these estimates is often the lack of data; Table 1.5 illustrates this point, simply there is currently not enough data to calculate C stocks and sequestration rates for many environments.

In comparison estimates have been made for the majority of Scotland's sedimentary environments. It is estimated the 18 Mt OC and 1738 Mt IC is stored in the top 10 cm of sediment, this makes the sediments highly important as they are capable of storing C for long periods of time in comparison to kelp and microalgae. These estimates suffer the same problem as other sedimentary C stock estimates (Table 1.3) in that they only focus on the top 10 cm, but when you consider that the sediments occupy 470807 km^2 18 Mt of OC seems to be a very low estimate. This total was later corrected upwards by several orders of magnitude (Burrows et al., 2017) to 592 Mt making the sediments the largest marine C store in Scotland.

Habitat	Extent (km^2)	OC Stock (Mt)	OC Sequestration Rate ($g\ C\ m^{-2}\ yr^{-1}$)	IC Stock (Mt)	IC Sequestration Rate ($g\ C\ m^{-2}\ yr^{-1}$)
Shelf Sediment Coarse(Top 10cm)	115004	0	0.2	798	1.05
Shelf Sediment Fine (Top 10cm)	171660	17.6	41.1	468	0.84
Offshore Sediment (Shelf/Deep)	183296	0.1	0.1	472	0.95
Sea loch: Mud	847	0.3	155.2		
Shelf Sediment (Revised Total)	**286664**	**592**			

Table 1.6 C stock estimates of Scotland sedimentary environments (Burrows et al., 2014)

1.4.1.1 Scotland's Fjords

Scotland's west coast is dominated by glacial geomorphology (sea lochs) resulting in 111 large fjords (over 2 km^2) and 100's of smaller inlets (Sharples and Edwards, 1989). Yet in terms of C we know very little about these environments which is odd when one considers the importance of the terrestrial C held within this region (Fig. 1.7). It has been estimated that the top 10 cm of sediment with Scotland's fjords hold 0.34 Mt of OC this is as previously discussed, is a vast underestimation of the true C stock for the sediment which can reach as far 70 m in depth (Baltzer et al., 2010). Our understanding of the source of the C and the rates at which it is buried in these systems is based on the limited work by Loh et al., (2008, 2010). Loh et al. (2008) which concluded that terrestrial OC was important to the development of the sedimentary C store in Loch Creran, but failed to quantify the proportion of terrestrial and marine C held within the sediment; later they quantified that terrestrial OC constitutes 1.4 - 4% of the sediment (Loh et al., 2010). This estimate of terrestrial OC held within the fjord surface sediments is significantly below the global average for fjords of 55 – 62% (Cui et al., 2016b) and due to the restrictive (largely land-locked) nature of the two fjords studied (Loch Creran and Etive) it is highly unlikely these estimates are correct. The C stred in fjord sediments were revisited by Burrows et al. (2017) when the C resources held within Scotland's Marine protected Area (MPA) network was quantified. Twelve fjords are included in Scotland's MPA network and it was estimated that they hold 0.22 Mt OC and 0.4 Mt IC within the top 10 cm of sediment (Table 1.7). These results bring into question the original Burrows et al. (2014) C stock estimate of 0.34 Mt OC for all 111 fjords in Scotland. As with the original report Burrows et al. (2017) found that the subtidal marine sediments were the most C rich marine environments.

Site	OC Stock (t)	OC Burial (t yr^{-1})	IC Stock (t)	IC Burial (t yr^{-1})
Loch Sunart	47673	877	70352	837
Loch Sween	36084	881	116488	1073
Loch Duich, Long and Alsh	49257	1326	80111	955
Loch Creran	19132	552	19464	297
Loch Laxford	8068	126	17717	178
Loch Moidart	3160	77	9442	89
Loch nam Madadh	17285	382	27708	324
Loch Roag	284	4	450	5
Loch of Stenness	9452	140	15357	172
Sullom Voe	29581	444	47525	530

Table 1.7 Sedimentary C stock estimates from fjords within the Scottish MPA network (Burrows et al., 2017)

The limited data and the quality of what is available means that Scotland and the mid-latitudes in general do not yet provide reliable sedimentary C estimates. An improved understanding of the quantity of C held within the sediments and the source of that C in Scottish fjords will enable to further constraint of the estimates of C burial and storage in the region, subsequently improving global estimates. Further by understanding the storage and origin of C at the land-ocean interface, we will improve estimates of Scotland's natural C capital through the inclusion of these forgotten stores.

Understanding the C in mid-latitude fjords is also important to understanding the future coastal arctic ocean. It has been suggested that present day Svalbard and Northern Norway are analogues for Scotland during the last glacial period (MacLachlan and Howe, 2010). Here we flip this relationship by gaining better understanding the C dynamics of Scottish mid-latitude fjords today we can better predict the processes which will govern C in the coastal arctic seas in the coming years.

1.5 Summary

Global marine sediments clearly play an important role in climate regulation through the burial and storage of C. While the rates at which C is buried in these sediments seems to be well characterised (Table 1.2) in reality they are based on very limited data and those data are geographically not well dispersed. To improve and further constrain the global rates at which C is buried in marine sediments, it is crucial to increase the number of regional/national studies focusing on different sedimentary environments.

Our understanding of the rates at which C is buried is rudimental but far exceeds our knowledge of the location and quantity of C stored in marine sedimentary environments. Currently, what sedimentary C stock estimates exist, only consider the top 10 cm of sediment (Table 1.3) and use a range of methodological approaches. This results in highly variable estimates which are clearly underestimations of the sedimentary C stock. Estimating the magnitude of these stores is highly important because they are a large forgotten piece of the global and natural C capital.

With calls for these sedimentary environments to be included in national C budgets, there is a strong imperative for a sound scientific foundation to guide any future policy decisions. We must improve our regional/local understanding of the locations and magnitude of the marine C stores, identify the source of the C and the rate at which C is buried. This can be achieved through a focused research programme on a number of different sedimentary environments around the world.

Fjords are one such environment; globally they have been shown to be “hotspots” for C burial and highly effective at capturing terrestrial C (Smith et al., 2014, Cui et al., 2016b). Globally fjords are estimate to bury 18 Mt of C annually but as with other sedimentary environments, these burial rates are based on minimal data, particularly from the mid-latitudes. For example, the global estimate of C burial in fjords only included one sediment core from a mid-latitude fjord (Loh et al. 2010). Similarly to the global outlook little is known about how much C is stored in fjordic sediments. As with all sedimentary environments through developing a better understanding of the size and long-term development of these C stores we will improve our comprehension of the global C cycle and provide a strong scientific foundation to guide future policy.

1.5.1 Aims and Objectives

The aim of this study is to evaluate and develop the current understanding of sedimentary carbon stores in the coastal ocean using Scotland as a natural laboratory. The focus of this study will be the fjords (Sea lochs) on the West coast of Scotland, using these environments we will explore these long-term sedimentary C stores and the mechanisms which govern their development. This will be possible through the following objectives:

1. Develop a methodological approach to quantify sedimentary C stores which is applicable to multiple environments in the world's oceans.
2. Quantify the sedimentary C stored in Scotland's fjords.
3. Understand the terrestrial environment's role in the supply of C to the coastal ocean.
4. Develop a long-term understanding of the evolution of the sedimentary C stores through time.

1.5.2 Thesis Structure

The style of this thesis is constructed as a classical monograph with the distinction that a number of the chapters have been written-up as stand-alone manuscripts, some of which have been published. This chapter presents an introduction to carbon in the coastal ocean, while Chapter 2 describes the generic analytical methods used throughout this study. Chapters 3-6 are written as independent chapters in expanded manuscript format; they included detailed discussion of the state of the art literature and include chapter-specific methodological sections beyond that found in Chapters 1 and 2. Chapter 3 describes the methodological development to quantify fjordic sedimentary C stores; Chapter 4 presents the use of light stable isotopes as a fingerprinting tool to quantify terrestrial C input; Chapter 5 utilises the methodological approach developed in Chapter 3 to calculate the first national sedimentary C stock estimate for the coastal ocean. Finally, Chapter 6 describes the evolution of a coastal sedimentary C store through the Holocene. Chapter 7 relates all the data gathered in this study to draw together conclusions based on the individual chapters.

Chapter 2

Materials and Methods

2.1 Overview

This chapter provides an overview of the generic sampling and analytical methods used in this study; Chapters 3-6 detail the application of these methods. Details on the use of specialised methodologies (volumetric modelling, Bayesian Mixing Models, etc.) can be found within the Chapters that they are utilised.

2.2 Sampling

This study utilised several sediment sampling techniques to collect surficial and integrated depth records. The coring equipment used included a multi-corer, sholkovitch corer, gravity corer and a giant piston corer, while surface samples were collected using van-veen grab samplers of differing sizes. All the coring equipment uses the simple principle of gravity to drive the sampler into sediment, most corers are weighted (normally with lead) to assist gravity and increase sediment penetration and recovery.

The length of core recoverable by each of the different corers varies (Fig.2.1); multi and sholkovitch corers collect samples of < 1 m in length and are designed to capture the undisturbed water sediment interface. Gravity coring methods are capable of recovering long sediment cores, in this study two different corers were used which were capable of recovering cores of 3 m (SAMS) and 6 m (BGS) respectively. Though gravity coring is one of the best methods for collecting long cores the technique can disturb the top portion of the core and the loss of the top 10 cm is not unusual, to combat this issue it is common that a multi-core is taken at the same location to assure the full sediment record is collected. Giant piston coring does use the gravity principle but it is a sampling method with greater complexity.

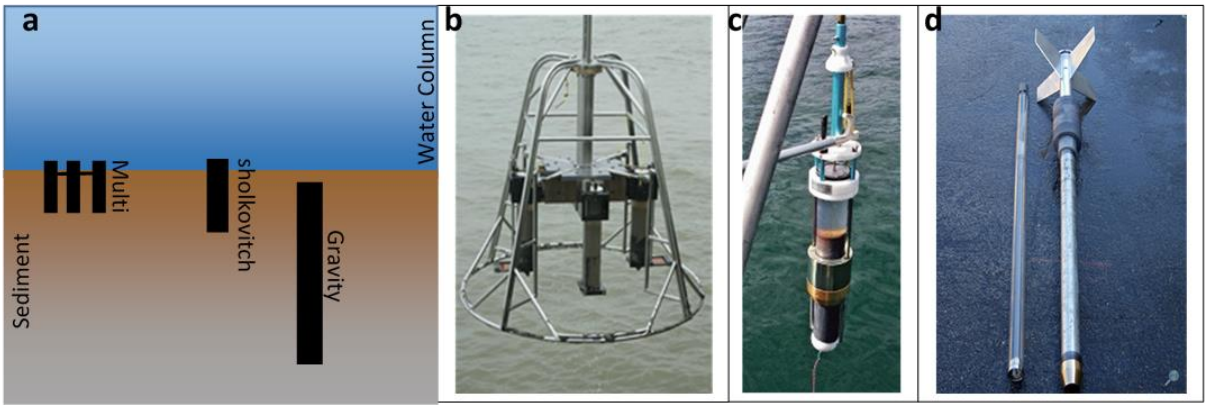

Figure 2.1 Details on the standard coring methods utilised (a) comparison of depth range and sample recovery **(b)** multi-corer **(c)** Sholkovitch corer **(d)** Gravity corer**.**

The study used the CALYPSO giant piston corer on board the *Marion Dufresne* (Fig.2.2). The CALYPSO is a giant corer that uses a Kullenberg piston. This technique is considered one of the most practical and useful coring methods for obtaining marine sediment cores of up to 60 m long. Normal operation of the corer follows five steps outlined in Figure 2.2. The corer is slowly lowered into the water column were the descent can take up to 2 hours before the counter weight reaches the seabed. After the counterweight reaches the seabed the trigger is activated and the corer is released, the corer falls and penetrates the marine sediment.

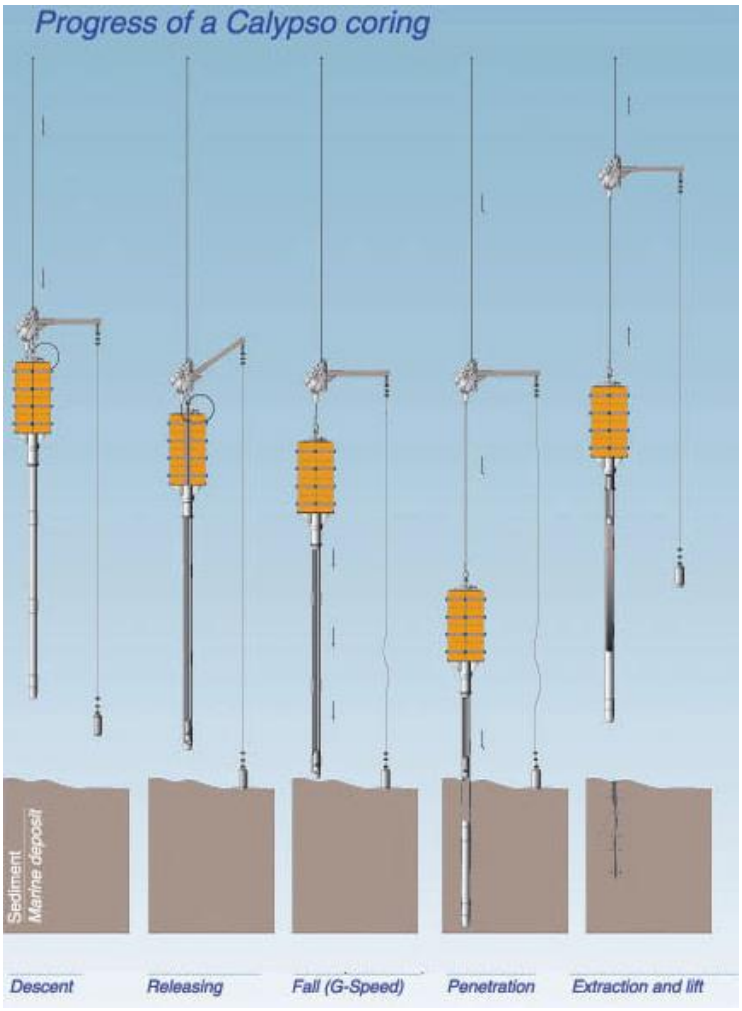

Figure 2.2. Simplified use of the CLAYPSO giant piston corer (Source: *institut-polaire.fr*).

The piston is used to ensure that the corer's internal pressure conditions are constant throughout its length, to minimize the deformation of the sediments. However, as the piston undergoes acceleration during coring a depression in the interior of the sediment forms this creates a stretching effect, whereby the sediments near the tube walls suffer a distortion that must be accounted for before interpolation.

Surface samples were collected using a van veen grab sampler (Fig.2.3).Though this technique is described as surface sampling method in reality it collects composite sample from the around the top 10 cm of sediment.

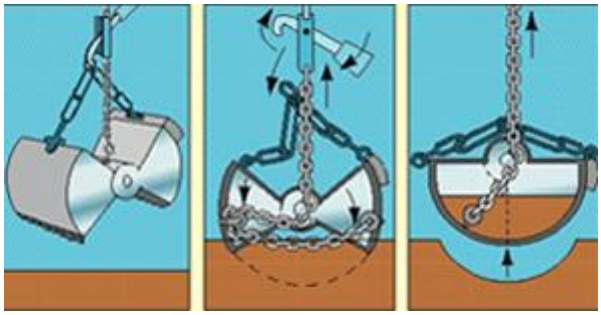

Figure 2.3. Operation of a Van Veen grab sampler (Source: *kmtsubmarine.com*)

Each technique has advantages and disadvantages ranging from sample recovery to the size of ship needed to operate the equipment. Through the use of several of the methods the disadvantages of one technique can normally be offset against the advantages of another (i.e. multi corer + gravity corer).

2.3 Physical and Sedimentological Properties

2.3.1 Water Content and Bulk Density

Bulk density and water content though simple measurements play a crucial role in this study and are key to calculating the mass of sediment and C density within the fjords. Bulk density is defined as the mass of sediment per unit volume of sediment. Bulk density considers both the solids and the pore space, depending on if the pore spaces are free of water bulk density can either be reported as either wet or dry bulk density. To measure these properties the methodology of Dadey et al. (1992) is followed, where a discrete sample of known volume (normally 5 cm^3) is weighed before and after overnight drying at 105°C. This allows the calculation of the wet and dry bulk density as well as the water content as follows:

Wet Bulk density (g cm^{-3}) = Wet mass (g) / Sample volume (cm^3)

Dry Bulk density (g cm^{-3}) = Dry mass (g) / Sample volume (cm^3)

Water Content (%) = (Wet Mass (g) – Dry Mass (g)) / Wet mass (g)

2.3.2 Magnetic Susceptibility

Magnetic susceptibility is a measure of the magnetic properties of a material. The susceptibility indicates whether a material is attracted into or repelled out of a magnetic field. Quantitative measures of the magnetic susceptibility provide insights into the structure of materials. In this study the magnetic susceptibility is used as a proxy of minrogenic input to the sediments (i.e. high magnetic susceptibility indicates minerogenic material).

Magnetic Susceptibility was measured using the Barrington suite of equipment, simply 1 cm^3 of dry sediment was powdered and placed in a Teflon cuvette where the magnetic susceptibility was measured using the MS2G Single Frequency Sensor. Magnetic susceptibility is reported in SI units (magnetic flux density) either in uncorrected form or correct for volume.

2.3.3 Particle Size and Sortable Silt.

Particle size distribution of the sediment was measured using laser granulometry. This technique can measure the size range of organic matter + mineral component of the sediment or the mineral component alone. To measure the organic matter + mineral component no sample preparation is required. To measure the mineralogical material the organics and carbonate material must be removed. This is achieved through the addition of 30% H_2O_2 to facilitate the removal of the organic component and 10% HCL to remove any carbonate.

Once prepared the samples are ready to be analysed. Laser granulometry measures the angular variation in intensity of light scattered as a laser beam passes through a dispersed particulate sample (Fig.2.4). Large particles scatter light at small angles relative to the laser beam and small particles scatter light at large angles. The angular scattering intensity data is then analysed to calculate the size of the particles responsible for creating the scattering pattern. The particle size is reported as a volume equivalent sphere diameter.

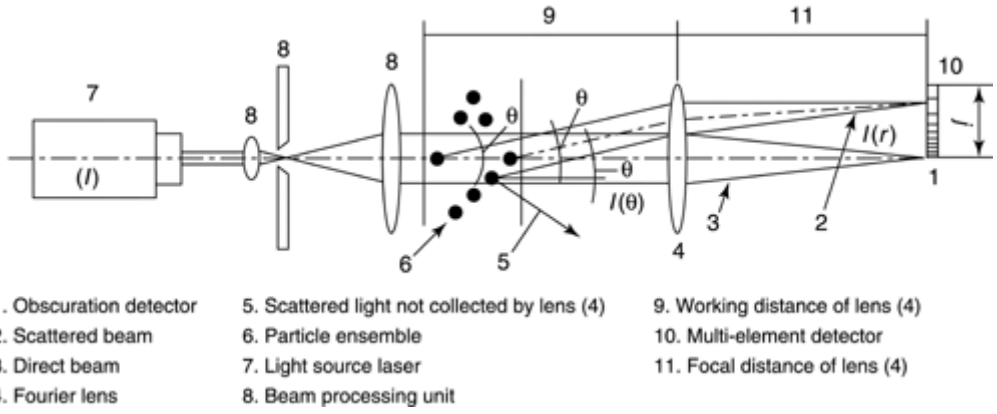

Figure 2.4. Schematic of the operation of a standard laser granulomtry system (Source: *malvern.com*)

Sortable Silt can be used as a proxy to infer current speeds (McCave et al. 1995). Silt within the size 10-63 µm size distribution display size sorting in response to hydrodynamlc processes and its properties may be used to infer current speed. The sortable silt proxy is often reported as either the 10-63 µm mean size or the percentage 10-63 µm of the fine fraction. Sortable silt can be calculated from data produced by laser granulometry but the use of a sedigraph is often preferred (McCave et al., 1995).

2.4 Bulk Organic Matter Geochemistry

Technological advances have improved our ability to characterise and distinguish between organic matter sources through the use of elemental, isotopic (bulk and compound specific), and chemical biomarker methods. These tools differ in their ability both to identify specific sources of organic matter and to represent bulk organic matter (Fig.2.5). This section provides a general overview of the techniques used in this study to characterise organic matter sources in the marine environment.

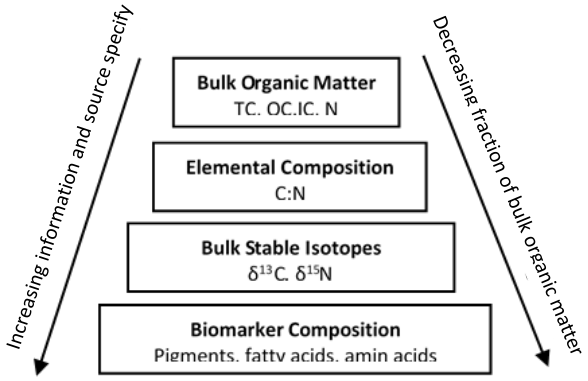

Figure 2.5 Overview of the approaches for characterising organic matter with differing levels of complexity.

2.4.1 Elemental Analysis (C & N)

The abundance and ratios of elements important in biological cycles (C,N) provide the basic information about organic matter sources and cycling. When bulk OC measurements are combined with additional elemental information, as in the case of atomic C to N, basic source information can be inferred about algal and vascular plant sources (Meyers, 1997). The broad range of C:N ratios across sources of organic matter in the biosphere demonstrate how such a ratio can provide an initial proxy for determining source information.

2.4.1.1 Measuring Elemental Content

This technique places pre-prepared sample capsules into an automatic sampler. They are then dropped into a combustion furnace held at 1200 °C where they are combusted in the presence of oxygen. The capsules flash combust causing the temperature in the furnace to rise to ca. 1600°C. The gaseous products of combustion are swept in argon (alternatively Helium) stream over a Cr_2O_3 combustion catalyst and silver wool to remove halides. The resultant gases (N_2, NO_x, CO_2) are then swept through a reduction stage of pure copper wires held at 800°C removing any remaining oxygen. The gases are passed through magnesium perchlorate trap to remove water. The N is directly channelled to the Thermal Conductivity Detector (TCD) while the other gases are trapped awaiting sequential analysis (Fig.2.6) The TCD senses changes in the thermal conductivity of the gases and compares it to a reference flow of carrier gas. Since most compounds have a thermal conductivity much less than that of the common carrier gases, the carrier gas thermal conductivity is reduced; this reduction allows the quantification of the elements. The TCD has a detection limit of < 40ppm for both C and N.

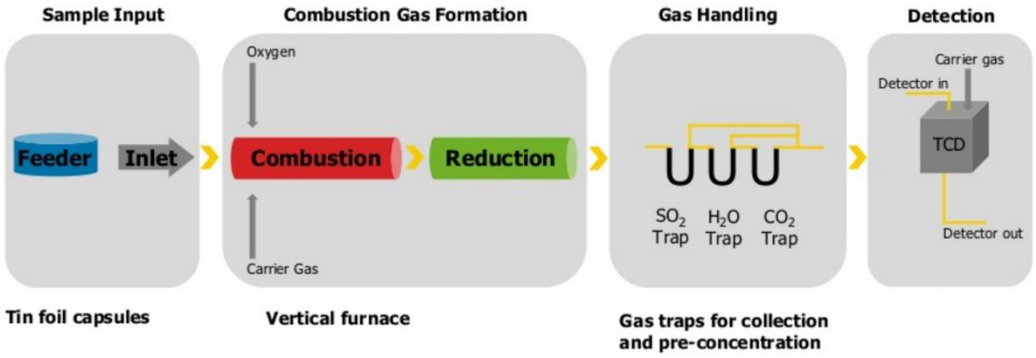

Figure 2.6. Schematic of the standard operation of an Elementar EA (Source: Elementar.de)

2.4.1.2 Sample Preparation

Samples must be prepared before analysis can take place; this normally entails the sample being freeze dried or dried at a low temperature (40°C). The dry sample is then milled to a fine powder. A subsample (normally 10 ± 1 mg) of the powder is then placed in a tin capsule which is sealed ready for analysis. This preparation method is designed to measure TC, N, H and S. To measure OC and IC the samples must be reanalysed with an additionally step to remove one of the C phases. The removal of OC can be

achieved through a Loss on Ignition step where the OC is burned away at 550°C for 4 hours this technique is rarely used and is best suited for carbonate rich marine sediments. More commonly the IC is removed through the addition of acid; this can be done a number of ways with different acids (HCl, Phosphoric, Sulfurous acid). The standard methodology (Verardo et al., 1990, Nieuwenhuize et al., 1994) involves the powdered sample (normally 10 ± 1 mg) being placed in a silver capsule with acid (10% HCL) being directly added, the samples are left over night to assure total IC removal. The alternative acidification method uses the acid fumigation technique (Harris et al., 2001), where the wetted powdered samples again in silver capsules are place in a desiccator for 8 hours with concentrated (~ 37%) HCL. The fumes from the acid are absorbed by the sample as it dries, with the uptake of acid removing any IC. Though widely used studies suggest that exposing organic material to concentrated acid may have a detrimental impact on elemental and isotopic quantification especially the measurement of N (Kennedy et al., 2005). Once the samples are prepared they can be analysed (Section 2.4.1.1). Once the TC and either of the other types of C (OC or IC) are quantified the remaining C phase can be calculated following:

$$TC = OC + IC$$

2.4.1.3 Inter- Laboratory Comparison

During this study elemental analysis was undertaken in five laboratories (University of St-Andrews, University of Florida (UF), NERC Life Science Mass Spectrometry Facility (NERC LSMSF), Scottish Association of Marine Science (SAMS) and the commercial OEA labs using three differently manufactured EA's (Thermo, Costech and Elementar). To assure the quality and the reproducibility of the data collected an inter-laboratory comparison exercise was undertaken.

The inter-laboratory comparison measured the OC and N content of 98 marine sediment and 16 terrestrial samples on an Elementar vario EL cube located at the University of St-Andrews. The 114 samples were chosen from a sample set with existing data collected from the other four laboratories.

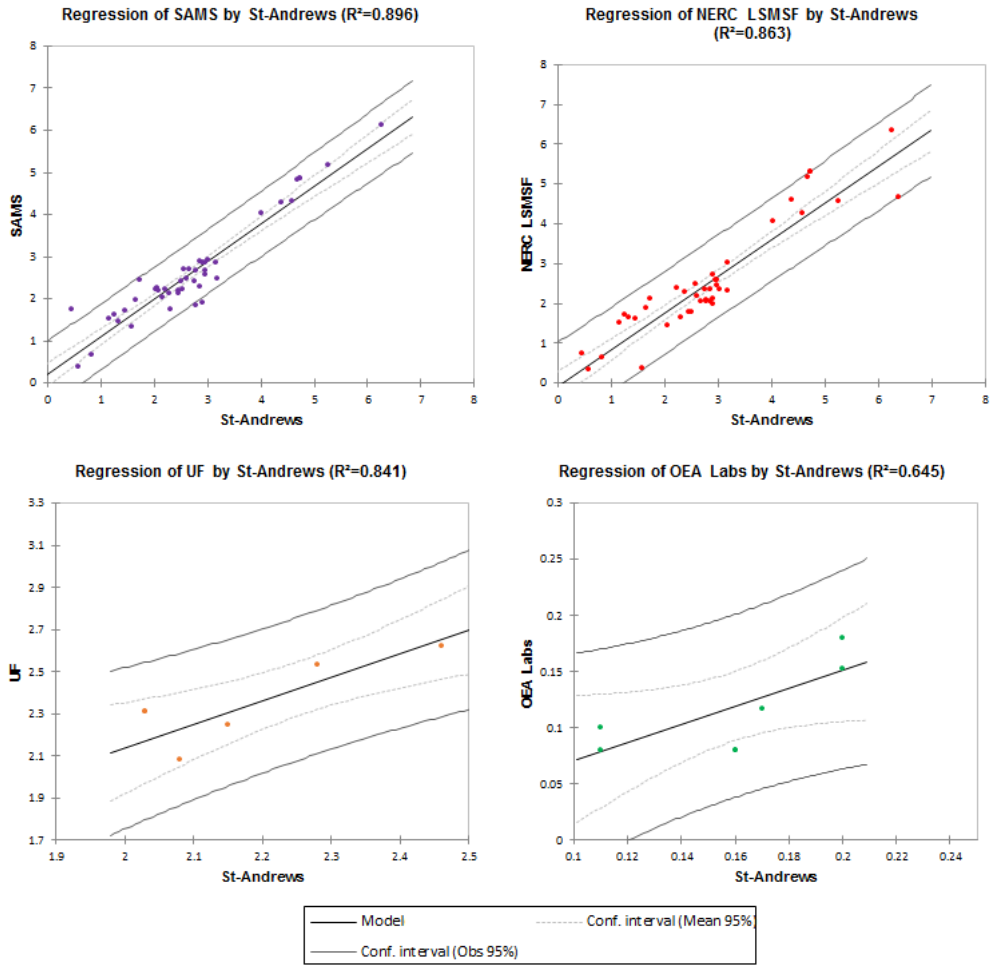

Figure 2.7. Comparison of organic carbon (OC) measurements of marine sediment samples made at St-Andrews to the other labs.

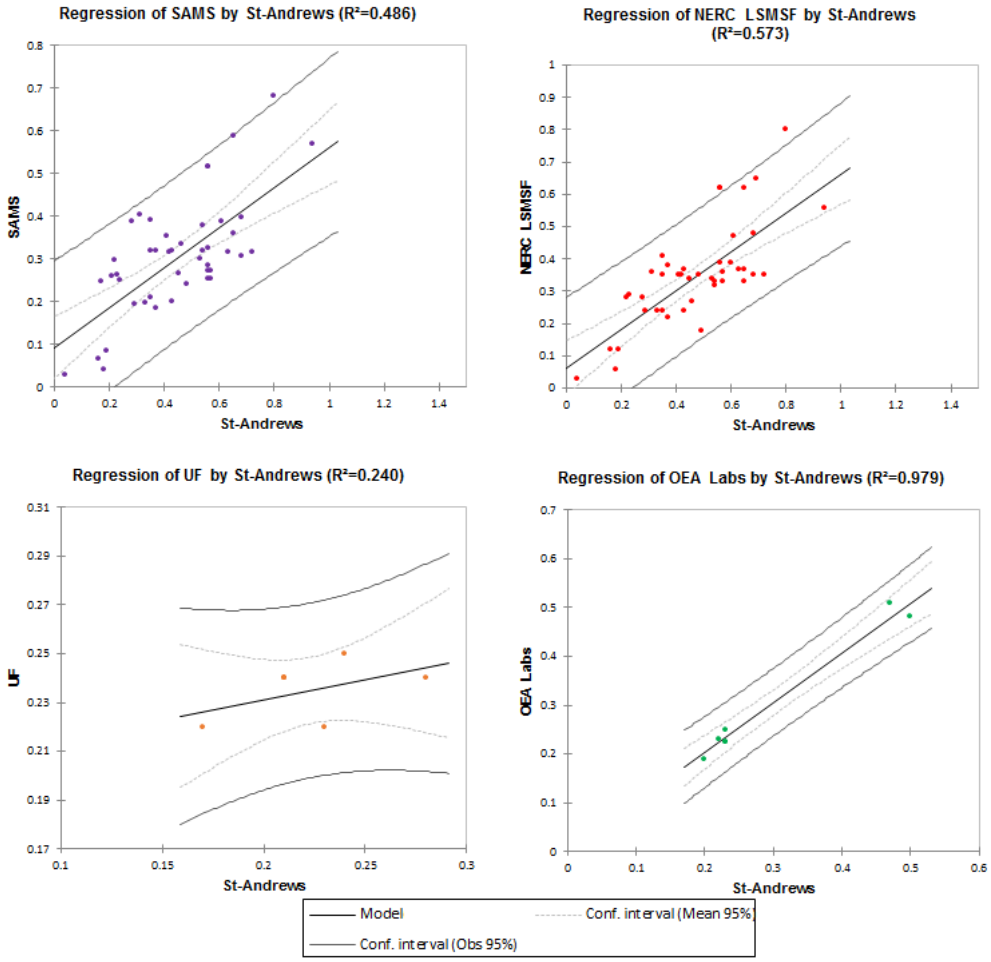

Figure 2.8. Comparison of nitrogen (N) measurements of marine sediment samples made at St-Andrews to the other labs.

When compared the OC data produced at the four external labs compares favourably to that of produced at St-Andrews (Fig.2.7). Both the data produced at SAMS and the NERC LSMSF are statistically similar to the data produced at St-Andrews (Table 2.1). The data produced by UF and OEA labs shows the greatest variation in comparison to St-Andrews but this is likely a product of the smaller sample set used for both these comparisons.

	SAMS	NERC LSMSF	UF	OEA Labs
Similarity	0.946	0.996	0.917	0.803

Table 2.1 Statistical analysis (Similarity) comparing the OC data produced at St-Andrews to that of the other four laboratories marine sediment samples.

	SAMS	NERC LSMSF	UF	OEA Labs
R^2	0.896	0.863	0.841	0.645
Adjusted R^2	0.893	0.859	0.801	0.557
P-Value	0.1140.140	0.1510.257	0.3180.013	0.7100.001

Table 2.2 Statistical analysis (Goodness of fit) comparing the OC data produced at St-Andrews to that of the other four laboratories marine sediment samples.

The N data varies more than OC between the four laboratories (Fig.2.7) though broadly the % N content of the marine sediments measured at the four laboratories are comparable with the St-Andrews data. Statistically the data produced at the NERC LSMSF and OEA Labs shows the greatest level of statistical similarity (Table. 2.3) with the data produced at UF having the weakest relationship (Table.2.4) likely due to sample preparation method. The samples analysed at UF were exposed to concentrated (~ 37 %) HCL acid through the acid fumigation (Harris et al., 2001) technique of carbonate removal; the other laboratories used the direct acidification method (Verardo et al., 1990, Nieuwenhuize et al., 1994) where weak (10 %) HCL is directly added to the sample. The results suggest that the difference in preparation method does not impact the quantification of OC but the N content can be unduly impacted.

	SAMS	NERC LSMSF	UF	OEA Labs
Similarity	0.697	0.757	0.489	0.989

Table 2.3. Statistical analysis (Similarity) comparing the N data produced at St-Andrews to that of the other four laboratories marine sediment samples.

	SAMS	NERC LSMSF	UF	OEA Labs
R^2	0.896	0.863	0.841	0.645
Adjusted R^2	0.893	0.859	0.801	0.557
P-Value	0.1140.140	0.1510.257	0.3180.013	0.7100.001

Table 2.4. Statistical analysis (Goodness of fit) comparing the N data produced at St-Andrews to that of the other four laboratories marine sediment samples.

In addition to the marine sediment samples 16 terrestrial samples were also analysed (Fig.2.8); unlike the sediment samples no preparation was required (i.e. addition of acid). Statistically both the OC and N data from both laboratories show a strong similarity (Table 2.5) and are strongly correlated (Table 2.6). The N data produced by both laboratories is strongly correlated more so than previous comparison this is likely due to the lack of acid treatment.

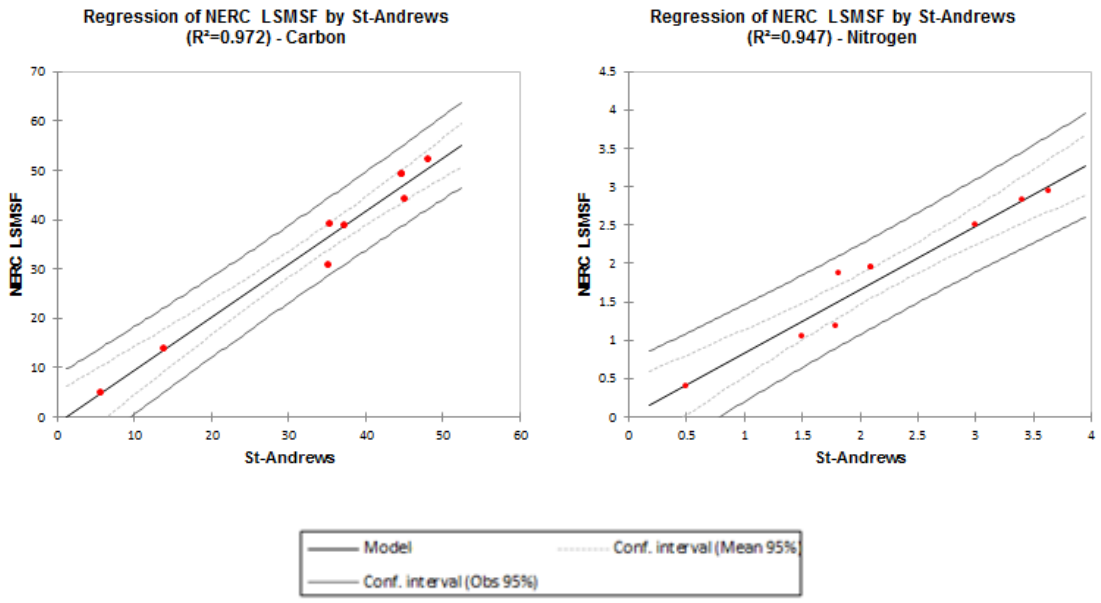

Figure 2.9. Comparison of organic carbon (OC) and nitrogen (N) measurements made at St-Andrews to the other labs.

	OC	N
NERC LSMSF	0.986	0.973

Table 2.5. Statistical analysis (Similarity) comparing the OC and N data produced at St-Andrews to that of the other four laboratories for terrestrial organic materials.

	OC	N
R^2	0.972	0.947
Adjusted R^2	0.968	0.938
P-Values	0.0469.110	0.0890.051

Table 2.6. Statistical analysis (Goodness of fit) comparing the OC and N data produced at St-Andrews to that of the other four laboratories terrestrial organic materials.

The results of the inter-laboratory comparison indicate that the data produced in the different laboratories is good quality and largely reproducible in the different settings and using different analytical equipment. The exception is the N data produced at UF with samples exposed to concentrated acid. This data supports the idea that exposure to concentrated acid can impact the measurement of N as previously discussed in Section 2.4.1.1. To assure this did not impact the quality of this study all samples analysed using this preparation method at UF where reanalysed at the University of St-Andrews using the direct acidification method (Verardo et al., 1990, Nieuwenhuize et al., 1994). Further statistical data from the inter-comparison exercise can be found in Appendix A.

2.4.2 Stable Isotopes ($\delta^{13}C$, $\delta^{15}N$, $\delta^{18}O$)

Stable isotopes compliments bulk elemental analysis and is widely used in the fields of ecology, geochemistry, limnology and oceanography, providing information about the sources and cycling of bulk organic matter pools (dissolved, particulate, and sedimentary). Stable isotope studies in marine geochemistry have incorporated the use of a variety of light elements, including H, C, N, O and S. The use of stable isotopes has contributed to insight insights about food web structure and organic matter sources over contemporary, historical, and geological timescales.

2.4.2.1 Isotope Theory

The main elements of interest in this study are C and N in the organic matter and O in the carbonate of shell material. Each of these contains isotopes which are forms of the same element differing only by mass due to having a different number of neutrons (Fig.2.10). C has two stable isotopes (^{12}C and ^{13}C), similarly N has two stable isotopes (^{14}N and ^{15}N) and O has three stable isotopes (^{16}O, ^{17}O and ^{18}O). The stable isotopes of an element have almost identical chemical properties. Yet the differences in masses between them can cause chemical, biological and physical processes to discriminate against one of them thereby altering the proportions present.

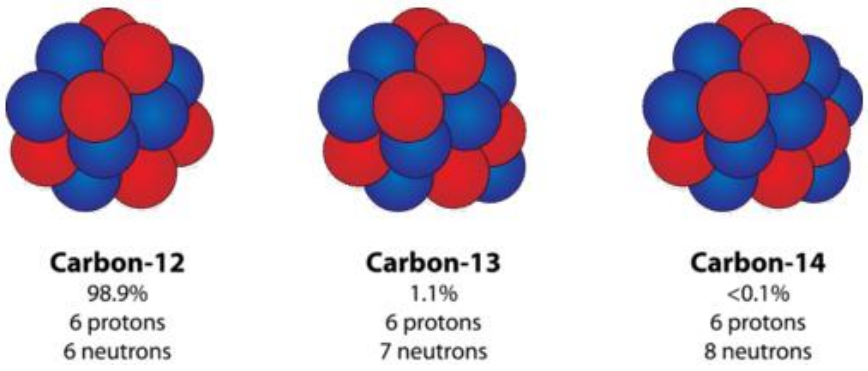

Figure 2.10. Nuclei of the three isotopes of carbon. Almost 99% of naturally occurring carbon is ^{12}C, whose nucleus consists of six protons and six neutrons. ^{13}C and ^{14}C, with seven or eight neutrons, respectively and have a much lower nuclei abundance. (Source: *chem.libretexts.org*).

2.4.2.2 Stable Isotope Notation

Stable isotopes are reported as a ratio, relative to a standard. The ratio (*R*) of carbon, nitrogen and oxygen isotopes are measured as the abundance of the least abundant (i.e. ^{13}C) isotope to that of the most abundant isotope (i.e. ^{12}C) and reported relative to the isotope ratio of a standard as follows (Farquhar et al., 1982):

$$\delta^{a}E = \left(\frac{Rsample}{Rstandard} - 1\right) \times 1000$$

Where E is the element, a is the atomic mass of its heaviest isotope. The δ value is multiplied by 1000 and reported in parts per thousand (‰ or per mil).

2.4.2.3 Measurement of Stable Isotopes

The most common method to measure stable isotopes is isotope ratio mass spectrometry (IRMS). A mass spectrometer is an instrument for separation of molecules based upon their mass-to-charge ratio. In IRMS the mass spectrometer used separates isotopes of different mass within a magnetic field and precisely measures the ratio of two, or more, isotopes. Depending on the sample matrix there are multiple routes for the sample to be introduced to the IRMS, in this study to determine $\delta^{13}C$ and $\delta^{15}N$ in organic matter the main route is through a coupled EA (Section 2.4.1), where a sample is combusted in a EA with the gases being channelled to an IRMS after the quantification of the element in the TCD. The N_2 and CO_2 are separated by a packed column gas chromatograph held at an isothermal temperature. The resultant chromatographic peaks sequentially enter the ion source of the IRMS where they are ionised and accelerated. Gases of different mass are separated in a magnetic field and simultaneously measured by a Faraday cup universal collector array. For N_2, masses 28, 29 and 30 are monitored and for CO_2, masses 44, 45 and 46 (Fig.2.11).

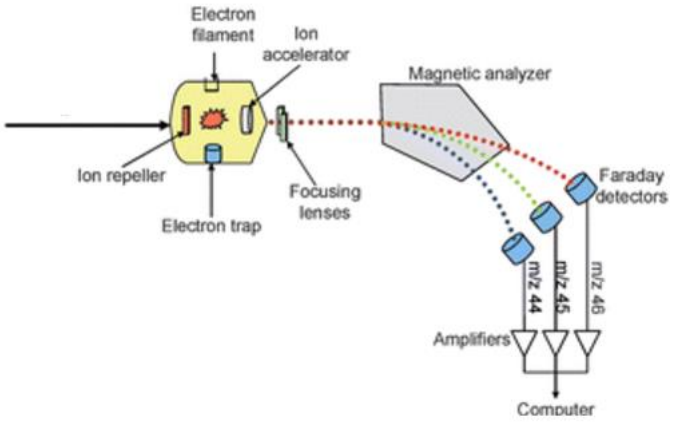

Figure 2.11. Schematic of a standard IRMS with the arrow entering the system representing EA and gas bench input (Muccio and Jackson, 1999).

For the determination of $\delta^{18}O$ in carbonate (i.e. foraminifera), the bulk material must first be converted to pure CO to permit analysis by IRMS. In this technique, samples are placed in clean glass test tubes. They are then exposed to phosphoric acid where the carbonate is converted to CO in the presence of glassy carbon. The gases are extracted from the test tube using an automated Gas Bench, the gases are passed through magnesium perchlorate trap where water is removed, while any traces of CO_2 is removed by a Carbon absorption trap. CO is separated by a packed column gas chromatograph held at an isothermal temperature. The resultant chromatographic peak enters the IRMS where it is ionised and accelerated. Gas of different mass are separated in a magnetic field then simultaneously measured on a Faraday cup universal collector array. For CO, masses 28, 29 and 30 are monitored (Fig.2.11). The data produced by this methodology is reported as with the δ notation which represents the observed isotopic ratio relative to a standard (Table 2.7)

Element	Standard	Abbreviation
C	Vienna PDB	VPDB
N	Atmospheric N2	AIR
O	Vienna Standard Mean Ocean Water	VSMOW
	Vienna PDB	VPDB

Table 2.7. Stable isotope standards

2.5 Organic Geochemistry

The complex nature of organic matter in the marine environment and the limitations of bulk measurements results in the need for another method to discriminate between organic matter sources. Chemical biomarkers have become widespread in limnology and oceanography due to the complexity and variety of organic matter source in the fresh and marine aquatic environments. Biomarkers are defined as complex organic compounds composed of C, H and other elements, which occur in sediments, rocks, and crude oils, and show little to no change in their chemical structure from their precursor molecules that existed in living organisms (Hunt et al., 1996; Peters et al., 2005; Gaines et al., 2009). Biomarkers can provide insights about present and past aspects of Earth history and are especially suited to developing a better understanding of the biogeochemical processes within aquatic environments, including riverine, estuarine, and oceanic ecosystems (Bianchi and Canuel, 2011).

2.5.1 Lipids: Hydrocarbons

Sources of natural hydrocarbons delivered to marine environments include autochthonous sources such as algae and bacteria as well as allochthonous inputs from terrestrial plants (Cranwell, 1982; Meyers and Ishiwatari, 1993; Meyers, 1997). A summary of hydrocarbon biomarkers representing these sources is provided in Table 2.8.

Compound of Proxy	Source	Reference
n-Alkanes with C_{15},C_{17}or C_{19}	Algae	Cranwell (1982)
n-Alkanes with C_{21}, C_{23} or C_{25}	Aqautic macrophytes	Ficken et al. (2000)
Long-Chain *n*-Alkanes	Terrestrial plants	Eglinton and Hamilton (1967)
n-Alkanes C_{20}-C_{40}	Petroleum	Peters et al. (2005)
Unresolved complex mixture	Petroleum	Peters et al. (2005)
IP25	Sea ice diatoms	Belt et al. (2007)
P_{aq}	Aquatic macrophytes	Ficken et al. (2000)
TAR_{HC}	Terrestrial to Aquatic Ratio	Meyers (1997)
Heneidosahexaene	Diatoms	Lee and Loeblich (1971)
Highly Branched isoprenoids	Plankton	Freeman et al. (1994)
Very Long Chain alkenes	Microalgae	Volkman (2005)
Pristane	Zooplankton	Blumer et al. (1964)
Phytane	Methanogenic bacteria	Risatti et al. (1984)
Diploptene	Methanogens	Freeman et al. (1994)
Pentamethyleicosane (PME)	Methanogens	Tornabene and Langworthy (1979)
Lycopane	Photoautotrphic organisms	Tornabene and Langworthy (1979)
C_{30} isoprenoids	Methanogens	Volkman and Maxwell (1986)
Hop-9(11)-ene	Photosynthetic bacterium	Howard (1980)

Table 2.8. Examples of Hydrocarbon biomarkers (adapted from Bianchi and Canuel, 2011)

Hydrocarbons biomarkers (Fig.2.12) from bacterial sources occur in the form of open chains, generally with carbon chain lengths between C_{10} and C_{30}. Phytoplankton, are usually characterised by low concentrations of hydrocarbons (3–5% of the lipid fraction). The hydrocarbon fraction of phytoplankton is generally dominated by saturated and unsaturated hydrocarbons having both straight and branched chains. Marine algae typically synthesize *n*-alkanes with chain lengths ranging from C_{14} to C_{32}. The ratio of even to odd numbered homologues is frequently close to one in marine algae (Bianchi and Canuel, 2011).

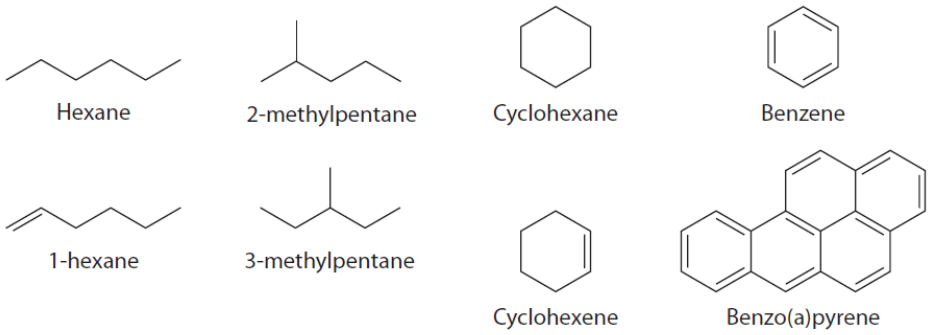

Figure 2.12. Examples of different hydrocarbon structures (Bianchi and Canuel, 2011)

In contrast terrestrial vascular plants are dominated by long-chain *n*-alkanes in the range C_{23} to C_{35}. In vascular plants, the distribution of *n*-alkanes is usually dominated by odd numbered homologues with C_{27}, C_{29}, and C_{31} as the dominant compounds. The carbon number at which the *n*-alkane distribution maximizes (C_{max}) can sometimes be a diagnostic tracer for different plant sources (Rogge et al., 2007). Submerged macrophytes often have biomarker compositions which lie between algae and terrestrial plants. Aquatic macrophytes are generally characterised by mid-chain-length *n*-alkanes with odd-numbered homologues. Previous studies have shown that submerged and floating aquatic plants have *n*-alkane distributions that maximize at C_{21}, $C_{23,}$ or C_{25} (Cranwell, 1984; Viso et al., 1993; Ficken et al., 2000).

2.5.2 Lipid: Fatty Acids

Fatty acids are classes of lipid biomarker and this class of biomarkers has been applied to a wide variety of environmental studies, including characterisation of organic matter sources in marine systems, analysis of the nutritional value of organic matter, trophic studies, and microbial ecology. Characteristics (Fig.2.13) of fatty acids that contribute to

their usefulness as biomarkers include (**i**) their unique distributions in various organisms (archaebacteria, eubacteria, microalgae, higher plants), (**ii**) distinct structural features indicative of their sources, and (**iii**) the fact that individual compounds and fatty acid classes exhibit different reactivity (Bianchi and Canuel 2011). This range in reactivity largely derives from variations in functional group composition and carbon chain length (Canuel and Martens, 1996; Sun et al., 1997). Most fatty acids occur in esterified forms in neutral and polar lipids.

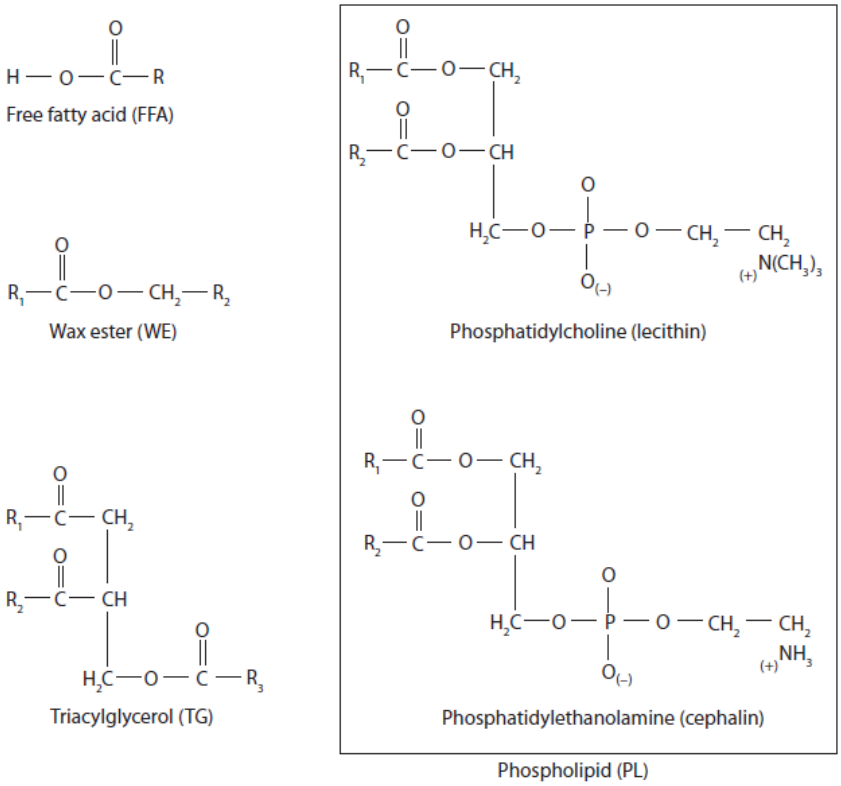

Figure 2.13. Example of free fatty acids and lipid subclasses composed of fatty acids (Bianchi and Canuel 2011).

Fatty acids are among the most versatile classes of lipid biomarker compounds and have been used widely to trace sources of organic matter in aquatic environments. This is because individual compounds, and groups of compounds, can be attributed to microalgal, bacterial, fungal, marine faunal, and higher plant sources (Table 2.9), providing a tool to identify sources of organic matter (Volkman et al., 1998). While fatty acids can provide qualitative information about the dominant sources of organic matter, it is difficult to extrapolate quantitative contributions of organic matter from specific sources because lipid content varies with tissue type, changes in life cycle, and

environmental conditions. Higher plants and microbes, for example, may change the proportion of fatty acids in response to changes in temperature (Yano et al., 1997).

Fatty Acid Feature	Source
Short chain (14:0, 16:0, 18:0)	Non-specific (marine and terrestrial; bacteria, plants and animals)
Long Chain (24:0, 26:0, 28:0)	Higher plants (vascular)
Monounsaturated Short Chain (16:1 and 18:1)	Non-specific (some isomers may be source specific)
Polyunsaturated	Marine and aquatic phytoplankton zooplankton and fish.
Methylbranched Chains (iso and anteiso)	Bacteria
Internally Branched and cycloalkyl	Fungi and bacteria (Eubacteria)
Hydroxy	Mostly Bacteria
Diacids	Higher plants, Bacterial oxidation of other compounds.

Table 2.9 Structural features of fatty acids and their use to identify organic matter source (adapted form Bianchi and Canuel 2011).

2.5.3 BIT Index

Glycerol dialkyl glycerol tetraether (GDGT) also provide useful biomarkers for examining contributions of terrigenous carbon to bulk organic matter. The branched and isoprenoid tetraether (BIT) index (the ratio of marine and terrestrial GDGT membrane lipids) has been shown to correlate with the amount of fluvial organic carbon buried in marine sediments (e.g., Hopmans et al., 2004; Herfort et al., 2006; Weijers et al., 2006). When the BIT index equals zero, it signifies the absence of branched GDGTs (or absence of terrestrial material). In contrast, a BIT index equal to one indicates the absence of crenarchaeol (absence of marine material).

In a recent study conducted off the coast of Washington State (USA), the BIT index was compared to other measures of terrigenous organic matter such as lignin phenols and $\delta^{13}C$ (Walsh et al., 2008). Surprisingly, the BIT index did not correlate well with either $\delta^{13}C$ or lignin phenols and suggested much lower contributions from terrigenous sources of organic matter. The authors concluded that the discrepancy may be due to differences

in the sources of terrigenous organic matter, since the BIT index likely reflects contributions from soils and peats, while lignin phenols trace inputs from vascular plants. As a result, care must be used in interpreting the BIT index, particularly in environments where soils and peats, are not the dominant sources of terrigenous organic matter. Other more recent studies also supported this idea of BIT being used more ideally as a biomarker of soils (Belicka and Harvey, 2009; Weijers et al., 2009; Smith et al., 2010).

2.5.4 Analysis of Lipids

Fatty acids are typically extracted from a sample matrix (e.g., particulate matter, sediment,) using a combination of organic solvents, with a portion of the solvent mixture including a polar solvent (e.g., chloroform and methanol, 2:1, v:v) (Bligh and Dyer, 1959; Smedes and Askland, 1999). A variety of extraction methods can be used, including soxhlet extraction, sonication, microwave extraction, or accelerated solvent extraction (ASE) (e.g., MacNaughton et al., 1997; Poerschmann and Carlson, 2006). Often, total fatty acids are analyzed following saponification (base hydrolysis) of the lipid extract. However, additional information can be gained if fatty acids with specific lipid subclasses are separated chromatographically (Fig. 2.14). In this case, the lipid extract is first separated into compound classes using adsorptive chromatography and the lipid subclasses of interest are then saponified (Muri and Wakeham, 2006; Wakeham et al., 2006).

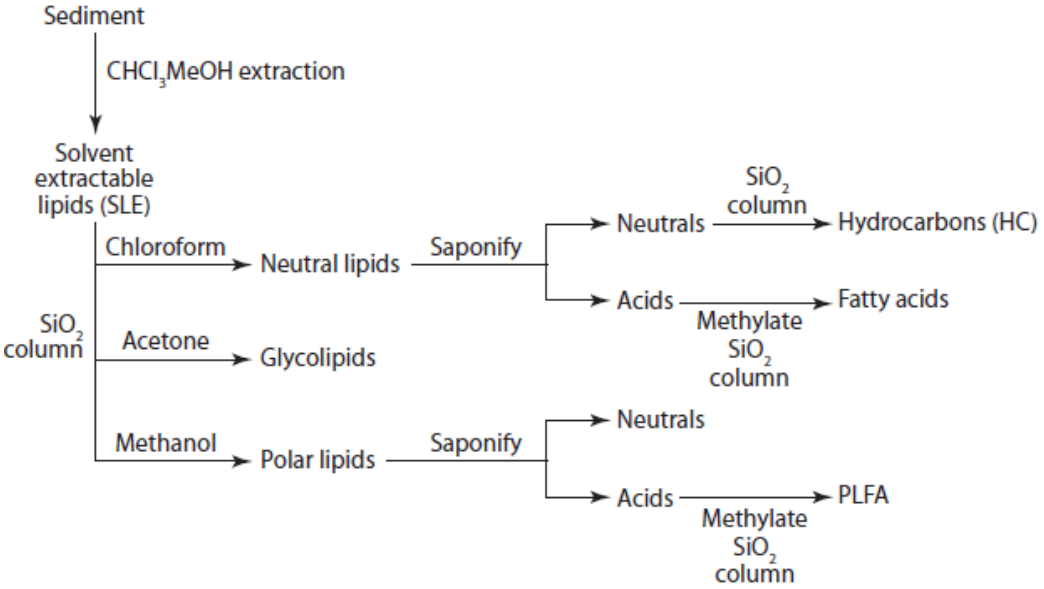

Figure 2.14. Schematic showing separation of different lipid classes by polarity and subsequent saponification and methylation of neutral lipids and carboxylic acids. (Wakeham et al., 2006.)

Following saponification, fatty acids are generally converted to methyl *esters* for subsequent analysis by gas chromatography. This can be achieved through a variety of methods, including in methanol (Grob, 1977; Metcalfe et al., 1966), Fatty acid methyl esters (FAME) are typically analysed by gas chromatography–flame ionization detection (GC-FID) using a polar column (Fig.2.15).

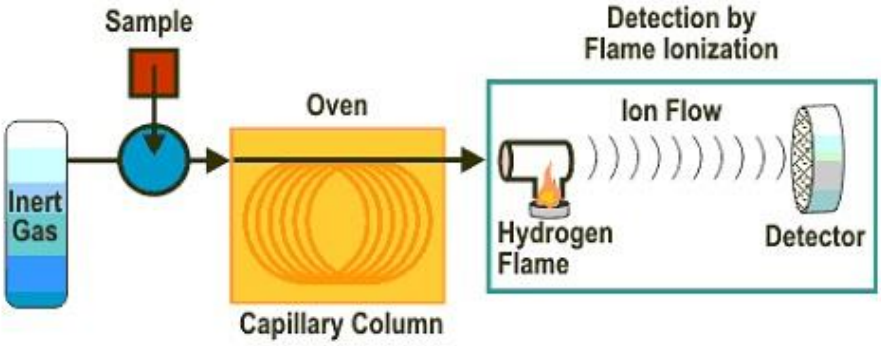

Figure 2.15. Schematic of the standard operation of GC-FID (source: *chromatographyscience.co.uk*)

2.6 Inorganic Geochemistry

Alongside the bulk and organic geochemistry the inorganic characteristic of sediments can provided valuable information on past environments and present day processes. This study utilises destructive Inductively Coupled Plasma Mass Spectrometry (ICP-MS) techniques and non-destructive ITRAX core scanning to better understand the past environment and the anthropogenic pressure on the environment.

2.6.1 ICP-MS

ICP-MS is a destructive method which allows the determination of elements with atomic mass ranges 7 to 250 (Fig.2.16) from a wide variety of substances. ICP-MS combines a high-temperature Inductively Coupled Plasma source with a mass spectrometer. The ICP source converts the atoms of the elements in the sample to ions. These ions are then separated and detected by the mass spectrometer. Unlike older method (i.e. atomic absorption spectroscopy), which can only measure a single element at a time, ICP-MS has the ability to scan for all elements simultaneously.

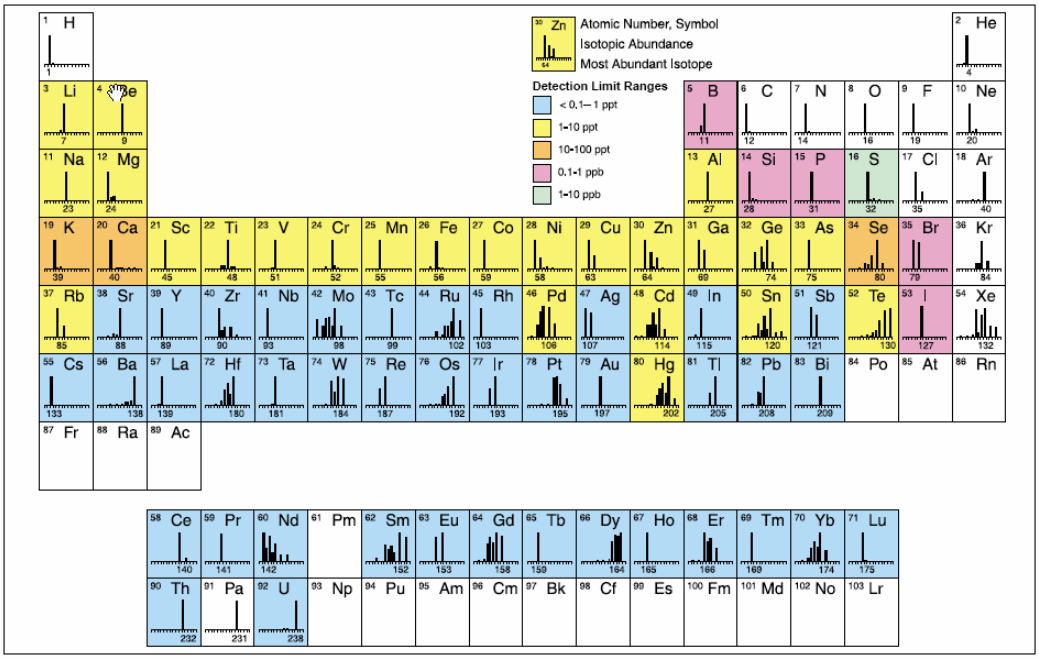

Figure 2.16 Approximate detection capabilities of the ELAN 6000/6100 quadrupole ICP-MS. (Source: *PerkinElmer, Inc.)*

Samples are typically introduced into the ICP-MS as an aerosol, either by aspirating a liquid or dissolved solid sample (Nitric acid commonly used to dissolve solids) into a nebuliser or using a laser to directly convert solid samples into an aerosol (Laser Ablation-ICP-MS). Once aerosolised the sample are introduced into the ICP torch, where the elements in the aerosol are converted ionized gas. Once the elements in the sample are converted into ions, they are then brought into the mass spectrometer via the interface cones (Fig.2.17) allowing the quantification of the elements present in the sample.

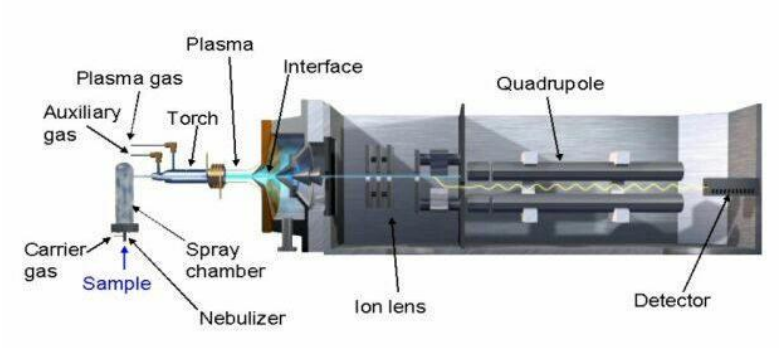

Figure 2.17 Simplified schematic of an Quadrupole ICP-MS (Source: PerkinElmer, Inc.)

2.6.2 ITRAX Core Scanning

ITRAX core scanning collects high resolution (resolution > 100 µm) elemental data from split sediment core sections. ITRAX core scanners utilise Energy Dispersive X-ray Fluorescence techniques (ED-XRF) an non-destructive method to collect a range of elemental data (Si-U); this method has many advantage over the traditional Wavelength Dispersive X-ray Fluorescence (WD-XRF) outlined in Table 2.10.

	ITRAX (ED-XRF)	**WD-XRF**
Optical image and high-resolution X-radiograph provided	Yes	No
Sample preparation and preparation requirement	Non-destructive	Semi-destructive (pellets) or destructive beads, requires 3 g or more of sample
Practical scanning resolution	> 100 µm	5000 µm
Time to acquire major and minor element data from a 1 m long core 500 µm scanning increments	16 hours	10 working days
Normal detection limits (100 s)	9000 ppm Si 60 ppm Ti 5 ppm Sr	50 ppm Si 10 ppm Ti 0.5 ppm Sr

Table 2.10. Comparison between ITRAX and conventional WD-XRF

ITRAX scanning does have advantages over traditional WD-XRF but there are disadvantages. The technique has poorer detection limits so measuring light elements (i.e. Al) and elements of low abundance can be difficult (Rothwell and Croudace.2015). It is also crucial to remember that the technique is semi-quantitative, there are statistical techniques to ground-truth the data with selective discrete sampling (Weltje and Tjallingii. 2008) but this only further constrains the semi-quantitative nature of ITRAX data.

2.6.2.1 Operation of the ITRAX

The ITRAX scanner firstly scans the core to map the surface topography using a laser rangefinder this allows the X-ray detector to be kept at a constant distance from the core surface. A continuous-strip X-radiograph, can be collected immediately before to the

XRF scan using a CCD line camera. The count time for each measurement is then defined (normally 60 to 100 seconds). The X-ray beam used to irradiate the core is generated using a 3kW Mo X-ray tube and is focused through a flat wave guide. The recorded spectra are deconvolved to construct profiles of peak area integrals for individual elements and Rayleigh and Compton scattering peaks with the element peak area reflecting the element abundances.

2.7 Geochronology

The requirements for this study is to chronological constrain Holocene marine sediment records. Thus radiometric dating techniques have been utilised as they have the ability to date material from the present day back 50,000 years. The methods chosen are radiocarbon dating (^{14}C), Lead-210 (^{210}Pb) and Cesium-137 (^{137}Cs) as they have the ability to date material and different resolutions over the Holocene.

2.7.1 Radiocarbon (^{14}C)

Radiocarbon (^{14}C) produced by the reaction of cosmic rays with atmospheric atoms such as N_2, O_2, and others to produce broken pieces of nuclei, which are called spallation products (Suess, 1958, 1968) (Fig.2.17). Some of these spallation products are neutrons that can interact with atmospheric atoms to produce additional products, which include ^{14}C and other radionuclides (^{3}H, ^{10}Be, ^{26}Al, ^{36}Cl, ^{39}Ar, and ^{81}Kr) (Broecker and Peng, 1982).

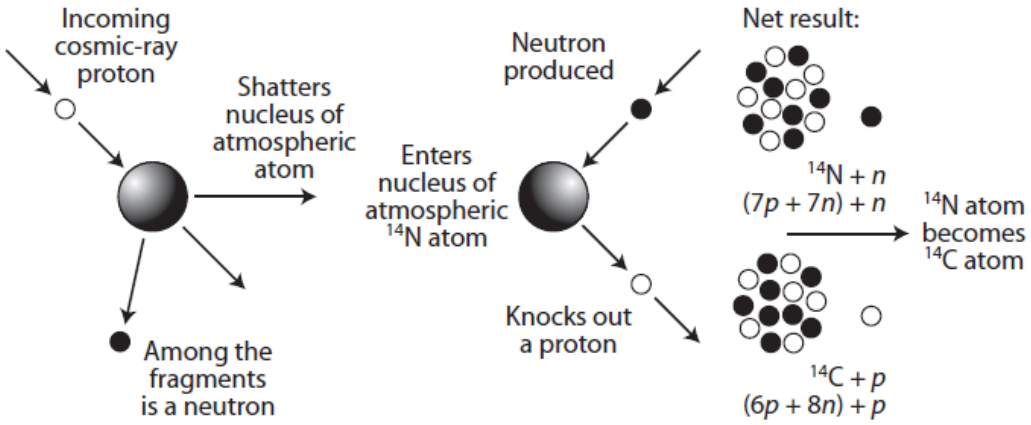

Figure 2.17 The formation of 14C in the atmosphere. (Adapted from Broecker and Peng, 1982.)

The ^{14}C atoms formed in the atmosphere become oxidized and form $^{14}CO_2$, which is mixed throughout the atmosphere (Libby, 1952). This ^{14}C becomes incorporated into other reservoirs, such as the biosphere, as plants fix carbon during the process of photosynthesis. Living plants and animals in the biosphere contain a constant level of ^{14}C, but, when they die there is no further exchange with the atmosphere and the activity of ^{14}C decreases with a half-life of 5730 ± 40 years. This provides the basis for establishing the age of fossil remains.

2.7.1.1 Measuring ^{14}C

Three principal techniques have been used to measure ^{14}C content of a given sample - gas proportional counting, liquid scintillation counting, and accelerator mass spectrometry (AMS). Gas proportional counting is a conventional radiometric dating technique that counts the beta particles emitted by a given sample. Beta (β) particles are products of ^{14}C decay. In this method, the C sample must first be converted to CO_2 before measurement. Liquid scintillation counting is another radiocarbon dating technique from the 1960's. In this method, the sample is in liquid form and a scintillator is added. This scintillator produces a flash of light when it interacts with a β particle. A vial with a sample is passed between two photomultipliers, and when both devices register the flash of light a count is made.

AMS is the modern and most commonly used ^{14}C measurement method (Fig.2.18). In this method, the ^{14}C content is directly measured relative to the ^{12}C and ^{13}C present. The method counts the number of C atoms present in the sample and the proportion of the isotopes. The greatest advantage that AMS ^{14}C analysis has over the older methods is small sample size. AMS need as little as 20 mg and as high as 500 mg for certain samples whereas conventional methods need at least 10 g in samples like wood and charcoal and as much as 100 g and sediments. Additionally; AMS measurements usually achieve higher precision and lower backgrounds than the traditional radiometric dating methods.

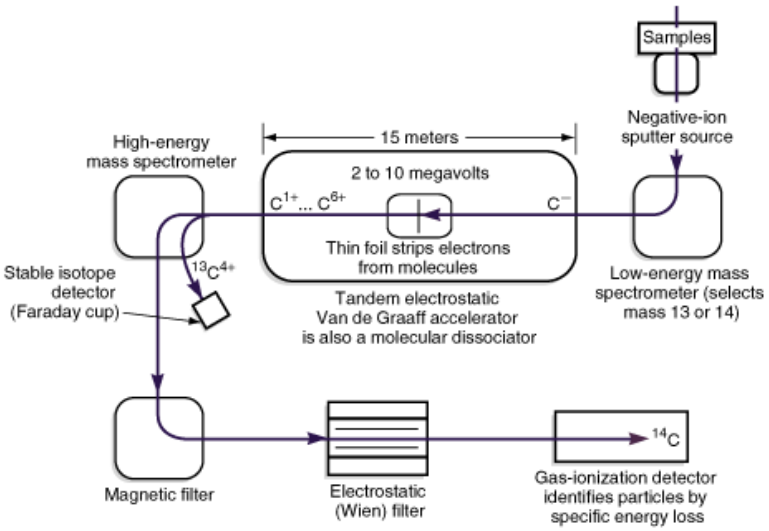

Figure 2.18. Schematic of the standard configuration of a conventional AMS (Source: *Beta Analytical*)

The principal modern standard used for ^{14}C measurements is Oxalic Acid I and II obtained from the National Institute of Standards and Technology (NIST). This oxalic acid came from sugar beets in 1955 and 1977 respectively. Around 95% of the ^{14}C activity of Oxalic Acid I is equal to the measured radiocarbon activity of the absolute radiocarbon standard— wood from 1890 unaffected by fossil fuels.

2.7.1.2 Radiocarbon Dating

Radiocarbon dating is one of the most widely used dating methods in archaeology and environmental science. It can be applied to most organic materials and is capable of dating material from between 1950 AD back to about 50,000 years ago. Nuclear weapons testing in the 1950's and 60's irreversible altered the atmospheric concentration of ^{14}C which has meant that dating material using the radiocarbon method beyond this time period is not possible, therefore 1950 can be referred to as present day and is a marker for the modern period.

Radiocarbon dating uses the known half-life (5730 ± 40 years) of ^{14}C combined with the knowledge that once an organism dies the C within is no longer replaced. Using this relationship it is possible to quantify the point at which that organism died in time which provides a chronological constraint to a stratigraphy. There are two sets of complications with this approach, firstly the ^{14}C concentration of the atmosphere has not always been constant; in reality it has varied significantly in the past. This complication can be overcome with by calibration of the radiocarbon dates against material of known age (tree rings). Calibration curves are developed from measurements on tree rings, speleothems, marine corals and samples from sedimentary records with independent dating are all compiled into calibration curves (Reimer et al., 2013, Reimer. 2013) by the IntCal group. Using these calibration curves you can match the ^{14}C content of a sample to the curve and calculated the calibrated age of the sample. Figure 2.19 illustrates how radiocarbon measurements are calibrated, the grey curve represents ^{14}C content of a sample, the blue line represents the ^{14}C calibration curve (Reimer. 2013) created from hundreds of samples with a known age that have been measured for ^{14}C content through matching the ^{14}C content of the sample to the calibration curve we can extrapolate the age of the sample.

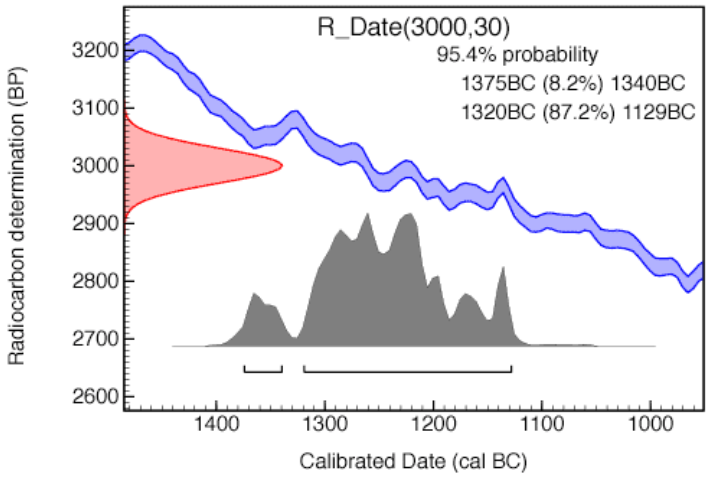

Figure 2.19. Example plot shows how the radiocarbon measurement 3000 ± 30BP would be calibrated (Source: *c14.arch.ox.ac.uk*)

Radiocarbon dating is further complicated when the C within a sample has not taken a straightforward route from the atmosphere to the organism. This commonly come in two forms – contamination and a reservoir effect. Contamination where material from the surrounding environment (i.e. organic sediment) becomes incorporated within the sample resulting in a mixture of C with a different ^{14}C contents; this is commonly not a problem if the chemical pre-treatment has been carried out correctly. The reservoir effects occur when reaches an organism not directly from the atmosphere (i.e. the ocean). As the ^{14}C composition of the oceans differs from that of the atmosphere, this can lead to incorrect dating. In recent years calibration curves (Reimer. 2013) have been developed specifically for the marine environment to overcome this issue at a global scale but local/regional corrections are still required and in many area this is still lacking.

2.7.2 Radiometric Dating (^{210}Pb, ^{137}Cs)

Radiometric dating utilises short lived radioactive isotopes (^{210}Pb, ^{7}Be, ^{137}Cs) to measure sedimentary dynamics over the last 100 to 150 years (Fig.2.20). The technique uses the same methodological approach as radiocarbon dating (Section 2.7.1.2), simply each isotope has known half-life and by measuring the concentration of that isotope at a known depth allows the age of that depth to be calculated. The most common isotopes used in the marine sediment studies are ^{210}Pb and ^{137}Cs.

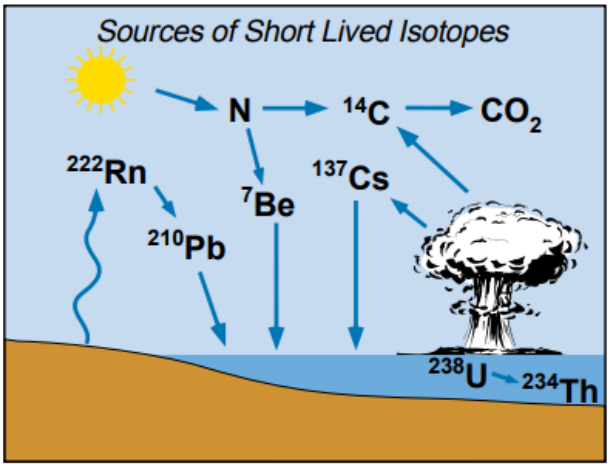

Figure 2.20. Sources of short lived radioactive isotopes in the environment (source: *USGS*)

2.7.2.1 Lead-210 (^{210}Pb)

^{210}Pb has a half-life of 22.3 years and is a member of the ^{238}U series. ^{210}Pb forms from the decay of its intermediate parent, ^{222}Rn, which rapidly decays to form ^{210}Pb. This isotope has a residence time in the atmosphere of around 10 days before it is removed by precipitation. The reactive lead is then rapidly adsorbed to and incorporated into the depositing sediment. This flux produces a concentration of "unsupported" ^{210}Pb (lead whose activity in the sediment is higher than that of its radium grandparent, ^{226}Ra). Dates of sediment deposition are calculated by determining the decrease in ^{210}Pb activity at each selected sediment interval; this decrease is a function of time. If the initial concentration of ^{210}Pb is known, or is estimated using ^{7}Be data, then the age of a sediment interval is calculated by the following:

$$T_{age} = \left(\frac{A_{210_{Pb_0}}}{A_{210_{Pb_h}}}\right) \times 1/\lambda$$

Substituting the constants:

$$T_{age} = \left(\frac{A_{210_{Pb_0}}}{A_{210_{Pb_h}}}\right) \times 1/0.03114$$

Where $A_{210_{Pb_0}}$ is the unsupported ^{210}Pb activity in disintegrations per minute at time zero (the present), $A_{210_{Pb_0}}$ is the activity in disintegrations per minute at depth h, and λ is the decay constant for ^{210}Pb. An idealised plot of ^{210}Pb activity and depth will be an exponentially decreasing curve approaching the supported value (Figure 2.21)

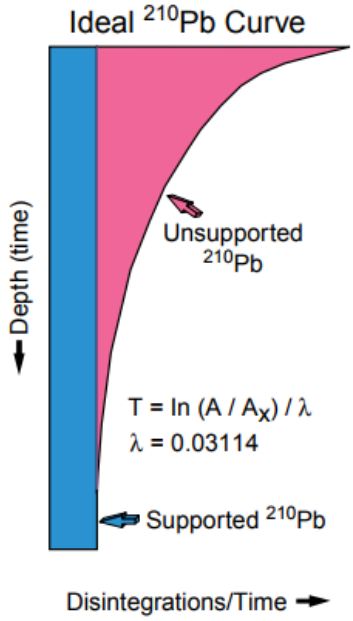

Figure 2.21. Idealised plot of ^{210}Pb activity and depth (source: *USGS*)

2.7.2.2 Cesium-137 (^{137}Cs)

^{137}Cs has a half-life of 30.3 years and is a thermonuclear by-product. Its presence in natural systems is directly related to atmospheric thermonuclear activity. The curve below shows that ^{137}Cs fallout production and deposition began at approximately 1952; deposition peaked during 1963 and 1964. Under ideal conditions the sediment profile should mimic the ^{137}Cs production (Fig.2.22). However, the inability to accurately sample small intervals, and the mixing of the sediment by organisms, often cause deviations from the ideal profile.

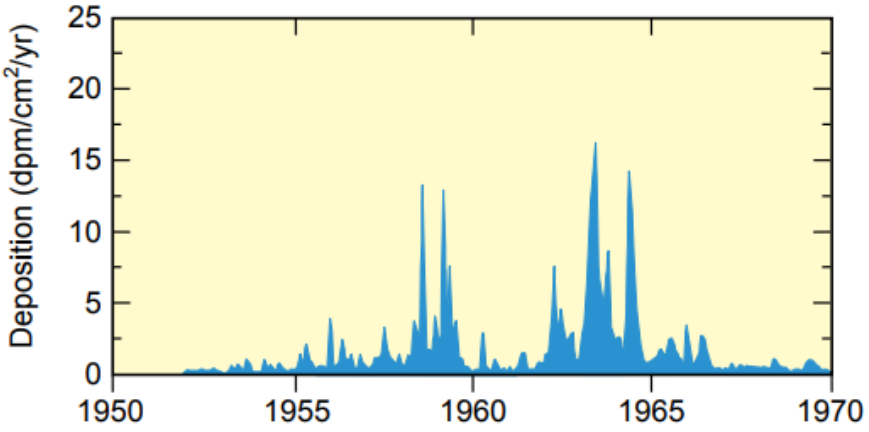

Figure 2.22.. ^{137}Cs fallout in the northern hemisphere (source: *USGS*)

2.7.2.3 Measuring ^{210}Pb and ^{137}Cs

Measurement of ^{210}Pb activity within a sample is undertaken using gamma (γ) spectrometry. Gamma spectrometry relies on the measurements of gamma photons emitted by ^{210}Pb, ^{214}Pb and ^{214}Bi isotopes. Analysis of the ^{210}Pb gamma spectrum data allows the calculation of total activity of ^{210}Pb, while the activity of ^{214}Pb and ^{214}Bi combines to allow the calculation of autigenic ^{210}Pb activity. Small masses of samples and the low energy nature of gamma photons emitted by ^{210}Pb require the utilisation of a thin-wall well type germanium detector. The detector used is 45 mm high and 46 mm in diameter; the well is Ø = 8 x 35.5 mm. The detector's well contains a portion of sediment of precisely measured mass (approx. 1.2 g). Each sample is placed in the detector and measured for not less than 24 hours. The ^{210}Pb, ^{214}Pb and ^{214}Bi activities were calculated by analyses of appropriate gamma spectrum. Similarly both ^{134}Cs and ^{137}Cs isotopes release gamma particles as the decay therefore gamma spectrometry

again is the preferred analytical method. The methodology is the same as measuring ^{210}Pb with the exception that ^{134}Cs and ^{137}Cs activity is extracted from the outputted gamma spectrum. Validation of results is independently verified using a numerical model of lead and Cesium photon behaviour (Appleby and Oldfield. 1978).

This method does not come without issues, the first of which is bioturbation. Since the method determines the age from direct measurements of the sediment any disturbance can be problematic. Therefore caution is required when interpreting the results, within the literature it is widely recognised that it is highly likely that some level of bioturbation will have taken place which can be accounted for through the use of appropriate metrics (Szmytkiewicz and Zalewska., 2013, Carvalho et al. 2011). Yet recently there have been calls to abandon this method (Middleburg. 2017) as it is deemed to be impossible to determine the magnitude of disturbance caused by bioturbation, though this is extreme it further highlights the need to be cautious in interpreting radiometric dating results. The second issue is one that cannot be avoided; these short lived radioactive isotopes have far shorter half-life's than ^{14}C. Lead^{210} has a half-life of 22.3 years which allows chronologies to be created back to approximately 1880 AD.

Chapter 3

A Sedimentary Carbon Inventory for a Scottish Fjord: An Integrated Geochemical and Geophysical Approach

Based Upon: Smeaton, C., Austin, W. E. N., Davies, A. L., Baltzer, A., Abell, R. E., and Howe, J. A.: Substantial stores of sedimentary carbon held in mid-latitude fjords, *Biogeosciences*, 13, 5771-5787, doi:10.5194/bg-13-5771-2016, 2016.

Author Contributions: Craig Smeaton and William E. N. Austin conceived the research and wrote the manuscript, to which all co-authors contributed data or provided input. Craig Smeaton conducted the research as part of his PhD at the University of St. Andrews, supervised by William E. N. Austin, Althea L. Davies and John A. Howe. Craig Smeaton wrote this chapter, expanding on the detail provided by Smeaton et al., 2016.

3.1 Introduction

The rising prominence of blue carbon i.e. carbon (C) which is stored in coastal ecosystems, notably, mangroves, tidal marshes, seagrass meadows and their sediments has forced a reassessment of our knowledge of C in the coastal ocean (Nellemann et al., 2009). In recent years there have been a number of reviews highlighting knowledge gaps (Bauer et al., 2013; Cai et al., 2011; Duarte, 2016) and the limited understanding of both the C sources and sinks in the coastal ocean (Bauer et al., 2013). Quantifying the stores of C in the coastal ocean is the first step to a better understanding of coastal carbon dynamics. Global C burial in the coastal zone is estimated in the region of 237.6 Tg yr^{-1} with approximately 126.2 Tg yr^{-1} of C being buried in depositional areas, i.e. estuaries and the shelf (Duarte et al., 2005). However, high levels of uncertainty due to the lack of regional and national coastal sedimentary C inventories means these global estimates cannot be confirmed or further constrained.

One of the rare examples of a national marine C inventory was carried out by Burrows et al. (2014), who produced preliminary estimates of blue and sedimentary carbon in Scottish territorial waters; they calculated that the sediments in these waters stored 1757 Mt C, with coastal and offshore sediments acting as the main repositories. Burrows et al. (2014) suggested that the majority of this organic carbon (OC) was held in fjord sediments.

It has long been known that fjords are important stores of C (Syvitski et al., 1987) and that C burial in sediments is the most significant mechanism of long-term (> 1000 years) OC sequestration in the coastal ocean setting (Hedges et al., 1995). These carbon accumulation and burial processes have been investigated in the fjordic systems of New Zealand (Pickrill, 1993; Knudson et al., 2011; Hinojosa et al., 2014; Smith et al., 2015), Chile (Sepúlveda et al., 2011), Alaska (Cui et al., 2016) and the high latitudes of NW Europe (Winkelmann and Knies, 2005; Müller, 2001; Kulinski et al., 2014; Duffield et al. 2017), yet the mid-latitude fjords of Scotland have been largely overlooked, with only limited data available (Loh et al., 2008). Smith et al. (2015) brought much of the available data together and showed that globally fjordic systems act as a CO_2 "buffer" by efficiently capturing and burying labile terrestrially derived OC and preventing it from entering the adjacent ocean system where it is prone to recycling. They calculated that 11 % of annual global marine carbon sequestration occurs within fjords.

Despite these findings, much of the global research to assess and quantify C stocks is disproportionately skewed towards the terrestrial environment (e.g. Yu et al., 2010). This trend is also found at the regional scale as for example in Scotland, where there have been multiple studies quantifying the carbon held within the soils (Aitkenhead and Coull, 2016; Bradley et al., 2005; Chapman et al., 2013) and peats (Howard et al., 1995; Cannell et al., 1999; Chapman et al., 2009).

In addition to the challenges of access and cost in sampling these environments when compared to the adjacent terrestrial environment, it might also be argued that the sparsity of marine sedimentary C inventories is due to the lack of a robust methodology to quantify these C stores. Syvitski et al. (1987) commented that "the development of a methodological approach to quantify the C in the sediment of a fjord must be a priority", yet in the subsequent years there has been relatively little progress towards this goal.

The absence of a robust methodology to quantify the C held in marine sediments is illustrated by Burrows et al. (2014), who estimated that there is 0.34 Mt OC stored in the sediments of Scottish fjords. However, these calculations only take into account an estimate of OC in the top 10 cm of sediment, despite the fact that sediment depths of > 25 m are common in Scottish fjords (Baltzer et al., 2010; Howe et al., 2002). Therefore, it is likely that current best estimates of the quantity of OC within these systems as a whole have been significantly underestimated and that the presence of significant quantities of inorganic carbon (IC) held within fjord sediments (Nørgaard-Pedersen et al., 2005) has been overlooked.

To address these gaps, this study combines geochemical, geophysical and geochronological techniques to produce a methodology capable of delivering quantitative first-order estimates of the mass of C stored within the sediment of a fjord with the aim of achieving the goal set out by Syvitski et al. (1987). This work provides the first carbon inventory for a fjord and further contributes to the emerging evidence that these fjords are globally important sites for the burial of C as set out by Smith et al. (2015) and Cui et al. (2016b).

3.2 Study Area

The study focuses on Loch Sunart, a fjord on the west coast of Scotland (Fig. 3.1). It is 30.7 km long and covers an area of 47.3 km^2 with a maximum depth of 145 m. It consists of three basins separated by shallow rock sills. The inner basin is separated from the middle basin by a sill at approximately 6 m depth, while the middle and outer basins are separated by a sill at approximately 31 m depth (Edwards and Sharples, 1986; Gillibrand et al., 2005). The silled nature of the bathymetry allows the fjord to act as a natural sediment trap for both terrestrial and marine-derived materials (e.g. Nørgaard-Pedersen et al., 2006). Though the sills are shallow they do not restrict the exchange of marine water in the fjord basins (Gillibrand et al., 2005) and therefore Loch Sunart has well oxygenated bottom waters (Gillibrand et al., 2006).

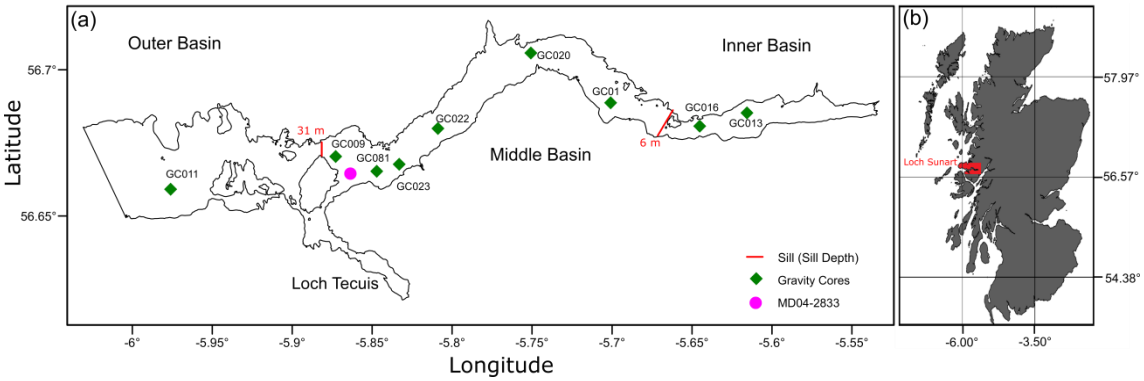

Figure 3.1. Maps of Loch Sunart illustrating **(a)** the three basins and the sediment core locations and **(b)** Loch Sunart in a Scottish context.

Loch Sunart's catchment covers 299 km^2; the main tributaries of the fjord are the rivers Carnoch and Strontian; the latter has a mean daily discharge of 1409 x 10^3 m^3 (2009–2013). The mean annual precipitation in Loch Sunart's catchment is 2632 ± 262 mm (Capell et al., 2013). The combination of small catchment size and high precipitation means that the flow network is sensitive to precipitation changes which can result in a flashy flow regime (Gillibrand et al., 2005).

The catchment is largely dominated by high relief and poorly developed soils. The bedrock consists primarily of igneous and metamorphic rocks, overlain by gley and podzol soils with limited peat in the upper catchment (Soil Survey of Scotland, 1981). Exposed rock is common on the steep slopes. Much of the catchment's vegetation can be found by streams or on the shore of the fjord and is dominated by both commercial

forestry and natural woodlands; there is only very limited agriculture within the catchment. The combination of steep, exposed slopes, poorly developed soil, a reactive river network and poorly developed vegetation typically results in high surface runoff and sediment transport (Hilton et al., 2011).

The characteristics of Loch Sunart and its catchment are representative of fjords across mainland Scotland (Edwards and Sharples, 1986), with the possible exception of Loch Etive which has a permanently hypoxic upper basin (Friedrich et al., 2014). The fjords of the Scottish islands (Shetland, Orkney and the Western Isles) differ from their mainland counterparts in that they are generally shallower and have catchments characterised by lower relief and are largely dominated by peat or peaty soil (Soil Survey of Scotland, 1981). Syvitski and Shaw's (1995) table of generalised fjord characteristics allows us to compare the fjords of mainland Scotland to other fjordic systems globally. The fjords of the Norwegian mainland, Canada and Fiordland, New Zealand (Hinojosa et al., 2014), are characterised by similar climate, geomorphology, river discharge, basin water temperature and sedimentation rate to the fjords of Scotland. The fjords of mainland Scotland differ significantly from those in Greenland, Alaska, Svalbard and the Canadian Arctic, many of which still have active glaciers, resulting in very different sediment input regimes.

3.3 Seismic Data Acquisition and Processing

To measure bedrock bathymetry and sediment depths, a seismic geophysical survey of Loch Sunart took place in 2002 aboard the RV Envoy (Fig.3.2). A SIESTEC Boomer system was used to create seismic profile data throughout the fjord. The data were recorded using an Elics–Delph data acquisition system coupled to the Differential Global Positioning System (DGPS). The Boomer system operated on a frequency of 1 to 10 kHz and had a pulse duration of 75 to 250 ms at a power of 150 J. The system has a depth resolution of 25 cm and can penetrate 100 m in soft sediment (Simpkin and Davis, 1983). A total of 34 transects of the fjord were acquired (Fig.3.2). The survey achieved an average penetration of 50 m; gas blanking prevented the signal from penetrating the sediment in some areas (Baltzer et al., 2010).

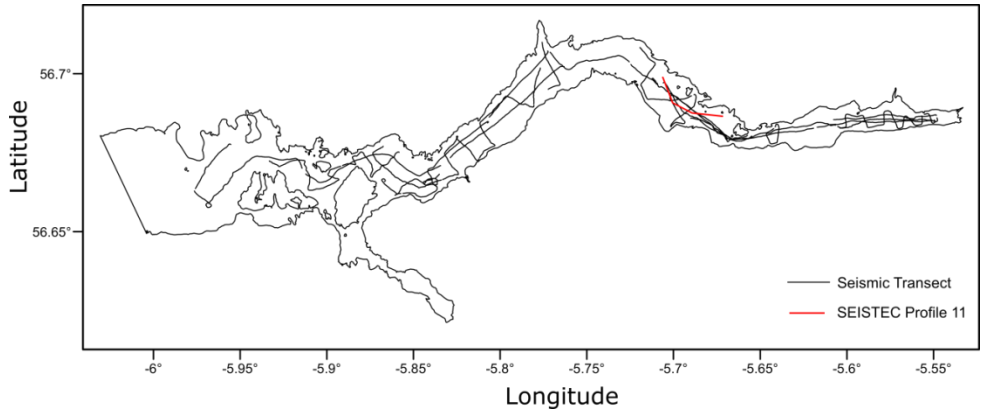

Figure 3.2. Map of the 34 seismic transects undertaken in Loch Sunart with SIESTEC profile 11 highlighted.

3.3.1 Defining Sedimentary Horizons

Each seismic profile was combined with the DGPS data and processed with the Petrel (Schlumberger) software package. Subsequent analysis was undertaken using the open-source SeiSee (DMNG) software package. Initial interpolation, following the methodology of Baltzer et al. (2010), defined the different seismic horizons (H) and the layers between the horizons which are defined as seismic units (U) numbered 1 to 3 from the basement horizon upwards (Fig. 3.3). The compilation of the horizons and units allows the construction of an equivalent seismic stratigraphy for each sediment core and for the fjord as a whole. Using SeiSee, points were picked along each of the four horizons, creating polylines. Each polyline was split into points at 0.25 m intervals and each point was assigned an x, y, z coordinate that represents its geographic location and depth (relative to mean sea level).

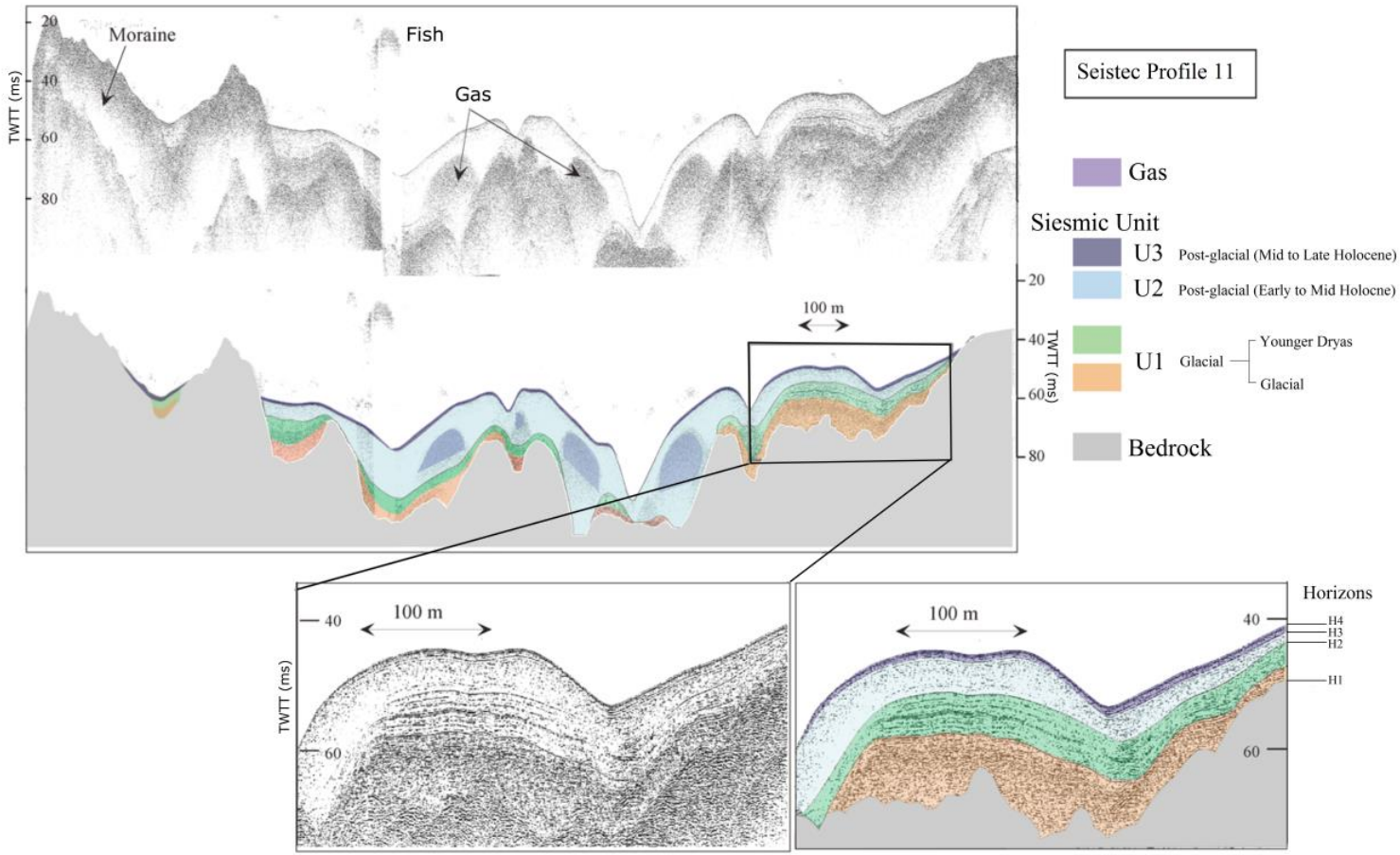

Figure 3.3. SIESTEC profile 11: a characteristic seismic profile displaying the four seismic horizons (H1, H2, H3 and H4) and the three seismic units (U1, U" and U3) with the depth indicated as two way travel time (TWTT), adapted from Baltzer et al. (2010).

3.4 Sediment Sampling

Eight sediment cores (Table 3.1) were collected from Loch Sunart (Fig.3.1) in 2001 using a gravity corer (GC) as part of the HOLSMEER (Late Holocene Shallow Marine Environments of Europe) project. This was supplemented with further sampling on a follow-up cruise on board the RV Calanus in August 2013 where a short GC was collected to fill a gap between the original coring sites. These cores capture the postglacial history of sediment accumulation within the fjord, as confirmed by ^{14}C basal dates (Section 3.7.2) Additionally, to obtain sediment of inferred glacial origin for geochemical analysis we accessed the lower sections of core MD04-2833 (Section VIII (1050–1200 cm) (Baltzer et al., 2010). This was recovered using the CALYPSO giant piston corer from the R/V Marion Dufresne in July 2004 as part of the IMAGES (International Marine Past Global Changes Study) project.

Core ID	**Basin**	**Position** (Lat, Long)	**Water Depth** (m)	**Recovery** (m)
GC009	Middle	56.672056, -5.867083	107	1.41
GC011	Outer	56.759861, -5.969639	91	2.45
GC013	Inner	56.681306, -5.629528	58	1.67
GC016	Inner	56.680944, -5.642333	58	0.56
GC020	Middle	56.704278, -5.751333	105	2.38
GC022	Middle	56.680333, -5.804944	120	2.46
GC023	Middle	56.665917, -5.840361	87	2.89
GC081	Middle	56.668972, -5.863278	58	3.63
GC01	Middle	56.696806, -5.704972	42	0.21
MD04 2833	Middle	56.665500, -5.859667	38	12

Table 3.1 Details of the sediment cores extracted from Loch Sunart that were used in this study.

3.5 Sediment Analysis (Methods)

3.5.1 Physical Characteristics

Detailed sediment logging was undertaken for each of the cores (Appendix A). The gravity cores were sub-sampled at 10 cm intervals and high-resolution sampling at 1 cm intervals was undertaken on the short core (GC01). Section VIII of glacial sediment core MD04-2833 was sub-sampled at 12 cm intervals. Each sub-sample was split for physical property and geochemical analyses. The wet (WBD) and dry bulk density (DBD) of the sediment was calculated following Dadey et al. (1992), while porosity was calculated using the methodology of Danielson and Sutherland (1986).

3.5.2 Bulk Elemental Analysis

To quantify the total carbon (TC) content, each sub-sample was freeze-dried and milled to a fine powder. A 20 ± 2 mg aliquot was placed in a tin capsule and measured on a COSTECH Elemental Analyser (EA) calibrated with acetanilide (Verardo et al., 1990; Nieuwenhuize et al., 1994). Precision of the analysis is estimated from repeat analysis of standard reference material B2178 (Medium Organic content standard from Elemental Microanalysis, UK) with C = 0.07 % and N = 0.02 % (n = 8).

To quantify OC, the process was repeated with the addition of HCl to remove the IC. After acidification, vessels were placed in a vacuum desiccator to remove any remaining CO_2 and the sample was then freeze-dried to remove the HCl (Loh et al., 2008). IC was calculated from the difference between TC and OC measurements. The mean standard deviations (1 σ) of TC and OC triplicate measurements (n = 10) were 0.04 % and 0.17 % respectively.

3.5.2 Sediment Geochronology

Basal radiocarbon dates for five of the gravity cores were obtained by accelerator mass spectrometer (AMS) radiocarbon dating of marine carbonate material (mollusc). This was carried out at the University of Aarhus, Denmark (AAR), Centre of Accelerator Mass Spectrometry, USA (CAMS), and the NERC Radiocarbon Laboratory, Scotland (SUERC). The radiocarbon dating was used to validate the Holocene chronology of the seismic stratigraphy. A single MD04-2833 sample was processed at Laval University,

Canada (UL), to confirm that the sediment was early postglacial in age. Dates were calibrated using OxCal 4.2.4 age modelling software (Bronk Ramsey, 2009; Bronk Ramsey and Lee, 2013), applying the Marine13 curve (Reimer et al., 2013) and the regional marine radiocarbon reservoir age correction: ΔR value of −26 ± 14 yr (Cage et al., 2006).

3.6 Quantifying and Characterising Sediment

3.6.1 Digital Terrain Models (DTMs)

The points collected from each seismic horizon were connected to form a DTM of that horizon. This was achieved using spatial modelling techniques in ArcGIS. The compiled x, y, z data were statistically tested to determine the gridding technique best suited to the interpolation of the data. Eleven gridding techniques were subjected to cross validation (Chiles and Delfiner, 1999) (Table 3.2). The residual Z mean value and standard deviation were examined; the technique with the lowest residual Z mean and standard deviation for each horizon (and the data set as a whole) was chosen as the gridding technique best suited to the interpolation of the data. Kriging, with linear interpolation (Cressie, 1990) and a 100 by 1000 node structure, performed best and was chosen to create computationally efficient DTMs for each seismic horizon.

3.6.2 Volumetric Calculations

The horizon DTM grids were used to calculate the volume of sediment in each seismic unit and, by extension, within the fjord as a whole. By subtracting one DTM grid from another (e.g. surface DTM minus bedrock DTM) the volume between the grids was calculated. Three different numerical integration algorithms were used for this calculation (Eqs. 1, 2, 3). The net volume is reported as the mean of these three calculations. In the following formulae Δ_x represents the grid column spacing, Δ_y represents the grid row spacing, $G_{i,j}$ represents the grid node value in row *i* and column *j* and A_i represents the abscissa (Press et al., 1988).

Trapezoidal Rule

The pattern of coefficients is {1,2,2,2,…,2,2,1}: $A_i = \frac{\Delta x}{2}[G_{i,1} + 2G_{i,2} + 2G_{i,3} \cdots + 2G_{i,nCol-1} + G_{i,nCol}]$

$$Volume \approx \frac{\Delta y}{2}[A_1 + 2A_2 + 2A_3 + \cdots 2A_{nCol-1} + A_{nCol}]$$

Extended Simpson's Rule

The pattern of coefficients is {1,4,2,4,2,4,2,…,4,2,1}:

$$A_i = \frac{\Delta x}{3}[G_{i,1} + 4G_{i,2} + 2G_{i,3} + 4G_{i,4} + \cdots + 2G_{i,nCol-1} + G_{i,nCol}]$$

$$Volume \approx \frac{\Delta y}{3}[A_1 + 4A_2 + 2A_3 + 4A_3 + \cdots + 2A_{nCol-1} + A_{nCol}]$$

Extended Simpson's 3/8 Rule

The pattern of coefficients is {1,3,3,2,3,3,2,…,3,3,2,1}:

$$A_i = \frac{3\Delta x}{8}\left[G_{i,1} + 3G_{i,2} + 3G_{i,3} + 2G_{1,4} + \cdots + 2G_{i,NCol-1} + G_{i,nCol}\right]$$

$$Volume \approx \frac{3\Delta y}{8}\left[A_1 + 3A_2 + 3A_3 + 2A_3 + \cdots + 2A_{nCol-1} + A_{nCol}\right]$$

Basin	Horizon	Kriging (Linear Interp)		Inverse Distance to Power		Minimum Curvature		Modified Shepard's Method		Natural Neighbour		Nearest Neighbour		Radial Basin Function		Triangulation (Linear Interp)		Moving Average		Local Polynomial	
		Z Mean	Z St.dev	Z Mean	Z St.dev	Z Mean	Z St.dev	Z Mean	Z St.dev	Z Mean	Z St.dev	Z Mean	Z St.dev	Z Mean	Z St.dev	Z Mean	Z St.dev	Z Mean	Z St.dev	Z Mean	Z St.dev
Inner	Surface	0.148	5.381	0.795	7.543	0.166	9.342	0.341	6.404	0.373	4.460	0.080	8.421	-0.308	21.696	0.217	4.459	-1.606	23.948	1.591	12.011
	Holocene Int	0.115	5.513	0.521	7.533	0.108	8.996	0.101	6.292	6.422	13.139	0.347	8.302	0.405	64.849	0.208	4.680	-1.658	23.899	1.586	11.403
	G/PG Interface	0.147	5.574	0.304	7.398	0.077	9.208	0.096	6.237	0.216	4.692	0.215	7.731	-0.315	38.672	0.203	5.113	-1.383	21.752	1.673	11.193
	Bedrock	-0.065	7.780	-0.544	10.188	-0.518	10.074	0.129	7.985	-0.643	7.003	-0.180	10.415	-0.685	22.481	-0.681	6.902	1.634	24.276	-2.317	14.082
Middle	Surface	0.122	5.498	0.801	8.098	0.134	9.897	0.435	5.999	0.408	4.988	0.067	9.811	-0.598	23.67	0.345	5.587	-1.789	21.900	1.498	12.098
	Holocene Int	0.098	5.332	0.634	8.456	0.105	8.213	0.114	6.001	5.221	11.945	0.387	9.765	0.376	71.897	0.303	4.987	-1.854	22.897	1.556	13.001
	G/PG Interface	0.169	5.781	0.299	8.398	0.104	9.346	0.088	6.567	0.111	5.091	0.211	8.931	-0.387	32.677	0.567	5.987	-1.765	23.876	1.603	10.998
	Bedrock	-0.076	6.987	-0.448	9.972	-0.678	11.087	0.469	8.532	-0.632	6.782	-0.204	11.678	-0.703	21.567	-0.456	7.032	1.345	21.478	-2.222	15.073
Outer	Surface	0.156	5.398	0.786	8.034	0.176	9.456	0.289	6.867	0.556	5.123	0.089	9.002	-0.445	26.643	0.311	4.898	-1.675	23.674	1.547	12.002
	Holocene Int	0.101	5.545	0.456	7.001	0.087	7.891	0.105	6.345	7.991	13.456	0.378	9.832	0.378	67.789	0.356	4.698	-1.798	22.111	1.497	12.768
	G/PG Interface	0.134	5.678	0.201	7.457	0.108	9.679	0.078	6.389	0.321	5.897	0.198	10.432	-0.378	43.734	0.689	6.023	-1.666	21.896	1.634	11.034
	Bedrock	-0.045	8.012	-6.045	9.986	-0.789	9.789	0.156	7.765	-0.687	7.015	-0.163	13.001	-0.801	24.834	-0.389	7.091	1.456	22.134	-2.980	15.002
Total Times Methodology Ranked in the Top 3		21		0		10		11		9		5		0		12		0		0	

Ranking	
1st	
2nd	
3rd	

Table 3.2. Cross validation results (Residual Zmean & Zst.dev) for the three basins of Loch Sunart.

3.6.3 Sediment Mass Quantification

The mean DBD for each seismic unit was calculated and assigned to the equivalent seismic unit within each core. The spatial distribution of the DBD for each seismic unit was modelled, again using Kriging (with linear interpolation). The resulting contour plot was integrated with the volumetric model for each seismic unit to calculate the dry mass of the sediment held within that seismic unit. The integration process calculates the volume of sediment held within each of the DBD contours and multiplies that volume with the associated DBD value to calculate the mass of sediment.

3.6.4 Sedimentary Carbon Quantification

The same methodology used to integrate the volume and density data was used to combine bulk elemental data with the sediment dry mass calculations. Mean values for TC, OC and IC in each seismic unit were assigned to the seismic units from the available core data. Kriging (with linear interpolation) was again used to create contour maps representing the quantity of TC, OC and IC in each seismic unit, and the mass of sediment held between the contours was multiplied by the percentage of OC and IC, quantifying the mass C held within the fjord's sediment. Finally, we calculated how effectively the fjord stores C (C density) as a depth-integrated average value per km^2 for both the postglacial and glacial-derived sediments. This measure allows the fjord's C stores to be directly compared with other C stores (peatlands, soil, etc.).

3.6.5 Carbon Accumulation and Burial

Sedimentation rates (SRs) were calculated as an approximation for the postglacial sediment burial history using basal ages and linear interpolation to the core top, assuming a contemporary surface. We recognise that the calculations will be relatively crude and do not take into consideration factors such as compaction and possible changes in sedimentation rate through time, but they provide initial insight into the variability of SRs within the fjord and allow first order C accumulation rates (CARs) to be estimated. The SRs were converted to CARs using Eq. (4). The %OC, %IC, bulk density and porosity data used for these calculations were based upon a mean value for the postglacial unit of each dated core.

$$\text{CAR} = \%\text{C} \times \text{SR} \times (\text{porosity} - 1) \times \text{wet bulk density}$$

As there is no available data on how efficiently OC is buried in the sediment of Scottish sea fjords, burial efficiencies of 64 % (Sepúlveda et al., 2005) and 80 % (Smith et al., 2015) were used to convert CARs to carbon burial rates (CBRs) (low and high). The Scottish system have a more open circulation than NZ fjords but are more restricted than those found in Chile therefore we believe the range of burial efficiencies used will be broadly representative to the Scottish fjords. For the purposes of this study and in the absence of reliable estimates of burial efficiency, we assume that the IC accumulation rates equal the IC burial rates. These CBRs were, in turn, used to calculate the long-term annual average burial of OC and IC; while potentially very useful for understanding the dynamics of carbon deposition, such estimates should be treated with caution.

3.7 Results

3.7.1 Seismic Interpretation

Four horizons were identified throughout the fjord (Fig.3.3): these represent the basement (H1) and the sediment water interface (H4) with two intermediate horizons (H2 and H3). Core stratigraphies (Baltzer et al., 2010) indicate that H2 divides the postglacial and glacial sediment, while H3 splits the postglacial sediment into two units. The seismic data display a fifth horizon between H1 and H2 which is only present in the inner basin and partially in the middle basin. We interpret this as glacial sediment from the Younger Dryas, as confirmed by radiocarbon dating (Baltzer et al., 2010; Mokeddem et al., 2010); for the purposes of this paper, the horizon was amalgamated with H2.

A seismic stratigraphy was developed based on these horizons (Fig.3.3). U1 is interpreted as glacial sediment based on the observation of the short, discontinuous seismic reflections which are synonymous with poorly sorted material; the unit varies in thickness but never drops below a minimum thickness of 10 m. U2 is found throughout the fjord with an average thickness of 5 to 10 m; the unit drapes over U1. U3 is the uppermost unit and has a homogenous thickness of around 1m; it is characterised by laminated acoustic reflections. Both U2 and U3 are interpreted as postglacial infill of the fjord; though clear in the seismic geophysics, the boundary between U2 and U3 is poorly defined in the sediment lithology (Supplement). Similar patterns in seismic stratigraphy have been observed throughout the west coast of Scotland (Binns et al., 1974a, b; Boulton et al., 1981; Howe et al., 2002).

We compared our interpretation of the seismic data to the seismic interpretation of Baltzer et al. (2010); this exercise was designed to test the replicability of our interpretation and allow potential uncertainties in the seismic interpolation to be built into our future applications. The comparison identified small differences in the depth of H1 (−0.17 m), H2 (+0.34 m) and H3 (−0.22 m). These differences were integrated into the volumetric calculations as an error term.

3.7.2 Sediment Geochronology

The calibrated age for the basal sediment from MD04-2833 (Section VIII) was 17041 +/- 312 cal BP. This, combined with the characteristic glacial core lithology of poorly sorted sedimentary material, indicates that these sediments were deposited during the retreat of the British ice sheet (BIS) at the end of the last glacial period, around 13 500 to 17 000 cal BP (Clark et al., 2010; Scourse et al., 2009; Wilson et al., 2002). Calibrated radiocarbon dates for the gravity cores (Table 3.3) indicate that these cores are comprised of sediment that was accumulated during subsequent postglacial period, the Holocene.

By comparing the radiocarbon chronologies with the seismic stratigraphy we can test the seismic interpolation and further constrain the age of each seismic unit. The seismic unit for the equivalent depth of each of the radiocarbon samples has been compiled (Table 3.3), then compared to the seismic unit that the sample would fall into based on age alone as per the Baltzer et al. (2010) chronostratigraphy. Of the 18 samples tested, 15 have estimated ages which match the appropriate seismic units. Three samples (all from GC023) have ages which are apparently too young for their corresponding seismic unit; this suggests a possible problem with the dating of this particular core, rather than the interpolation of the seismic geophysics. Close inspection of the seismic profile suggests that sediment slumping could be an issue at the core site. This test signifies that our interpolation of the seismic geophysics is accurate and that the chronostratigraphy developed for MD04-2833 (Baltzer et al., 2010) can be applied throughout Loch Sunart. The dated samples are in agreement with the seismic interpretation, suggesting that both U2 and U3 are of Holocene origin. Similarly, we can further constrain the age of the seismic units with U2 representing the early to mid-Holocene and U3 mid to late Holocene sedimentary sequences.

Laboratory Code	Core ID	Depth (cm)	^{14}C Age, BP (No Correction)	Calibrated ^{14}C Age (cal BP)	Seismic Unit	
					Depth eqv.	Age eqv.
AA-48108	GC009	140	9827 ± 49	10801 ± 93	U2	U2
SUERC 65990	GC011	60	2837 ± 35	2625 ± 66	U3	U3
SUERC 65991	GC011	120	9890 ± 38	10878 ± 87	U2	U3
SUERC 65992	GC011	170	11266 ± 40	12760 ± 61	U2	U2
AA-48109	GC011	231	12181 ± 58	13658 ± 90	U1	U1
AA-48107	GC013	113	1716 ± 32	1294 ± 35	U3	U3
SUERC 65995	GC016	30	1865 ± 35	1438 ± 51	U3	U3
SUERC 65994	GC020	9	683 ± 35	357 ± 44	U3	U3
SUERC 65993	GC020	19	3067 ± 37	2864 ± 57	U3	U3
AA-48106	GC020	126	11652 ± 74	13160 ± 90	U2	U2/U1
AA-51569	GC023	30	340 ± 60	64 ± 51	U3	U3
SUERC-681	GC023	49	1215 ± 47	788 ± 58	U3	U3
SUERC-677	GC023	58	1322 ± 43	886 ± 55	U3	U3
AA-51570	GC023	73	1430 ± 55	1011 ± 66	U3	U3
SUERC-679	GC023	111.5	1695 ± 57	1274 ± 59	U2	U3
SUERC-680	GC023	250	2180 ± 61	1801 ± 80	U2	U3
CAMS-82821	GC023	286	2425 ± 40	2099 ± 70	U2	U3
UL 2853	MD04-2833	745	14420 ± 210	17041 ± 312	U1	U1

Table 3.3. Radiocarbon ages from Loch Sunart cores. Ages were calibrated using OxCal 4.2.4 (Bronk Ramsey., 2009 & Bronk Ramsey & Lee., 2013) with the Marine13 curve (Reimer et al. 2013) and regional correction of ΔR value of -26 ± 14 yr (Cage et al. 2006). All ages are calibrated at 95.4% probability and the mean age has been determined from the minimum and maximum calibrated ages. Additionally; we list the seismic unit assigned to each sample based on depth and compare this to the age equivalent (eqv.) seismic unit based on Baltzer et al. (2010).

3.7.3 Sediment Analysis

3.7.3.1 Bulk Density Measurement

Mean DBD was calculated for U1, U2 and U3 from each core. Figure 3.4 displays the DBD results, which are arranged to mirror the spatial distribution of the cores, from the inner basin to the outer basin. U1 sediment is characterised by the single section of MD04-2833, which has a mean DBD of 2.19 ± 0.09 g cm^{-3}. This is within the range estimated for other Northern Hemisphere fjords (Pedersen et al., 2012; Forwick et al., 2010; Baeten et al., 2010). DBD increases down each core as a result of sediment dewatering in response to compaction. GC011 is the only core where U3 has a higher DBD than the underlying U2, most likely due to large quantities of shell in the upper part of the core. U1 has the highest DBD; this is likely to reflect both the type of sediment deposited during glacial retreat and long-term compaction over the postglacial period.

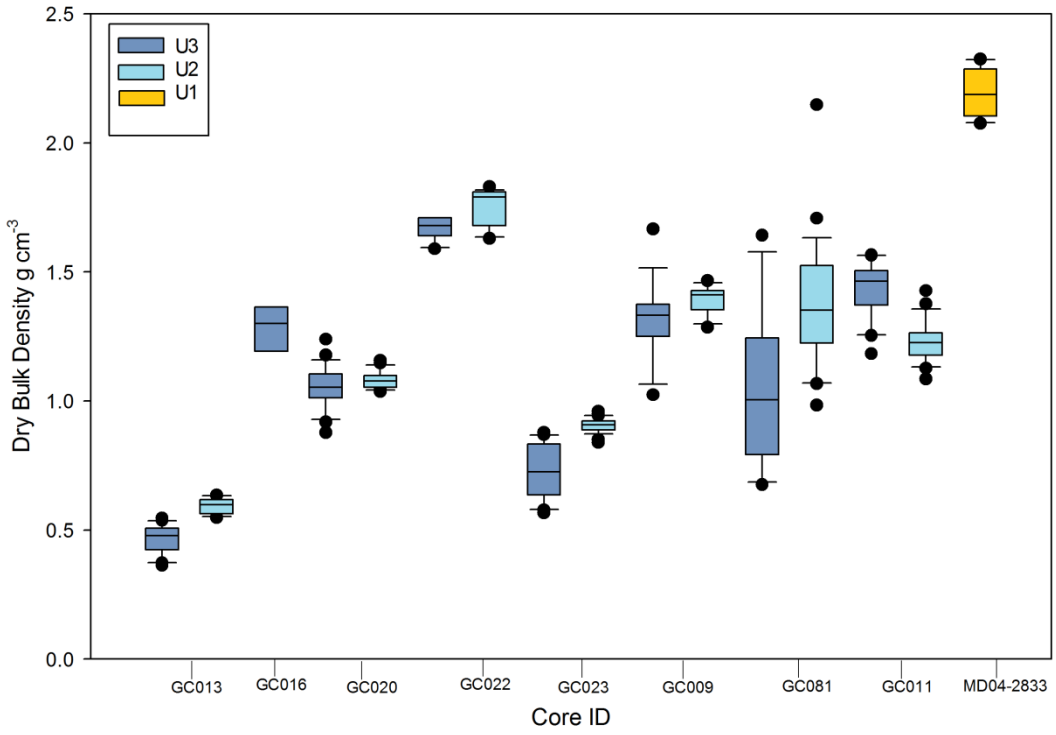

Figure 3.4. Dry bulk density from each of the sediment cores corresponding to seismic units 1, 2 and 3.

3.7.3.2 Bulk Elemental Analysis

Mean quantities of OC and IC have been calculated for U1, U2 and U3 (Fig. 3.5). Values for U1 were calculated using the basal sediments from MD04-2833 (Section VIII). There are clear temporal and spatial trends, with U3 consistently containing a greater quantity of OC than U2, while the proportion of sedimentary OC generally decreases seawards, away from the inner basin. The opposite is true for sedimentary IC, which generally increases seawards away from the inner basin.

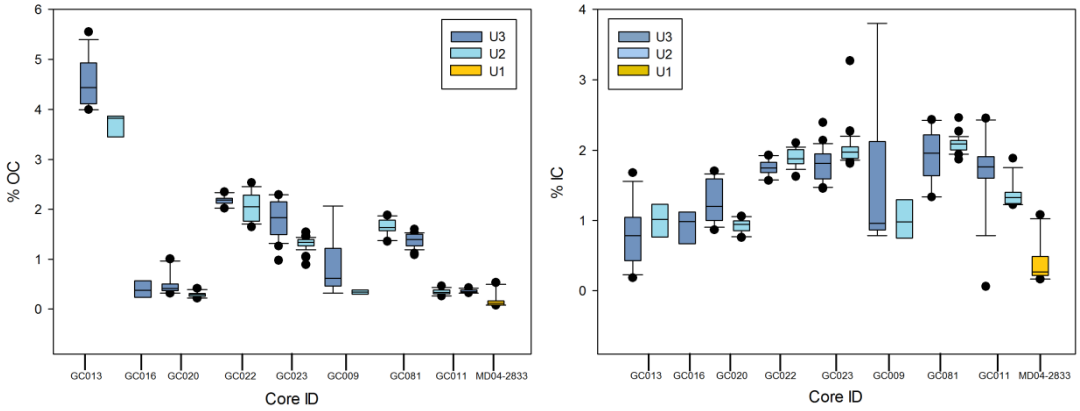

Figure 3.5. %OC and %IC values from each of the sediment cores corresponding to seismic units 1, 2 and 3.

3.7.4 Sediment and Carbon Quantification

3.7.4.1 Volumetric Modelling

The interpolation of the seismic profiles led to the creation of four DTMs (Fig 3.6) which represent horizons H1 to H4. To determine the accuracy of the models, the DTM for H4 was compared to an existing high-resolution bathymetric model of the fjord (Bates et al., 2004). The coordinates (x, y, z) of key high and low points (n = 12) were compared between surveys; the mean divergence between surveys was calculated as x = −0.56 m, y = −0.81 m and z = 0.21 m. Although the H4 DTM slightly negatively offsets the x and y and overestimates the z coordinates of these points, the general location and pattern of these seabed features compare favourably.

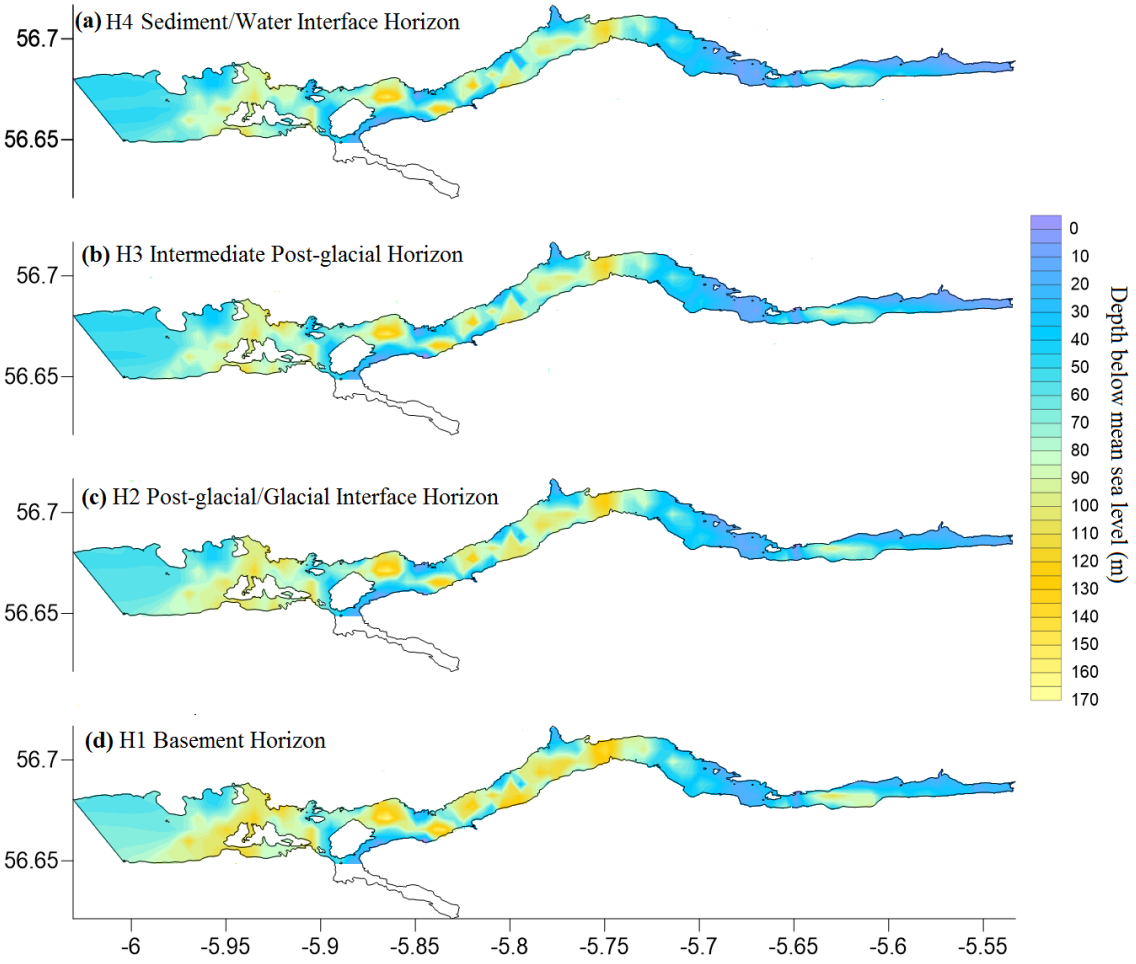

Figure 3.6. Digital terrain models illustrating the topography of the different seismic horizons **(a)** H4 sediment water interface **(b)** H3 intermediate post-glacial horizon **(c)** postglacial/glacial interface **(d)** Basement (Bedrock).

The DTMs and numerical integration algorithms were combined to calculate the volume of sediment held within each seismic unit. A further subdivision by basin and according to postglacial (U2 and U3) and glacial (U1) sediment origin has also been undertaken (Table 3.4). The fjord as a whole contains a greater volume of glacial (6.00 × 108 m3 ± 1.89 %) than postglacial sediment (5.31 × 108 m^3 ± 7.39 %). Comparison of the three basins indicates that the middle basin contains the greatest combined (postglacial + glacial) volume of sediment (3.04 × 107 m^3 ± 5.30 %) followed by the outer (1.60 × 107 m^3 ± 5.74 %) and inner basins (4.17 × 106 m^3 ± 4.48 %).

Basin	**Layer**	**Volume**	
		Mean (m^3)	%RSD
Inner	PG	2869825.90	6.48
	G	1301836.56	1.89
Middle	PG	23046267	7.26
	G	7363034.04	1.89
Outer	PG	13371884	7.90
	G	2667373.2	1.89
Loch Sunart	PG	530872293	7.39
	G	599731882	1.89
	Total	**1130604175.55**	**3.61**

Table 3.4. Sediment volume calculated as the mean of the three numerical integration algorithms; the error is reported as relative standard deviation (%RSD) which integrates the uncertainty in the seismic interpolation and the standard deviation of the numerical integration algorithms. The data are reported for the post-glacial (PG) and glacial (G) sediment in each of the basins within Loch Sunartat the basin level.

3.7.4.2 Sediment Mass Quantification

The mean DBD for U2 and U3 were modelled (Fig. 3.7) to determine the variability in spatial distribution throughout the fjord. The spatial pattern of DBD is similar in both U2 and U3, with lower values in the inner basin (U2: 0.47 g cm^{-3}, U3: 0.59 g cm^{-3}), rising through the middle basin where it peaks at 1.75 and 1.67 g cm^{-3} for U2 and U3 respectively. The transition between the middle and outer basins is characterised by low DBD values (U2: 0.72 g cm^{-3}, U3: 0.91 g cm^{-3}); from this low point the DBD rises towards the seaward end of the fjord.

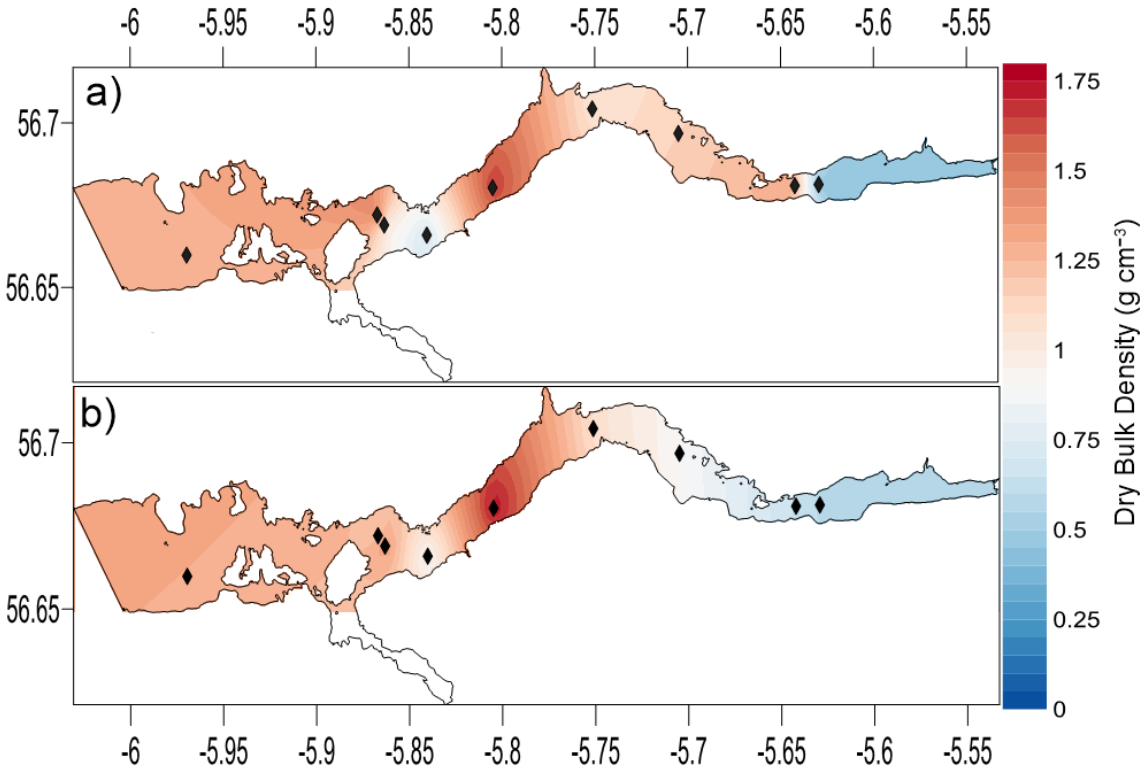

Figure 3.7. Contour maps showing the output of the spatial distribution model for the mean dry bulk density of **(a)** U3 and **(b)** U2. Sampling locations indicated with black diamonds.

The model output was integrated with the volumetric data (Section 3.7.4) to calculate the mass of postglacial sediment (Table 3.5). Since we have only derived a single mean DBD value for U1, it was applied throughout the fjord to calculate the mass of sediment held within this unit. The fjord holds an estimated total of 1928.3 ± 7.3 Mt of sediment, comprising 652.1 ± 6.6 Mt of postglacial material and 1276.2 ± 8.9 Mt of glacial sediment. The inner basin holds the least sediment, followed by the outer basin, with the middle basin acting as the main store of sediment in Loch Sunart.

Basin	Layer	Mass (Mt)	TC (Mt)	OC (Mt)	IC (Mt)
Inner	PG	27.1 ± 3.0	1.3 ± 0.2	1.1 ± 0.1	0.3 ± 0.2
	G	126.7 ± 7.2	0.8 ± 0.6	0.2 ± 0.2	0.6 ± 0.4
Middle	PG	421.5 ± 7.3	14.1 ± 0.3	7.1 ± 0.3	7.0 ± 0.2
	G	738.3 ± 9.6	4.0 ± 0.9	1.2 ± 0.3	2.8 ± 0.6
Outer	PG	203.5 ± 11.1	4.5 ± 0.3	1.3 ± 0.1	3.2 ± 0.2
	G	411.2 ± 9.8	2.2 ± 0.8	0.7 ± 0.1	1.6 ± 0.6
Loch Sunart	PG	652.1 ± 6.6	19.9 ± 0.3	9.4 ± 0.2	10.1 ± 0.2
	G	1276.2 ± 8.9	7.0 ± 0.8	2.1 ± 0.3	4.9 ± 0.6
	Total	**1928.3 ± 7.3**	**26.9 ± 0.5**	**11.5 ± 0.2**	**15.0 ± 0.4**

Table 3.5. Mass of sediment held with Loch Sunart and the mass of the total carbon (TC), organic carbon (OC) and inorganic carbon (IC) held within Loch Sunart's postglacial (PG) and glacial (G) sediment.

3.7.4.3 Sedimentary Carbon Quantification

Using a similar approach, the mean OC and IC were spatially modelled throughout the fjord. The output for U3 is illustrated in Fig. 3.8. As before, the model outputs for U2 and U3 were integrated with the sediment mass data in order to quantify the mass of TC, OC and IC held within the postglacial and glacial sediments (Table 3.5). Single mean values for TC, OC and IC were again used to calculate their respective mass of C within the sediment of U1.

The sediment in Loch Sunart is estimated to contain 26.9 ± 0.5 Mt of C, incorporating 11.5 ± 0.2 Mt OC and 15.0 ± 0.4 Mt IC. Although the mass of glacial sediment is higher, the postglacial sediments contain a larger quantity of C (19.9 ± 0.3 Mt). The quantity of C held within each of Loch Sunart's basins varies: the lowest amount is found in the inner basin (2.1 ± 0.5 Mt), followed by the outer basin (6.7 ± 0.6 Mt). The sediment of the middle basin holds significantly more C than both the inner and outer basins combined, estimated at 18.1 ± 0.7 Mt C. This indicates that the middle basin is the main repository for sedimentary C in Loch Sunart.

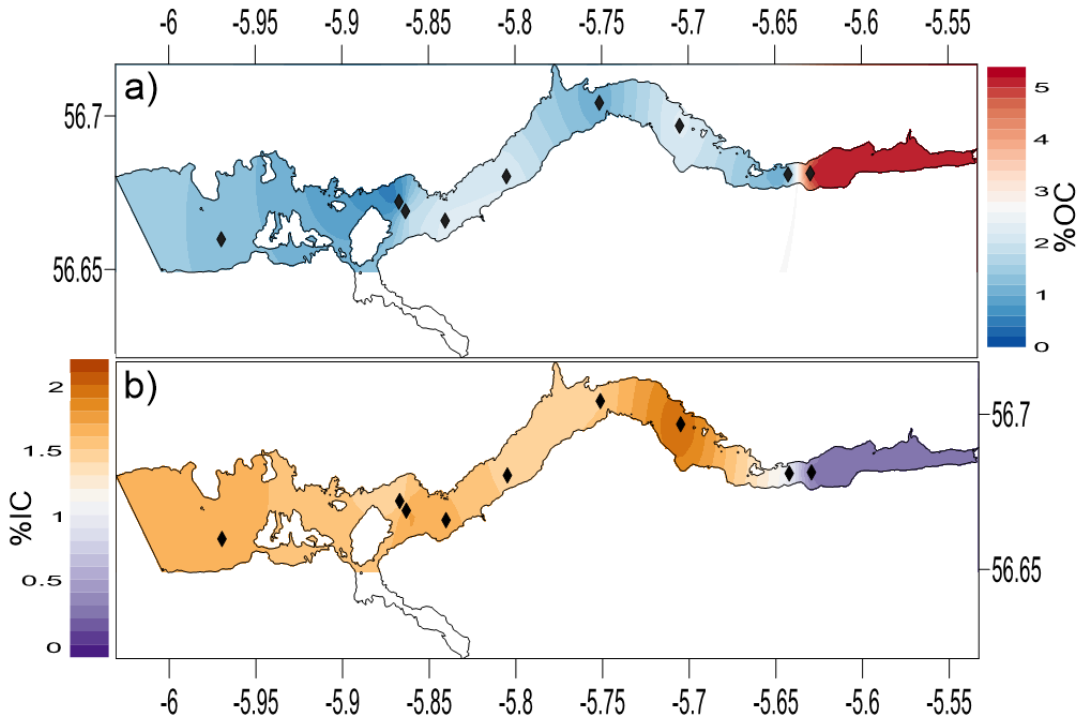

Figure 3.8. Output of spatial distribution model for **(a)** organic carbon (OC) and **(b)** inorganic carbon (IC) in U3. Sampling locations indicated with black diamonds.

How effectively the fjord stores C is measured by the C density (Table 3.6) with OC:IC ratios used to illustrate the split between the two forms of C. Loch Sunart is characterised by an OC:IC ratio of 0.74 and has an average C density of 0.560 Mt C km^{-2} , which can be further broken down to a postglacial C density of 0.412 Mt C km^{-2} and a glacial C density of 0.148 Mt C km^{-2} . The C density can also be illustrated at the individual basin (Table 3.6) level, with the postglacial sediments of the inner, middle and outer basins characterised by OC:IC ratios of 4, 1 and 0.42, illustrating the transition from OC as the dominant component in the upper fjord to IC dominated sediment at the seaward end of the fjord. The middle basin is the most effective at storing postglacial OC followed by the inner and outer basin. Similarly, the middle basin is most effective at storing IC, but in contrast to the effective storage of OC, the outer basin ranks second followed by the inner basin for IC. The glacial material held within the fjord as a whole is characterised by an OC: IC ratio of 0.42 with a mean OC density of 0.044 Mt km^{-2} and IC density of 0.104 Mt km^{-2}.

C Inventories	Area (km^2)	TC (Mt)	C Density (Mt km^{-2})	OC Density (Mt km^{-2})	IC Density (Mt km^{-2})	Reference
			Postglacial			
Inner Basin	5.5	1.3	0.238	0.191	0.047	This study
Middle Basin	24.7	14.1	0.570	0.285	0.284	
Outer Basin	17.1	4.5	0.263	0.077	0.184	
			Glacial			
Inner Basin	5.5	0.8	0.147	0.044	0.104	
Middle Basin	24.7	4.0	0.161	0.047	0.113	
Outer Basin	17.1	2.2	0.129	0.038	0.091	
Postglacial	47.3	19.9	0.412	0.199	0.213	
Glacial	47.3	7.00	0.148	0.044	0.104	
Loch Sunart	47.3	26.9	0.560	0.242	0.318	
			2 m Depth			
Peatlands*	17270	1620		0.094		Chapman et al., 2009
Organo-Mineral Soil*		754				Bradley et al., 2005
Mineral Soil*		498				
			1 m Depth			
Peat	17369	813.9		0.047		Aitkenhead and Coull ,2016
Alluvial Soil	1657	40.8		0.025		
Alpine Soil	3825	145.7		0.038		
Bare Ground	1672	50.5		0.030		
Brown Earth	15971	590.3		0.037		
Gley	15963	645.4		0.040		
Podzol	18159	536.6		0.029		
Ranker	2531	82.6		0.033		
Regosol	437	19.0		0.044		

*Both studies calculated the soil C stocks excluding IC data therefore the stocks only represent the OC held within these stocks.

Table 3.6. The C density of Loch Sunart's postglacial and glacial sediments in comparison to Scottish terrestrial C stores.

3.7.4.4 Carbon Accumulation and Burial

The estimated SRs vary between the sedimentary basins of the fjord, with the most rapid rates in the inner basin recorded in core GC013 (0.087 cm yr^{-1}). The middle and outer basins have lower SRs as shown by cores GC020 (0.025 cm yr^{-1}) and GC011 (0.017 cm yr^{-1}). The calculated organic carbon accumulation (OCAR) and burial (OCBR) rates for Loch Sunart are presented in Table 3.7 alongside rates from other fjords globally. Our estimates are in line with the fjords of New Zealand (Pickrill, 1993; Knudson et al., 2011; Hinojosa et al., 2014; Smith et al., 2015), Alaska (vegetated) (Cui et al., 2016) and Chile (Sepúlveda et al., 2011); they are somewhat lower than the glaciated fjords of NW Europe (Winkelmann and Knies, 2005; Müller, 2001; Kulinski et al., 2014). Although not

shown in Table 3.7, the calculated inorganic carbon accumulation rates (ICARs) range between 0.69 and 36.89 g IC m^{-2} yr^{-1}, resulting in long-term annual average estimates of IC burial of between 56 and 1.7 × 10^3 t for the fjord as a whole.

3.7.5 Uncertainty

The joint geophysical and geochemical methodology outlined (Fig. 3.9) provides a robust approach to allow the first quantification of total sedimentary C stocks in a fjord setting. An important part of estimating sedimentary C stocks should be the quantification of uncertainty associated with these estimates. There are several types of uncertainty that can influence sedimentary carbon estimations (Fig.3.9), including interpolation, algorithmic, analytical, sampling and extrapolation uncertainty. Several of these types of uncertainties are easily dealt with statistically: for example the analytical uncertainties of what have been quantified through triplicate measurements. The sampling uncertainty of a stratigraphic sequence (i.e. spatial variability of C content in relation to sampling density) can be overcome by calculating the mean and standard deviation to create composite values that are representative of the seismic unit as a whole. We integrated the quantifiable uncertainties at each calculation step (Fig. 3.9). By calculating composite standard deviations we are able to propagate the uncertainties throughout the C quantification process. In the interpolation of the seismic geophysics, it is difficult to fully quantify the uncertainty involved in the process. We utilised the five-step framework of Bond et al. (2007) designed to reduce uncertainty in this process and additionally integrated a validation step using radiocarbon dating of sedimentary cores (see Sect. 3.7.2). This allows us to reduce the uncertainties associated with the seismic interpretation, although we recognise that some uncertainty remains (e.g. highly variable patterns of sediment thickness) which cannot be fully quantified without extensive and costly survey, sampling and dating effort. Within this framework of uncertainty, we consider our method to give a robust estimate for the carbon stocks present.

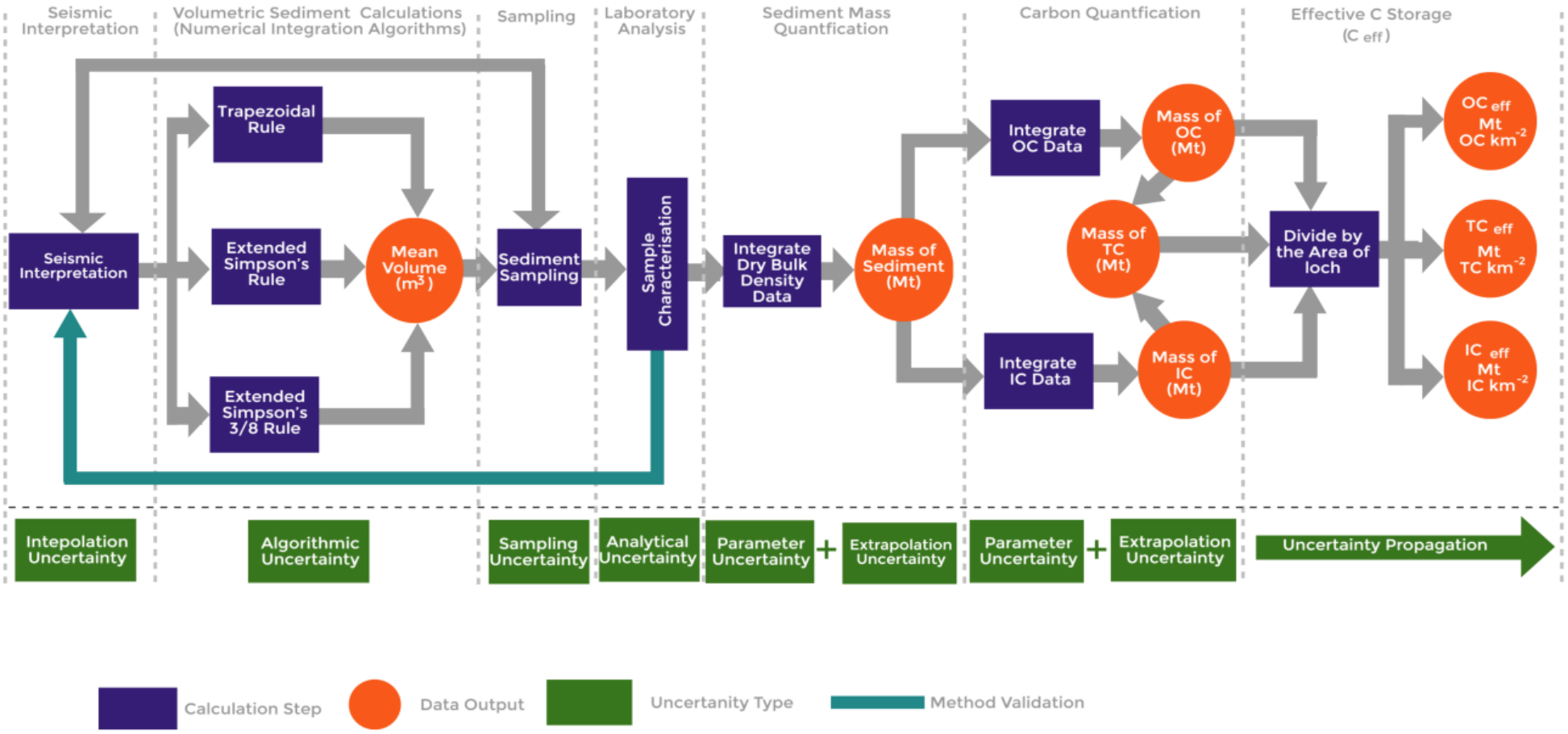

Figure 3.9. Flow diagram detailing the steps towards calculating the sedimentary C stocks within a fjord with the known uncertainties specified

Location	Area (km^2)	SR ($cm\ yr^{-1}$)	OC Accumulation Rate ($g\ m^{-2}\ y^{-1}$)		OC Burial Rate ($g\ m^{-2}\ y^{-1}$)		OC Burial (Tonnes yr^{-1})		Reference
			Min	Max	Min	Max	Min	Max	
Loch Sunart	47.3	0.017-0.089	3.0	32.1	1.89[a]	25.68[b]	8.9×10^1	1.2×10^3	This Study
NW Europe/Artic									
Loch Creran	13.3	0.2-0.5			21.9	193.45	2.9×10^2	2.6×10^3	Loh et al., 2008
Nordasvannet Fjord	4.6				2.2		1.0×10^1		Winkelmann and Knies 2005
Storfjord	14249				21.0	40.0	3.0×10^5	5.7×10^5	Müller. 2001
Kongsfjorden	817				9	13	7.4×10^3	1.0×10^4	Kulinski et al., 2014
Canada/Alaska									
Saguenay Fjord	360				24.5	291.0	8.8×10^3	1.0×10^5	St-Onge and Hillaire-Marcel. 2001
Vegetated Alaskan Fjords					13	82			Cui et al., 2016b
Glaciated Alaskan Fjords					30	1113	5.7×10^5	7.6×10^5	
Chile									
Jacaf Fjord	236	0.28	33.4	40.8	21.0	25.7	5.0×10^3	6.1×10^3	Sepúlveda et al., 2011
Ventisquero Sound	7.2	0.74	69.3	82.5	43.7	52.0	3.1×10^2	3.7×10^2	
Puyuhuapi Fjord	111	0.25	11.0	34.2	6.9	21.6	3.1 x1 0^3	9.6×10^3	
Aysen Fjord	340	0.24	10.5	20.7	6.6	13.1	2.3×10^3	4.4×10^3	
Quitralco Fjord	116	0.47	4.6	55.3	2.9	34.8	3.3×10^2	4.0×10^3	
Cupquelan Fjord	125	0.14	1.9	8.4	1.2	5.3	1.5×10^2	6.6×10^2	
New Zealand									
Milford Sound	25.3	0.268	23.2		18.6		4.7×10^2		Knudson et al., 2011
George Sound	32.9	0.087	3.63		2.90		9.5×10^1		
Thompson Sound	49.3	0.113	10.6		8.48		4.18×10^2		
Nancy Sound	13.9	0.204	32.6		26.1		3.62×10^2		Pickrill. 1993
Doubtful Sound	83.7	0.079	23.2		18.6		1.6×10^3		Smith et al., 2015
Breaksea Sound	61.5	0.038	9.07		7.26		4.5×10^2		
Dusky Sound	181	0.012	2.31		1.85		3.3×10^2		
Long Sound	93	0.094	16.0		12.8		1.2×10^3		
Dusky Sound	181	0.16	44	68	35.2[a]	54.4[a]	6.4×10^3	9.8×10^3	Hinojosa et al., 2014
Doubtful Sound	83.7	0.38	115	169	92[a]	135.2[a]	7.7×10^3	1.1×10^4	
George Sound	32.9	0.10	4.8		3.84[a]		1.3×10^2		
Thompson Sound	49.3	0.06-0.17	15.2		12.16[a]		6.0×10^2		

(**a**) OC Burial rate calculated assuming a burial efficiency of 80% (Smith et al. 2015). (**b**)OC Burial rate calculated assuming a burial efficiency of 63% (Sepúlveda et al., 2005).

Table 3.7 Sedimentation, OC accumulation and OC burial rates for Loch Sunart in comparison to global fjords.

3.8 Discussion: A New Sedimentary C Inventory for Scottish Coastal Waters

The development of this methodology has allowed the estimation of the sedimentary C stocks stored in a mid-latitude fjord. An estimated 26.9 ± 0.5 Mt C has been accounted for within our study site (Loch Sunart). The only directly comparable estimation for sedimentary C stocks is the report by Burrows et al. (2014), where they calculated that 0.3 Mt OC was stored in all 110 Scottish fjords. In comparison, our findings estimate that Loch Sunart alone holds 11.5 Mt OC. However, Burrows et al. (2014) focused on the top 10 cm of sediment because data availability and the lack of a robust methodology made it impossible to calculate the entire sedimentary C stock; this has resulted in a significant underestimation of the quantity of C held within the sediment of these fjords. Additionally, Burrows et al. (2014) did not consider IC to be a major component in these sediments; instead the authors focused on Scottish fjords largely as OC stores. In contrast, our results demonstrate that Loch Sunart stores 15.0 Mt IC in comparison to 11.5 Mt OC. The general lack of IC data for the coastal environment makes it difficult to assess how representative Loch Sunart is of these coastal sedimentary IC stores; however, our results do highlight the potential significance of IC as a major component of sedimentary C stores in these depositional environments. Our results also highlight that fjords in general (Smith et al., 2015) act as an OC rich sediment transition zone between terrestrial and oceanic environments.

Loch Sunart's sediment currently holds 11.5 Mt OC with an additional estimated range of between 1.2 and 89 × 10^3 t of OC buried annually. This highly localised OC trapping in the coastal zone may reduce reworking and remineralisation of the suspended and deposited material which would have otherwise have been released as CO_2 through biotic decomposition processes (Smith et al., 2015).

Globally, terrestrial C stores have received much more attention than their marine counterparts, with significant focus on quantifying forest (Köhl et al., 2015) and soil C stocks (Köchy et al., 2015; Scharlemann et al., 2014). The compilation of known stocks and burial rates of C in the coastal environment by Duarte et al. (2005) highlighted that the coastal ocean constitutes a large store of carbon, which remains poorly understood. The focus of Duarte et al. (2005) was to highlight that the vegetated coastal zones (i.e. salt marsh, seagrass and mangroves) bury and store significant quantities of C and that these stores should be further investigated and recognised in policy outputs. However, they largely overlooked the importance of what they described as depositional areas (estuaries and the shelf sea) as long-term repositories of OC detritus from the vegetated

coastal environment (Krumhansl et al., 2012), and they did not consider terrestrial OC inputs. While the paper recognised that coastal (and shelf) depositional areas are important stores of sedimentary C globally, almost no consideration has been given to how these areas vary in terms of their capacity to store C.

Furthermore, if we consider the range of estuarine environments (e.g. fjord, delta, coastal plain, bar-built and tectonic), it is clear that the characteristics of each type of estuary will impact the manner in which C is buried and stored. For example, the restricted nature of fjords will be conducive to sediment capture and effective C storage when compared to more open estuarine environments which experience greater flushing. Globally, the rates at which fjords accumulate and bury OC is reasonably well defined (Table 3.7). This study adds data for the under-represented mid-latitude fjords which are comparable to other vegetated fjordic systems around the world (Pickrill, 1993; Sepúlveda et al., 2011; Knudson et al., 2011; Hinojosa et al., 2014; Smith et al., 2015). Additionally, for the first time, we cautiously report IC accumulation and burial rates for a fjord. The burial of IC has been overlooked in fjordic systems and requires further investigation to quantify its importance to the broader coastal C cycle.

Our initial work suggests that the sedimentary environments classed as depositional areas by Duarte et al. (2005) could be further expanded upon to include fjords as a separate component, and this recommendation is supported by Smith et al. (2015), who indicated that fjords are “hot-spots for OC burial” and should be considered separately from estuaries when investigating global ocean OC burial. Currently, there are insufficient globally available data to advocate fjords being categorised as a separate component in global coastal C stores; however, the standardised methodology outlined (Fig.3.9) provides a framework to investigate this process further.

At the national level there has been a significant focus on quantifying Scottish soil C stocks, with much attention given to the peatlands (Aitkenhead and Coull, 2016; Bradley et al., 2005; Chapman et al., 2009). Peat and other organic rich soils cover 66 % of Scotland and account for 50 % of all the United Kingdom’s soil C stocks (Cummins et al., 2011). The Scottish peatlands store an estimated total of 1620 Mt C (Chapman et al., 2009) over an area of 17270 km^2, while the other soils hold 2110.9 Mt C over 60215 km^2 (Aitkenhead and Coull, 2016). In comparison to these figures, the quantity of C stored in Loch Sunart is small, but the fjord itself only covers an area of 47.3 km^2. When the fjord’s C density is compared to how effectively Scotland’s soils and peatlands store C (Table 3.6), we can see that, when normalised as a store per unit area basis, Loch Sunart stores

significantly more C than the soils of Scotland. The fjord has a C density of 0.568 Mt C km^{-2} compared to 0.094 and 0.035 Mt C km^{-2} for the peatlands and other soils of Scotland. Our results suggest that Loch Sunart is one of the most effective stores of C in Scotland and highlight the potential of the sediment in these mid-latitude fjords to hold a significant quantity of C. Many of these terrestrial C stores are, of course, vulnerable to rapid and long-term environmental change; the Scottish terrestrial C stocks are at risk from erosion (Cummins et al., 2011) and even fire (Davies et al., 2013), both of which are increasing in extent and frequency because of anthropogenic activities. In comparison, a fjord's geomorphology combined with its depth gives sedimentary C stores a level of protection not afforded to terrestrial C stores. This does not mean that the sedimentary C in sea lochs is invulnerable, but rather that it is buffered from the immediate effects of chemical, biological and physical environmental change during interglacial periods. Over longer time frames these sedimentary stores are scoured out by glacial advances, resulting in the material being transported to the adjacent shelf and slope (Jaeger and Koppes, 2016). Further investigation is required to better understand the processes governing the transfer of material to the shelf and what impact this has on the quality of OC in coastal sediment stores (Smith et al., 2015).

The methodology outlined in this paper provides an analytical framework for calculating the carbon stocks in other fjordic systems, as well as environments with restricted sediment exchange processes such as estuaries, freshwater lakes and artificial systems (e.g. reservoirs and irrigation pools).

3.9 Conclusion

The integration of the geochemical and geophysical techniques outlined provides a robust and repeatable methodology to quantitatively calculate the volume of sediment and make first-order estimations of carbon stored within fjordic sediments. Using this methodology we have shown that Loch Sunart, a fjord on the west coast of Scotland, holds approximately 26.9 Mt C, which is equivalent to double Scotland's CO_2 emissions for 2014. While these individual fjord stores may be small in comparison with Scotland's peatland and soil C stocks, we show they are potentially far more effective stores of both OC and IC than Scotland's terrestrial habitats (area-normalised comparison). The results from this study suggest that the sediment in Scotland's 110 fjords (Edwards and Sharples, 1986) represent a potentially significant, yet currently largely unaccounted for repository of both OC and IC. These fjords act to trap sediment and reduce the remineralisation of OC into the atmosphere. Additionally, the C held within these 110 fjords is likely to represent a significant portion of Scotland's natural carbon capital (natural assets from which humans derive a wide range of services) that has not yet been considered at the marine ecosystem, global C cycle and policy level. Without a better understanding of these globally significant stores of marine sedimentary C, it remains difficult to fully quantify the coastal C cycle. However, evidence suggests that these fjordic environments play an important role in buffering the release of CO_2 through the storage of large quantities of C in these sediments. Future applications of the methodology outlined in this study to different fjord types and locations offer the potential to estimate the fjordic sedimentary C stores at regional, national and global scales through appropriate upscaling.

.

Chapter 4

Source to Sink: Tracing the Origin of Organic Carbon in a Mid-Latitude Fjord

Based Upon: Smeaton, C. and Austin, W.E.N. (2017). Sources, sinks, and subsidies: Terrestrial carbon storage in mid-latitude fjords. *Journal of Geophysical Research: Biogeosciences*, 122.

Author Contributions: Craig Smeaton and William E. N. Austin conceived the research and wrote the manuscript. Craig Smeaton conducted the research as part of his PhD at the University of St. Andrews, supervised by William E. N. Austin, Althea L. Davies and John A. Howe. Craig Smeaton wrote this chapter, expanding on some of the detail provided by Smeaton and Austin, 2017.

4.1 Introduction

The burial and storage of organic carbon in the coastal ocean is a key component of the carbon cycle at both local and global scales (Bauer et al., 2013). Globally, an estimated 276.6 Mt of C is buried in the coastal zone each year, with approximately 126.2 Mt buried in depositional areas, i.e. estuaries and the adjacent continental shelf (Duarte et al., 2005). An improved understanding of the factors regulating these C fluxes and their sources and an ability to account for the carbon stored in these coastal sediments remain important global challenges, with far reaching implications for integrating the coastal ocean into global carbon budgets (Bauer et al., 2013).

A key component of our understanding of the coastal carbon cycle is the growing recognition of significant terrestrial OC subsidies into coastal marine sediments. The proximity of the coastal ocean to the terrestrial biosphere means that both environments have a closely interlinked C cycle. The terrestrial environment is an important source of both particulate (POC) and dissolved (DOC) organic carbon to the coastal ocean (Bianchi et al., 2011). Current global fluvial OC input to the coastal ocean is estimated to be 500 Mt C yr^{-1} with between 30-70 % of this total being utilized biologically or stored in some form in the coastal ocean (Bauer et al., 2013). It has been suggested that the coastal ocean provides an important climate regulating service (Smith et al., 2015) by preventing much of this subsidized terrestrial OC from reaching the continental shelf/open ocean, where the potential for remineralization and loss to the atmosphere as CO_2 is enhanced. While there has recently been progress at the global scale in estimating the magnitude of the OC subsidy provided by the terrestrial environment to coastal sediments, the long-term storage of this OC at the local and regional scales remains poorly constrained. Without a good understanding of these local and regional processes we are unlikely to improve on the current global estimates and, in turn, provide the necessary constraint to quantify the magnitude of terrestrial OC subsidy to the coastal ocean.

Fjords are natural sediment traps at the land–ocean interface and effectively serve to highlight the global importance of the terrestrial OC subsidy to the costal ocean. The burial and long-term storage of OC in fjords is known to be significant (Smith et al., 2015, Smeaton et al., 2016) but, as with the majority of coastal environments, the long-term terrestrial OC subsidy into these systems is poorly constrained. Fjords are known to be global hotspots for OC burial, capturing approximately 11% of the total OC buried in marine sediments annually (Smith et al., 2015). The largely land-locked nature of fjords

and their natural capacity to trap sediment suggests a significant proportion of the buried OC should be of terrestrial origin (OC_{terr}). It has been estimated that 21 ± 16 Mt of OC is buried in fjords annually with approximately 55% of this carbon originating from terrestrial sources (Cui et al., 2016 a). Studies to determine the sources of coastal OC have largely been focused in the high latitude fjords of New Zealand (Smith et al., 2015, Hinojosa et al., 2014, Cui et al. 2016a, b), Chile (Bertrand et al., 2011, Sepulveda et al., 2011, Silva et al., 2011) and Svalbard (Faust et al., 2014, Koziorowska et al., 2016), with only limited data available for mid-latitude fjords (Loh et al., 2008). While these studies show the presence of significant amounts of OC_{terr} in fjordic sediments, the net long-term terrestrial subsidy to coastal sedimentary OC stores over extended (decadal to millennial) time periods remains poorly constrained.

Here we determine the origin(s) of the OC held within the marine sediment of a mid-latitude fjord. In conjunction with total marine sedimentary OC stock estimations (Smeaton et al., 2016) we make a direct comparisons between estimates of postglacial OC_{terr} stored in the fjord sediment and the OC_{terr} held within the soil and living biomass of the adjacent catchment. As in previous studies, we demonstrate a significant mid-latitude OC_{terr} contribution into the sediment stores of the adjacent coastal ocean. However, we also highlight that while significant terrestrial “losses” are generally well known, they remain largely unaccounted for as a net OC subsidy to long-term coastal marine sediment stores. Here we set-out a framework for the quantification of C in adjacent terrestrial and coastal sedimentary environments which helps to highlight the very significant OC_{terr} subsidy received by coastal marine sediments.

4.2 Study Site

Loch Sunart (56.708 , -5.749), a fjord on the west coast of Scotland (Fig.4.1), is one of the longest fjords in Scotland (30.7 km) with a maximum depth of 145 m. The fjord consists of three basins separated by sills at depths of 6 m and 31 m (Gillibrand et al., 2005). In addition, Loch Teacuis a small branch fjord (5.8 km long) connects into the middle and outer basin of Loch Sunart. It has been calculated that Loch Sunart holds 1928.3 ± 7.3 Mt of sediment of which an estimated 9.4 ± 0.2 Mt of postglacial OC is stored (Smeaton et al., 2016).

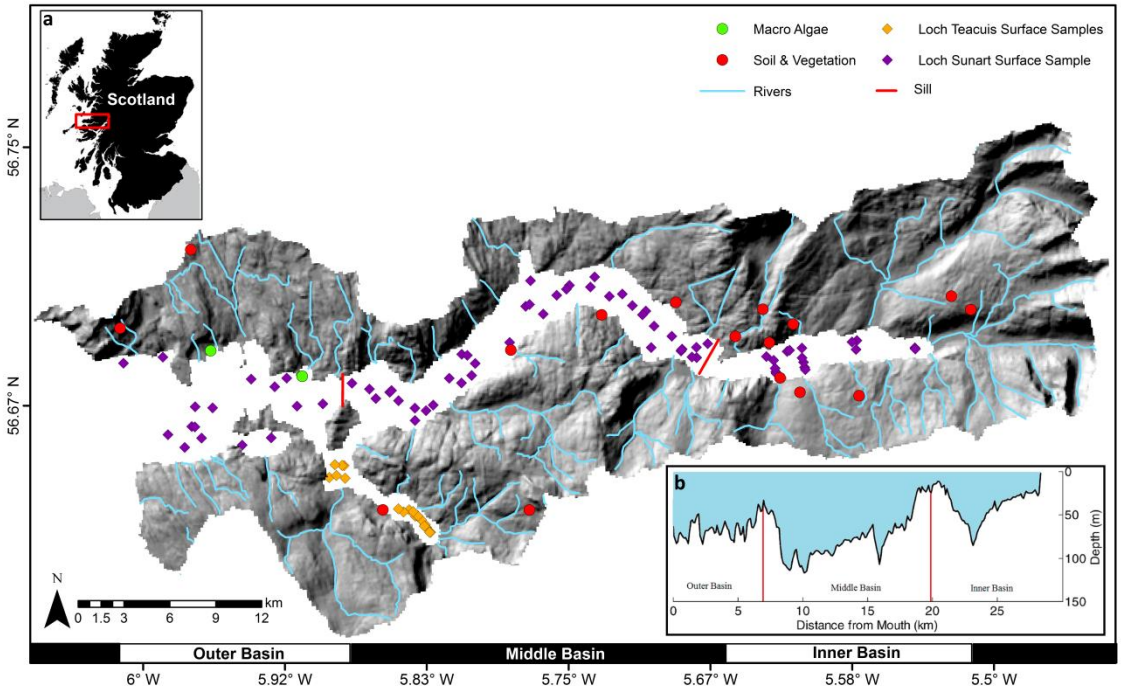

Figure 4.1. Map of Loch Sunart illustrating the topography and drainage network of the catchment. Sampling sites are highlighted: Loch Sunart (purple diamonds), Loch Teacuis (orange diamonds), soil and vegetation (red circles) and macro algae (green circles). (**a**) Overview map illustrating the location of Loch Sunart in context to Scotland (**b**) Bathymetric profile of Loch Sunart developed utilizing data from Bates et al. (2000), Baltzer et al. (2010).

The combined catchments of Loch Sunart and Loch Teacuis cover an area of 299 km^2; the main tributaries of the fjord are the rivers Carnoch and Strontian that both enter Loch Sunart's upper basin; the latter has a mean daily discharge of 1409 x 10^3 m^3 (2009–2013). The catchment is covered by carbon rich soils (Fig.4.2) with 63 % of the soil consisting of peaty gleys (Soil Survey of Scotland. 1981). The mean depth of the soil is approximately 50 cm with an estimated maximum depth of 100 cm (Bibby et al. 1982). The vegetation and land cover is largely dominated by acid grassland, coniferous forest and broad leave woodland (Morton et al., 2011) (Fig.4.2). The catchment geology consists of metamorphic and igneous rocks with minimal input potential from petrogenic/fossil carbon into the local system. The characteristics of Loch Sunart's catchment are similar to most mid-latitude fjords of mainland Scotland (Edwards and Sharple. 1986) and are comparable to systems in New Zealand, Norway and Canada (Syvitski and Shaw. 1995, Howe et al., 2010).

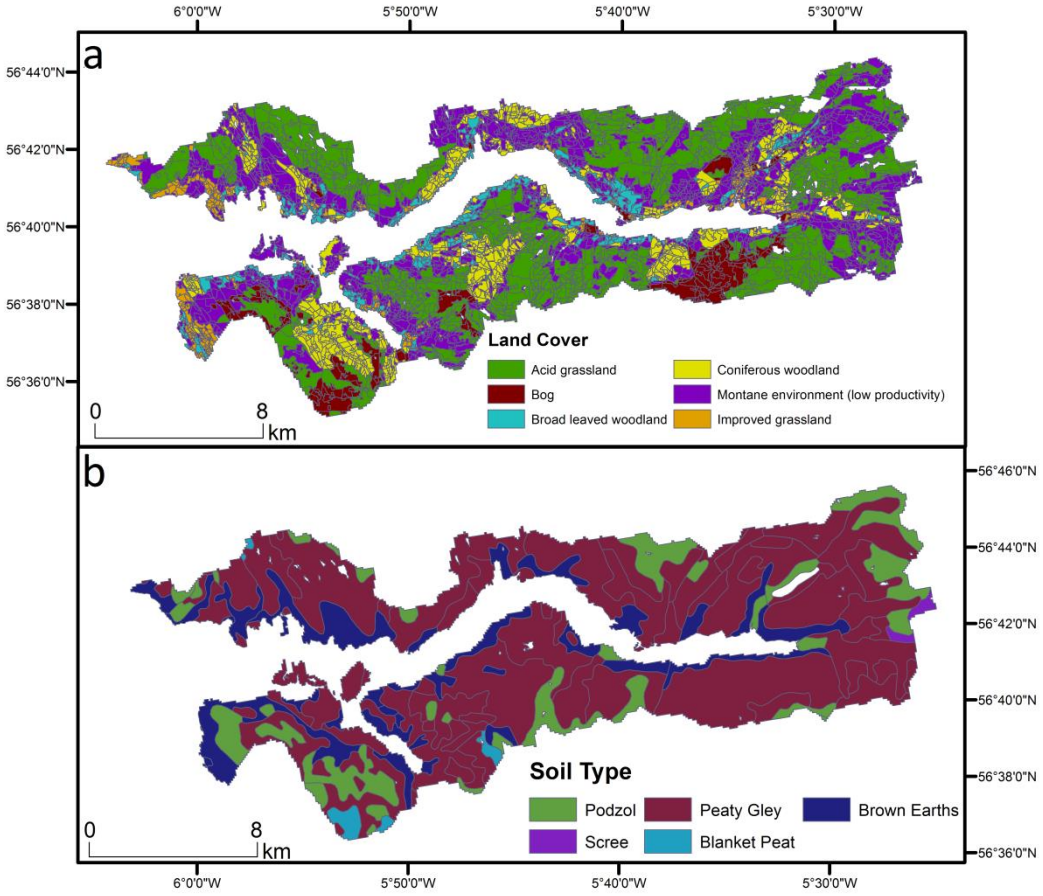

Figure 4.2. Maps illustrating the characteristics of the combined catchment of Loch Sunart and Teacuis. (**a**) Land Cover (Morton et al., 2011). (**b**) Soil Type (Soil Survey of Scotland. 1981).

4.3 Methods

4.3.1 Overview

Bulk elemental data and stable isotope values have extensively been used to identify the source of OC in coastal systems (Thornton and McManus. 1994, Gordon and Goni. 2003, Sepulveda et al., 2011, Silva et al., 2011, Smith et al., 2010, Hinojosa et al., 2014, Cui et al., 2016b). End-member mixing models developed by Thornton and McManus (1994) and further developed by Gordon and Goni (2003) provide a quantitative framework to assess the relative inputs of OC_{terr} and OC_{mar} into marine sediments. These techniques have been furthered by the introduction of Markov chain Monte Carlo (MCMC) methodologies (Li et al., 2014) and standalone Bayesian isotope mixing models (Arendt et al., 2015, Morris et al., 2015). These mixing models use elemental ratios and stable isotope values to separate the terrestrial and marine components; OC_{terr} is isotopically lighter and has a high C:N ratio in comparison to OC_{mar} (Redfield et al., 1963, Peter et al., 1978, Meyers. 1994, Bauer et al., 2013). However caution must be applied to the interpretation of down core data because syn- and post-depositional degradation of different components of OC can alter the isotopic and elemental values of the overall sediment. The gradual downcore loss of labile OC below the sediment surface means that the resultant net OC_{terr} may increase in relative abundance as the more labile OC_{mar} is degraded. For the purposes of this study we focus only on surface samples which are considered to best reflect the primary signal at the sea floor.

4.3.2 Sampling

Surface sediment samples (n= 98) were collected from Loch Sunart and Teacuis using a Van Veen grab sampler from the head to the mouth of each fjord (Fig.4.1). In total 83 samples were collected from Loch Sunart and 15 from Loch Teacuis (Appendix C). Soil and vegetation samples were collected from throughout the catchment (Fig.4.1) to help characterize the range of terrestrial source values used in later modelling. In total, 12 soil samples were collect covering the full range of soil types in the catchment (Fig.4.2). Additionally, eight samples of living and dead vegetation were collected representing the three dominant groups of vegetation (grasses, coniferous, broadleaved woodland) in the catchment. In order to represent the marine source values for macro-algae, samples were collected from Glenborrodale Bay (56.676, -5.906) and Camas Fearna (56.684, -5.960) within Loch Sunart (Fig.4.1). Further samples of phytoplankton, zooplankton and benthic micro-algae were provided by Marine Scotland Science from their sampling/monitoring station in Loch Ewe (57.849, -5.649) in North West Scotland. Detailed description of all samples collected can be found in Table.4.1.

Sample ID	Lat & Long	Description	$\delta^{13}C_{org}$ (‰)	$\delta^{15}N$ (‰)	OC (%)	N (%)	C:N
Soil 1	56.700, -5.687	Gley (Peaty Gleys)	-28.4	4.4	13.18	0.85	18.09
Soil 2	56.702, -5.525	Gley (Peaty Gleys)	-27.7	2.9	38.68	1.82	24.79
Soil 3	56.693, -5.618	Brown Soil (Brown Earth)	-28.0	4.8	13.83	1.19	13.56
Soil 4	56.717, -5.972	Blanket Peat (Dystrophic)	-27.6	2.9	44.22	2.83	18.23
Soil 5	56.633, -5.773	Blanket Peat (Dystrophic)	-27.9	1.9	28.51	1.90	17.51
Soil 6	56.669, -5.579	Gley (Peaty Gleys)	-28.3	2.3	31.03	2.94	12.31
Soil 7	56.695, -5.730	Gley (Peaty Gleys)	-28.1	3.4	17.35	1.59	12.73
Soil 8	56.684, -5.783	Brown Soil (Brown Earth)	-27.9	1.4	40.64	2.50	18.97
Soil 9	56.691, -6.013	Podzol (Humus-iron podzols)	-26.7	7.1	5.05	0.40	14.73
Soil 10	56.675, -5.625	Brown Soil (Brown Earth)	-27.6	5.2	17.26	1.44	13.98
Soil 11	56.675, -5.625	Podzol (Humus-iron podzols)	-27.7	1.9	3.37	0.08	49.15
Soil 12	56.633, -5.859	Brown Soil (Brown Earth)	-27.8	3.8	16.43	1.29	14.86
Veg 1	56.687, -5.632	Coniferous Forest (Mulch)	-29.7	0.3	47.96	1.80	31.09
Veg 2	56.687, -5.632	Coniferous Forest (Needles)	-30.3	1.7	52.34	0.91	67.10
Veg 3	56.671, -5.614	Coniferous Forest (Needles)	-29.6	0.5	51.69	1.20	50.25
Veg 4	56.671, -5.614	Coniferous Forest (Twiggy)	-29.3	1.7	51.41	1.28	46.86
Veg 5	56.689, -5.652	Deciduous Forest (Mulch)	-28.4	-0.2	49.9	2.20	26.46
Veg 6	56.689, -5.652	Deciduous Forest (Leaf Matter)	-28.5	-0.2	49.29	1.95	29.49
Veg 7	56.697, -5.635	Acid Grass	-27.4	4.5	37.12	3.50	12.37
Veg 8	56.697, -5.513	Acid Grass	-27.9	4.3	42.47	4.20	11.80
MacA 1	56.684, -5.960	*Fucus Vesiculosus*	-19.7	5.6	39.04	3.06	14.88
MacA 2	56.684, -5.960	*Fucus Spiralis*	-19.1	6.2	39.14	2.87	15.91
MacA 3	56.684, -5.960	*Fucus Vesiculosus*	-18.5	5.9	38.73	3.02	14.96
MacA 4	56.684, -5.960	*Ulva Compressa*	-18.4	5.9	26.31	2.07	14.83
MacA 5	56.676, -5.906	*Fucus Vesiculosus*	-17.2	5.9	38.62	2.81	16.03
MacA 6	56.676, -5.906	*Silvetia Compressa*	-18.7	6.0	40.32	2.87	16.39
MacA 7	56.676, -5.906	*S. Latissima*	-16.8	6.7	26.63	2.45	12.68
MacA 8	56.676, -5.906	*S. Latissima*	-16.8	6.7	27.9	2.21	14.73
Phyto 1	57.849, -5.649	Bulk Phytoplankton	-21.5	5.4	14.98	2.41	7.25
Phyto 2	57.849, -5.649	Bulk Phytoplankton	-21.4	5.3	13.75	3.15	5.09
Zoop 1	57.849, -5.649	Copepods	-21.9	5.8	48.00	10.41	5.38
Zoop 2	57.849, -5.649	Euphausiids	-20.2	7.2	41.20	10.21	4.71
BMicA	57.849, -5.649	Bulk Benthic Microalgae	-17.4	-1.0	38.01	7.10	6.25

Table 4.1. Detailed description of catchment and marine samples collected to represent the local terrestrial and marine environments with their associated bulk elemental and stable isotope values (relative to VPDB).

4.3.3 Bulk and Stable Isotope Analysis

The surface, catchment and marine samples were analysed to determine bulk elemental and stable isotope values. Each sample was freeze dried and homogenized; approximately 12 mg of processed sediment was weighed out into tin capsules and a further 12 mg was weighed into silver capsules. The samples encapsulated in silver underwent acidified to remove carbonate. After drying for 24 hrs at 40°C, OC and $\delta^{13}C_{org}$ were measured using an elemental analyser coupled to an isotope ratio mass spectrometer (IRMS) at the NERC Life Science Mass Spectrometer Facility (Lancaster, UK). The samples in the tin capsules were analysed for total carbon (TC), total nitrogen (TN) and $\delta^{15}N$ at the same facility. The standard deviation of $\delta^{13}C_{org}$ and $\delta^{15}N$ triplicate measurements (n=15) were 0.07 ‰ and 0.17 ‰ respectively. $\delta^{13}C_{org}$ and $\delta^{15}N$ values are reported in standard delta notation relative to Vienna Pee Dee Belemnite (VPDB) and air, respectively. By analysing $\delta^{15}N$ separately we negate the potential risk of the acid fumigation step altering the $\delta^{15}N$.The quantity of inorganic carbon (IC) in each sample was calculated by subtracting the OC from TC. C:N ratios are reported as molar ratios where C:N= (OC/12)/(TN/14).

4.3.4. Terrestrial and Marine Source Characterisation

For the purposes of the binary mixing model mean values are required for the local terrestrial and marine environments to act as source inputs to the model. To represent the terrestrial environment two source values were calculated; one representing the local soil and vegetation and the second using values derived for land cover over the entirety of Scotland (Thornton et al., 2015). These terrestrial source values are represented by the weighted mean, the weighting for these calculations were produced through examination of soil and land use maps (Morton et al., 2011, National Soil Survey. 1981) (Fig.4.2). The weighting for all calculations are detailed in Table 4.2. Similarly, a representative marine source value was determined by using the phytoplankton, zooplankton, macro algae and benthic micro algae bulk elemental ratio and stable isotope values. In the absence of specific data to constrain these marine source contributions, we assumed that each marine component contributed equally to the marine source value.

Source	Weighting (%)					
	Gley	**Podzol**	**Brown Earths**	**Blanket Peat**		
Soil	62.81	31.44	4.37	1.38		
	Coniferous	**Broad Leave**	**Grass**			
Vegetation	39.27	18.74	41.99			
	Soil	**Vegetation**				
Terrestrial (Soil + Veg)	50	50				
	Broad Leave Woodland	**Coniferous Woodland**	**Montane (Low Productivity)**	**Improved Grassland**	**Rough Grassland**	**Bog**
Terrestrial (Land Cover)	8.12	17.01	18.2	4.54	44.59	7.54
	Macro Algae	**Phytoplankton**	**Zooplankton**	**Benthic Microalgae**		
Marine	25	25	25	25		

Table 4.2. Weightings (%) that were applied to calculate weighted means for each of the source values used in the mixing models. Data derived from the UK Land Cover Map 2007 (Morton et al., 2011) and Scotland's soil map (Soil Survey of Scotland. 1981).

The Bayesian mixing model can deal with additional source values and we have therefore split the terrestrial source mean value into its constituent components (i.e. soil and vascular plants). The soil source value was calculated to represent the distribution of soil types within the catchment; the weighting to calculate this mean source value was determined from values quoted in the National Soil Survey (1981). In addition, the weightings to calculate the vascular plant source value was produced through examination of the 2007 land cover map (Morton et al., 2011). The marine source value for the binary mixing model was also used with the Bayesian model approach.

4.3.5 End-Member Mixing Modelling

Initial analysis was carried out using a simple binary (or 2 end-member) mixing model designed to discriminate between OC_{terr} and OC_{mar} based upon the work of Thornton and McManus. (1994). $\delta^{13}C_{org}$ values and C:N ratios were used separately as tracers and applied to the mixing model (Equation. 1,2 and 3) to calculate the fraction of OC_{terr}.

Fraction $OC_{terr} = (\delta^{13}C_{mar} - \delta^{13}C_{terr}) / (\delta^{13}C_{mar} - \delta^{13}C_{sample})$
Fraction $OC_{terr} = (C{:}N_{mar} - C{:}N_{sample}) / (C{:}N_{mar} - C{:}N_{terr})$
Fraction OC_{terr} + Fraction $OC_{mar} = 1$

These equations were augmented by the application of Markov Chain Monte Carlo (MCMC) simulations to source variability in endmembers (Andersson. 2011, Li et al., 2014). The MCMC simulations were performed in the OpenBUGS software package (Lunn et al., 2009). Simply, 1,000,000 out of 100,000,000 random samples from a normal distribution of each end-member were taken to simultaneously populate the mixing models (Equation. 1 to 3). Through this process a significant number of solutions are generated which follow a normal distribution. The mean, range (minimum and maximum) and standard deviation of source contributions were calculated for each sample from the MCMC solutions available.

The binary mixing model approach was expanded upon using the open source Bayesian isotope mixing model FRUITS (Fernandes. 2014). Bayesian models overcome some of the problems of the simpler models discussed above. These models integrate MCMC simulations throughout the process and are capable of using multiple tracers (isotopic and non-isotopic); in this study $\delta^{13}C_{org}$, $\delta^{15}N$ and C:N ratios were jointly utilized as tracers. This approach enabled the estimation of the proportional contribution of terrestrial and marine derived OC and provided a direct comparison with the simpler binary models. We assumed that no isotope discrimination occurred between the source and incorporation into the surface sediment. We also assumed that the source values selected are representative of the entire region covered by the study. Work by Gordon and Goni (2003) showed that it was possible to split the terrestrial OC into inputs from soil (OC_{soil}) and vascular plants (OC_{vp}). However, the similarity of isotopic values of the terrestrial material within the study region make it difficult to separate the OC_{soil} and OC_{VP} components; for this reason a Bayesian approach was preferred over the standard 3-end-member mixing model (Gordon and Goni. 2003). To assure the quality of model outputs the best practices outlined by Phillips et al. (2014) were followed. The outputs

from the mixing models were used to spatially map the distribution of OC from different sources. The mapping was undertaken using a Kriging (with linear interpolation) gridding technique (Cressie. 1990).

4.3.6 Terrestrial and Marine OC Stocks and Burial

To determine the OC held in the soil and living biomass of the catchment we utilized the outputs from the Countryside Survey 2007 (Henrys et al., 2012, 2016). The data from this survey allows for catchment specific estimates of soil (top 15 cm) and above ground living carbon (Fig.4.3). Using Bibby et al. (1982) soil depth estimations (mean = 50 cm) for the region, we estimated the total OC stock held within the catchment.

The combination of the mixing model outputs allow, the OC_{terr} stock estimations for the top 15 cm (Fig.4.3) and postglacial sediment as a whole (Smeaton et al., 2016) to be derived. This calculation assumes that the OC_{terr} in the surface sediments is representative of the entire postglacial sediment sequence. In reality, the OC_{terr} input, burial and preservation will have changed through the postglacial period but, by assuming the modern sediments are characteristic of the postglacial sediment, we have been able to make first-order estimations of OC_{terr} content in the sediment.

The calculated OC stocks allow a like for like comparison of both the surface marine sediments and catchment soils (0 – 15 cm), as well as the OC_{terr} store (catchment vs fjord) as a whole. Additionally, through a normalization process according to the area of the postglacial store, a calculation of how effectively each environment stores OC_{terr} (terrestrial OC density) can be made.

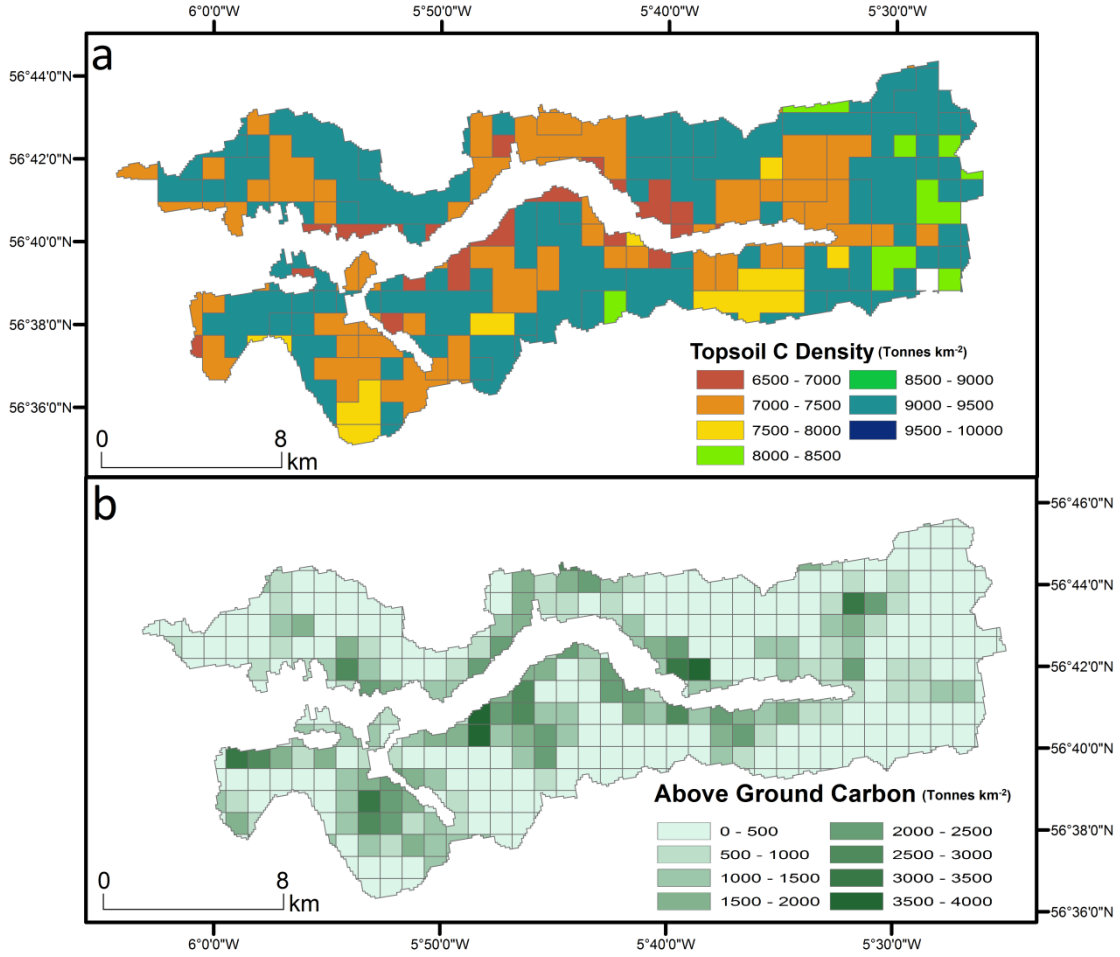

Figure 4.3. Maps illustrating (**a**) the topsoil carbon density (0 - 15 cm) (**b**) above ground carbon (living biomass). Maps produced from data collected for the Countryside Survey 2007 (Henrys et al,. 2012, 2016).

4.3.7 A Framework to Conceptualize OC_{terr} Subsidies.

We have used the methodology described above to estimate the quantity of OC_{terr} held in the surface sediments of the loch, as well as the living biomass and the topsoil of the catchment. To understand the OC_{terr} subsidies between terrestrial and coastal marine environments, there is also a need to better understand the transfer of OC from the catchment and the fate of that OC within the fjord. While a complete understanding of the fate of OC within the fjord environment is beyond the scope of this study, the burial of OC_{terr} can be calculated by combining the estimated proportion of OC_{terr} with the

previous estimated OC burial rates for Loch Sunart (Smeaton et al., 2016), these rates represent how much OC is buried annually and take into account the total OC lost during the burial process. To estimate how much OC is lost from the catchment we have used land cover data (Table.4.3) and regional soil erosion rates for each land cover type from the wider literature (Table 4.4)

Land Cover	Proportion of Catchment (%)	Area (km^2)	Minimum C (%)	Maximum C (%)
Woodland	25.13	75.14	13.18	31.03
Upland Heath	18.2	54.42	3.37	5.05
Improved Grassland	4.54	13.57	5.05	17.35
Grassland	44.59	133.32	5.05	17.35
Bog	7.54	22.54	28.51	44.22
Arable	0	0.00	-	-

Table 4.3. Catchment land cover (Morton et al., 2011) with associated carbon concentrations.

To validate this approach two checks were employed, first, we determined the loss of OC through the fluvial system (rivers and runoff) using the methodology set-out by Loh et al. (2008)(Equ. 4-7) combined with flow (Payne et al., 1989), catchment (Edwards and Sharples 1986) and soil C data from this study to estimate mean river discharge and OC loading.

$$\text{Fluvial Soil Export (g d}^{-1}\text{)} = \text{River Discharge (m}^3\text{ d}^{-1}\text{)} \times \text{Particle concentration (g m}^{-3}\text{)} \quad (4)$$

$$\text{Fluvial C loss (g d}^{-1}\text{)} = \text{Fluvial Soil Export (g d}^{-1}\text{)} \times \text{Carbon concertation (\%)} \quad (5)$$

$$\text{Annual C Loss (g)} = \text{Fluvial C loss (g d}^{-1}\text{)} \times 365 \quad (6)$$

$$\text{Annual C Loss (tonnes)} = \text{Annual C Loss (g)} \times 1000000 \quad (7)$$

Secondly the Revised Universal Soil Loss Equation (RUSLE) model (Panagos et al. 2015) was utilized to determine the potential soil erosion by water for the catchment. Through comparison of the fjord and catchment data we can begin to understand the linkages between the two environments in terms of OC supply and delivery. Despite the qualitative nature of this framework, it allows an opportunity to conceptualize the processes that govern the subsidy of OC_{terr} from the terrestrial to the adjacent coastal environment.

Land Cover	Soil Erosion Rate ($t\ km^{-2}\ yr^{-1}$)	Reference
Woodland		
Woodland	7	*Panagos et al.* [2015]
Disturbed Forest	10	*Borrelli et al.* [2016]
Disturbed Forest	6	*Borrelli et al.* [2016]
Undisturbed Forest	5.4	*Borrelli et al.* [2016]
Undisturbed Forest	4	*Borrelli et al.* [2016]
Upland Heath		
No Management (Average)	200	*Grieve et al.* [1994]
Forested	1300	*Grieve et al.* [1994]
Sheep Grazing	3400	*Grieve et al.* [1994]
Burning (Low)	600	*Grieve et al.* [1994]
Burning (High)	2600	*Grieve et al.* [1994]
Improved Grassland		
Improved Grassland	269	*Panagos et al.* [2015]
Pasture	202	*Panagos et al.* [2015]
Grassland		
Grassland	235.50	*Panagos et al.* [2015]
Pasture	202	*Panagos et al.* [2015]
Ley Grassland	114	*Knox et al.* [2015]
Bog		
North Esk	25	*Ledger et al.* [1974]
Hopes Reserviour	26	*Ledger et al.* [1974]
Glenfarg	26	*McManus and Duck.* [1985]
Glenfarg	31	*McManus and Duck*. [1985]
Earlburn	68	*Duck and McManus.* [1990]
North Third Reservoir	205	*Duck and McManus.* [1990]
Carron Valley	142	*Duck and McManus.* [1990]

Table 4.4 Land cover specific soil erosion rates from the literature.

4.4. Results

4.4.1 Bulk and Stable Isotope Analysis

Bulk elemental data show a clear distinction between the quantities of OC and IC held in the sediment of each sub-basin of the fjord. The quantity of OC in the surface sediment of Loch Sunart ranges from 8.86% to 0.35% declining in a seaward direction away from the head of the fjord. The sediment in the inner basin contains the most OC with a mean value of 3.07 ± 2.3%, declining to 2.11 ± 1.81% and 1.51 ± 0.98 for the middle and outer basins, respectively. Loch Teacuis's sediment has a mean value of 4.74 ± 1.72%. The quantity of IC in each basin in negatively correlated with the OC with sedimentary IC increasing in a seawards direction. The average C:N ratios were calculated for Loch Sunart (11.36 ± 5.64) and Loch Teacuis (11.22 ± 1.98).

Stable isotope ratios from the OC in surface sediments show a transition from isotopically depleted $\delta^{13}C_{org}$ signatures in the inner basin to more enriched values in the middle and outer basins (Fig.4.4). Samples from Loch Teacuis have depleted $\delta^{13}C_{org}$ values mirroring that of the inner basin of Loch Sunart. Sediment OC:N ratios remain consistent throughout the loch, but show greater variability in the inner basin of Loch Sunart. Similarly the $\delta^{15}N$ values of Loch Teacuis closely match that of the inner basin of Loch Sunart. The average $\delta^{13}C_{org}$ value for the fjord was -22.4 ± 1.1 ‰ for $\delta^{13}C_{org}$ and 6.4 ± 0.7 ‰ for $\delta^{15}N$. When compared to values from fjords around the world the $\delta^{13}C_{org}$ values appear typical, but $\delta^{15}N$ values are significantly more enriched than those reported from other fjord sediments (Table.4.5), likely due to a greater than average OC input from marine sources.

Fjord	Location	$\delta^{13}C_{org}$ (‰)	$\delta^{15}N$ (‰)	Reference
Loch Sunart	United Kingdom (Scotland)	-22.4 ± 0.1	6.4 ± 0.7	*This Study*
Inner Basin		-24.4 ± 0.5	6.1 ± 0.6	
Middle Basin		-22.6 ± 1.2	6.4 ± 0.7	
Outer Basin		-21.4 ± 1.8	6.6 ± 0.7	
Loch Teacuis		-24.8 ± 0.6	6.2 ± 0.7	
Loch Creran	United Kingdom (Scotland)	-24.7 to -21.3		*Loh et al.* [2008]
Loch Etive		-25.8 to -25.7		
Nordasvannet Fjord	Norway (Mainland)	-23.9		*Muller.* [2001]
Trondheimsfjord		-23.0 ± 1.1		*Fauest et al.* [2014]
Hornsund	Norway (Svalbard)	-24.45 ± 0.31	4.00 ± 0.48	*Koziorwska et al.* [2016]
Adventfjord		-25.16 ± 0.40	2.83 ±0.97	
Kongsfjord		-21.6 to -23.9		*Kulinski et al.* [2014]
Saguenay Fjord	Canada	-26.7 to -25.9	*St-Onge and Hillaire-Marcel.* [2001]	
Clayoquot Sound		-27.04 to -22.58		*Nuwer and Keil*.[2005]
Fiordland	New Zealand	-28.7 to -24.7		*Smith et al.* [2010]
		-25.10 ±2.59	4.55 ± 2.59	*Hinojosa et al.* [2014]
		-27.82 to -23.50		*Cui et al.* [2016a]
		-28.1 to -23.3		*Cui et al.* [2016b]
Norther Patagonia	Chile	-28.2 to -19.1	1.3 to 9.0	*Sepulveda et al.* [2011]
		-26.7 to -20.1		*Silva et al.* [2011]
Southern Patagonia		-22.1 to -19.7		*Silva and Prego.* [2002]

Table 4.5. Surface sediment $\delta^{13}C$ and $\delta^{15}N$ isotopic values (relative to VPDB) for Loch Sunart (broken down by basin) and Loch Teacuis. Listed for comparison are published equivalent isotopic values from the surface sediment of fjords around the world.

The results of the bulk elemental and stable isotope analyzes of the catchment and marine samples collected as source values for the mixing models are outlined in Table.4.1. As expected, the samples fall into two groups representing the terrestrial (soil and vegetation) and marine (phytoplankton, zooplankton, benthic micro algae and macro algae) environments (Fig.4.4).The marine sediment samples themselves fall between these two groups, suggesting a mixture comprised from these sources.

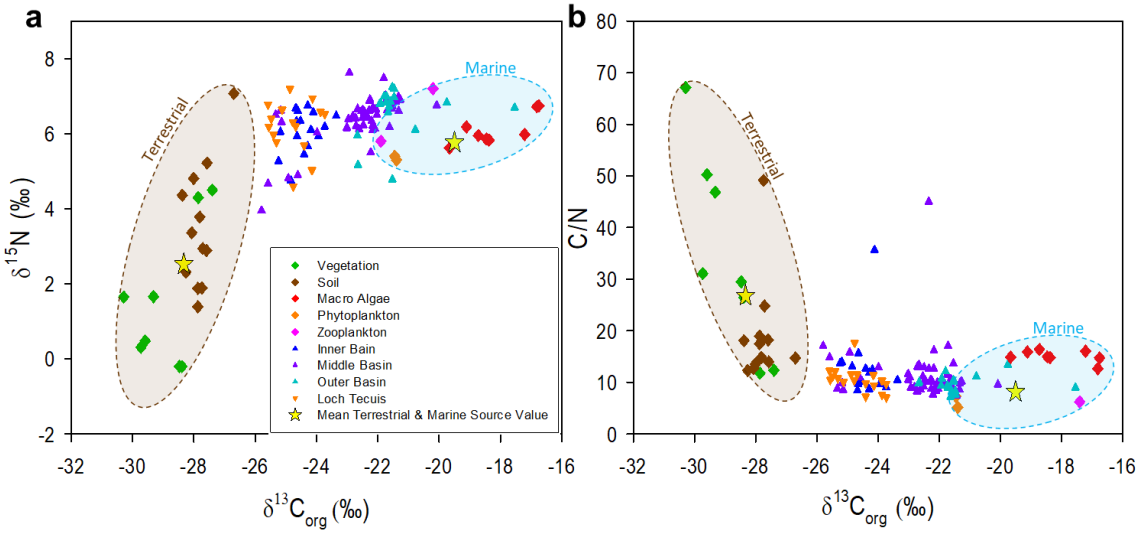

Figure 4.4. Cross plots (**a**) $\delta^{13}C_{org}$ versus $\delta^{15}N$ (**b**) $\delta^{13}C$org versus C:N in surface sediment of Loch Sunart and Tecuis with the shaded envelopes illustrating the range of the terrestrial and marine source values. Additionally, OC data from the grab samples show a relationship between the composition of the OC and the salinity gradient within the fjord (Fig.4.5).

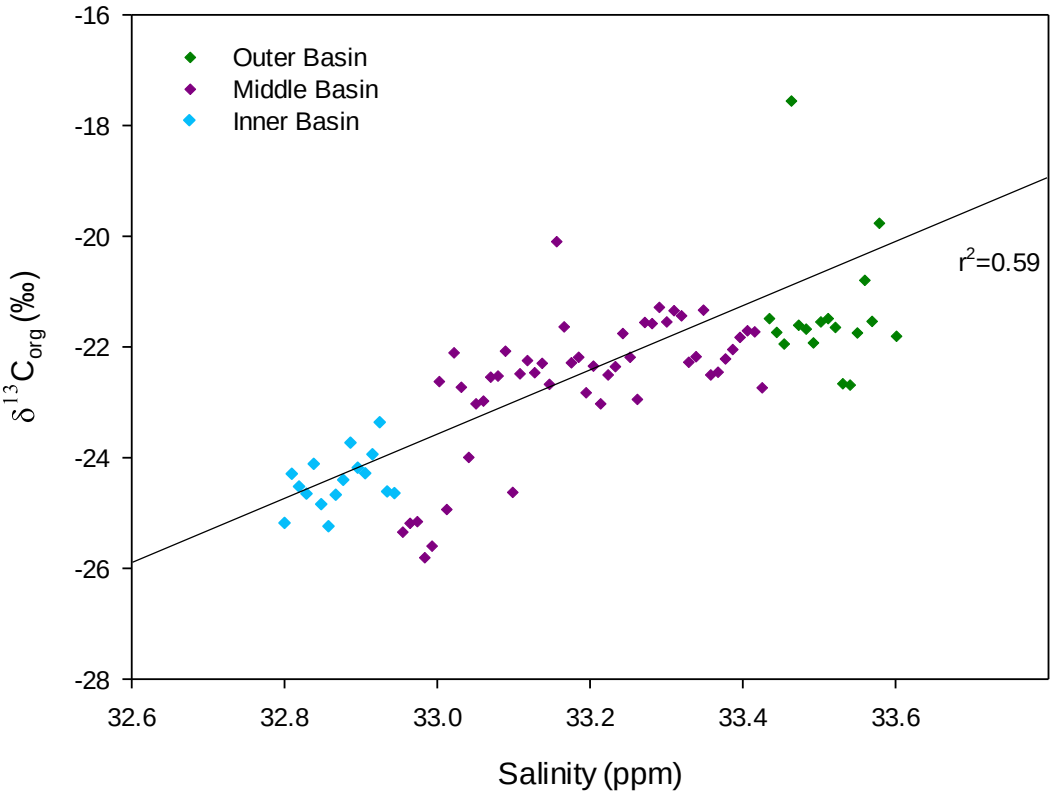

Figure 4.5. Cross plot illustrating $\delta^{13}C_{org}$ (‰) versus Salinity (ppm) of bottom water for each of the grab samples grouped by basin.

4.4.2 End-Member Mixing Model

4.4.2.1 OC Source Characterization

Each source was characterized and assigned a $\delta^{13}C_{org}$, $\delta^{15}N$ and C:N value (Table.4.6) which was utilized in both the binary and Bayesian mixing models. The composite marine source value corresponds well to other studies (Thornton and McManus. 1994, Cloern et al., 2007, Sepulveda et al., 2011, Hinojosa et al., 2014). The two methods of calculating the terrestrial source value have resulted in similar $\delta^{13}C_{org}$ and $\delta^{15}N$ values but the % OC and % N do vary significantly resulting in different C:N ratios. Despite differences between the methods, both results yield values which fall within the ranges found in the literature (Faganeli et al., 1988, Thornton and McManus. 1994, Mcleod et al., 2010, Sepulveda et al., 2011, Silva et al., 2011 Hinojosa et al., 2014). The values assigned to the soil match those found in the literature for Scottish soils in this region (Ficken et al., 1998, Schmidt et al., 2005). The values assigned to the vegetation source are consistent with grasses, coniferous and broadleaved trees (Cloern et al., 2007, Smith et al., 2010, Sepulveda et al., 2011, Silva et al., 2011).

Source	$\delta^{13}C_{org}$ (‰)	$\delta^{15}N$ (‰)	OC (%)	N (%)	C:N
Soil	-27.9 ± 0.4	3.5 ± 1.8	20.51 ± 8.52	1.46 ± 0.65	20.17
Vegetation	-28.6 ± 0.4	2.2± 2.4	45.97 ± 0.39	2.51 ± 0.01	29.47
Terrestrial (Soil +Veg)	-28.3 ± 0.7	2.5 ± 1.8	35.11 ± 9.56	1.84 ± 1.02	26.75
Terrestrial (Land Cover)	-28.1 ± 0.1	3.0 ± 0.2	18.54 ± 1.6	0.99 ± 0.07	25.79
Marine	-19.5 ± 0.6	4.2 ± 0.4	32.89 ± 3.01	5.36 ± 0.30	8.14

Table 4.6. Source type and their end-member values as used with mixing models.

4.4.2.2 End Member Mixing Modelling

The binary and Bayesian mixing models were run to determine the fraction of OC_{terr} within each of the surface samples. Each model was run separately with the terrestrial sources values derived from land cover and the composite soil/vegetation data (Table.4.6). The results produced using the different source values were combined to calculate the percentage of OC_{terr} within each sample. The average quantity of OC_{terr} was calculated for Loch Teacuis and each basin of Loch Sunart and the loch as a whole (Table.4).

Tracer	Inner Basin	Middle Basin	Outer Basin	Loch Sunart	Loch Teacuis
Two – End Member Model					
$\delta^{13}C_{org}$	58.6 ± 11.0	37.2 ± 12.2	23.8 ± 12.7	34.8 ± 12.3	63.1 ± 10.8
C:N	52.6 ± 24.7	45.1 ± 23.0	36.2 ± 20.7	42.7 ± 22.4	49.4 ± 23.9
Bayesian End Member Model					
$\delta^{13}C_{org}$, $\delta^{15}N$, C:N	61.4 ± 7.6	41.8 ± 9.8	36.1 ± 11.4	42.0 ± 10.1	64.8 ± 5.2

Table 4.7. Percentage of terrestrially derived OC held within the sediment of Loch Sunart and Loch Teacuis broken down by basin and mixing model.

The nature of the Bayesian model (i.e combining multiple tracers and MCMC integration) means that we have high confidence in the results; further supported by the binary mixing model results (Table.4.7). For the purposes of this study we have therefore used the Bayesian model results to assess the subsidy of OC_{terr} into the marine sediments of Loch Sunart. The greatest amount of OC_{terr} is found in the inner basin decreasing in the middle and outer basins. An estimated 42% of the OC in the surface sediment of Loch Sunart is terrestrial in nature, while 65% of Loch Teacuis's sediment originates from terrestrial sources. These subsidies are comparable to those reported by Cui et al. (2016a) who estimated that 55% of OC entering fjords globally is terrestrial in origin. However when spatially mapped there is a clear transition from the terrestrially dominated inner basin through to the largely marine influenced outer basin of the fjord (Fig.4.6). Our mapping also illustrates the similarity of OC_{terr} in the highly constricted Loch Teacuis and the inner basin of Loch Sunart. High quantities of OC_{terr} are found locally in the middle basin of Loch Sunart; these hotspots occur at the mouth of larger streams. More generally, there is likely to be diffuse OC_{terr} input down the length of fjord from non-point sources (i.e. hillside runoff) and from advective processes within the water column.

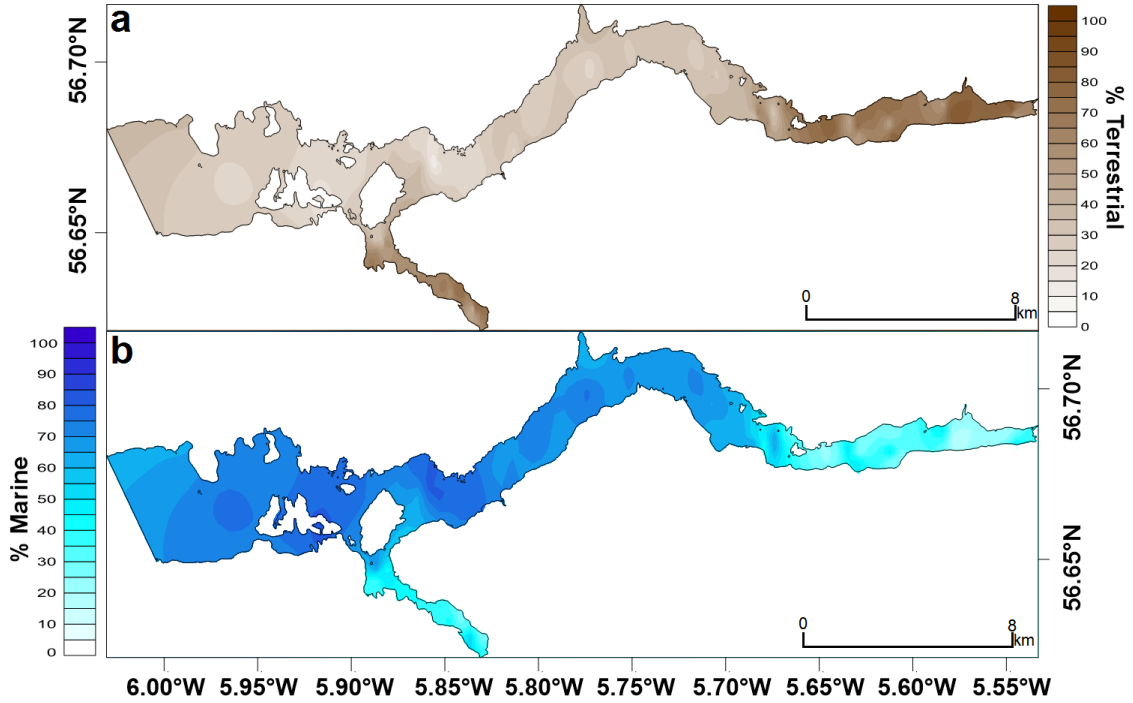

Figure 4.6. Modeled spatial distribution of (**a**) % terrestrial derived OC (**b**) % marine derived OC within the surface sediment of Loch Sunart and Loch Teacuis.

4.4.3 Terrestrial and Marine OC Stocks

By combining the postglacial stock (9.4 ± 0.2 Mt OC) and burial rate estimations (1.89-25.68 g m^{-2} y^{-1}) for Loch Sunart (Smeaton et al., 2016) with the % OC_{terr} calculated from this study (42.0 ± 10.1 % OC_{terr}) we estimated that the postglacial sediments hold 3.96 ± 0.1 Mt OC_{terr} with a further estimated 737 tonnes OC_{terr} being buried annually. We calculated the quantity of OC held in the living biomass of the catchment to be 0.28 Mt and estimated the soil OC content at 7.97 Mt OC; the catchment has a whole holds 8.25 Mt OC. Area normalized totals were calculated (Table.4.8) which show not unexpectedly that Loch Tecuis, as the most land locked location is the most effective at storing OC_{terr} followed by the inner basin of Loch Sunart (Fig.4.7).

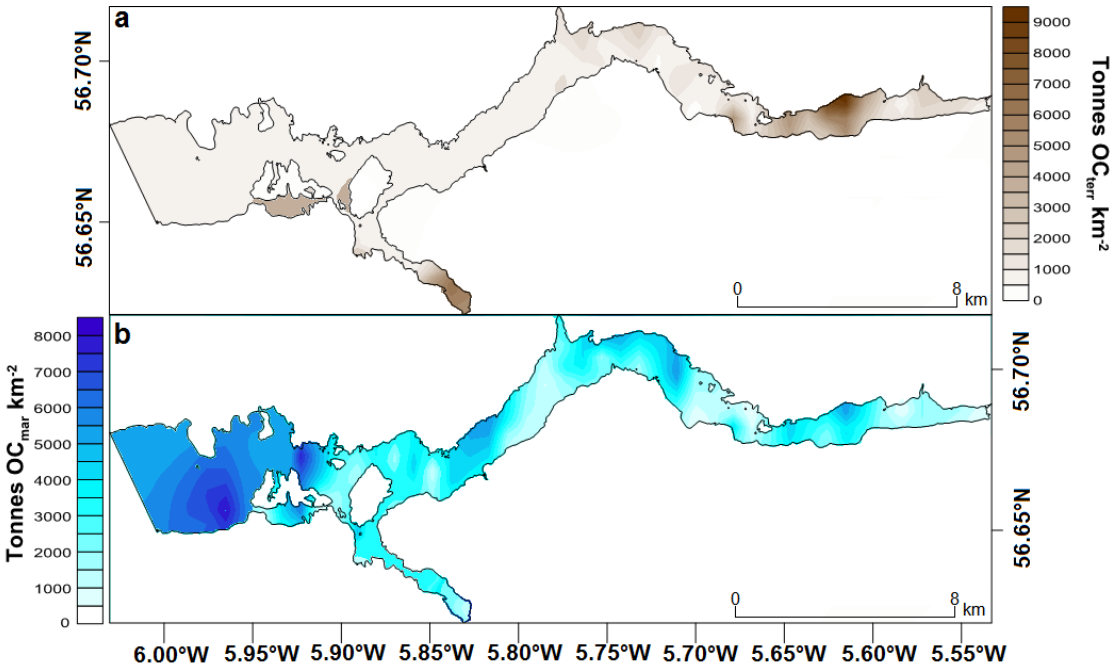

Figure 4.7. Area normalized (**a**) OC_{terr} (**b**) OC_{mar} stock estimations (tonnes OC km^{-2}) for the surface sediments (0 – 15 cm) of Loch Sunart and Tecuis.

When the depth integrated estimates of OC_{terr} stocks are area normalized, our results show that despite the significantly greater quantity of OC_{terr} held within the catchment the fjord sediments area a more effective store of OC_{terr}.

	Area (km^2)	Total OC (Mt)	Terrestrial OC (Mt)	Terrestrial $OC_{density}$ (Mt OC_{terr} km^{-2})
Catchment: Topsoil (Top 15 cm)	299		2.39	0.008
Catchment: Topsoil (50 cm)[a]	299		7.97	0.027
Catchment: Living Biomass	299		0.28	0.001
Catchment (Soil + Living Biomass)	**299**		**8.25**	**0.028**
Loch Sunart (Top 15 cm)	47.3	0.23	0.10	0.002
Inner Basin (Top 15 cm)	5.5	0.03	0.02	0.004
Middle Basin (Top 15cm)	24.7	0.15	0.06	0.003
Outer Basin (Top 15cm)	17.1	0.05	0.02	0.001
Loch Teacuis (Top 15cm)	2.2	0.02	0.01	0.005
Loch Sunart (Postglacial Sediment)[b]	**47.3**	**9.4**	**3.96**	**0.084**

a Calculated by applying surface soil OC values [Henry et al. 2012, Henry et al. 2016] to soil depth data (Bibby et al. 1982).

b Calculated by applying surface OC values to the postglacial sediment as quantified in Smeaton et al. (2016).

Table 4.8. Calculated OC and OCterr carbon stocks for the sediment and adjacent catchment of Loch Sunart. Additionally, the area normalized totals are listed indicating how effectively each environment stores OC.

4.4.4 First-order OC_{terr} Subsidy Estimates

This work has calculated that Loch Sunart's surface sediments (top 15cm) hold 0.1 Mt OC_{terr} (Table 4.8) and that an estimated further 737 tonnes OC_{terr} is added annually into this store. Through the use of the RULSE model (Fig.4.8) and fluvial C export calculations (fully detailed in Appendix C) we estimate that between 7,500 and 15,000 tonnes OC is lost annually from the catchment's soil. When used in conjunction with the fjord burial rates we calculate that between 5 to 10 % of the OC lost from the catchment is buried in the sediment. The additional ~ 90 % of missing OC_{terr} could be removed from the system through multiple pathways (Fig.4.9). The primary processes most likely to account for this missing OC_{terr} are (**i**) some of the OC_{terr} export may be in a dissolved rather than particulate form (Bianchi et al., 2011, Bauer et al., 2013), (**ii**) some of the eroded soils may not reach the fjord and may be deposited within the catchment (e.g. floodplains) (Wang et al. 2014), (**iii**) some of the OC_{terr} may be degraded and lost to the atmosphere during transport in the fluvial system (Dinsmore et al., 2013, Leith et al., 2015), within the water column of the fjord (Burt et al., 2013) and within the sediment itself (Arndt et al., 2013, Glud et al., 2016), (**iv**) some of the OC_{terr} may be exported

further offshore to the continental shelf and beyond (Haas et al., 2002, Bischoff et al., 2016, Painter et al., 2016) bypassing the coastal sediment. It is likely that other fjords may be more efficient traps of OC_{terr} than these results suggest; we know that Loch Sunart does not suffer from periods of water column hypoxia (Gillibrand et al., 2006) and the absence of this OC preservation mechanism likely results in lower OC_{terr} preservation in comparison to sites with hypoxic conditions (Woulds et al., 2007, Middelburg and Levin, 2009). Therefore, while certain process may both under and overestimate certain aspects of annual OC_{terr} gains and losses from the catchment to the fjord sediments, they do serve to provide an overview of OC_{terr} subsides to the coastal ocean.

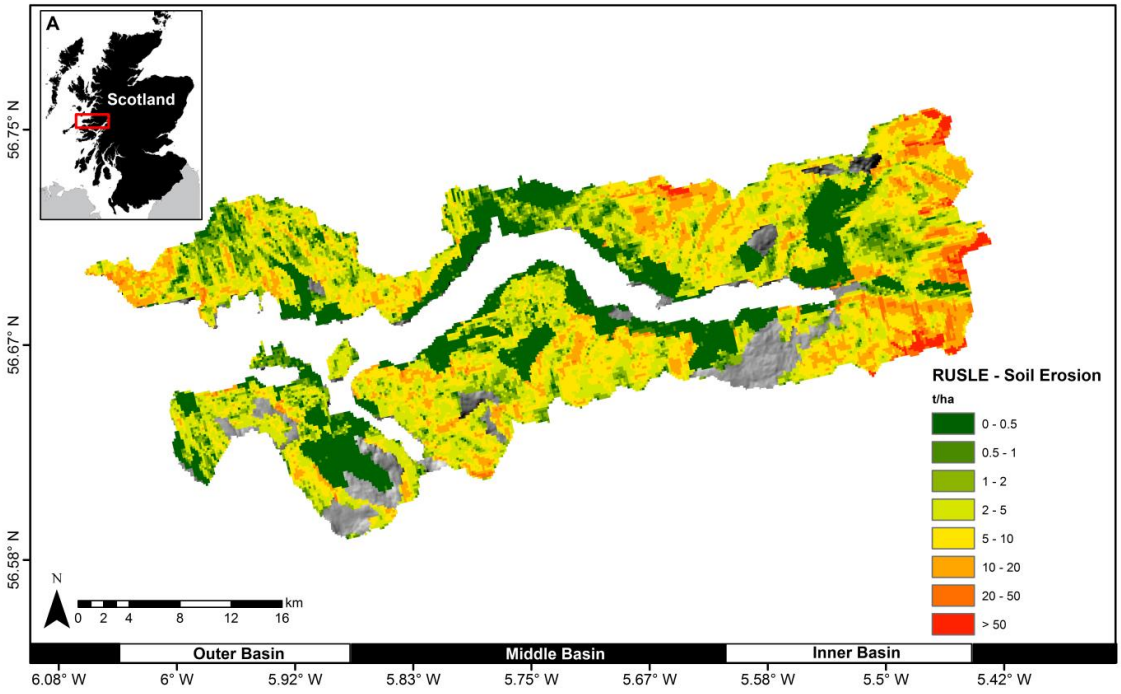

Figure 4.8. RULSE2015 model (Panagos et al., 2015) output for Loch Sunart's catchment illustrating the potential loss of soil caused through hydrological erosion.

The terrestrial subsidy of C into long-term marine sediment storage is far from being an efficient or straight-forward burial process (Fig.4.9). The fertilization of the coastal ocean through the input of OC_{terr} can result in increased primary production (Bianchi et al., 2011, Bauer et al., 2013) and, when combined with the high sedimentation rates found within fjords, creates a secondary, indirect pathway for OC_{terr} storage in these coastal

sediments. The mechanisms that regulate this system are well characterized (Burd et al., 2016), yet rates of exchange between these C pools are still poorly understood. For example, work focusing on a shallow coastal system estimated that >25% of the OC_{mar} reaching the sediment could be attributed to OC_{terr} fertilization of the marine system (Watanabe and Kuwe. 2015). While the typically deeper water depths found in fjords may reduce this estimate, it is clear that this process potentially provides an indirect secondary pathway for OC_{terr} to reach coastal marine sediment stores.

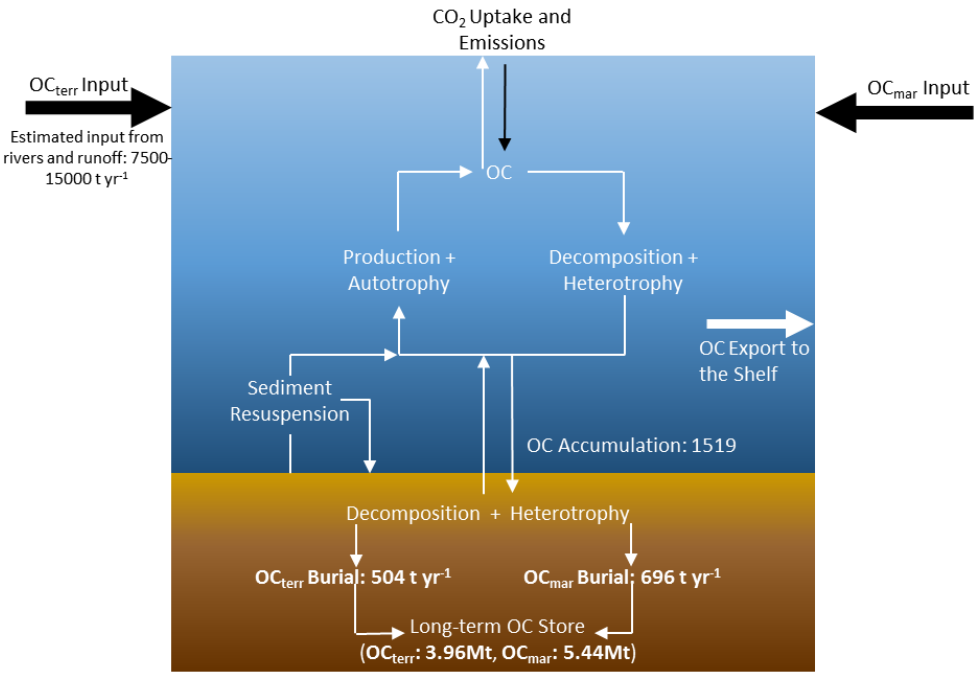

Figure 4.9. Conceptual diagram highlighting the pathways (white arrows) through which the OC input from external sources (black arrows) are processed within the water column and sediment of a fjord. Additionally, the mean values for soil erosion (t yr^{-1}), OC accumulation (t yr^{-1}) and burial (t yr^{-1}) calculated for Loch Sunart and its catchment are shown.

4.5. Discussion

The results of this study serve to highlight the important role that the terrestrial environment plays in contributing C to coastal sedimentary systems. We have estimated the quantity OC_{terr} stored in coastal marine sediment and compared it to that of the adjacent catchment. The results indicate that on a like for like basis (i.e. 0-15 cm) the catchment soil stores a greater amount of OC_{terr} than the marine sediment; similarly, the living biomass within the catchment holds more OC_{terr}. This is, of course, expected because both the soil and living biomass are wholly terrestrial in nature while the marine sediments have OC inputs derived from both the terrestrial and marine environment. While the living biomass of the catchment itself holds more OC_{terr} when normalized for area, the marine sediment is a more effective store of OC_{terr} (Table.4.8). Taking into consideration the full postglacial depth extent of these stores, the soils remain the largest store of C, but our results suggest that the coastal marine sediments provide a more effective long-term store of OC_{terr} than the adjacent terrestrial environment. Any direct comparison of these stores must consider their longevity as effective C stores. Storage potential varies significantly from short-term storage within the living biomass (days to decades) to the long-term storage of OC in soils and marine sediments (10^3 yrs). A further important and underreported consideration is the long-term stability of these stores. The terrestrial stores are vulnerable to short and long-term environmental change such as soil erosion (Cummins et al., 2011) and fire (Davies et al., 2013), both of which are increasing in regularity with growing climatic and anthropogenic pressure. In contrast, the often restricted nature of fjord hydrography combined with their deep coastal water setting can provide the OC stored in these sediments with a far greater level of protection than the adjacent catchments. This is not to imply that these marine stores will not be affected by recent anthropogenically-driven changes, but rather that in the short to medium-term they will be buffered from the immediate impacts of these alterations to the wider environment. It is therefore important to recognize that the subsidy of OC_{terr} from an inherently vulnerable terrestrial system to a potentially stable long-term store within coastal sediments may provide a previously unrecognized climate-regulating service.

To understand the OC_{terr} subsidy to the coastal sedimentary environment, a good understanding of the processes that govern the transfer of C from one pool to another (i.e. terrestrial to marine) is required. Examination of our results from the integrated catchment and fjord system suggest that different processes govern the different

environments. The terrestrial environment is dominated by cyclical processes (Kirkels et al., 2014), whereby the catchment itself constantly accumulates and erodes OC_{terr} stores while approaching a state of relative equilibrium. By contrast, the mechanisms that control and govern the post-glacial sedimentary storage of OC_{terr} in fjords are largely cumulative (Smith et al., 2015, Smeaton et al., 2016), with fluvial and hillside processes subsidizing the sediment with OC_{terr} at the same time that primary production within the fjord and adjacent seas contributes an OC_{mar} source to the same sediments. If we consider the fjord and its catchment as a single, integrated system, the OC_{terr} subsidy to coastal marine sediments becomes increasingly important as the main mechanism by which the system as a whole stores OC_{terr} over the long-term (i.e. interglacial periods). We hypothesis that the catchment may be approaching a state of equilibrium and that the annual new production of OC_{terr} may not be adding significantly to the terrestrial store. Ultimately, these systems may successfully store more OC_{terr} through the subsidy of C from the catchment to the coastal sediments. Through this process of C subsidy, coastal marine sediments become effective and stable long-term repositories for OC_{terr} storage. This new understanding highlights the growing imperative to critically re-evaluate terrestrial OC losses as net gains in the marine environment.

While the subsidy of coastal sediments with OC_{terr} may represent an effective mechanism for the long-term storage of OC, it remains unclear how these marine stores will respond to increased anthropogenic pressure on their adjacent catchments. Such pressures will certainly act to disturb catchment soils and vegetation and should therefore act to increase the soil, nutrient and associated OC_{terr} flux to the adjacent coastal ocean. It remains something of an open question as to whether or not the anthropogenically-driven OC_{terr} flux has enhanced C storage in coastal marine sediments, but it seems likely that this is happening and that it requires urgent quantification.

4.6 Conclusions

A comparison of Loch Sunart with other mid-latitude fjords (Edwards and Sharples 1986) and to fjords with similar glacial history (New Zealand, Norway and Canada) (Syvitski and Shaw. 1995) suggests that our findings are likely to be prevalent throughout many of these middle- and high-latitude coastal sedimentary systems. This work suggests that fjordic sediments contain significant stores of OC_{terr} and could potentially provide a largely unrecognized climate regulation service through the subsidy of OC_{terr} from the catchment to the adjacent marine environment. Within these environments it appears that OC_{terr} transfers from land to sea in recent times have been effectively transferring OC_{terr} from an inherently unstable store within the catchment to a far more stable and long-lived OC_{terr} store in marine sediments. Ironically, this probably means that fjordic marine sediment systems are a more effective long-term store of OC_{terr} than their adjacent terrestrial catchments.

Chapter 5

A National Assessment of Mid-Latitude Fjord Sedimentary C Stocks

Based Upon: Smeaton, C., Austin, W. E. N., Davies, A. L., Baltzer, A. and Howe, J. A.: Scotland's Forgotten Carbon, (2017) A National Assessment of Mid-Latitude Fjord Sedimentary Carbon Stocks, *Biogeosciences*.

Author Contributions: Craig Smeaton and William E. N. Austin conceived the research and wrote the manuscript, to which all co-authors contributed data or provided input. Craig Smeaton conducted the research as part of his PhD at the University of St. Andrews, supervised by William E. N. Austin, Althea L. Davies and John A. Howe. Craig Smeaton wrote this chapter, expanding on some of the detail provided by Smeaton et al., 2017.

5.1 Introduction

Globally there is growing recognition that the burial (Smith et al., 2015) and storage (Smeaton et al., 2016) of carbon (C) in coastal marine sediments is an important factor in the global carbon cycle (Bauer et al. 2013), as well as providing an essential climate regulating service (Smith et al., 2015). Coastal sediments have been shown to be globally significant repositories for C, with an estimated 126.2 Mt of C being buried annually (Duarte et al., 2005). Of the different coastal depositional environments, fjords have been shown to be 'hotspots' for C burial, with approximately 11 % of the annual global marine carbon sequestration occurring within fjordic environments (Smith et al., 2015). Although it is clear these areas are important for the burial and long-term storage of C, the actual quantity of C held within coastal sediment remains largely unaccounted for. This knowledge deficit hinders our ability to fully evaluate, manage and protect these coastal C stores and the climate-regulating service that they provide.

The quantification of C in fjordic sediments was identified as a priority by Syvitski et al. (1987), but little progress has been made towards this goal until recently. Our work presented here utilises and extends the joint geochemistry and geophysical methodology developed by Smeaton et al. (2016) by applying it to a number of mid-latitude fjords. Estimated sedimentary C stocks for individual fjords will be utilised to create the first national estimate of sedimentary C stocks in the coastal ocean and thus quantify an overlooked aspect of Scotland's natural capital.

5.2 Scotland's Fjords

The coastal landscape of the west coast and islands of Scotland is dominated by fjordic geomorphology (Cage and Austin, 2010; Nørgaard-Pedersen et al., 2006). Catchments totalling an area of 21,742 km^2 drain to the sea through fjords, thus transporting sediment from the C rich soils into the marine system (Bradley et al., 2005). There are 111 large fjords (over 2 km long, where fjord length is twice fjord width) (Fig.5.1) in Scotland (Edwards and Sharples, 1986), supplemented by a further 115 smaller systems. The 111 large fjords are the primary focus of this study because their size and heavily glaciated geomorphology (Howe et al., 2002) suggest they are likely to store significant quantities of postglacial sediment. Additionally, geomorphological and oceanographic datasets are readily available for these fjords.

Building on the work of Smeaton et al. (2016), which centred on Loch Sunart (56.705556, -5.737534), we focus on a further four fjords to develop site specific sedimentary C stock estimations, which then allow us to make more precise estimates for the same range of fjordic system types in Scotland. The chosen sites are Loch Etive (56.459224, -5.311151), Loch Creran (56.536970, -5.324578), Loch Broom (57.873974, -5.117443) and Little Loch Broom (57.872144, -5.316385)(Fig.5.1).

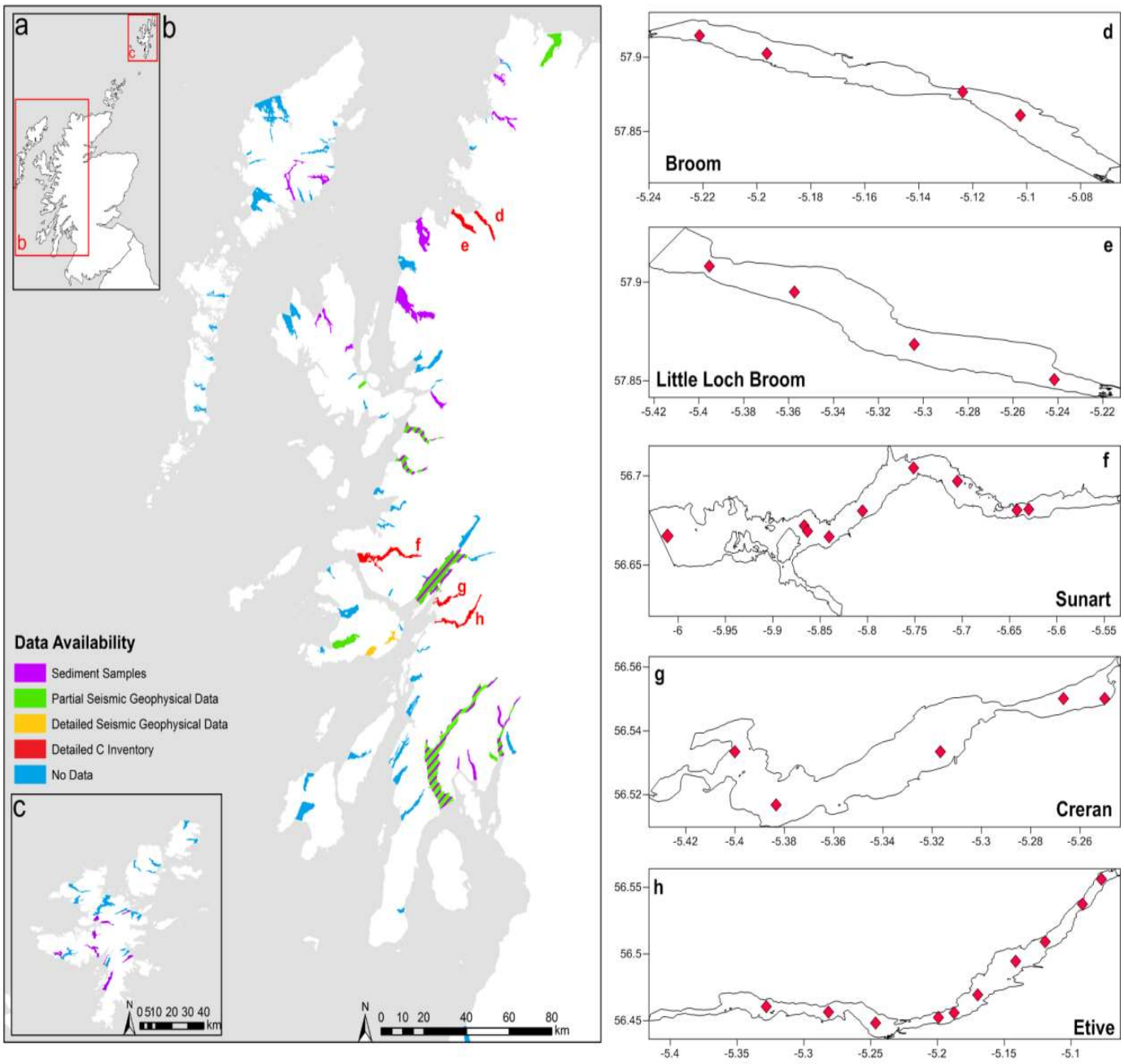

Figure 5.1. Map illustrating the location of Scotland's 111 fjords and the available data. Additionally, detailed maps present the sampling locations within (**D**) Loch Broom, (**E**) Little Loch Broom, (**F**) Loch Sunart (Smeaton et al., 2016), (**G**) Loch Creran (Loh et al., 2008) and (**H**) Loch Etive.

These fjords differ significantly in their physical characteristics (Table 5.1) and bottom water oxygen conditions. Hypoxic bottom water conditions are recognised as an important factor in C burial and preservation within depositional coastal environments (Middelburg and Levin, 2009; Woulds et al., 2007). However of these, 111 fjords, only Loch Etive's upper basin is known to be permanently hypoxic (Friedrich et al., 2014). Modelling of deep water renewal in the 111 fjords suggests that between 5 and 28 fjords, including Loch Broom and Little Loch Broom, could experience intermittent periods of hypoxia, while this is less likely in Lochs Sunart and Creran (Gillibrand et al., 2005, 2006). The fresh water to tidal ratio (Table 5.1) is a measure of how restrictive the fjords circulation is therefore it can be broadly linked to the presence of hypoxic bottom waters.

Fjord	**Length** (km)	**Area** (km^2)	**Mean Depth** (m)	**Max Depth** (m)	**Catchment Size** (km^2)	**Fresh/Tidal Ratio**	**Tidal Range**	**Rainfall**	**Run Off**
Loch Etive	29.5	27.7	33.9	139	1350	120.4	1.8	2500	3037.5
Loch Creran	12.8	13.3	13.4	49	164	12.5	3.3	2000	286.3
Loch Broom	14.7	16.8	27.3	87	353	14	4.5	1750	529.2
Little Loch Broom	12.7	20.4	41.7	110	167	5.5	4.5	1750	249.9
Loch Sunart	30.7	47.3	38.9	124	299	5.3	4	2000	523.2

Table 5.1. Key physical characteristics of each of the five fjords (Edwards and Sharples, 1986) selected to produce detailed estimates of sedimentary C stocks.

5.3 Towards a National Fjordic Sedimentary Carbon Inventory

5.3.1 Sample and Data Collection

This study applies the methodology of Smeaton et al. (2016) where sediment cores and seismic geophysical data were collected to four additional fjords. Figure. 5.1 shows the location of each of the long (>1 m) sediment cores extracted from the four fjords chosen to produce detailed sedimentary C stock estimates. With the exception of Loch Creran, where the required data were extracted from the available literature (Cronin and Tyler. 1980, Loh et al., 2008), each core was subsampled at 10 cm intervals for analysis. In total, 285 subsamples were collected from the sediment cores from Loch Etive (n= 133), Loch Broom (n= 78) and Little Loch Broom (n= 74). The data produced by Smeaton et al. (2016) for the glacially derived sediment in Loch Sunart were used as a surrogate for all glacial sediments in this study since MD04-2833 remains the only mid-latitude fjord core with chronologically constrained glacial sediment (Baltzer et al., 2010). Detailed seabed seismic geophysical data for Loch Etive (Howe et al., 2002) , Loch Creran (Mokeddem et al., 2015), Loch Broom (Stoker and Bradwell, 2009) and Little Loch Broom (Stoker et al. 2010) was compiled.

In addition, sediment surface samples (n= 61) and partial seismic surveys (n=5) have been collected from a number of additional fjords (Fig.5.1). These, in conjunction with data from the literature (Russell et al., 2010, Webster et al., 2004), provide a greater understanding of C abundance in these sediments and assist in constraining upscaling efforts. The full dataset is presented in the Table 5.2.

Fjord	ID	%TC	%OC	%IC	Location (Lat & long)
Gare Loch	GS 412	5.62	5.26	0.36	56.07633, -4.83017
Gare Loch	GS 414	4.38	3.83	0.55	56.0215, -4.79067
Loch Striven	GS 454	4.15	3.66	0.49	56.00417, -5.12333
Loch Striven	GS 456	3.91	2.31	1.60	55.96017, -5.08667
Loch Striven	GS 458	4.83	3.61	1.22	55.92067, -5.06217
Loch Riddon	GS 465	3.32	2.70	0.62	55.9535, -5.18933
Loch Portree	M 135	7.63	2.14	5.49	57.40967, -6.16117
Loch Long	GS 396	4.85	4.48	0.37	56.2015, -4.74567
Loch Long	GS 398	3.11	2.73	0.38	56.16433, -4.78917
Loch Long	GS 401	0.66	0.34	0.32	56.1025, -4.84883
Loch Goil	GS 402	7.10	4.54	2.56	56.16583, -4.90567
Loch Goil	GS 404	4.18	4.13	0.05	56.12267, -4.89483
Loch Fyne	GS 507	6.42	5.76	0.66	56.2655, -4.9305
Loch Fyne	GS 510	2.58	2.48	0.10	56.24166, -5.05233
Loch Fyne	GS 512	6.18	3.64	2.54	56.19017, -5.08733
Loch Fyne	GS 519	1.41	0.67	0.74	56.08083, -5.26933
Loch Fynne	GS 524	1.05	0.21	0.84	55.98833, -5.355
Loch Linnhe	56/06/134	0.23	0.14	0.09	56.685, -5.29333
Dale Voe	60-02/109	10.50	3.15	7.35	60.20667, -1.161767
Clift Sound	MD15-01	8.99	8.00	0.99	60.11943, -1.27727
Clift Sound	MD15-02	9.87	2.80	7.07	60.09987, -1.28453
Clift Sound	MD15-03	10.99	3.48	7.51	60.07995, -1.2975
Clift Sound	MD15-04	8.3	3.58	4.72	60.06635, -1.30778
Clift Sound	MD15-05	11.73	6.62	5.11	60.04765, -1.31588
Sand Sound	MD15-06	5.83	3.39	2.44	60.24485, -1.40295
Sand Sound	MD15-07	5.04	4.51	0.53	60.24477, -1.40418
Sand Sound	MD15-08	9.95	8.28	1.67	60.24477, -1.37952
Sand Sound	MD15-09	4.31	3.78	0.53	60.24178, -1.35835
Sand Sound	MD15-10	10.37	4.80	5.57	60.22822, -1.37052
Olna Firth	MD15-11	10.56	8.51	3.02	60.36277, -1.29588
Olna Firth	MD15-12	10.66	7.54	2.15	60.36425, -1.32315
Aith Voe	MD15-13	10.14	5.44	4.70	60.28945, -1.37488
Aith Voe	MD15-14	4.83	4.48	0.35	60.3055, -1.374
Busta Voe	MD15-15	40.71	38.38	2.33	60.39075, -1.36122
Busta Voe	MD15-16	33.96	7.68	26.28	60.38063, -1.35888
Busta Voe	MD15-17	24.15	3.76	20.39	60.3694, -1.37052
Vaila Sound	MD15-18	8.49	4.79	3.70	60.21943, -1.56408
Vaila Sound	MD15-19	7.42	3.51	3.91	60.213, -1.5624
Vaila Sound	MD15-20	8.14	4.07	4.07	60.21428, -1.58217
Vaila Sound	MD15-21	8.41	2.89	5.52	60.20567, -1.56747
Loch Ewe	GC009	7.20	0.48	6.72	57.906518, -5.687034
Loch Ewe	GS 1	3.59	2.34	1.25	57.847717, -5.626583
Loch Ewe	GS 2	5.49	2.26	3.23	57.847333, -5.628317
Loch Ewe	GS 3	5.53	2.91	2.62	57.848267, -5.625000
Loch Ewe	GS 4	5.28	2.09	3.19	57.845733, -5.646567
Loch Ewe	GS 5	2.64	1.55	1.09	57.833783, -5.651133
Loch Ewe	GS 6	3.82	1.28	2.54	57.816900, -5.635667
Loch Ewe	GS 7	6.13	5.29	0.84	57.796683, -5.629767
Loch Ewe	GS 8	5.72	5.18	0.54	57.787783, -5.634933
Loch Ewe	GS 9	4.44	3.68	0.76	57.786483, -5.634133

Table 5.2. Location and carbon content of the spot samples collected as part of effort to constraint the upscaled estimates.

5.3.2 Analytical Methods

Each of the subsamples was split for physical and geochemical analyses. The dry bulk density (DBD) of the sediment was calculated following Dadey et al. (1992). All samples were freeze dried, milled and analysed for total carbon (TC) and nitrogen (N) using a Costech elemental analysis (EA) (Verardo et al., 1990). Sub-samples of the same samples then underwent carbonate removal through acidification and were analysed by EA to quantify the organic carbon (OC) content. The inorganic carbon (IC) content of the sediment was calculated by deducting the OC from the TC. Analytical precision was estimated from repeat analysis of standard reference material B2178 (Medium Organic content standard from Elemental Microanalysis, UK) with C = 0.08 % and N = 0.02 % (n = 40).

5.3.3 Fjord Specific Sedimentary Carbon Inventories

Following the methodology of Smeaton et al. (2016), the geochemical and seismic geophysical data were combined to make first order estimates of the C held in the postglacial and glacial sediments of Loch Etive, Creran, Broom and Little Loch Broom. We then calculated how effectively the fjord stores C (C density) as a depth-integrated average value per km^2 for both the postglacial and glacial-derived sediments. Unlike Loch Sunart, where the sediment stratigraphy has robust chronological constraints (Cage and Austin, 2010; Smeaton et al., 2016), the four other fjords largely lack chronological evidence, with the exception of two cores from Loch Etive (Howe et al., 2002; Nørgaard-Pedersen et al., 2006). The lack of ^{14}C dating means we rely solely on the interpretation of the seismic geophysics to differentiate between the postglacial and glacial sediments. To ensure the consistency of this approach, previous seismic interpretations of Scottish fjordic sediments (Baltzer et al., 2010; Dix and Duck, 2000; Howe et al., 2002, Stoker and Bradwell, 2009, Stoker et al. 2010) were studied and a catalogue of different seismic facies compiled for use as a reference guide (Appendix D). Finally, we applied the framework set out in Smeaton et al. (2016) to reduce uncertainty in the interpretation of the seismic geophysics by testing seismic units against available dated sediment cores.

5.3.4 Upscaling to a National Sedimentary Carbon Inventory

Upscaling from individual to national coastal C estimates was key objective of this work. Two approaches were developed to upscale the five detailed sedimentary C inventories to a national scale stock assessment of C in the sediment of the 111 major Scottish fjords. Both approaches utilise the physical characteristics of the fjords to quantify the OC and IC held within the sediment. From these data we can also estimate the long-term average quantity of C buried each year. Currently the best estimate of when the west coast of Scotland was free of ice from the last glacial period is approximately 13.5 ka (Lambeck, 1993) though it could be argued that 15 ka or 11.5 ka BP would be more appropriate. Modelling of the retreat of the last ice sheet (Clark et al., 2012) suggests that a significant number of the fjords would have been ice free around 15 ka (Fig.5.2) and have the ability to start accumulating C. Alternatively 11.5 ka (Golledge, 2009) could be used as this date signifies the point the fjords became permanently ice free after the loss of ice associated with the Younger Dryas period. By dividing the total C held within the postglacial sediment in all the fjords by this range of dates we can calculate the long-term average quantity of C buried per year since the start of the postglacial period. Although the methodology is relatively crude and probably underestimates the quantity of C being buried each year, it does give a valuable first order insight into the long-term carbon sequestration service that fjords prove.

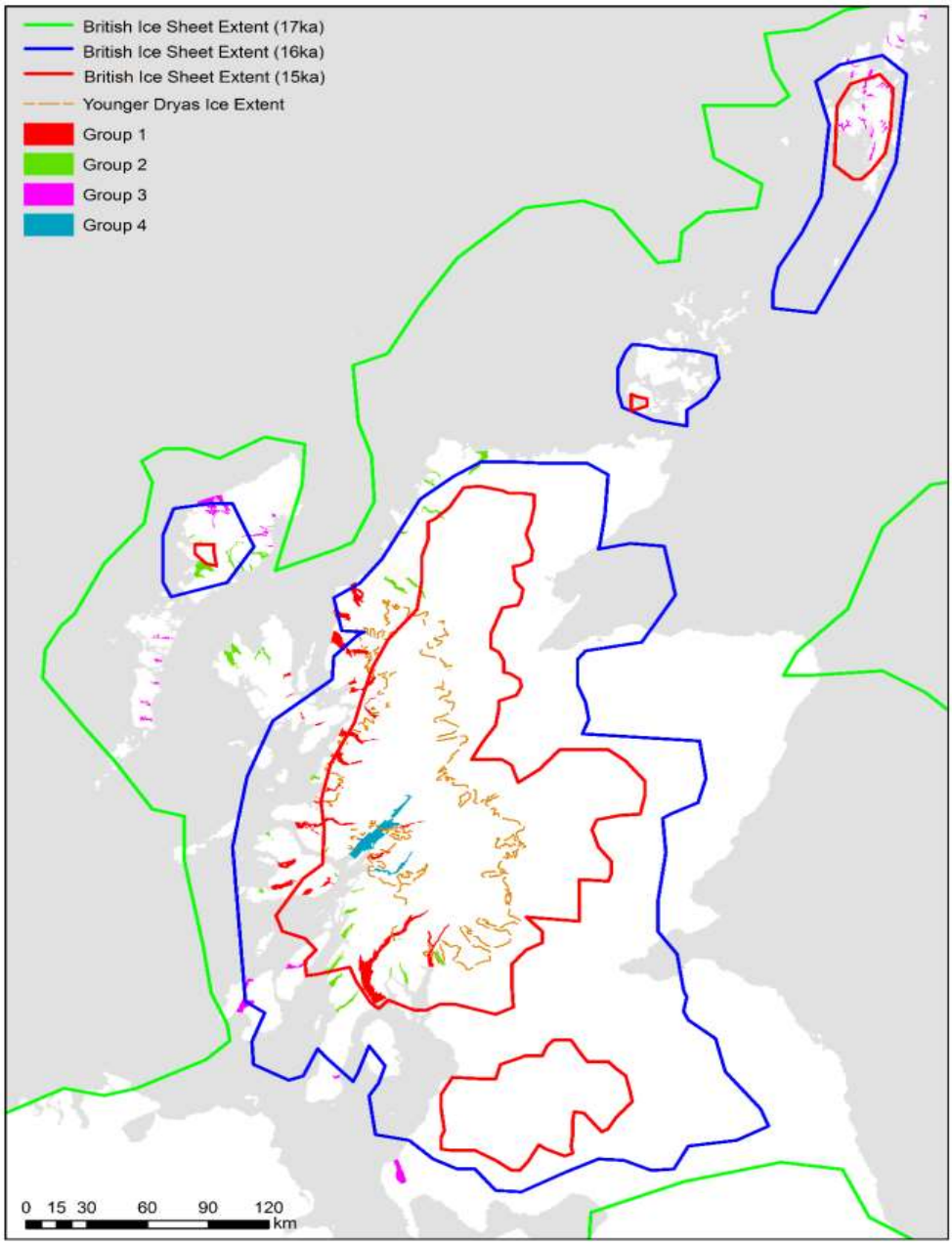

Figure 5.2. Scotland's fjords overlain by the model of the British Ice Sheet deglaciation (Clark et al., 2012) and the extent of the Younger Dryas ice sheet (Golledge. 2010).

5.3.4.1 Fjord Classification Approach

The first stage of upscaling involves grouping the 111 fjords using the physical characteristics identified in (Table 5.1), along with rainfall, tidal range and runoff data (Fig.5.3). Grouping was achieved by applying a k-means cluster analysis (1 x10^5 iterations) to all 111 fjords (Edwards and Sharples, 1986). This resulted in the delineation of four groups (Fig.5.4).

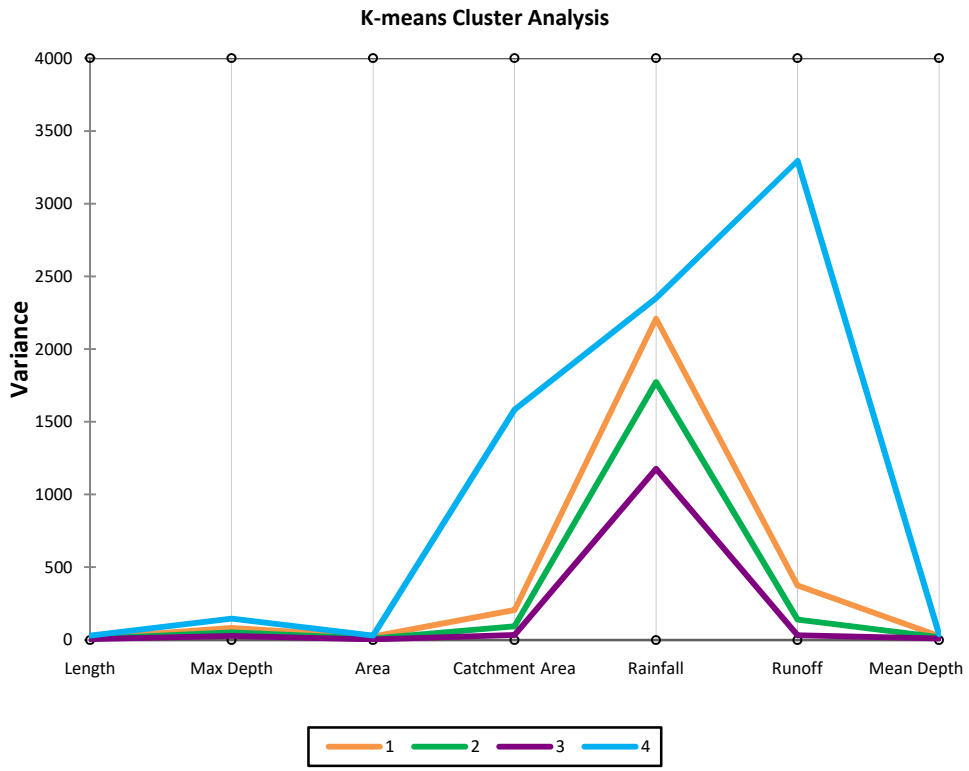

Figure 5.3. K-mean cluster analysis: Grouping determination based on variance in key fjord characteristics.

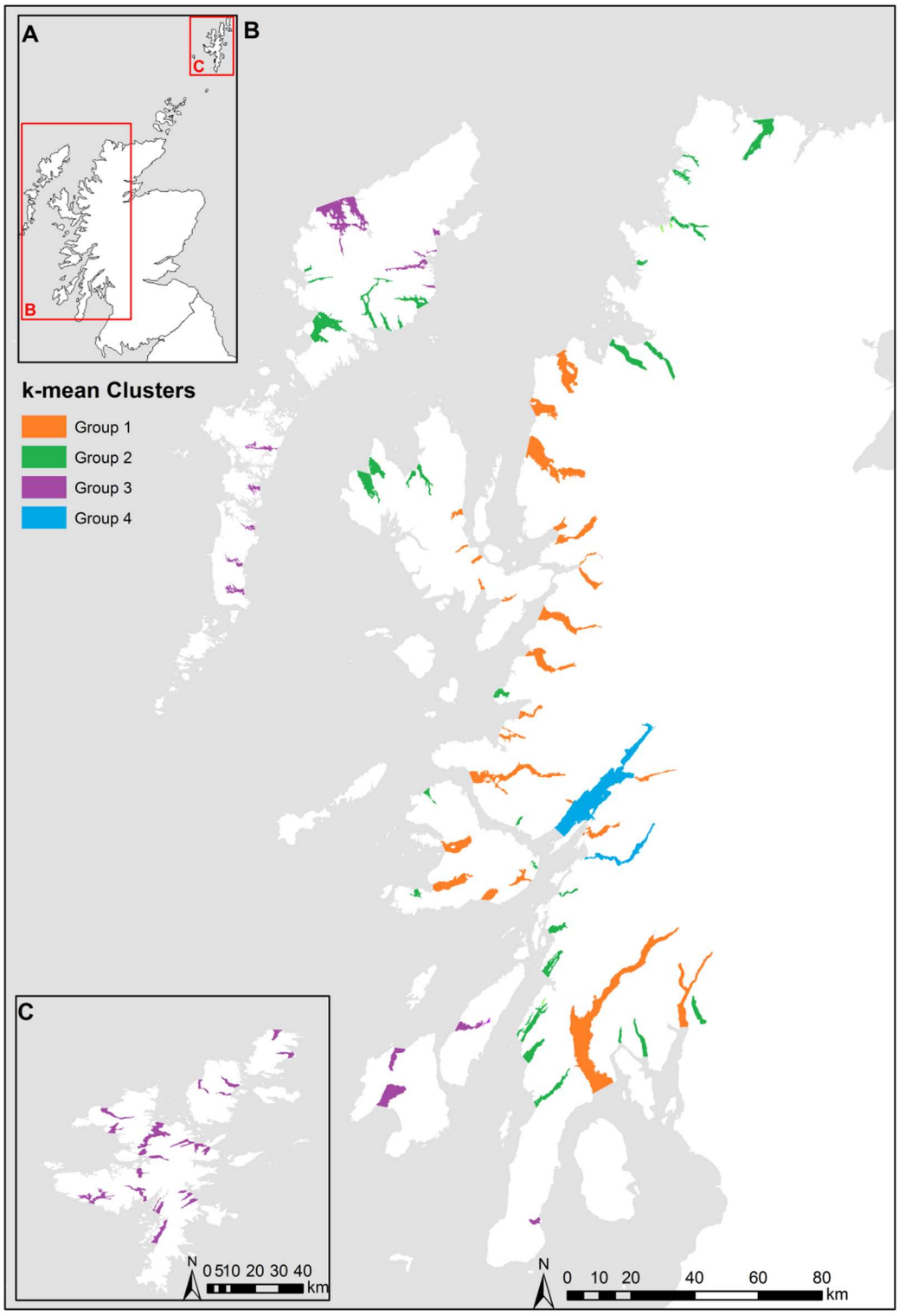

Figure 5.4. Output from the k-means analysis showing the spatial distribution of the four different groups of fjords

Group 1 comprises mainly mainland fjords which are the most deeply glaciated and have highly restrictive submarine geomorphology (Gillibrand et al., 2005); Loch Sunart and Creran fall into this category. Group 2 contains fjords from the mainland and the Inner Hebrides which tend to be less deeply glaciated and more open systems; Loch Broom and Little Loch Broom are part of this group. Group 3 includes the fjords on Shetland and the Outer Hebrides; these fjords are shallower and their catchments tend to be smaller and noticeably less glaciated. Group 4 consists of Loch Etive and Loch Linnhe; these fjords are outliers from the other groups and both have extremely large catchments in comparison to the others and were major glacial conduits for ice draining the central Scottish ice field at the last glacial period. This analysis suggest the level to which the fjords are glaciated is a defining factor to how they are classified. When mapped the ice thickness at the last glacial maximum (Lambeck et al. 1993) largely correlates with the groupings produced by the k-means analysis (Fig.5.5) with Group 1 under the maximum amount of ice, which reduces in thickness for each subsequent group.

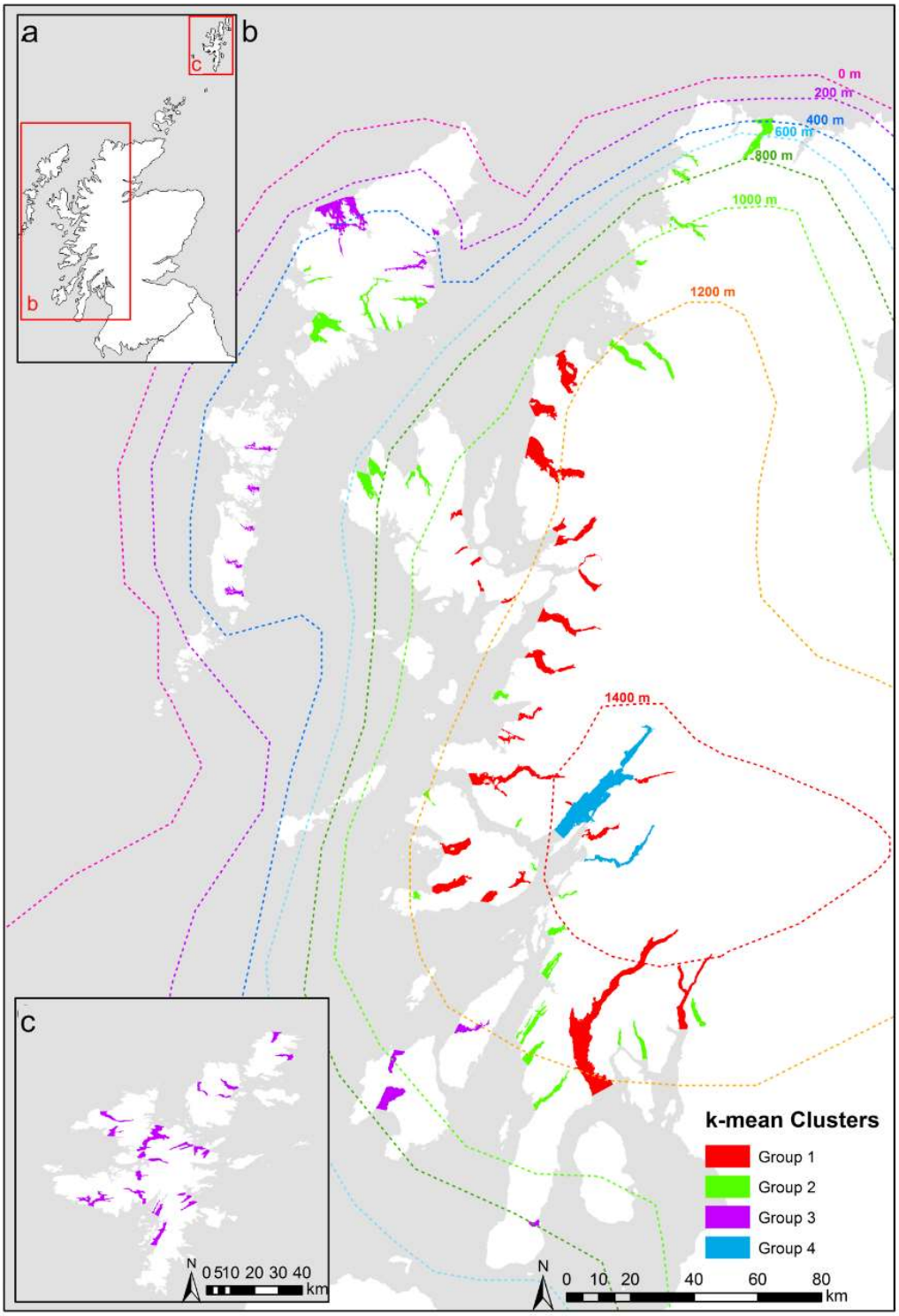

Figure 5.5. Scotland's fjords overlain by estimate ice thickness at the last glacial maximum (Lambeck. 1995)

Our case study fjords are thus representative of three of the fjordic groups that can be recognised at a national scale. Group specific postglacial and glacial OC and IC densities were calculated using the data from the detailed sedimentary C inventories available from our five sites. The Group specific OC and IC densities were applied to each fjord within a group, giving the total OC and IC stock for each fjord. Group 3 does not contain any of the five fjords for which there are detailed C stock estimations and Group 2 has therefore been chosen as a surrogate since the k-mean analysis indicates that Groups 2 and 3 have the greatest similarities.

5.3.4.2 Physical Attribute Approach

The physical characteristics of fjords (Table 5.1) have primarily governed the input of C into the fjord since the end of the last glaciation, when the majority of fjords became ice-free. We might therefore expect a relationship between the physical features of a given fjord and its accompanying catchment, and the C stored in its sediments. We use detailed sedimentary C stock estimations in conjunction with the physical characteristics (Edwards and Sharples, 1986) to determine which physical feature best correlates with the quantity of OC and IC held in the sediment. A statistical scoping exercise was therefore undertaken to determine which physical characteristics are best suited to the upscaling process. The results indicate that there are strong linear relationships between OC density and tidal range ($p = 0.012$, $R^2 = 0.909$), precipitation ($p = 0.003$, $R^2 = 0.961$), catchment area ($p = 0.023$, $R^2 = 0.860$) and runoff ($p = 0.019$, $R^2 = 0.877$). The correlation between these physical features and OC content fits well with our understanding of fjord processes, since tidal range is a proxy for the geomorphological restrictiveness of the fjord, while catchment size, precipitation and runoff govern the input of terrestrially-derived OC (Cui et al., 2016) into the fjord. The relationship between the IC stored in the sediment and a fjord's physical characteristics is less well-defined, with strong correlations identified between IC and the area of the fjord ($p = 0.009$, $R^2 = 0.925$) and the length of the fjord ($p = 0.016$, $R2 = 0.892$). Again, this fits with what we would expect: the larger/longer the fjord, the greater the opportunity for in-situ IC production (Atamanchuk et al., 2015) and remineralisation of OC (Bianchi et al., 2016). Each of these relationships were used to calculate the OC and IC stored in the postglacial sediment of each of the 111 fjords. The input of glacially-derived OC during the retreat of the ice sheet at approximately 13.5 ka -17 ka (Clark et al., 2012) is controlled by a more sporadic mechanisms (Brazier et al. 1988) governed by complex advance-retreat

ice margin dynamics during the deglaciation. This approach is therefore not suitable for estimating the C stored in the glacial sediment of the fjords

5.3.4.3 Constraining Estimates and Uncertainty

To determine the accuracy of both upscaling methodologies, we compared the total quantity of sedimentary OC and IC calculated for Lochs Sunart, Etive, Creran, Broom and Little Loch Broom by both upscaling approaches alongside detailed estimates of C held within the sediment of each of the five fjords. Although there are insufficient data to create additional detailed sedimentary C stock estimates at a national scale, there are enough data from some fjords to make broad estimations (Table.5.3). Seismic geophysical data from Lochs Hourn (57.125683, -5.589578), Eriboll (58.497543, -4.685106), Fyne (55.882882, -5.381012), Nevis (57.007023, -5.693133) and Lower Loch Linnhe (56.591510, -5.456910) allow us to estimate the minimum and maximum depth of postglacial sediment, while surface sample data from each loch enables us to estimate C content of the sediment. Using these data we can calculate basic estimates of postglacial OC and IC held within the sediment of these fjords as an additional check on the accuracy of the upscaling methodology.

Two metrics of uncertainty were employed: arithmetic and a confidence-driven approach. The arithmetic method follows the approach of Smeaton et al. (2016), whereby any known arithmetic uncertainty is propagated through all the calculations. However, as recognised by Smeaton et al. (2016), there are ‘known unknowns’ which we cannot reliably quantify. Therefore we have further employed a confidence-driven approach to assess the final C stock estimations for each fjord. Using a modified confidence matrix (Fig.5.6) following the protocols adopted in the IPPC 5th Assessment (Mastrandrea et al., 2010), we have semi-quantitatively assigned a level of confidence to the C estimates from each fjord. The matrix uses the results from the k-means analysis and the availability of secondary data (Supplemental Material) to assign a confidence level. For example, as described above (3.4.1) a fjord in the Outer Hebrides would fall into Group 3. As discussed, this group is without a detailed sedimentary carbon inventory and no other data are available to test the calculated C inventory. In this case, the C stock estimation for that fjord would be assigned a very low confidence level. In contrast, if the fjord fell into to Group 1, where there are similar fjords with detailed C stock estimations and further C and partial geophysical data were available to test the calculated C inventory, then a high confidence level is assigned. The five fjords with detailed sedimentary C inventories are the only sites, which have been assigned a confidence level of very high.

Fjord	Area (km^2)	Estimated Sediment Depth (m)		OC (%)		IC (%)		Basic Estimate OC (Mt)		Basic Estimate IC (Mt)		Upscaling Estimate OC (Mt)		Upscaling Estimate IC (Mt)	
		Min	Max	Min	Max	Min	Max	Min	Max	Min	Max	Min	Max	Min	Max
Loch Fyne	175.5	2	14.8	0.2	5.8	0.1	2.5	1.00	194.5	0.5	85.8	34.3	45.8	24.6	45.8
Loch Linnhe	213.2	1.2	15.7	0.2	2.7	0.1		0.76	117.0	0.3	3.9	36.7	42.9	18.4	23.1
Loch Hourn	33.7	3.3	11.0	0.5	3.0	-	-	0.71	14.65	-	-	4.7	6.6	3.7	6.7
Loch Nevis	28.7	1.5	12.5	1.0	4.3	0.2	4.4	0.55	19.9	0.12	20.5	3.9	5.6	3.1	5.6
Loch Long	33.6	2.8	10.1	0.3	4.5	0.3	0.4	0.42	19.8	0.39	1.7	6.0	6.57	4.62	6.57

Table 5.3. Basic sedimentary C stock estimates for five fjords calculated using partial geophysical data and surficial C data (%). Additional the sedimentary C stock estimates produced through the upscaling approach outlined is this work is displayed for comparison.

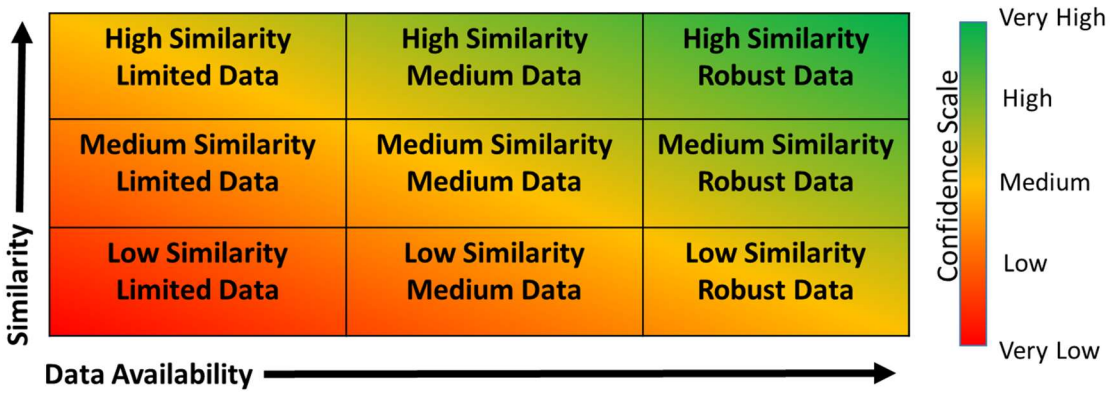

Figure 5.6. Matrix depicting the relationship between data availability, similarity to modelled fjords and confidence level. Adapted from IPCC 5th Assessment Report (Mastrandrea et al. 2010).

5.4 Interpretation and Discussion

5.4.1. Fjord Specific Sedimentary Carbon Inventories

Sedimentary analyses showed a broad similarity in dry bulk density values from the postglacial sediment of the five fjords, while the variability between the fjords is more clearly illustrated by the carbon concentrations (Fig.5.7). Lochs Broom, Sunart and Little Loch Broom are characterised by similar quantities of OC and IC. Although the TC content of the sediment in Loch Creran is comparable to the other fjords, the relative contribution of OC is higher, with a correspondingly lower quantity of IC in the sediment. Of the five lochs surveyed, the C content of Loch Etive's sediment is significantly different from the other sites. It has the highest TC content due to high quantities of OC found in the sediment. This is a possible consequence of hypoxic conditions in the inner basin, as discussed below. As expected, the highest dry bulk density values and lowest quantity of OC and IC occur in the glacial sediments at all sites.

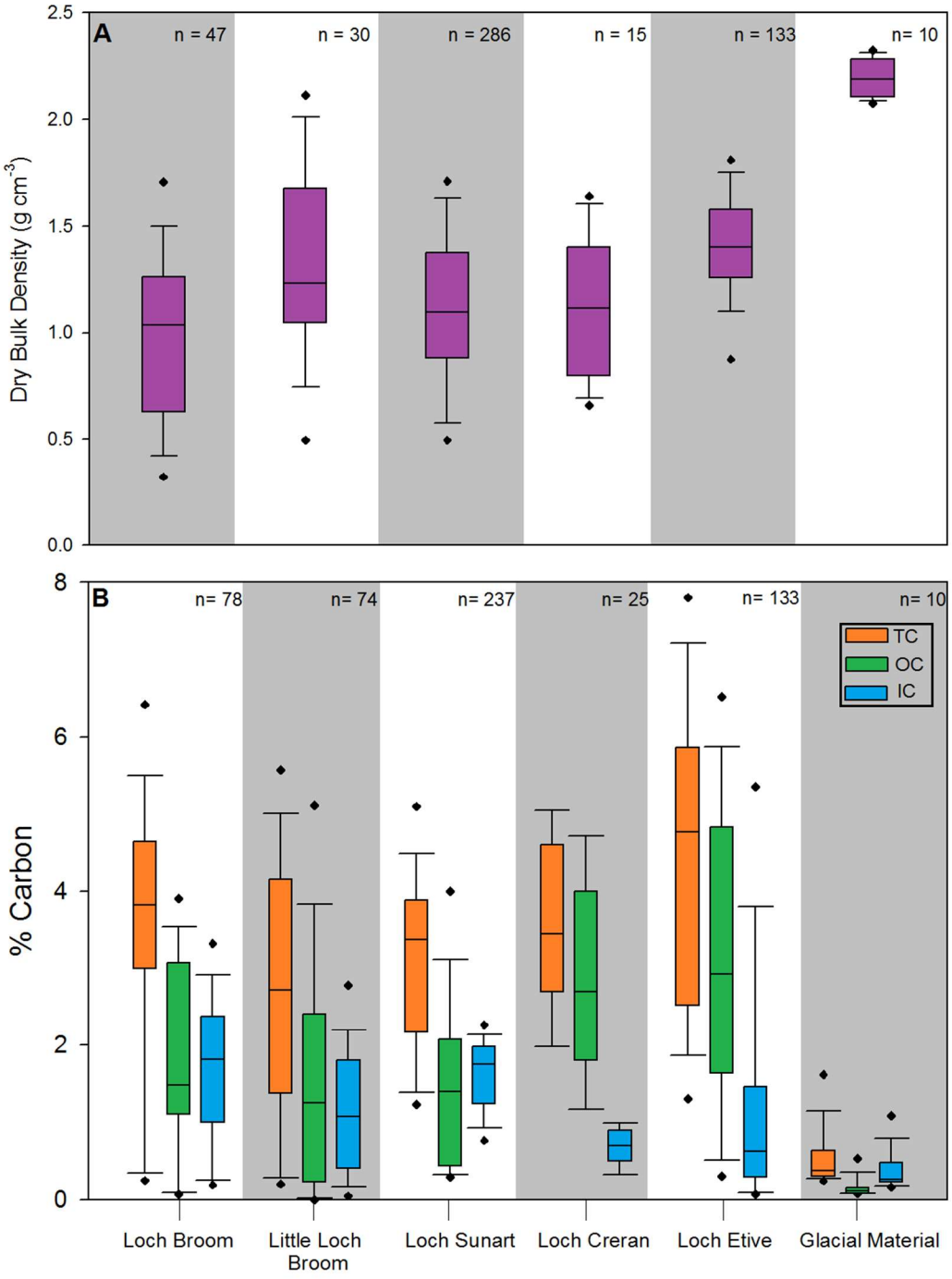

Figure 5.7. Boxplots illustrating the (**a**) dry bulk density and (**b**) carbon content (%) compiled from the sediment cores extracted from the five fjords central to this research. Data for the glacially derived sediments collected from Loch Sunart (MD04-2833) are also presented.

The total C held within each of the five fjords (Table 5.4) was calculated by combining the dry bulk density data, % C and sediment volume models (Fig.5.8, 5.9, 5.10). Loch Sunart (26.9 ± 0.5 Mt C) contains the largest sedimentary C store of the five fjords, closely followed by Loch Etive (21.1 ± 0.3 Mt C). In comparison, Lochs Creran, Broom and Little Loch Broom hold significantly less C. As indicated above, the postglacial sediments of Loch Etive hold the greatest quantity of OC (11.5 ± 0.4 Mt) with 7.76 Mt of that OC held in the upper hypoxic basin resulting in Loch Etive being the most effective store of OC (0.455 Mt OC km^{-2}).

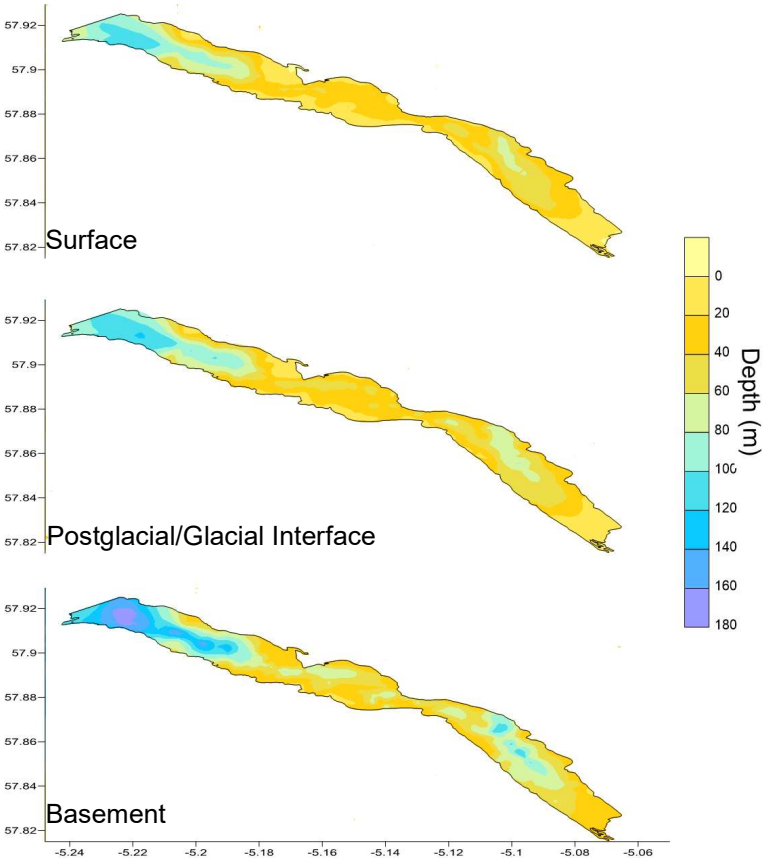

Figure 5.8. Loch Broom: Contour maps defining the topography of each seismic horizon from which the volume of sediment was calculated.

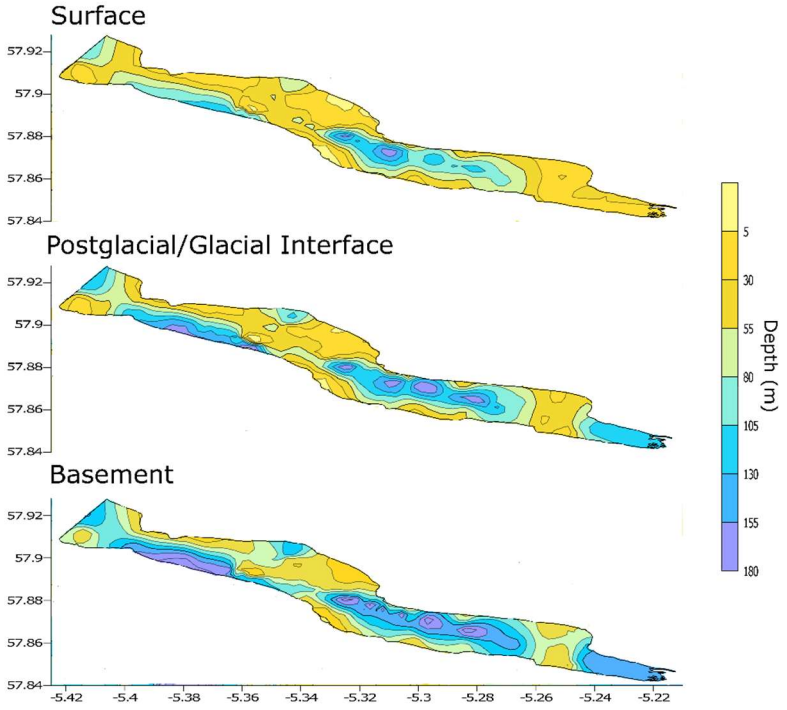

Figure 5.9. Little Loch Broom: Contour maps defining the topography of each seismic horizon from which the volume of sediment was calculated.

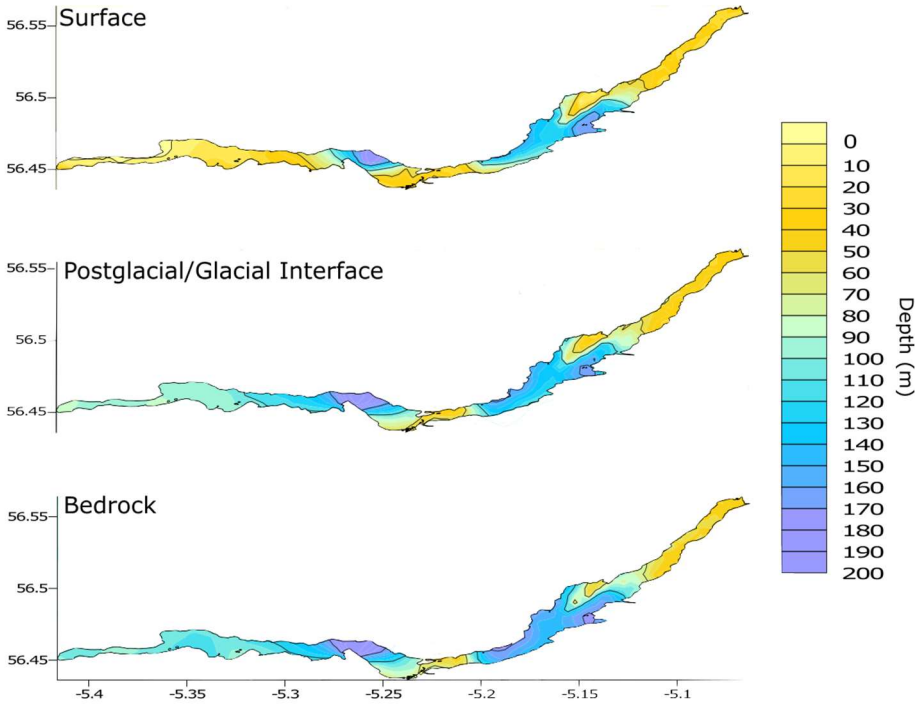

Figure 5.10. Loch Etive: Contour maps defining the topography of each seismic horizon from which the volume of sediment was calculated.

These results suggest that low oxygen conditions inhibit reworking and remineralisation of organics and the production of carbonate fauna (Woulds et al., 2016) Loch Sunart has large sills (Smeaton et al. 2016) and is one of the largest fjords in Scotland; these features favour the capture of terrestrial OC (Smeaton and Austin, 2017) and storage of large quantities of post-glacial OC (9.4 ± 0.2 Mt) and IC (10.1 ± 0.2 Mt). The quantities of C stored in the sediment of the smaller fjords are strongly linked to how restrictive the geomorphology of the fjord is. For example, the smallest quantity of IC is held within Loch Creran. This is in part be due to the shallow and narrow central sill which results in a terrestrially dominated system with high sedimentation rates (Loh et al., 2008) which increases the OC storage effectiveness (0.195 Mt OC km^{-2}) but reduces the IC storage effectiveness (0.068 Mt IC km^{-2}) as increased humic acid input from terrestrial sources (Bauer and Bianchi. 2011) results in lower pH which in turn reduces the suitability of the fjord for calcifying organisms (Khanna et al. 2013). In contrast, the relatively unrestricted geomorphology of Loch Broom results in the fjord being governed by marine processes. The greater marine influence results in these ecosystem being capable of supporting a greater range and abundance of calcifying organisms (e.g. foraminifera) which in-turn makes the sediments a highly effective store of IC 0.232 Mt IC km^{-2}. In contrast open systems are comparatively poor at capturing OC as illustrated by Little loch Broom (1.6 Mt OC). The glacial material contains less C than the postglacial sediments. The effective storage of C in the glacially-derived sediments of the five fjords is very similar, with the OC density ranging between 0.030 to 0.093 Mt OC km^{-2} and an IC density varying between 0.068 and 0.104 Mt IC km^{-2} (Table 5.4). The similarity of these results may be because the mechanisms governing the deposition of glacial sediment during the retreat of the British Ice Sheet (Brazier et al., 1988) were similar across the geographic range of the fjords, but it may also be a product of limited data availability for the glacial sediment.

Fjord		TC (Mt)	OC (Mt)	IC (Mt)	C $_{density}$ (Mt C km^{-2})	OC $_{density}$ (Mt OC km^{-2})	IC $_{density}$ (Mt IC km^{-2})
Loch Etive		**21.1 ± 0.3**	**12.6 ± 0.3**	**8.6 ± 0.3**	**0.77**	**0.46**	**0.31**
	PG	17.7 ± 0.4	11.5 ± 0.4	6.2 ± 0.3	0.64	0.42	0.22
	G	3.5 ± 0.2	1.1 ± 0.1	2.4 ± 0.2	0.13	0.04	0.09
Loch Creran		**4.8 ± 0.7**	**3 ± 0.5**	**1.8 ± 0.9**	**0.36**	**0.23**	**0.14**
	PG	3.5 ± 0.6	2.6 ± 0.7	0.9 ± 0.4	0.27	0.20	0.07
	G	1.3 ± 0.9	0.4 ± 0.1	0.9 ± 1.2	0.10	0.03	0.07
Loch Broom		**6.8 ± 0.4**	**2.9 ± 0.4**	**3.9 ± 0.4**	**0.41**	**0.17**	**0.23**
	PG	5.1 ± 0.5	2.4 ± 0.5	2.7 ± 0.4	0.30	0.14	0.16
	G	1.7 ± 0.3	0.5 ± 0.2	1.2 ± 0.3	0.10	0.03	0.07
Little Loch Broom		**7 ± 0.5**	**3.5 ± 0.5**	**3.5 ± 0.6**	**0.34**	**0.17**	**0.17**
	PG	3 ± 0.7	1.6 ± 0.6	1.4 ± 0.8	0.15	0.08	0.07
	G	4 ± 0.3	1.9 ± 0.2	2.1 ± 0.4	0.20	0.09	0.10
Loch Sunart		**26.9 ± 0.5**	**11.5 ± 0.2**	**15.0 ± 0.4**	**0.56**	**0.24**	**0.36**
	PG	19.9 ± 0.3	9.4 ± 0.2	10.1± 0.2	0.41	0.20	0.21
	G	7.0 ± 0.8	2.1 ± 0.3	4.9 ± 0.6	0.15	0.04	0.10

Table 5.4. Detailed sedimentary C stocks presented as total carbon (TC), organic carbon (OC) and inorganic carbon (IC) held within postglacial (PG) and glacial (G) sediment of the fjords. Additionally, we list the C density for each fjord as a measure of how effectively the sediment stores C.

5.4.2 A National Fjordic Sedimentary C Inventory

The results of the upscaling process suggest overall an estimated 640.7 ± 46 Mt C are stored in fjordic sediments of Scotland (Table 5.5), comprising 295.6 ± 52 Mt OC and 345.1 ± 39 Mt IC. The postglacial sediments are the main repository for much of this C, with almost equal amounts of OC and IC indicated by a OC:IC ratio of 1.17:1. In contrast, the glacial sediments are dominated by IC, with an OC:IC ratio of 0.33:1. This is most likely due to the glacial source material originating from scoured bedrock, and the absence of organic-rich soils and vegetation (Edwards and Whittington. 2010.). These estimates represent the first fully depth integrated sedimentary C inventory for any marine ecosystem

The storage of C is unevenly distributed between the 111 fjords; a small number of systems disproportionately contribute to the national sedimentary C total (Fig.5.11). The sediment of fourteen large fjords hold 65 % of the total C held Scotland's fjords (Table 5.6). Estimated C stocks for individual fjords can be found in the supplementary material.

	TC (Mt)	**OC** (Mt)	**IC** (Mt)
Postglacial	467.1 ± 65	252.4 ± 62	214.7 ± 85
Glacial	173.6 ± 18	43.2 ± 12	130.6 ± 22
Total	**640.7 ± 46**	**295.6 ± 52**	**345.1 ± 39**

Table 5.5. Total C stored in the sediment of Scotland's 111 fjords further broken down into the quantities of OC and IC stored is the postglacial and glacial sediments.

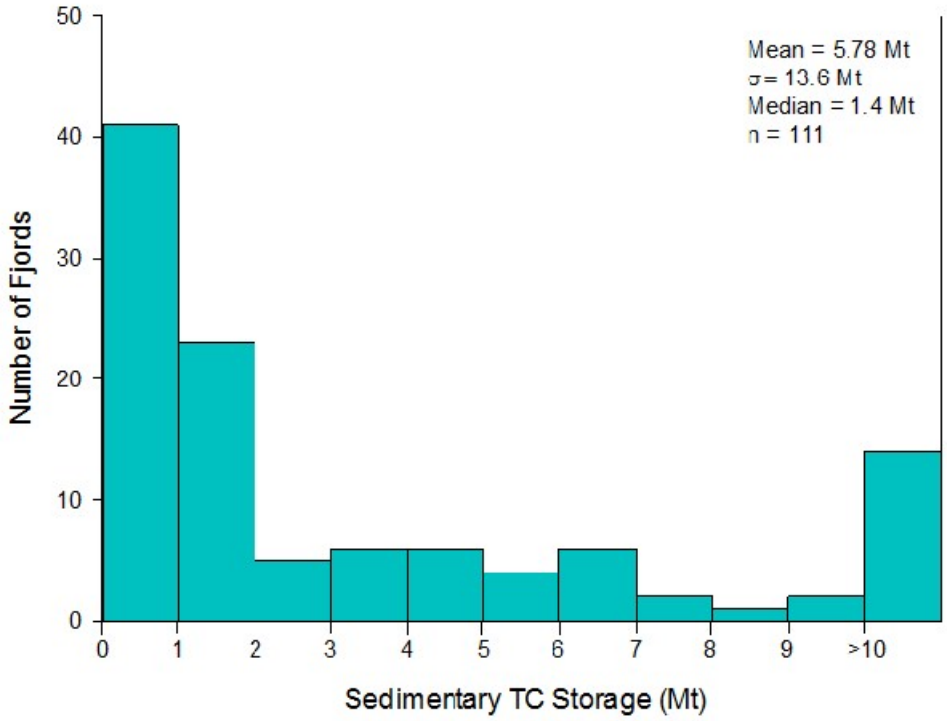

Figure 5.11. Frequency distribution of sedimentary TC stock estimates for the Scotland's 111 fjords.

Fjord	TC (Mt)	% of Scotland's Total of Fjordic Sedimentary C Stock
Loch Fyne	99.70	15.56
Loch Linnhe (Lower)	92.28	14.40
Loch Torridon	30.82	4.81
Loch Linnhe (upper) and Eil	27.82	4.34
Loch Sunart	26.50	4.14
Loch Ewe	21.82	3.41
Loch Etive	21.11	3.29
Long Clyde	16.60	2.59
Loch Hourn	15.41	2.41
Loch Ryan	14.35	2.24
Loch na Keal	14.29	2.23
Loch Nevis	13.08	2.04
Loch Scridian	12.01	1.87
Loch Carron	10.52	1.64

Table 5.6. Details of the fourteen fjords that disproportionately contribute to Scotland's Fjordic Sedimentary C stock.

In addition to quantifying the total C stored in these fjords, we also calculated the accuracy of the upscaling process and assigned a confidence level to each of the sedimentary C estimates using the confidence matrix (Fig.5.3). To test the accuracy of the upscaling approach, we compared the outputs from the fjord classification and physical attribute approach with the fjord-specific sedimentary carbon inventories (Fig.5.12). Both upscaling approaches produced outputs comparable to the detailed C inventories for the postglacial OC and IC. There is greater variation when we compare the outputs for the glacial material, but overall there is reasonable agreement between the different approaches. A secondary check was undertaken by comparing the estimated C stocks to data collected from spot samples and the literature. Sampling in the small, shallow Shetland voes recovered large quantities of shell material, which resulted in high IC content within the surface sediment (Average: 5.36 %). This corresponds well with the upscaling results, which suggests that these systems are more effective at storing IC than the majority of mainland fjords. Additionally, the C data collected from the spot samples from fjords out with the five case study fjords (Average OC: 3.09 %, Average IC: 1.66 %) and literature (OC: 0.48 % to 8.15 %) (Russell et al., 2010, Webster et al. 1998, Webster et al., 2004) corresponds well with the values used to create the detailed C inventory's (Table 5.4). As an additional check, we utilised the partial seismic data and the spot samples to make a crude sediment volume estimation. Sedimentary C stocks were then estimated based on the minimum and maximum

sediment depth, the fjord areas, C data, and the average dry bulk density value (1.3 g cm^{-3}) from all five case study fjords. These estimates are similar to that produced by the upscaling approaches.

The availability of data for the postglacial sediment means that we have medium to very high confidence in our estimates of the quantity of OC and IC stored in 74 of the 111 fjords. The remaining 37 fjords have been assigned a confidence level of low, with most originating from Group 3 of the k-means analysis where we recognise a shortage of data needed to constrain C stock estimates. The lack of data for glacially-derived sediment results in all except the five case study lochs being assigned a confidence level of very low to medium. Using these checks we believe that our first order estimate of the C stored in the sediment of Scotland's fjords and the associated uncertainties are realistic and robust. The confidence level assigned to each fjordic C estimate stock can be found in Appendix D.

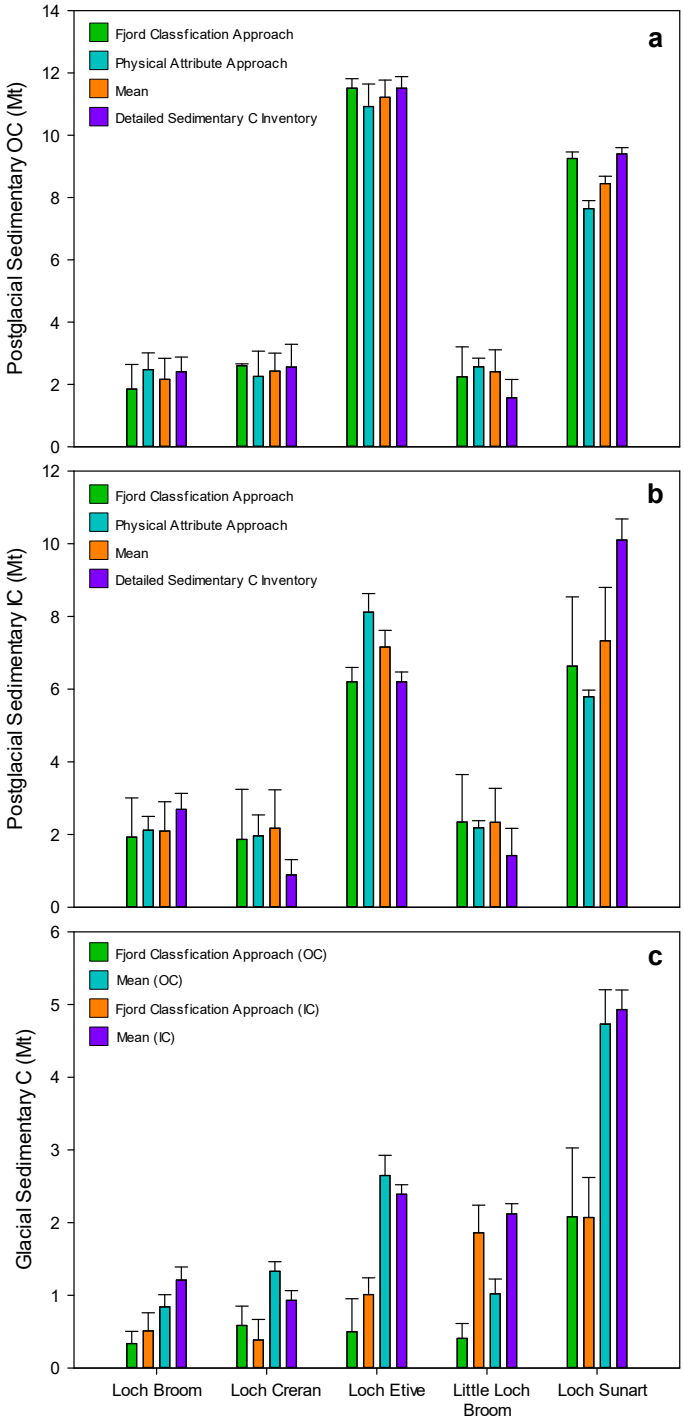

Figure 5.12. Comparison of the outputs from the two upscaling methods (fjord classification and physical attribute approaches) and the detailed C inventories for the 5 core fjords. (**a**) Postglacial organic carbon stocks (**b**) Postglacial inorganic carbon stocks (**c**) Glacial carbon stocks.

5.4.2.1 National Estimates of C Burial

Annually an estimated 31139- 40615 t of C is buried in the sediment of the 111 fjords, with OC contributing 16828 - 21949 t yr^{-1} and IC supplying 14311 -18666 t yr^{-1}. This annual burial of C has been suggested to provide a climate regulating service through C sequestration (Smith et al., 2015), yet efforts to fully quantify this mechanism have remained elusive. The results from this study indicate that fjords have been capturing OC since the retreat of the last ice sheet some of which that would have otherwise been lost to the open ocean, where it would be more readily remineralized (Middelburg et al. 1993, Bianchi. 2011). Although the results do little to resolve the mechanisms that govern this climate regulating service, they clearly show that fjords have been providing this service since the retreat of the last ice sheet and throughout the Holocene. This suggests that these systems have the capacity to adapt to future environmental change. Intriguingly, there is also the possibility that this process may have aided the capture of terrestrial C during the late Holocene and recent past (Smeaton and Austin, 2017).

5.4.2.2 Global Outlook

Given similarities between the mid-latitude fjords and coastal environments of New Zealand, Chile, Norway and Canada (Syvitski and Shaw, 1995), it is reasonable to suggest that our findings are relevant throughout these systems. The sediments within fjordic environments around the world potentially hold significant quantities of both OC and IC which have been overlooked in national and global carbon budgets. The joint geophysical and geochemical methodology used to quantify sedimentary C stocks coupled to the upscaling approach taken in this study is capable of providing nations around the world with the ability to quantify of their coastal sedimentary C stocks and reassess their nation's natural capital.

5.4.3 Comparison to Other Mid-Latitude Carbon Stocks: Significance and Vulnerability

The 640.7 ± 46 Mt of carbon held within the sediment of the fjords is one of the largest stores in Scotland (Fig.5.13). The fjordic sedimentary store is the largest of Scotland's coastal carbon stores (Burrows et al., 2014), exceeding both maerl and biogenic reefs which have been shown to be highly effective stores of both OC and IC (Van Der Heijden and Kamenos, 2015). In addition, fjord sediments hold a greater quantity of C than all the living vegetation in Scotland (Forestry Commission, 2015, Henrys et al., 2016, Vanguelova et al., 2013). While Scotland's soils (Aitkenhead and Coull, 2016) and in particular the peatlands (Chapman et al., 2009) contain a greater quantity of OC than the fjords, it must be remembered that the fjord sediments also hold IC and the areal extent of these stores differs greatly. When normalised by area (Fig.5.13), fjordic sediments emerge as a far more effective store of OC and IC than other Scottish C stores, on land or at sea.

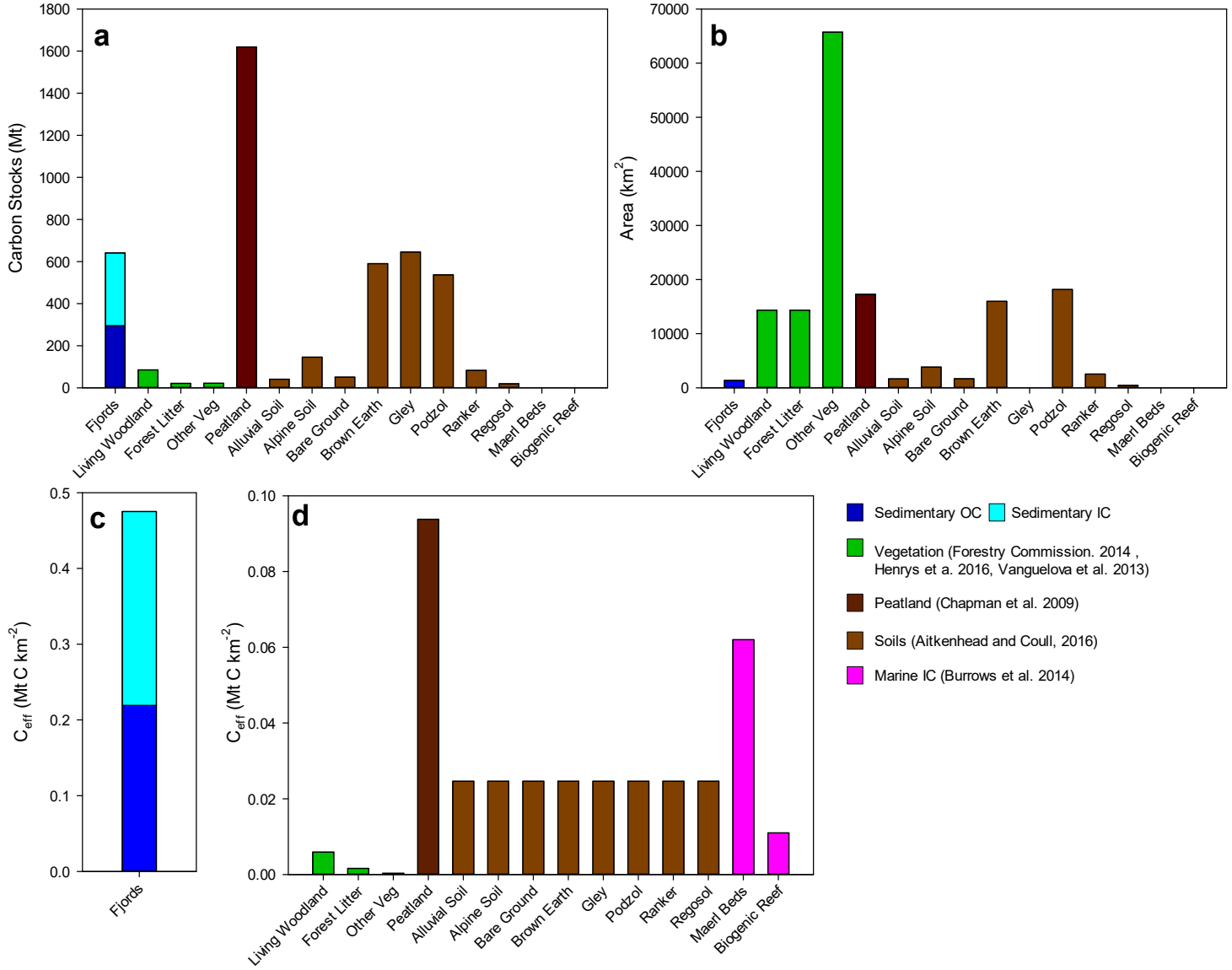

Figure 5.13. Comparison of the Scotland's national fjordic sedimentary C store other national inventories of C. (**a**) Carbon stocks (Mt) (**b**) Area of store (km^2) (**c**) Effective carbon storage (Mt C km^{-2}) for the 111 fjords. (**d**) Effective carbon storage (Mt C km^{-2}) for the other national C stores.

Radiocarbon dating (Nørgaard-Pedersen et al., 2006, Baltzer et al., 2010, Smeaton et al. 2016) shows that the fjords have been collecting sediment since the retreat of the last ice sheet (Clark et al., 2012), which results in these C stores likely being some of the oldest and most persistent in the UK. Of the terrestrial C stores, only soils and peatland have the potential to store C over similar timescales, but they are significantly more vulnerable to natural and anthropogenic disturbance than the fjordic sediments. Vegetation and soil C stores are at risk from rapid and long-term environmental change. These environments can lose significant quantities of C through soil erosion (Cummins et al., 2011), fire (Davies et al., 2013) and vegetation change (Jackson et al., 2002), disturbances which are increasing in regularity and severity with growing climatic and anthropogenic pressure. When we consider the marine sedimentary C stores through the same prism of environmental change, it is evident that the restricted geomorphology, water depth and relative remoteness of these stores affords them a level of protection not found in the terrestrial environment. However, this does not imply that coastal sedimentary C stores do not require careful management. For example, the remobilisation of C-rich sediments at the seafloor from direct physical disturbance poses an increased risk to these effective long-term C stores. The recognition of these coastal habitats for both their biodiversity and additional ecosystem functioning, including C sequestration and storage, represents an important emerging opportunity to designate and help create a new thinking in the establishment of marine protected areas. Taking into account the areal extent of fjords, their proximity to terrestrial sources and their longevity and stability, we suggest that fjordic sediments are the most effective systems for the long-term storage of OC in the UK and it is highly likely that fjords globally are just as effective as their mid-latitude equivalents at storing C.

5.5 Conclusion

The sediments of mid-latitude fjords hold a significant quantity of C which has largely been overlooked in global C budgets and which constitute a significant component of natural capital for Scotland and the UK. Our results indicate that the 640.7 ± 46 Mt C held within the sediments of these fjords is of similar, if not greater, magnitude than most terrestrial C stores. Fjords cover a small area in comparison with terrestrial C stores, but the stability and longevity of these coastal stores means that fjords are a highly effective long-term repository of C, surpassing the Scottish peatlands which have been the focus of intense research for decades. In contrast with their terrestrial equivalents, the magnitude of the fjord sedimentary C stores combined with their long-term stability emphasises the significant role that fjords and the coastal ocean, more generally, play in the burial and storage of C globally. This highlights the need for stronger international effort to quantify coastal sedimentary C stores and account for the C sequestration and associated climate regulating services which these subtidal environments provide.

Chapter 6

Holocene Evolution of a Coastal Sedimentary Carbon Store.

Based Upon: Smeaton, C, Cui, X, Bianchi, T.S, Cage, A.G., John A. Howe, J,A., Austin, W.E.N, Climatic and Human Drivers of Holocene Carbon Burial along the North Atlantic Margin – In Review in *Nature Communications*

Author Contributions: Craig Smeaton, Thomas Bianchi and William E. N. Austin conceived the research and wrote the manuscript, to which all co-authors contributed data or provided input. Craig Smeaton conducted the research as part of his PhD at the University of St. Andrews, supervised by William E. N. Austin, Althea L. Davies and John A. Howe. Craig Smeaton wrote this chapter, expanding on the detail provided by Smeaton et al., 2016.

6.1 Introduction

Millennial-scale climate variability of the sub-polar North Atlantic is a characteristic of Holocene marine, ice core, and numerous terrestrial archives (Fig.6.1), however the underlying drivers of this variability and its influence on terrestrial and marine ecosystems are poorly understood (Mayewski et al., 2004). Atmospheric forcing of Atlantic meridional overturning circulation (AMOC), linked to persistent mode changes in the strength of the winter North Atlantic Oscillation (NAO) during the past millennium (Ortega et al., 2015; Trouet et al., 2009), is a plausible underlying climate forcing mechanism that may have persisted throughout the post-deglacial Holocene epoch (Thornalley et al., 2009). In fact, the impact of AMOC and NAO variability in the Holocene on terrestrial ecosystems sensitive to climate forcing (Knight and Harrison, 2012; Seddon et al., 2016) is gaining attention. The challenge lies in understanding the long-term interactions of climate and humans on the terrestrial environment (Mills et al., 2016).

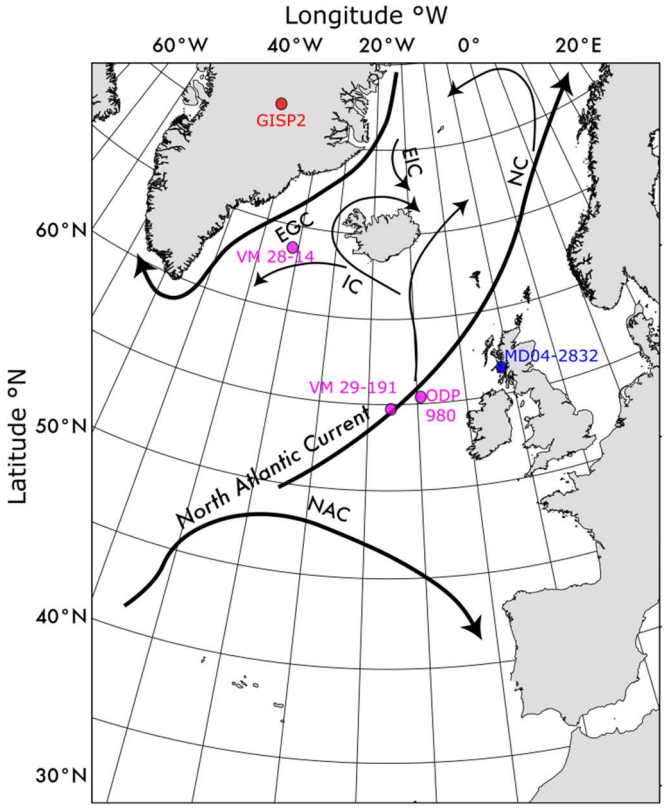

Figure 6.1. North Atlantic Ocean circulation. Location of core MD04-2832 (blue dot), GISP2 and cores VM 28-14,VM29-191 (Bond et al., 2001) and ODP Site 980 (Oppo, McManus and Cullen, 2003) presented alongside the principal surface currents: **NAC**, North Atlantic Current; **IC**, Irminger Current; **NC**, Norwegian Current; **EGC**, East Greenland Current and **EIC**, East Iceland Current.

Humans have been relentless in their ability to alter the terrestrial landscape (Guthrie, 2015), thereby disrupting terrestrial ecosystems (Baker, 1995; Dainese et al., 2017). However, separating complex interactive effects of humans and climate on these ecosystems remains a difficult problem. For example, were humans the main driver of terrestrial ecosystem disturbance in the late Holocene, or did their actions merely enhance the vulnerability of these systems to then be further altered by climate change? If so, these synergistic effects on terrestrial ecosystems will likely respond in a complex non-linear fashion. In the North Atlantic, attempts have been made at the land-ocean interface, using certain aquatic systems as repositories of carbon storage to separate the effects of climatic and human forcing on past alterations in terrestrial ecosystems (Randsalu-Wendrup et al., 2016; Zillén and Conley, 2010); this work has largely been focused in the Baltic Sea region. While this work was successful in reconstructing more regional effects of humans and climate in the Baltic watershed, an aquatic repository situated farther to the west may provide a more suitable location for linking humans to the tele-connections of North Atlantic climate forcing.

Recently, there has been an interest in the role of fjords as global hotspots for sediment and carbon (C) burial (Cui et al., 2016a; Smith et al., 2015) and storage (Smeaton et al., 2016). The unique abilities of these estuarine systems to store carbon, due in part to their deep glacial geomorphology and typically low oxygenated bottom waters, make these systems ideal for reconstructing regional climate change (Cage and Austin, 2010; Faust et al., 2016) and potentially separating the timing and potential drivers of past climatic versus human changes upon the terrestrial landscape. Moreover, fjords located more directly at the interface of North Atlantic climatic drivers (e.g., western UK, Iceland, and Greenland) may offer a more direct linkage for past effects between human and climatic drivers on the landscape. Here, we present a sediment record from Loch Sunart, a fjord on the west coast of Scotland (Fig.6.1) in an attempt to unravel the terrestrial ecosystems response to major phases of North Atlantic climate reorganization and human disturbance through the late Holocene. The fjords along the west coast of Scotland are ideally situated for coupling to North Atlantic circulation (Austin et al., 2006; Gillibrand et al., 2005) and, unlike Greenland and Iceland, have stronger and longer historical records of human occupation and environmental disturbance (Smout, 1993; Tipping, 2013).

6.2 Methods

6.2.1 Sampling

A 22.5 m giant piston core (MD04-2832) was collected from the middle basin of Loch Sunart (Fig.6.2) in 2004 from the French research vessel *Marion Dufresne II* as part of the IMAGES programme. In addition to MD04-2832 a gravity core (PM06-GC01) and a multi-core (PMO6 MC01) was collected at the same site on board the *RV Prince Madog* in 2006. The cores were split and taken to the University of St-Andrews where they were sub-sampled at 10 cm intervals for analysis.

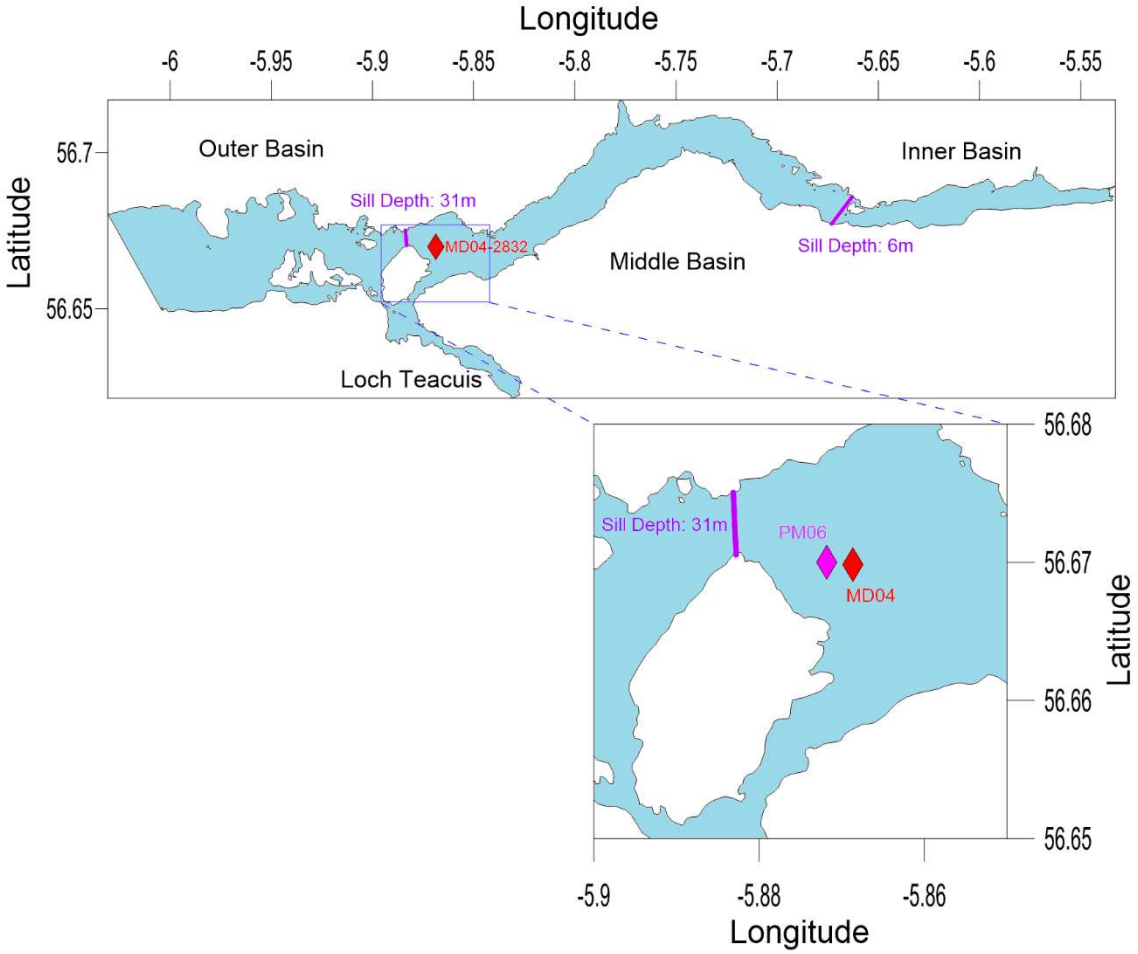

Figure 6.2. Location map of Loch Sunart indicating the MD04 (MD04-2832, MD04-2831) and PM06 (PM06-GC01, PM06-MC01) coring sites.

6.2.2 Core Chronology

Shell material was collected from the length of the core for Accelerator Mass Spectrometry (AMS) dating. In total 22 samples underwent ^{14}C measurement from MD04-2832, PM06-GC01 and PM06-MC01C (Table 6.1) at the Aarhus AMS Centre (AAR) and Scottish Universities Environmental Research Centre (SUERC). Ages were calibrated using OxCal 4.2.4 (Bronk Ramsey, 2009; Bronk Ramsey and Lee, 2013) with the Marine13 curve (Reimer, 2013) and regional correction of 1R value of −26 ± 14 yr (Cage et al., 2006). All ages are calibrated at 95.4 % probability and the mean age has been determined from the minimum and maximum calibrated ages.

Sample ID	Core	Depth (cm)	^{14}C age, yr BP	Error (±)
AAR-11340	PM06-MC01	28.5	476	25
AAR-11332	MD04-2832	35.5	485	24
AAR-11341	PM06-MC01	37.5	568	27
AAR-11342	PM06-MC01	44.5	408	22
AAR-11343	PM06-MC01	47.5	532	31
AAR-11333	MD04-2832	52.5	427	32
AAR-11345	PM06-GC01	62.5	550	25
AAR-11334	MD04-2832	63.5	428	26
AAR-11346	PM06-GC01	92.5	674	76
AAR-11347	PM06-GC01	111.5	818	24
AAR-11336	MD04-2832	119.5	604	37
AAR-11337	MD04-2832	137.5	686	25
AAR-11338	MD04-2832	246.5	1167	24
SUERC-12424	MD04-2832	305	1511	35
AAR-11339	MD04-2832	334.5	1687	28
SUERC-12426	MD04-2832	440	2231	35
SUERC-12137	MD04-2832	1090	4285	35
SUERC-12138	MD04-2832	1350	4625	35
SUERC-10444	MD04-2832	1780	6296	39
SUERC-7316	MD04-2832	1980	6590	35
SUERC-10443	MD04-2832	2250	7142	40

Table 6.1. Radiocarbon ages from Loch Sunart cores MD04-2832, PM06-GC01 and PM06-MC01.

Additionally; a ^{210}Pb chronology was developed for core PM06-MC01 (Table 6.2). The analyses were undertaken at Copenhagen University.

Depth Interval (cm)	^{210}Pb age (year)	Date (year AD)
0.5 – 1.0	1 ± 1	2005 ± 1
9.5 – 10.0	15 ± 10	1991 ± 10
19.0 – 20.0	30 ± 19	1976 ± 19
30.0 – 31.0	47 ± 30	1959 ± 30
36.0 – 37.0	56 ± 36	1950 ± 36
37.0 – 38.0	58 ± 37	1948 ± 37

Table 6.2. ^{210}Pb age and standard deviation errors measured on bulk sediments from PM06-MC01.

The ^{210}Pb and ^{14}C ages were combined to create a full chronology for core site MD04-2832. The methodology used to splice these chronologies is fully discussed in Cage and Austin (Cage and Austin, 2010). To fully understand chronological uncertainty both the ^{14}C ages and ^{210}Pb dates were used in combination with the Bayesian age modelling software BACON (Blaauw and Christeny, 2011). An age models was created representing the full 8000 year record (Fig.6.3). A tephra horizon representing the Landám event (871 ± 1 AD) was identified at 325-330 cm in core MD04-2831 (Cage et al., 2011). As core MD04-2831 was collected in close proximity to MD04-2832 the tephra was used as a test of the age model's accuracy. When compared, the tephra and Bayesian age estimates correspond strongly, validating the models.

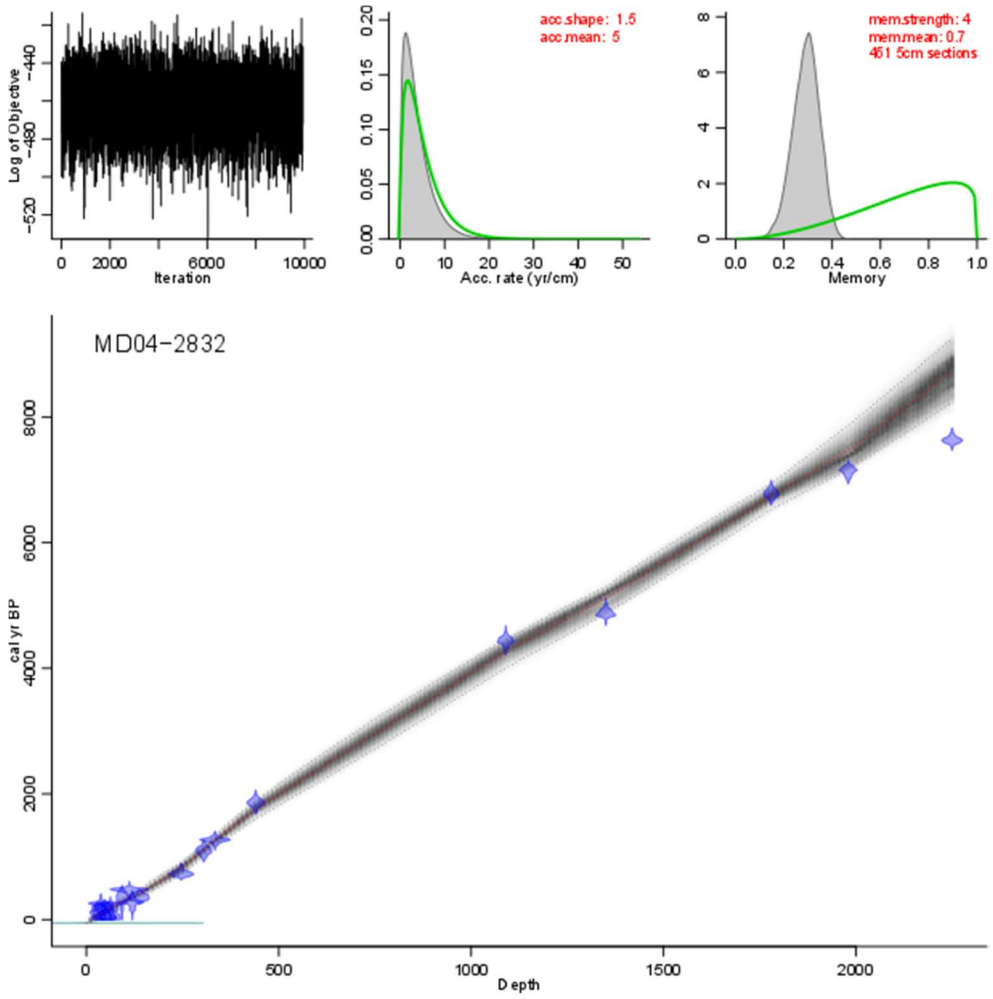

Figure 6.3. Bayesian age model for the based on ^{14}C and ^{210}Pb data from cores MD04-2832, PM06-GC01 and PM06-MC01.

6.2.3 Paleoclimate Reconstruction

Stable oxygen and carbon isotopes were measured on 20-30 hand-picked individuals of the infaunal benthic foraminifera species *Ammonia beccarii*. Samples were cleaned in ethanol, dried at 40°C and run on a Gasbench autosampler coupled to an isotope ratio mass spectrometer (Delta Plus XP, Thermo Finnigan) at the University of St. Andrews. Stable isotope compositions are reported relative to the Vienna Pee Dee Belemite (VPDB) using the NBS-19 standard. Precision of 0.07‰ is based on an internal Carrara marble standard.

6.2.4 Physical Properties Analysis

Water content, bulk density and porosity of the sediment were measured at 10 cm intervals following the standard methodological approaches (Dadey et al., 1992; Danielson and Sutherland, 1986). Magnetic susceptibility (SI units) was measured using a Bartington MS2 system linked to MS2E core logging sensor; measurements were taken at 2 cm resolution. Samples for particle size analysis were prepared using the standard methodology (Jiilavenkatesa et al., 2001); briefly an aliquot of sample material was digested in 30% H_2O_2 to remove organics followed by 10% HCl to remove carbonate, finally the sample was soaked in a 5% Sodium hexametaphosphate $(NaPO_3)_6$ solution to prevent flocculation. The prepared samples were measured on a Laser Granulometer (LS230) at the University of St. Andrews. The mean sortable silt was calculated from the 10-63μm particle size fraction following the standard methodology (McCave et al., 1995).

6.2.5 Geochemical Analysis

Total organic carbon (% OC) and stable carbon isotope analyses ($\delta^{13}C_{org}$) of the sediments were carried out at the University of St. Andrews following standard methodologies (Nieuwenhuize et al., 1994; Verardo et al., 1990). Measurements were made using an elemental analyser (COSTECH) interfaced with an isotope ratio mass spectrometer (Delta Plus XP, Thermo Finnigan). Carbon isotope ratios were calculated in δ notation relative to the Vienna Pee Dee Belemnite (VPDB) standard. The precision of duplicate measurements was ±0.1‰.

A suite of metals where measured using inductively coupled plasma mass spectrometry (ICP-MS). Samples preparation followed the standard method (McLaren 1990), where sample aliquots were digested in 2% HNO_3 before analysis on a Thermo X'Series II ICPMS at the University of St-Andrews.

6.2.6 Biomarkers

Analysis of alkanes and fatty acids was based on a modified method of Cui et al. (2016b). Briefly, ~1 g samples were extracted on accelerated solvent extractor (ASE) using dichloromethane (DCM): methanol (MeOH) (9:1 v:v). After being saponified with KOH in

MeOH, “neutral” and “acid” fractions were sequentially extracted with hexane and hexane: DCM (4:1 v:v). The former fraction containing alkanes were analysed on the gas chromatography – flame ionization detector (GC-FID) for alkane concentrations. The latter fraction containing fatty acids (FA) were then derivatized using boron trifloride (BF3) in MeOH, re-extracted using DCM, and eluted using DCM on a Pasteur pipette column. Fatty acid methyl ester (FAME) samples were analysed on the same GC-FID as above. The concentrations of alkanes and fatty acids were calculated and corrected with internal standards (C_{34} alkane isomer, C_{19} FA) and mix standards of alkanes and FAMEs. ALK $C_{25\text{-}35}$ is calculated as the sum of the odd chain C_{25} to C_{35} alkanes, while ALK $C_{24\text{-}36}$ is the sum of even chain C_{24} to C_{36} alkanes. ALK P_{aq} is the ratio of C_{23} and C_{25} alkanes over the sum of C_{23}, C_{25}, C_{29}, C_{31} alkanes. Short chain fatty acids (SCFA) is calculated as the sum of C_{12} to C_{18} fatty acids, while long chain fatty acids (LCFA) is calculated as the sum of C_{24} to C_{32} fatty acids. Terrestrial to aquatic ratios of fatty acids (TAR_{FA}) is the ratio of C_{24}, C_{26} and C_{28} fatty acids over the sum of C_{12}, C_{14}, C_{16}, C_{24}, C_{26}, C_{28}. Finally, the ratio of fatty acids to alkanes (FA/ALK) is the ratio of $C_{24\text{-}32}$ fatty acids to $C_{24\text{-}36}$ alkanes.

Analysis of glycerol dialkyl glycerol tetraethers (GDGTs) was based on the method of Liu et al. (2016) and Smith et al.(2010). Shortly, ~1 g of sediment samples were sonicated and extracted using DCM: MeOH (9:1 v:v) using an ultra-sonicator. The extracts were re-concentrated in hexane and analysed on a liquid chromatography – mass spectrometry (LC–MS). Quantification of GDGTs was achieved by using a synthesized tetraether surrogate standard and focusing on targeted ions (e.g., *m/z* 1292) on the LC–MS. Branched/isoprenoid tetraether (BIT) index (Hopmans et al., 2004) is calculated as the ratio of three branched GDGTs (I, II, and III) to the sum of branched and crenarchaeol GDGTs. The targeted *m/z* of the four compounds are 1022, 1036, 1050, and 1292 for branched I, II, III and crenarchaeol GDGTs.

6.2.7 Sedimentation and OC Accumulation Rates

Sedimentation rates (cm yr^{-1}) were calculated using the output from the Bayesian age model at 100 and 500 year intervals. OC accumulation rates (OCAR) where calculated for each interval using the standard methodology (Loh et al., 2010; Smith et al., 2015). Briefly, the average bulk density, porosity and %OC was calculated for each of the time intervals allowing the OCAR to be calculated following:

OCAR = %OC x sedimentation rate x (1 - porosity) x wet bulk density

6.2.8 REVELS Modelling

We estimate past regional vegetation composition using the regional estimates of vegetation abundance from large sites (REVEALS) modelling approach (Sugita, 2007). REVEALS is a Landscape Reconstruction Algorithm (LRA) (Sugita, 2007) which transforms pollen proportions into estimates of vegetation cover at a regional scale. We utilised the REVEALSinR model which is part of the DISQOVER package for R. REVEALSinR implements the REVEALS model (Theuerkauf et al., 2016) and integrates Lagrangian stochastic dispersal modelling (Kuparinen et al., 2007). Data for two independent sites (i.e. pollen counts) were taken from the European Pollen Database (www.europeanpollendatabase.net). The sites where chosen due to their proximity to our study area, availability of suitable chronological constraints and full pollen counts.

6.3 Regional Response to North Atlantic Climate

Loch Sunart (Fig.6.2), is separated from the coastal ocean by a 33 m deep sill, which allows for direct sub-surface exchange and communication of shelf salinity and temperature into the main basin (Gillibrand et al., 2005). The main basin core site (MD04-2832) is therefore directly influenced by the hydrography of the Scottish Shelf, where northward flowing Scottish Coastal Current (SCC) waters are influenced by the intrusion of North Atlantic water onto the shelf (Gillibrand et al., 2005; Inall et al., 2009). Using $\delta^{18}O$ composition from benthic foraminifera at the core site as a measure of the interplay between the salinity and temperature of seawater (O'Neil, 1969) illustrates pronounced millennial-scale variability of up to 1 ‰ over the Holocene (Fig.6.4). This Holocene variability in $\delta^{18}O$ corresponds to both North Atlantic climate reconstructions (Bond et al., 2001; Oppo et al., 2003; Thornalley et al., 2009) as well as chemical records from the Greenland Ice Sheet Project 2 (GISP2) (Fig.6.4).

The most pronounced feature of the Loch Sunart record occurs shortly after 6000 cal. BP, when $\delta^{18}O$ values reach their lowest (0.9 ‰) and then increase abruptly shortly before 5000 cal. BP (Fig 6.4). The timing of this event is broadly coincident with the decreasing relative North Atlantic Deep Water contribution inferred from benthic foraminiferal $\delta^{13}C$ from ODP Site 980 (Fig.6.1), which began at ~6500 cal. BP (Oppo et al., 2003). At the same time, the GISP2 ice core record suggest major atmospheric reorganization (Meeker and Mayewski, 2002). This, in conjunction with increase in the relative abundance of haematite-stained grains in northeast North Atlantic cores between 6000-5000 cal. BP (Bond et al., 2001), suggests an expansion of the polar vortex and a shift towards winter-like conditions at high latitudes.

The Sunart record shows minimal response from the terrestrial ecosystem to this large climate reorganisation. However, this response may be masked by effects of Relative Sea Level (RSL) during this period. The relatively steady, long-term fall in Holocene RSL (Fig. 6.4) since 7500 cal. BP (Shennan et al., 2005) will have effectively reduced sill depth from ~41 m (mid-Holocene) to 33 m (present) and modified sub-surface exchange and bottom currents with the coastal waters. The increased openness of the fjord at this time allows greater exchange between the coastal and fjord waters resulting in the lowest OC values (0.9% OC) with much of that buried OC originating from marine sources, as illustrated by the shift in C/N ratio (Fig.6.4). This is further supported by the steady increase in the mean sortable silt size due to a reduction in the winnowing of fine particles due to the alterations of bottom water currents (Fig.6.4).

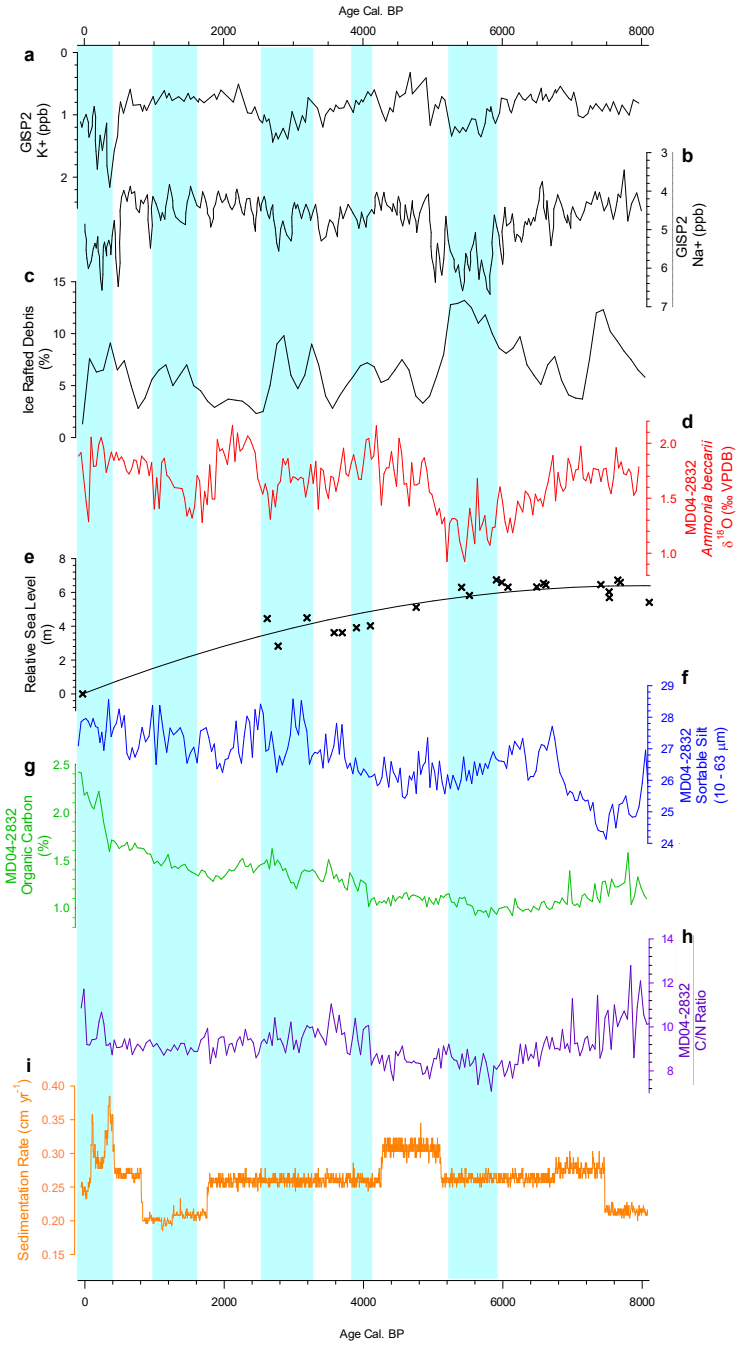

Figure 6.4. Age calibrated MD04-2832 record in the context of North Atlantic Holocene paleoclimate records (**a**) Gaussian smoothed (200 yr) GISP2 sodium (Na+; parts per billion, ppb) ion proxy for the Icelandic Low (**b**) Gaussian smoothed (200 yr) GISP2 potassium (K+ ; ppb) ion proxy for the Siberian High (Mayewski et al., 2004; Meeker and Mayewski, 2002). (**c**) Pervasive millennial-scale cycle illustrated by ice rafted debris (%) from cores VM-28-14 and VM-29-191 (Bond et al., 2001). (**d**) MD04-2832 foraminifera (Ammonia beccarii) δ18O (‰ VPDB) record as a proxy for basin temperature/salinity. (**e**) Regional relative sea level (Shennan et al., 2005) (**f**) MD04-2832 sortable silt mean size (after removal of biogenic components) record as a proxy for bottom current (**g**) MD04-2832 organic carbon (%) (h) MD04-2832 C/N ratio. Vertical shading represent the Rapid Climate Change timing tuned to the GISP2 chronology (Mayewski et al., 2004). (**i**) Sedimentation rate (cm yr^{-1}) calculated from the Bayesian age model (Fig.6.3).

Regional landscape vegetation reconstructions, which are decoupled from RSL (Fig.6.5), indicate that over this period the woodland coverage was not adversely impacted by this climate reorganisation. For example, around Gallanech Beg (Fig.6.5b) woodland increased and this likely further stabilised the terrestrial ecosystem (Achat et al., 2015). Interestingly, this masking effect dissipates as we transition away from the mid-Holocene RSL highstand. At this time, we begin to see periods of increased terrestrial input in Loch Sunart, as indicated by coarser sortable silt and increasing C/N ratios, which coincide with periods of rapid North Atlantic climate change (Fig.6.4). This pattern holds throughout the Holocene until late in the record where we observe disproportional increases in terrestrial inputs that seem de-coupled to climate change, suggestive of another driver linked with this nonlinear terrestrial response. This is the time when humans began shaping the landscape.

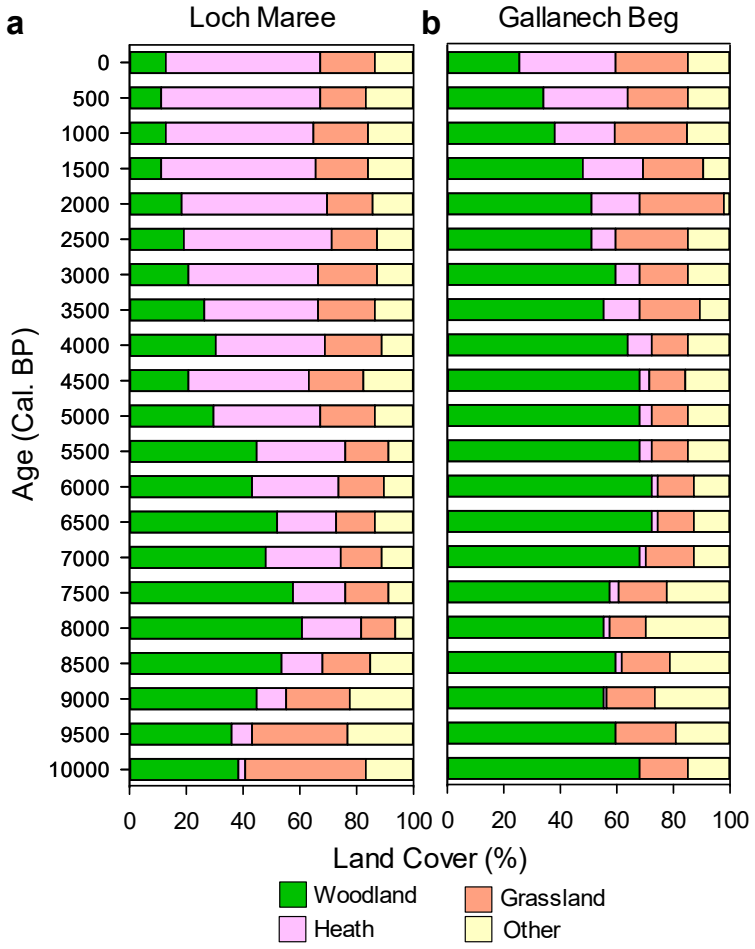

Figure 6.5. Estimated Holocene regional vegetation cover types for West Coast of Scotland derived from the REVEALS modelling. (**a**) Loch Maree(Birks, 1972) (**b**) Gallanech Beg (Davies, 1997). Pollen counts available from the European Pollen Database (www.europeanpollendatabase.net).

6.4 The Human Dimension

Humans have been a feature of the North Atlantic coastal landscape of Europe for the last 0.5 Ma years (Cohen et al., 2012) and the west coast of Scotland has been occupied since the Palaeolithic period (Mithen et al. 2015). It is believed that the region surrounding Loch Sunart was permanently settled at approximately 4000 cal. BP (Bishop et al., 2015; Tipping, 2013).The earliest anthropogenic alteration to leave a lasting legacy on the environment was the removal of woodlands (Smout, 1993), which destabilised soils (Achat et al., 2015,Macklin et al. 2000), thereby enhancing the release of C from the watershed. Regional landscape reconstructions (Fig.6.5) from the North and South of our study site both show that woodland cover begins to decline at 5500-4500 cal. BP, which corresponds with the start of long-term increased inputs of OC to Loch Sunart's sediments (Fig.6.4). The coarser grain size and higher C/N ratios further suggest this increased input of OC is terrestrial in origin, likely as a consequence of soil destabilisation due to woodland removal. The removal of these woodlands initiated landscape reorganisation of vegetation with the appearance of more pioneering plant species and grasslands, which initially dominated the partially deforested landscape before being replaced by heath and grassland communities (Fig.6.5). This shift of vegetation is common throughout Scotland and the North Atlantic region (Fyfe et al., 2013; Williams et al., 2002). Heath plants, such as heather, have the ability to stabilise soils (Panagos et al., 2015), but are vulnerable to grazing pressure (Hartley and Mitchell, 2005) (i.e. sheep and deer) and less adaptable to climate alterations compared to the earlier pioneering plant species (Coll et al., 2016). Interestingly, through plant succession the catchment recovered from the initial human impact of large-scale deforestation, but the widespread change in vegetation probably resulted in the catchment being more vulnerable to future climatic and/or anthropogenic changes.

The last millennium has seen an unprecedented anthropogenic pressure placed on the catchment to provide resources for the growing local and national populations in Scotland (Fig.6.6). Much of this pressure has centred on the river networks and the River Strontian in particular were most of the population in the region has settled.

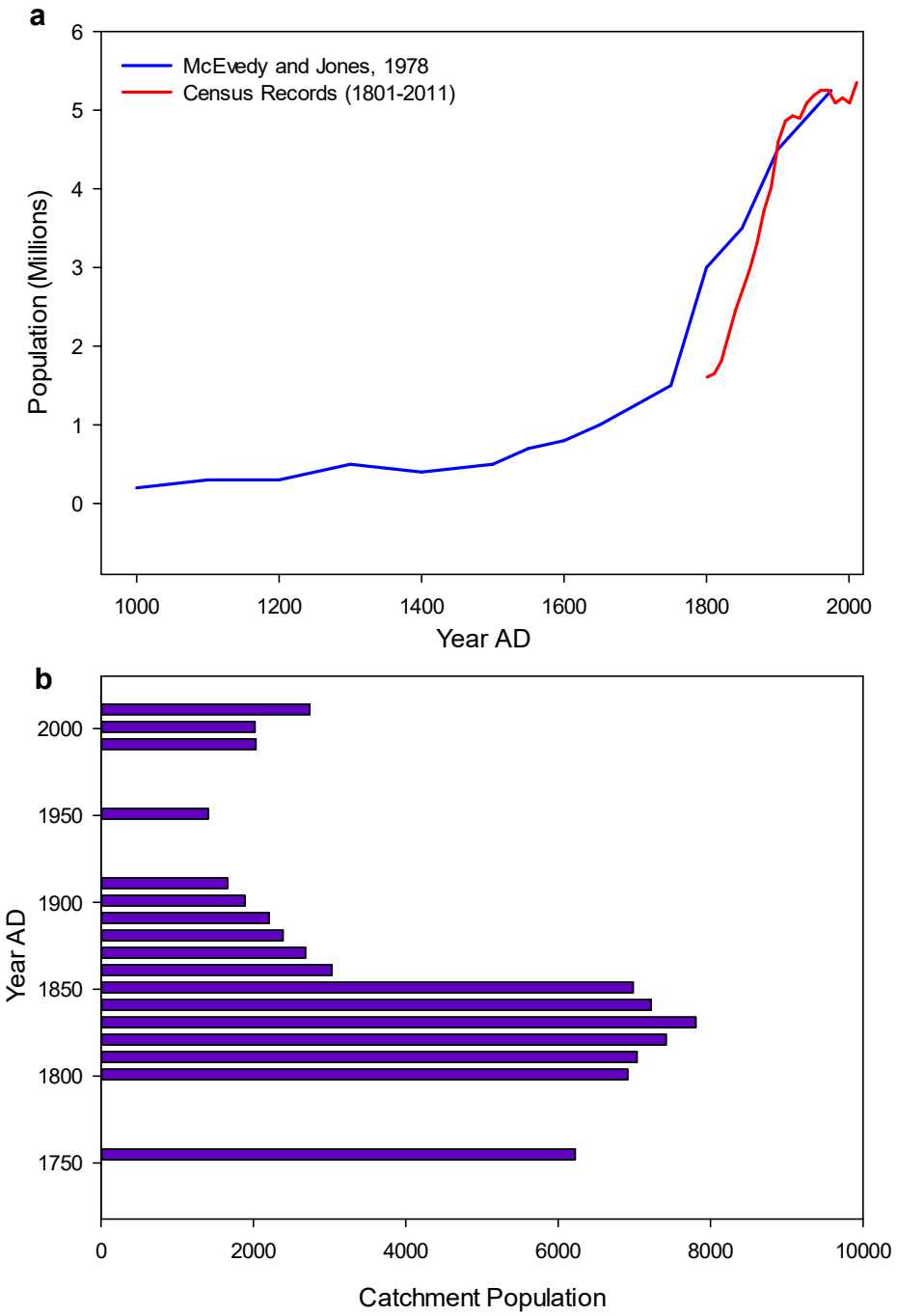

Figure 6.6. Estimates of the total population of (**a**) Scotland for the last millennium, (McEvedy and Jones, 1978) illustrated alongside 1801-2011 census data (National Records of Scotland). (**b**) Loch Sunart catchment population 1755 to 2011. 1755 record derived from Webster's Analysis of population, 1755. 1801-1951 data accessed from the National Records of Scotland (www.nrscotland.gov.uk/research/guides/census-records). 1991-2011 data accessible from Scotland's census (http://www.scotlandscensus.gov.uk/).

Early in the last millennium, sediment records from Loch Sunart show that the catchment was in a steady state, but this state was disturbed at approximately 1520 ± 63 AD when there is a significant change in the record towards greater terrestrial input (Fig.6.7) which could be attributed to anthropogenic disturbances. During this time period (16th Century) in the vicinity of the Sunart catchment, scrub was being removed from the landscape to improve grazing and local charcoal production (Tipping, 2013), which in turn reactivated lower slope erosion mobilization soil materials (Brazier and Ballantyne, 1989). It should also be noted that early geomorphological instability (15th century) recorded in the region was likely due to woodland and scrub removal (Ballantyne, 1991, Ballantyne 2008). The initial phase of this disturbance resulted in a pulse of coarse grained minerogenic material being delivered to Loch Sunart sediments - likely due to erosion of deep soils which correspond to terrestrial geomorphological records (Ballantyne, 1991; Brazier and Ballantyne, 1989). This high minerogenic input resulted in a dilution effect, lowering the %OC in fjord sediment. The initial pulse of lithic material was followed by an increased input of terrestrial OC (1584 ± 58 AD), as evidenced by a decrease in $\delta^{13}C_{org}$ from -14.9 ‰ to -20.5 ‰ (Fig. 6.7) which is supported by the long chain fatty acids and the Alkane lipids both of which represent vascular plant inputs. The BIT index (Fig 6.7) also indicates that during this period there was an increase of soil derived C being transported to the sediments of the fjord. This pattern is comparable in other local fjord sedimentary records (Nørgaard-Pedersen et al., 2006), therefore we can suppose the Sunart record is reflective of regional terrestrial responses. Although these values are still within the range of marine-derived OC, there is a clear trend towards greater terrestrial inputs in a region of the fjord known to be strongly influenced by marine input (Smeaton and Austin, 2017). This shift towards greater terrestrial input is further supported by the biomarker profiles which all indicate an increase in terrestrial OC input to the sediments. Additionally, throughout this time period marine inputs remained stable, as indicated by constant Crenarchaeol concentrations, both the sediment and OC normalized values, suggesting that the changing OC in Loch Sunart's sediment was driven by terrestrial inputs (Fig.6.8). Interestingly, during this period of increased OC input the stable marine inputs to the fjord sediments suggest these terrestrial OC inputs were not accompanied by higher inputs of nutrients, such as P, as previously shown in the Baltic Sea (Randsalu-Wendrup et al., 2016; Zillén and Conley, 2010). Unfortunately, no macronutrient (e.g., P and N) measurements have been made in Loch Sunart for comparison.

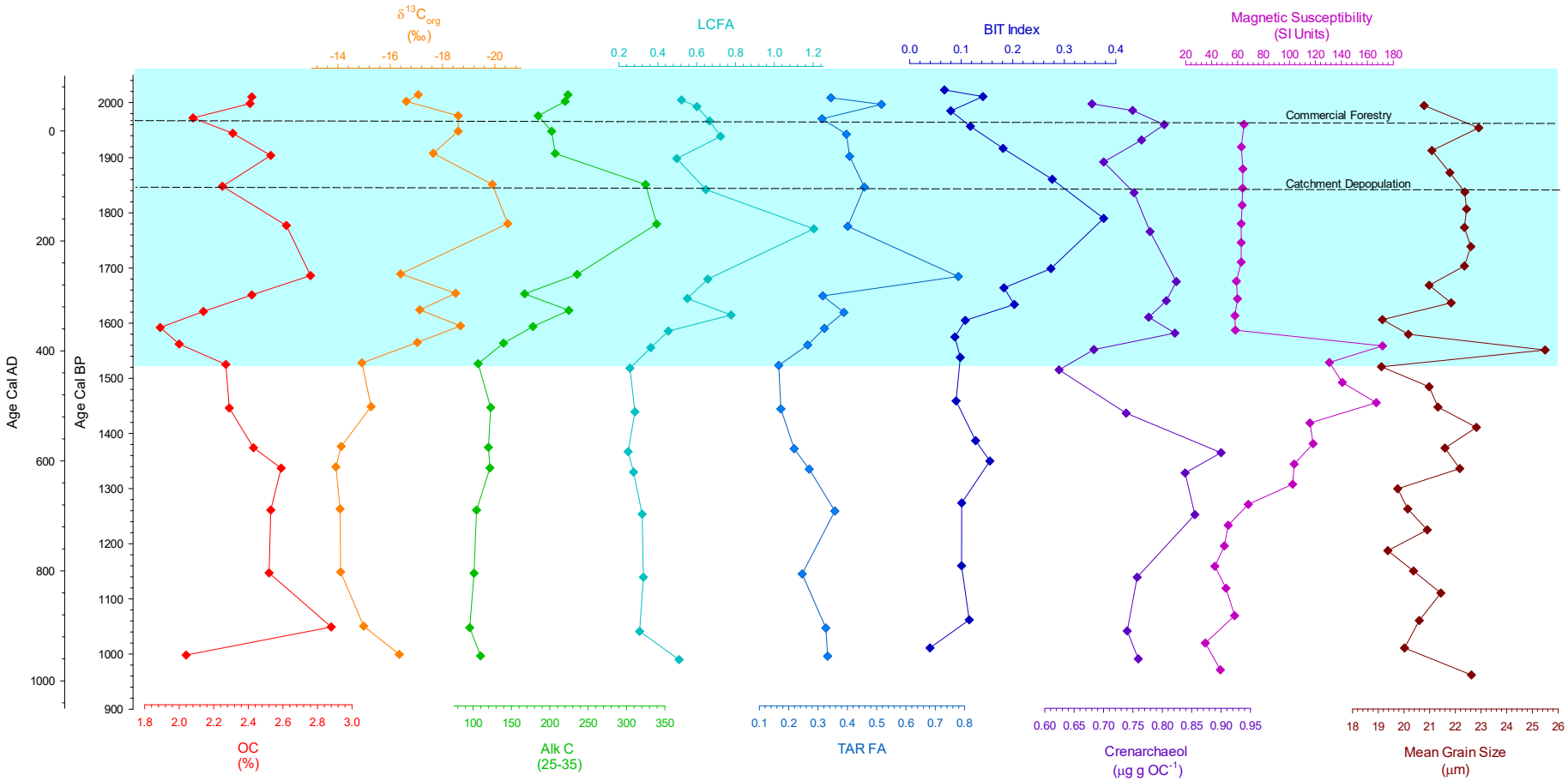

Figure 6.7. Bulk elemental, biomarker and physical property profiles of core MD04-2832 spanning the last 1000 years.

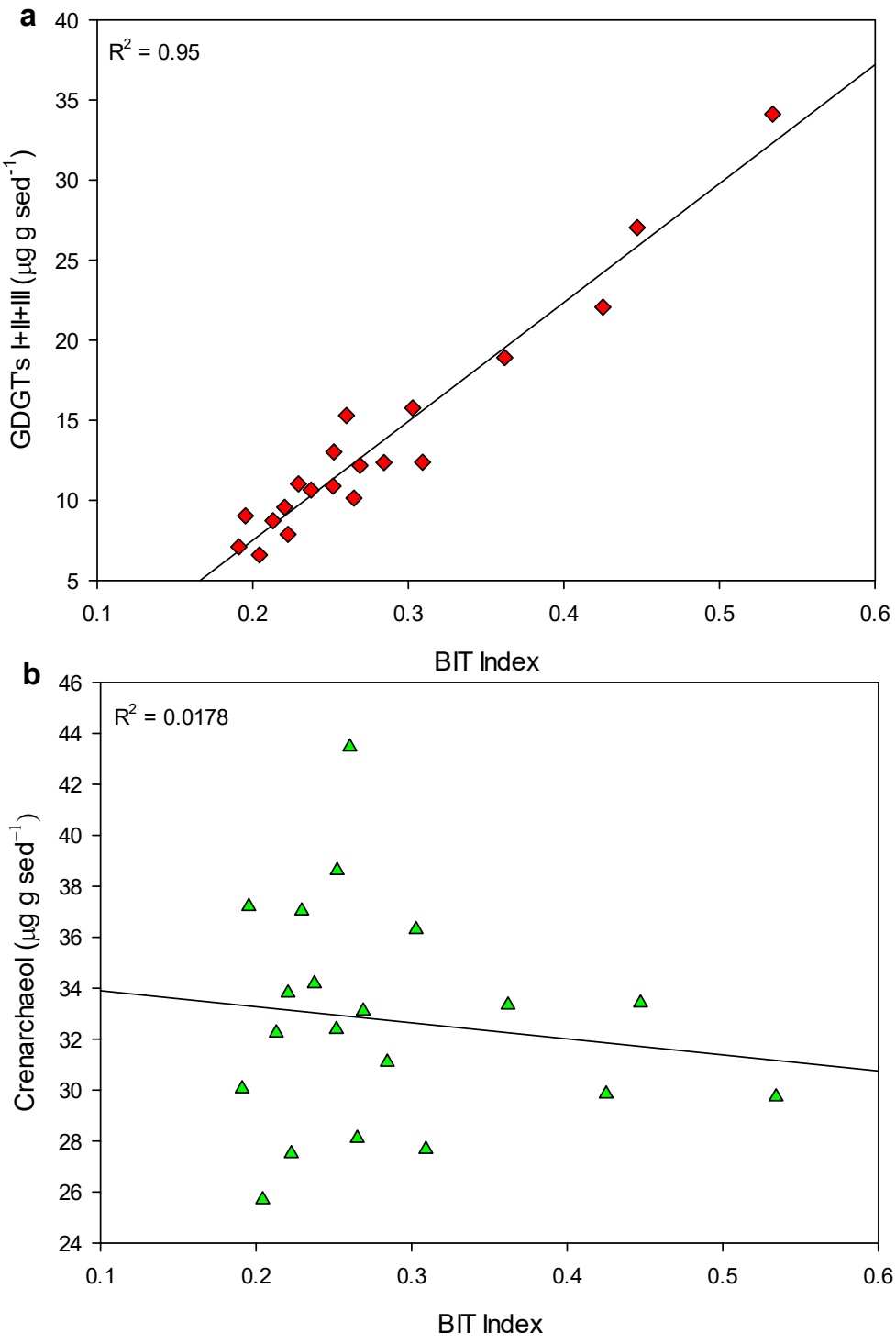

Figure 6.8. BIT index regression plots (**a**) BIT Index vs GDGT's I+II+III (µg g sed^{-1}) (**b**) BIT Index vs Crenarchaeol (µg g sed^{-1}).

The decline in terrestrial inputs to Loch Sunart sediments in the early to mid-1800's suggests a return to pre-1520 levels based on chemical biomarkers and bulk OC proxies. This change could be due to the exhaustion of erodible soil materials, or more likely the recovery of vegetation and stabilisation of the catchment. Although this is a time when Scotland's urban population experienced a period of rapid growth, the rural population of Scotland's west coast was in decline due the Highland Clearances, which saw tenants evicted from the land through the 18th and 19th centuries. This, in combination with the 1846 potato famine, triggered a severe depopulation within the Sunart region and beyond (Fig.6.6). This significant reduction in population (44 % decrease) reduced the human pressures on the catchment, allowing for partial vegetation recovery thereby reducing the terrestrial inputs to fjord sediments. Nevertheless, at this time of forced emigration from the region, the advancement of technological innovation began as a new stage of human development in the catchment that essentially occurred in two phases. Firstly, mining in the area started as early as 1722, with lead , nickel and silver being mined sporadically through the following centuries (Fig 6.9). Mining in the catchment ceased in 1990, but left a lasting legacy in the sediment record. The second phase of the post-industrial era was heralded by the introduction of commercial forestry. While it is true that woodlands in the catchment had been managed since at the beginning of the 18th century (Sansum et al., 2005), the scale of disturbance associated with the introduction of the Forestry Act of 1919 had never been witnessed before. In particular, wide spread planting in the catchment occurred in the 1950's; this is reflected in Loch Sunart's sediment record showing increase terrestrial inputs from this point onward (Fig. 6.7). Although small shrub succession and even mature tree stands will lead to stabilization of soils, catchment disturbances associated with tree planting initially resulted in a pulse of coarse-grained material being mobilized and transported to Loch Sunart, diluting the bulk OC in sediments, followed rapidly (1964 ± 8 AD) by a sharp increase in terrestrial OC. Interestingly, this initial response of OC dilution, via coarse lithic material inputs from eroding soils, is similar to that observed during the 1520 event, albeit markedly smaller.

The pressure humans have exerted on the catchment from the late 18th century to the present day (Fig.6.9) is several orders of magnitude more intense than before the 1520 AD event, yet the terrestrial response to these later catchment alterations are somewhat muted in comparison (Fig. 6.7). Therefore, it is unlikely that human activity is the sole driver of this intense response from the terrestrial environment. It is here, that we posit the role of climatic change needs to be considered to better explain these catchment responses and temporal differences.

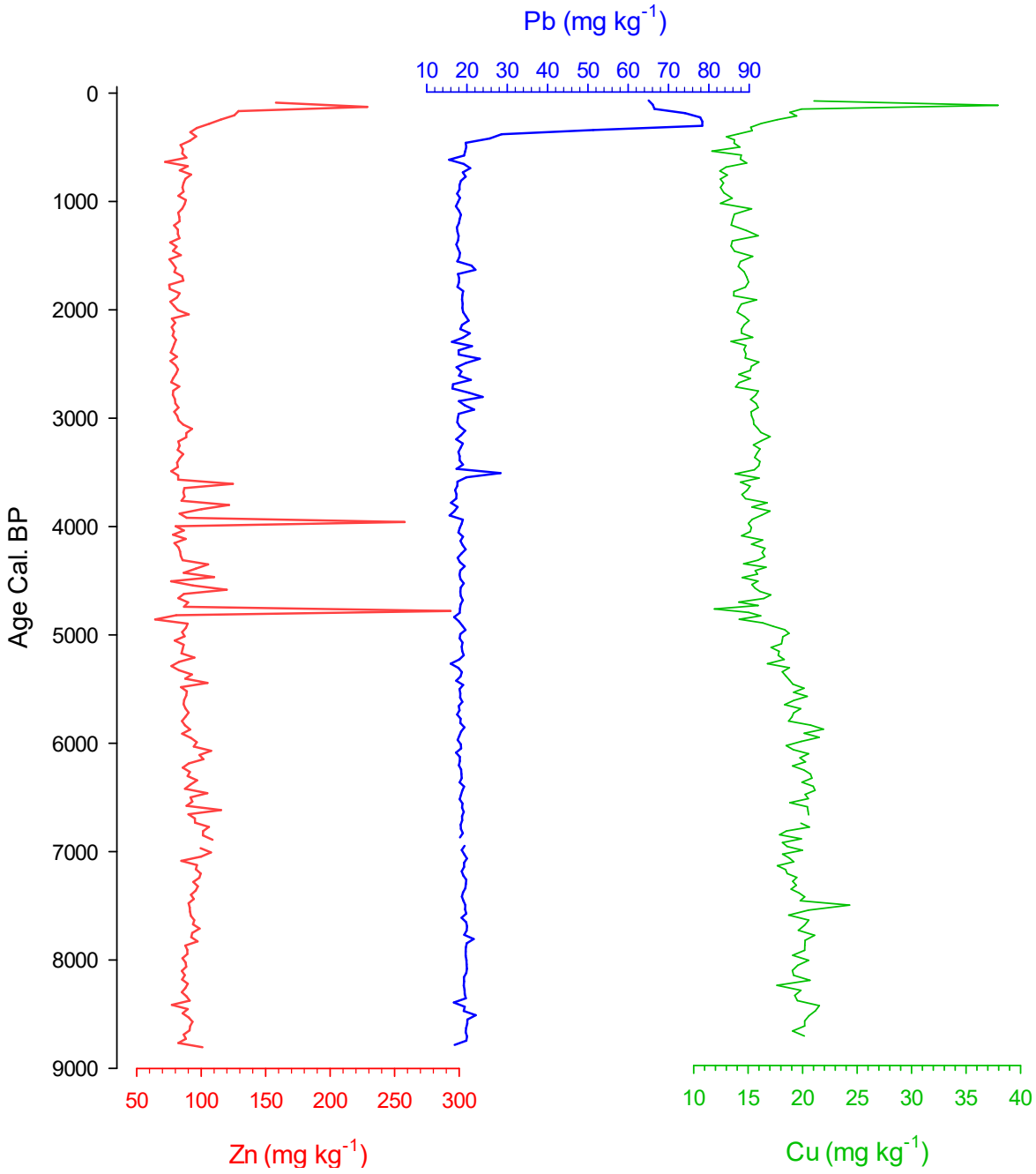

Figure 6.9. MD04-2832 down core profiles of the metals (Zn; Zinc, Pb; Lead) mined and those associated with the mined ore (Cu; Copper) from the catchment from the early 1700's

6.5 Climate vs Human Drivers

Was the AD 1520 event due to an increase in anthropogenic or climatic pressure, or both? The MD04-2832 record suggests that the terrestrial environment at this likely responded to a synergistic interactive effect between climate and humans. For example, in AD 1450 (within chronological uncertainty of AD 1520) there is a shift in the NAO from a negative to positive phase (Ortega et al., 2015; Trouet et al., 2009), which would have created a wetter and warmer atmosphere over NW Europe. Moreover, peatbog water table (Charman et al., 2006; Langdon et al., 2003) and tree ring temperature reconstructions (Rydval et al., 2017) from Scotland further confirm this widespread atmospheric reorganisation and corroborates a wetter environment. The Sunart catchment has been shown to be sensitive to NAO-forcing, whereby the switch in the phase of NAO (Gillibrand et al., 2005), could actually begin to destabilize the catchment for soil and C loss. In particular, during the dry negative NAO phases the catchment would build and store soil materials, which could then quickly be lost during the shift to a positive, wetter phase of the NAO. There have, of course, been similar changes to climate and phase of the NAO throughout the Holocene (Fig.6.4) yet, with this preliminary destabilization effect of human disturbances within the catchment, it appears that a major reorganization in the mode of the NAO over the North Atlantic at AD 1450 may have acted as a trigger to this heightened terrestrial response.

We suggest that the long-term alterations of the terrestrial environment by humans further sensitized the catchment to climatic forcing. The shift in the NAO with the associated preliminary diffuse destabilization of the catchment, resulted in a more vulnerable terrestrial ecosystem, and the crossing of a “tipping point” that allowed for the significant mobilization of terrestrial OC to fjords sediments observed in 1520 AD (Fig.6.7). These types of synergistic interactions between climate and humans, further support the importance of non-linear response of the environment to climate change that need to be considered in climate modelling (Ahlström et al., 2012; Overland et al., 2016; Sun and Mu, 2017), This coupling of climate and human drivers at the start of the 16th century provides a unique and useful example of how depositional environments at the land-ocean transition, like fjords, particularly when they are located at the interface of large-scale climatic oscillations, can be used to understand climate versus human-induced changes across the landscape of the late Holocene.

The idea of the modulation of the C cycle by our early ancestors as a marker of the Anthropocene has been posited (Boyle et al., 2011; Ruddiman and Ruddiman, 2013)

and we contend this tipping-point threshold reached in the early 16th century indicates regional onset of the Anthropocene, in this case, by their actions to destabilize what aspects of landscapes by allowing climate to act as a driving mechanism to deliver terrestrial soil carbon into a long term marine store. Alternatively, as the long history of woodland decline illustrates (Fig.6.5), our early human ancestors were clearly active in these landscapes, removing trees and preconditioning their environment long before (5500-4500 cal. BP) these notional initiation dates for the Anthropocene.

The anthropogenic disturbance of the catchment from the mid-18th century onwards has been orders of magnitude more severe than before the 1520 AD event therefore it is reasonable to assume the catchment and the C held within in its biosphere is in a perilous position.

6.6 Carbon Burial

Future shifts in climate have the potential to facilitate large scale terrestrial responses in the form of soil and C loss, further increasing the importance of the coastal ocean and fjords in capturing terrestrial C. While fjords are known hotspots for C burial (Smith et al., 2015) and storage (Smeaton et al., 2016) the effectiveness of these environments as OC sinks over Holocene timescales is now evident (Fig.6.10). Falling RSL over the Holocene restricted the input of marine derived OC which caused the initial drop in OCAR. By the mid-Holocene increasing terrestrially derived input (Fig.6.4) stabilised OC accumulation. This stability suggests that Loch Sunart's sediments have been long-term hotspots for the burial and storage of C (Smeaton et al., 2016; Smith et al., 2015) throughout the mid- to late Holocene.

During the last millennium this stability has been disrupted with a 48 % rise in OCAR in comparison to the average over the preceding 6500 years. The rise in OCAR during the last millennium (Fig.6.10b) has been linked to increased terrestrial input (Fig.6.7) driven by climatic and anthropogenic pressure on the catchment. Over the last millennium there have been two significant increases in sedimentation rate (SR) (Fig.6.10c) which correspond to the early 16th Century climate event and the post-industrial era (~1850 AD) disturbances of the catchment. Both increases in SR are followed by an increase in OCAR of an equivalent magnitude. These increases can be extreme and rapid but they also return to the Holocene norm quickly after each event (Fig.6.10) This demonstrates that fjords respond to change and have the capacity to capture and bury OC at greater rates than the long-term averages. This adaptability of the coastal ocean, and fjords, in particular in trapping terrestrial OC released by climatic and anthropogenic activities may represent an unrealised yet significant long-term buffer in the global climate system.

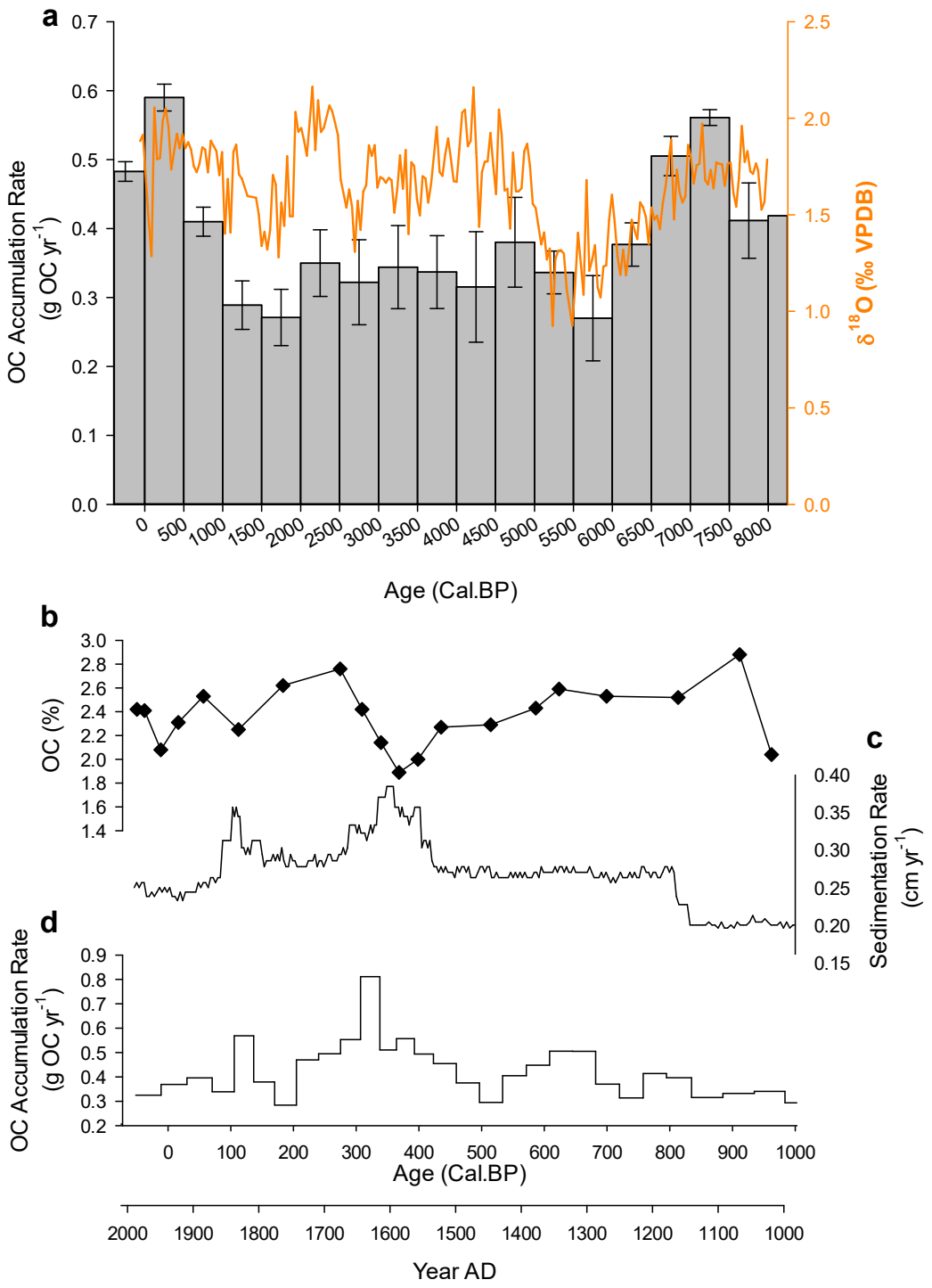

Figure 6.10. (a) Holocene OC accumulation rates for site MD04-2832 overlain by the foraminifera $\delta^{18}O$ record **(b)** % OC (**c**) Sedimentation and (**d**) OC accumulation rates for the last 1000 yrs.

6.7 Conclusion

During the Holocene North Atlantic terrestrial ecosystems and their associated carbon stores were under pressure from both millennial-scale climate variability and increasing anthropogenic activity. We have shown that both climate and humans are drivers of terrestrial ecosystem destabilization allowing C to be transferred to the coastal marine environment. The results indicate that climate and human activity independently drove changes to the catchment but during times in the past when both these drivers were coupled, the terrestrial response was pronounced. Long-term sustained human disturbance sensitized the catchment to climate forcing, suggesting that catchment tipping points were the result of pre-Anthropocene human disturbance. The results highlight the long-term importance of fjords as hotspots for carbon burial and the potential role of terrestrial carbon subsidy to the coastal ocean as an overlooked buffer in the global climate system.

Chapter 7

Conclusion

7.1 Synthesis

This project set out to develop our understanding of C held within the sediments of fjords and to highlight the scale of the role they may play in global climate regulation. Using Scotland, a region largely devoid of data, as a natural laboratory the project sought to quantify the C stored within the sediments of fjords, identify and map the sources of that C and determine how these coastal C stores formed through time.

Understanding the quantity of C held within marine sediments, and fjords in particular was highlighted as a priority research question in 1987 (Syvitski et al., 1987), yet little has been achieved towards this goal. The main hurdle to the production of C stock estimates for marine sediments is the lack of a methodological approach capable of integrating the full depth of sediment held within these environments. Using a combination of seismic geophysics and geochemistry a new methodological approach has been developed (Chapter 3) to achieve this goal. The new methodology provides a platform to develop sedimentary C stock estimations for fjordic environments but it is also applicable to other environments which have similar issues in determining the full depth of sediment; these range from freshwater lakes, shelf sediments, blue carbon habitats (saltmarsh, seagrass and possibly mangroves) and potentially even terrestrial environments such as peatlands. Importantly, the new methodology where possible attempts to quantify the uncertainties in the estimations, recognising that these estimates are not perfect but they do represent the first steps to a better understanding of C stored in marine sediments.

The development of this new methodological approach provided a framework for the first time to examine a nation's marine sedimentary C resource. By utilising the joint geophysical and geochemical methodology in a number of different fjords with differing physical characteristics, an upscaling protocol was developed to estimate the sedimentary C stock of Scotland's fjord network. This full depth integrated sedimentary C stock estimate for Scotland's fjords is a first and provides useful insights into a largely forgotten C store. The results showed that the fjord sediments store around one third of the C held within Scotland's C rich terrestrial environment but when normalized for area the fjords are a far more effective C store. The results also highlight the importance of integrating the true depth of sediments into C stock estimation as the fjords hold a greater quantity of OC than previous estimates of Scotland's entire EEZ (Burrows et al., 2014).

One of the major unanswered questions that we sought to address was how does the C rich terrestrial environment interact with the coastal ocean. Using a stable isotope

approach combined with Bayesian mixing modelling, it was shown that 42 – 65 % of the OC held within Loch Sunart was terrestrial in origin which is comparable to global estimates (Cui et al., 2016b). The results from this work suggested that the sediments of these fjords were potentially better long-term stores of terrestrial C than the local terrestrial environments from which much of the OC is derived.

The results from this study have shown that there are significant quantities of C held within the sediments of the Scottish fjords and that they are closely linked to the terrestrial environment. It is clear that these environments are highly important for C burial and potentially climate regulation. Yet in Scotland and around the world little is known about the long-term role these environments have played in climate regulation and what has driven the development of the C stores. The work presented in Chapter 6 showed the complex nature of climate and human interactions which have driven the development of these C stores. The results indicate that the fjords have been burying and storing C at a consistent rate for much of the Holocene, suggesting these systems have been playing an important role in long-term global climate regulation. Further the results indicate that these systems are adaptive to change and do have the capability to capture and bury greater quantities of C under changing climatic and human pressure.

The findings of this study significantly improve our understanding of C in Scotland's fjords. This new understanding is both important within a Scotland/UK context and at the global scale. Within a Scottish context, this work has highlighted the importance of the coastal ocean and fjords in particular. Through the quantification of this forgotten C it has been shown that the coastal marine environment can store major quantities of C equivalent to that held in the highly C rich terrestrial environment. Scotland's terrestrial environments have been the focus of significant C research in the preceding decades, within this research there has been a prevailing view that once the C enters an estuary it is lost. In truth the coastal ocean has the ability to capture a portion of this lost C. This study shows that the C stored in the coastal marine environment makes up a significant proportion of Scotland's national C resource; highlighting the need for the two research communities to come together.

Our improved understanding of Scotland's fjords has global implications. Firstly the previously data devoid mid-latitude fjords now have robust data sets which can be used to better constrain global C burial rates within fjords (Smith et al., 2014) and the proportion of terrestrial C held in fjord sediments (Cui et al., 2016b). The work also highlights that our global knowledge of the location and magnitude of these sedimentary

C stores still remains poor. Without this basic understanding of the current C stocks it is difficult to truly understand how significant the C fluxes are (i.e. relative to C stock).

Beyond the science it is obvious that there is policy interest in understanding the C held within marine sediments. At the simpler end of this spectrum, using the C stored in these environments as a policy mechanism to get areas of the seabed protected or to develop management strategies seems an obvious and sensible route forward. While we argue that these marine sedimentary C stores are stable and buffered from the immediate impact on environmental change further work does have to be conducted to better understand the risks to the sedimentary C. If the precautionary principle is followed, these C stores would be designated and given protection until it was proved otherwise. The data produced from this study does highlight these C stores as being of national importance and that protection may be warranted. With our current understanding of C held within the sediments of Scotland's fjords I believe this is the most that can be advocated for at this time.

Finally, what of the calls for the definition for Blue Carbon to be extended to include these sedimentary environments? While it is easy to understand why these calls are being made it should be remembered that these systems are fundamentally different. In my view, it would be inappropriate to expand the BC definition to include these sedimentary environments. If this is attempted there is a real risk that the momentum behind BC that has been built over the last decade could be weakened at a time when it is needed more than ever with the ongoing loss of intertidal BC habitat. Rather, it's time for the marine sedimentological community to communicate the importance of these subtidal sedimentary ecosystems as important sites of C burial and storage. There is already a strong scientific foundation (possibly stronger than current BC science) that could be built on, yet the marine sedimentological community have been reluctant to communicate the importance of these non-charismatic environments, it may be time to take some cues from the BC community.

7.2 Future Work

This project has been successful in quantifying the sedimentary C held within Scotland's fjords and improving our understanding of the source of that C and how these stores have developed through time. The results from this study fill a data void in the mid-latitudes and will be crucial in constraining global estimates of C burial and storage. This is not to say our understanding of C in these environments both in Scotland or globally is perfect but essential steps forward have been taken.

Globally, the only fully depth integrated C stock estimates for the marine environment are the fjords in this study (Chapter 5). Therefore, the most obvious route for future work is to apply the joint geophysical and geochemical methodology developed within this project (Chapter 3) to other fjord systems around the world and to other coastal or shelf environments (estuaries, enclosed basins, etc.). Additionally, there is scope to refine these methodologies to improve our understanding of C held within marine sediments. This includes the introduction of Markov chain Monte Carlo (MCMC) modelling to the quantification of individual sedimentary stocks, this approach will allow the uncertainties in the calculations to be better constrained. Further, the upscaling approach could be improved using more complex numerical methodologies, this will be reliant on the production of several more detailed C stock estimates to test future numerical upscaling approaches.

The biggest issue that must be overcome both in the Scottish context and more globally is to improve our understanding of the spatial heterogeneity of fjordic and more generally marine sediments. When calculating C burial rates and C stocks it is largely assumed that the sediments are homogeneous. This can be seen in the global C burial estimates (Smith et al., 2014, Cui et al., 2016b) which calculate these rates from individual cores then apply those rates to the area of the fjord, this assumes the fjords are evenly covered in the same sediment type and sedimentation and C dynamics are identical throughout the fjord, we know this not to be true. Through the use of seismic geophysics the methodological approach developed to quantify the C in individual fjords (Chapter 3) does deal with some of these issues. The methodology could be further improved with the addition of more sediment cores laterally across the lochs but this would have significant cost implications. The approach we used to map the terrestrial C in the fjord sediments (Chapter 4) does utilise a high sampling frequency which does overcome the spatial heterogeneity of the sediment but we do assume the fjord's seabed is totally covered in sediment. Finally in Chapter 5 when upscaling, we again assume that the

sediment coverage equals the area of the fjord. To overcome the issue of the spatial heterogeneity of sediment we must bring techniques together; multibeam bathymetry, for example provides a platform to map the seabed and understand the distribution of different seabed types. This combined with high frequency sampling will allow us to better constrain C burial rates as well as C stocks in these environments.

This study has been able to provide new data on C buried over Holocene timescales, but current C accumulation rates and how the C is incorporated into the long-term store remains an unknown in a Scottish and mid-latitude context. There is a requirement to undertake further radiometric dating (^{210}Pb and ^{137}Cs) of sediment cores from different basins in different fjords, in order to understand the C burial rates. An interesting science questions are how do modern C burial rates compare to long-term C burial rates based upon ^{14}C dating and when is C truly buried as a stable long-term store?

How these sedimentary environments are linked to other ecosystems (terrestrial, BC, etc.) and what is the origin of the C held with in fjord sediments, remain important questions. At the moment, using stable isotopes we can broadly identify if the C originates from terrestrial or marine sources (Chapter 4) but as shown in Chapter 6, molecular biomarkers can further unravel the source of C held within the sediment. Both stable isotope and biomarker techniques need to be further applied across a variety of spatial and temporal scales.

A highly significant question not touched upon is this study is how stabile are these C stores to future environmental change? These sedimentary environments hold large quantities of C but we know little about how physical, biological or chemical alterations to the environment will impact the C. We expect that the depth of these fjords will buffer them from the immediate impact of climate change but further information on both their physical and geochemical stability is required.

Globally I believe the next steps for this type of research is to move away from the *status quo* to a new paradigm. Currently the wider C research community tends to focus in on single environments such as forests, peatland, saltmarsh or fjords. However, there needs to be a shift towards not only understanding how C is stored in these environments but also the transfers between them; in essence an earth system approach. This approach could be employed at the catchment scale all the way to a global understanding. Taking this approach forward, Scotland, is an ideal natural laboratory to test these concepts and answer these globally important questions as the environments are C rich, easily

accessible, data is available and there is a willingness to support this type of research from many quarters.

7.3 Final Comments

To conclude, this study has shown the importance of the coastal ocean and fjords in particular as long-term stores of C. These largely forgotten C stores have been burying C since the retreat of the last ice sheets and a providing a long-term climate regulation service. In the future this climate service is going to become increasingly relevant in efforts to mitigate against climatic and human extremes. This improved understanding provides a strong foundation to be built upon with further research and policy development.

References

Achat, D. L. et al. (2015) 'Forest soil carbon is threatened by intensive biomass harvesting.', *Scientific reports*. Nature Publishing Group, 5, p. 15991.

Ahlström, A. et al. (2012) 'Robustness and uncertainty in terrestrial ecosystem carbon response to CMIP5 climate change projections', *Environmental Research Letters*, 7, p. 044008.

Aitkenhead, M. J. and Coull, M. C., (2016), Mapping soil carbon stocks across Scotland using a neural network model, *Geoderma*, 262, 187–198.

Aller, R.C., Blair, N.E., (2004). Early diagenetic remineralization of sedimentary organic C in the Gulf of Papua deltaic complex (Papua New Guinea): net loss of terrestrial C and diagenetic fractionation of C isotopes. *Geochimica et Cosmochimica Acta* 68, 1815-1825.

Aller, R.C., Blair, N.E., (2006). Carbon remineralization in the Amazon–Guianas tropical mobile mudbelt: a sedimentary incinerator. *Continental Shelf Research* 26, 2241-2259.

Almahasheer, H. *et al.* (2017) 'Low Carbon sink capacity of Red Sea mangroves', *Scientific Reports*. Springer US, (June), pp. 1–10. doi: 10.1038/s41598-017-10424-9.

Alongi DM. (2002). Present state and future of the world's mangrove forests. Environ Conserv 29: 331–49.

Andersson, A., (2011), A systematic examination of a random sampling strategy for source apportionment calculations, *Science of the Total Environment*, v. 412-413, p. 232–238.

Appleby, P.G. and Oldfield, F.,(1978). The calculation of lead-210 dates assuming a constant rate of supply of unsupported Pb-210 to the sediment. *Catena*, 5: 1-8.

Arendt, C.A., Aciego, S.M., and Hetland, E.A., (2015), An open source Bayesian Monte Carlo isotope mixing model with applications in Earth surface processes: *Geochemistry Geophysics Geosystems*, v. 18, no. 1-2, p. 1541–1576.

Arnarson, T.S., Keil, R.G., (2007). Changes in organic matter–mineral interactions for marine sediments with varying oxygen exposure times. *Geochimica et Cosmochimica Acta* 71, 3545-3556

Arndt, S., Jørgensen, B. B., Larowe, D. E., Middelburg, J. J., Pancost, R. D. and Regnier, P., (2013), Quantifying the degradation of organic matter in marine sediments : A review and synthesis, *Earth Sci. Rev*., 123, 53–86.

Atamanchuk, D., Kononets, M., Thomas, P. J., Hovdenes, J., Tengberg, A. and Hall, P. O. J.,(2015), Continuous long-term observations of the carbonate system dynamics in the water column of a temperate fjord, *J. Mar. Syst*., 148, 272–284.

Austin, W. E. N., Cage, A. G. and Scourse, J. D. (2006) 'Mid-latitude shelf seas: a NW European perspective on the seasonal dynamics of temperature, salinity and oxygen isotopes', *The Holocene*, 16(2006), pp. 937–947.

Avelar, S., Voort, T. S. Van Der and Eglinton, T. I. (2017) 'Relevance of carbon stocks of marine sediments for national greenhouse gas inventories of maritime nations', *Carbon Balance and Management*. Springer International Publishing.

Baeten, N. J., Forwick, M., Vogt, C. and Vorren, T. O., (2010), Late Weichselian and Holocene sedimentary environments and glacial activity in Billefjorden, Svalbard, *Geol. Soc. London, Spec. Publ*., 344(1), 207–223.

Baker, W. L. (1995) 'Longterm response of disturbance landscape to human intervention global change', *Landscape Ecology*, 10(3), pp. 143–159. doi: 10.1007/BF00133028.

Ballantyne, C. K. (1991) 'Late Holocene erosion in upland Britain: climatic deterioration or human influence?', *Holocene*, 1(1), pp. 81–85.

Ballantyne, C. K. (2008) After the ice: Holocene geomorphic activity in the Scottish Highlands, Scottish *Geographical Journal*.

Baltzer, A., Bates, R., Mokeddem, Z., Clet-Pellerin, M., Walter-Simonnet, A.-V., Bonnot-Courtois, C. and Austin, W. E. N, (2010), Using seismic facies and pollen analyses to evaluate climatically driven change in a Scottish sea loch (fjord) over the last 20 ka, *Geol. Soc. London, Spec. Publ*., 344(1).

Bao, R., McIntyre, C., Zhao, M., Zhu, C., Kao, S.-J., Eglinton, T.I., (2016). Widespread dispersal and aging of organic carbon in shallow marginal seas. *Geology* 44, 791-794

Barbier, E. B., Hacker, S. D., Kennedy, C., Koch, E. W. and Stier, A. C., (2011), The value of estuarine and coastal ecosystem services, Ecol. Monogr., 81(2), 169–193.

Bates, C. R., Moore, C. G., Harries, D. B., Austin, W. and Lyndon, A. R., (2004), Broad scale mapping of sublittoral habitats in Loch Sunart, Scotland. *Scottish Natural Heritage Commissioned Report No. 006* (ROAME No. F01AA401C).

Bauer, J. E. and Bianchi, T. S., (2011), Dissolved Organic Carbon Cycling and Transformation, Elsevier Inc., *Treatise on Estuarine and Coastal Science*, 5, 7-762012.

Bauer, J.E., Cai, W.J., Raymond, P. A, Bianchi, T.S., Hopkinson, C.S., and Regnier, P. A. G., (2013), The changing carbon cycle of the coastal ocean.: *Nature*, v. 504, no. 7478, p. 61–70.

Beaumont, N. J., Jones, L., Garbutt, a., Hansom, J. D. and Toberman, M.,(2014), The value of carbon sequestration and storage in coastal habitats, Estuar. Coast. Shelf Sci., 137, 32–40.

Bellassen, V. and Luyssaert, S.(2014), Managing forests in uncertain times, *Nature*, 506, 6–8.

Belt, S. T., G. Massè, S. J. Rowland, M. Poulin, C. Michel, and B. Leblanc. (2007). A novel chemical fossil of palaeo sea ice: IP25. Organic Geochemistry 38: 16–27.

Bergamaschi, B.A., Tsamakis, E., Keil, R.G., Eglinton, T.I., Montluçon, D.B., Hedges, J.I., (1997). The effect of grain size and surface area on organic matter, lignin and carbohydrate concentration, and molecular compositions in Peru Margin sediments. *Geochimica et Cosmochimica Acta* 61, 1247-1260.

Bertrand, S., Hughen, K.A., Sepúlveda, J., and Pantoja, S., (2012), Geochemistry of surface sediments from the fjords of Northern Chilean Patagonia (44-47°S): Spatial variability and implications for paleoclimate reconstructions: *Geochimica et Cosmochimica Acta*, v. 76, p. 125–146.

Bianchi, T. S. et al. (2017) 'Centers of Organic Carbon Burial and Oxidation at the Land-Ocean Interface', Organic Geochemistry.

Bianchi, T. S., Schreiner, K. M., Smith, R. W., Burdige, D. J., Woodard, S. and Conley, D. J., (2016), Redox Effects on Organic Matter Storage in Coastal Sediments During the Holocene : A Biomarker / Proxy Perspective, *Annu. Rev. Earth Planet. Sci.*, 44, 295–319.

Bianchi, T.S and Canuel, E.S., (2011), Chemical biomarkers in aquatic ecosystems, Princeton University Press

Bianchi, T.S., (2011), The role of terrestrially derived organic carbon in the coastal ocean: a changing paradigm and the priming effect.: *Proceedings of the National Academy of Sciences of the United States of America*, v. 108, no. 49, p. 19473–81.

Bianchi, T.S., and M.A. Allison. (2009). Large-river delta-front estuaries as natural "recorders" of global environmental change. Proc. *Nat. Acad. Sci.:* 106 (20): 8085-8092.

Bianchi, T.S., Mitra, S., McKee, B.A., (2002). Sources of terrestrially-derived organic carbon in lower Mississippi River and Louisiana shelf sediments: implications for differential sedimentation and transport at the coastal margin. *Marine Chemistry* 77, 211-223.

Bibby, J.S., Hudson, G. and Henderson, D.J. (1982), Soil and Land Capability for Agriculture: Western Scotland. Handbook to accompany the 1:250 000 scale Soil and Land Capability for Agriculture maps, Sheet 4. The Macaulay Institute for Soil Research. Aberdeen.

Binns, P. E., Harland,R. & Hughes, M. J., (1974a), Glacial and post glacial sedimentation in the sea of the Hebrides. *Nature*, 248, 751–754.

Binns, P. E., Mcquillin,R.& Kenolty, N.,(1974b), The geology of the sea of the Hebrides. Institute of Geological Sciences 73/14.

Birks, H. H. (1972) 'Studies in the vegetational history of Scotland. A radiocarbon-dated pollen diagram from Loch Maree Ross, and Cromatry', *New Phytologist*, 71, pp. 731–754.

Bischoff, J., Sparkes, R. B., Do, A., Semiletov, I. P., Dudarev, O. V, Wagner, D., Rivkina, E., Dongen, B. E. Van and Talbot, H. M., (2016), Source , transport and fate of soil organic matter inferred from microbial biomarker lipids on the East Siberian Arctic Shelf, *Biogeosciences*, 4899–4914.

Bishop, R. R., Church, M. J. and Rowley-Conwy, P. A. (2015) 'Firewood, food and human niche construction: The potential role of Mesolithic hunter-gatherers in actively structuring Scotland's woodlands', *Quaternary Science Reviews*. Elsevier Ltd, 108, pp. 51–75..

Blaauw, M. and Christeny, J. A. (2011) 'Flexible paleoclimate age-depth models using an autoregressive gamma process', *Bayesian Analysis*, 6(3), pp. 457–474.

Blair, N.E., Leithold, E.L., Ford, S.T., Peeler, K.A., Holmes, J.C., Perkey, D.W., (2003). The persistence of memory: the fate of ancient sedimentary organic carbon in a modern sedimentary system. *Geochimica et Cosmochimica Acta* 67, 63-73.

Bligh, E. G., and W. J. Dyer. (1959). A rapid method of total lipid extraction and purification. *Canadian Journal of Biochemistry and Physiology* 37: 911–917.

Blumer, M., M. M. Mullin and D. W. Thomas. (1964). Pristane in the marine environment. *Helgoland Marine Research* 10: 187–201.

Bond, C. E., Gibbs, A. D., Shipton, Z. K. and Jones, S., (2007), What do you think this is? "Conceptual uncertainty" In geoscience interpretation, *GSA Today*, 17(11), 4–10,

Bond, G. et al. (2001) 'Persistent solar influence on North Atlantic climate during the Holocene.', *Science*, 294(5549), pp. 2130–2136.

Borrelli, P., Lugato, E., Montanarella, L., and Panagos, P., (2016). A New Assessment of Soil Loss Due to Wind Erosion in European Agricultural Soils Using a Quantitative Spatially Distributed Modelling Approach. *Land Degradation & Development*, In Press.

Boulton, G. S., Chroston,P.N.& Jarvis, J. A., (1987), marine seismic study of late Quaternary sedimentation and inferred glacier fluctuations along western Inverness–shire, Scotland. *Boreas*, 10, 39–51.

Boyle, J. F. et al. (2011) 'Modelling prehistoric land use and carbon budgets: A critical review', *The Holocene*, 21(5), pp. 715–722.

Bradley, R.I., Milne, R., Bell, J., Lilly, A.., Jordan, C. and Higgins, A., (2005), A soil carbon and land use database for the United Kingdom. Soil Use and Management, 21, 363–369.

Brandano, M., Cuffaro, M., Gaglianone, G. and Petricca, P., (2016), Evaluating the Role of Seagrass in Cenozoic CO2 Variations, *Front. Environmnetal Sci*., 4(November), 1–9,

Brazier, V. and Ballantyne, C. K. (1989) 'Late Holocene debris cone evolution in Glen Feshie, western Cairngorm Mountains, Scotland', *Transactions of the Royal Society of Edinburgh: Earth Sciences*, 80(1), pp. 17–24.

Brazier, V., Whittington, G., Ballantyne, C.K., (1988), Holocene debris cone evolution in glen Etive Western Grampian Hhghlands, Scotland, *Earth Surface Processes and Lanscapes*, 13, 525-531.

Briand, MJ, Bonnet, X, Goiran, C, Guillou, G and Letourneur, Y, (2015) , Major Sources of Organic Matter in a Complex Coral Reef Lagoon: Identification from Isotopic Signatures ($\delta^{13}C$ and $\delta^{15}N$)., *PloS one*, 10, (7), p. e0131555..

Bridgham SD, Megonigal JP, Keller JK, (2006). The carbon balance of North American wetlands. *Wetlands* 26: 889–916

Bröder, L, Tesi, T, Andersson, A, Eglinton, TI, Semiletov, IP, Dudarev, O V, Roos, P and Gustafsson, Ö, (2016), Organic Geochemistry Historical records of organic matter supply and degradation status in the East Siberian Sea, *Organic Geochemistry*, 91, pp. 16–30.

Bröder, L., Tesi, T., Salvadó, J.A., Semiletov, I.P., Dudarev, O.V., (2016). Fate of terrigenous organic matter across the Laptev Sea from the mouth of the Lena River to the deep sea of the Arctic interior. *Biogeosciences* 13, 5003-5019.

Broecker, W.S, Peng, T, Beng, Z, (1982). Tracers of the Sea, Lamont-Doherty Geological Observatory, Columbia University Press.

Bronk Ramsey, C. (2009) 'Bayesian Analysis of Radiocarbon Dates', *Radiocarbon*, 51(1), pp. 337–360.

Bronk Ramsey, C. and Lee, S, (2013), Recent and planned developments of the program OxCal. *Radiocarbon*, 55(2-3), 720-730.

Burd, A.B., Frey, S., Cabre, A., Ito, T., Levine, N.M., Lønborg, C., Long, M., Mauritz, M., Thomas, R.Q., Stephens, B.M., Vanwalleghem, T., and Zeng, N., (2016), Terrestrial and marine perspectives on modeling organic matter degradation pathways: *Global Change Biology*, v. 22, no. 1, p. 121–136.

Burdige DJ (2005) The burial of terrestrial organic carbon in marine sediments: A reassessment. *Global Biogeochemical Cycles*.

Burrows M.T., Kamenos N.A., Hughes D.J., Stahl H., Howe J.A. and Tett P., (2014), Assessment of carbon budgets and potential blue carbon stores in Scotland's coastal and marine environment. *Scottish Natural Heritage Commissioned Report No. 761*.

Cage, A. G. and Austin, W. E. N. (2010) 'Marine climate variability during the last millennium: The Loch Sunart record, Scotland, UK', *Quaternary Science Reviews*. Elsevier Ltd, 29(13-14), pp. 1633–1647.

Cage, A. G. et al. (2011) 'Identification of the Icelandic Landnám tephra (AD 871 ± 2) in Scottish fjordic sediment', *Quaternary International*, 246(1-2), pp. 168–176.

Cage, A.G., Heinemeier, J. and Austin, W.E.N., (2006), Marine radiocarbon reservoir ages in Scottish coastal and fjordic waters, Radiocarbon, Vol 48, Nr 1, 31–43.

Cai WJ (2011) Estuarine and coastal ocean carbon paradox: CO2 sinks or sites of terrestrial

Cannell, M.G.R., Milne, R., Hargreaves, K.J., Brown, T.A.W., Cruickshank, M.M., Bradley, R.I., Spencer, T., Hope, D., Billett, M.F., Adger, W.N. and Subak, S., (1999), National inventories of terrestrial carbon sources and sinks: The UK experience. *Climatic Change*, 42, 505–530.

Canuel, E. A., and C. S. Martens. (1996). Reactivity of recently deposited organic matter: Degradation of lipid compounds near the sediment–water interface. *Geochimica et Cosmochimica Acta* 60: 1793–1806.

Capell, R., Tetzlaff, D. and Soulsby, C., (2013), Will catchment characteristics moderate the projected effects of climate change on flow regimes in the Scottish Highlands ?,*Hydrological Processes* , 699 (December 2012), 687–699.

Carvalho, F. P., Oliveira, J. M. and Soares, A. M. M. (2011) 'Sediment accumulation and bioturbation rates in the deep Northeast Atlantic determined by radiometric techniques', *ICES Journal of Marine Science*, 68(3), pp. 427–435.

Chapman, S. J., Bell, J., Donnelly, D. and Lilly, A., (2009), Carbon stocks in Scottish peatlands, *Soil Use Manag*., 25(2), 105–112.

Chapman, S.J., Bell, J.S., Campbell, C.D., Hudson, G, Lilly, A., Nolan, A.J., Robertson, A.H.J., Potts, J.M., and Towers, W., (2013), Comparison of soil carbon stocks in Scottish soils between 1978 and 2009, *European Journal of Soil Science*, 64, (4), pp. 455–465.

Charman, D. J. et al. (2006) 'Compilation of non-annually resolved Holocene proxy climate records: Stacked Holocene peatland palaeo-water table reconstructions from northern Britain', *Quaternary Science Reviews*, 25(3-4), pp. 336–350.

Charman, D.,(2002), Peatlands and Environmental Change, Wiley, Chichester.

Chen, G., Azkab, M. H., Chmura, G. L., Chen, S., Sastrosuwondo, P., Ma, Z., Dharmawan, I. W. E., Yin, X. and Chen, B., (2017), Mangroves as a major source of soil carbon storage in adjacent seagrass meadows, Sci. Rep., (January), 1–10.

Chiles, J.P., and Delfiner.P., (1999), Geostatistics: Modeling Spatial Uncertainty. John Wiley and Sons, New York, 695.

Chmura GL, Anisfeld SC, Cahoon DR, and Lynch JC. (2003).Global carbon sequestration in tidal, saline wetland soils. *Global Biogeochemical Cycles* 17: 1111; doi:10.1029/2002GB001917.

Chung, I. K., Beardall, J. and Mehta, S. (2011) 'Using marine macroalgae for carbon sequestration : a critical appraisal', *Journal Applied Phycology*, 23, pp. 877–886.

Chung, I. K., Beardall, J. and Mehta, S.(2011), Using marine macroalgae for carbon sequestration : a critical appraisal, J. Appl. Phycol., 23, 877–886.

Clark, C. D., Hughes, A. L. C., Greenwood, S. L., Jordan, C., and Petter, H., (2012), Pattern and timing of retreat of the last British-Irish Ice Sheet, *Quaternary Sci. Rev*., 44, 112–146, doi:10.1016/j.quascirev.2010.07.019, 2012.

Cloern, J.E., Canuel, E. A, Harris, D., and May, N., (2007), Stable Carbon and Nitrogen Isotope Composition of Aquatic and Terrestrial Plants of the San Francisco Bay Estuarine System*: Limnology and Oceanography*, v. 47, no. 3, p. 713–729

Cohen, K. M. et al. (2012) 'The earliest occupation of north-west Europe: A coastal perspective', *Quaternary International.* Elsevier, 271(January 2015), pp. 70–83.

Cole JJ, et al. (2007) Plumbing the global carbon cycle: Integrating inland waters into the terrestrial carbon budget. *Ecosystems* (NY) 10:171–184.

Coll, J. et al. (2016) 'Projected climate change impacts on upland heaths in Ireland', *Climate Research*, 69(2), pp. 177–191.

Coppola, L., Gustafsson, Ö., Andersson, P., Eglinton, T., Uchida, M., Dickens, A., (2007). The importance of ultrafine particles as a control on the distribution of organic carbon in Washington Margin and Cascadia Basin sediments. *Chemical geology* 243, 142-156.

Cranwell, P. A. (1982). Lipids of aquatic sediments and sedimenting particulates. *Progress Lipid Research* 21: 271–308.

Cressie, N. A. C. (1990), The Origins of Kriging, *Math. Geol.,* 22, 239– 252.

Cronin,J.R.& Tyler, I. D., (1980), Organic carbon in a Scottish sea loch. In: Albaiges, J. (ed.) *Analytical Techniques in Environmental Chemistry*. Pergamon Press, Oxford, 419–426,

Cui, X, Bianchi, TS, Savage, C and Smith, RW, (2016c) 'Organic carbon burial in fjords: Terrestrial versus marine inputs', Earth and Planetary Science Letters. Elsevier B.V., 451, pp. 41–50. doi: 10.1016/j.epsl.2016.07.003.

Cui, X., Bianchi, T.S., Hutchings, J.A., Savage, C., and Curtis, J.H., (2016a), Partitioning of organic carbon among density fractions in surface sediments of Fiordland, New Zealand: *Journal of Geophysical Research: Biogeosciences*, v. 121, no. 3, p. 1016–1031.

Cui, X., Bianchi, T.S., Jaeger, J.M., Smith, R.W., (2016b). Biospheric and petrogenic organic carbon flux along southeast Alaska. *Earth and Planetary Science Letters* 452, 238-246.

Cui, X., Bianchi, T.S., Savage, C., (2017). Erosion of modern terrestrial organic matter as a major component of sediments in fjords. *Geophysical Research Letters* 44, 1457-1465.

Cummins, R., Donnelly, D., Nolan, A., Towers, W., Chapman, S., Grieve, I., and Birnie, R. V., (2011). Peat erosion and the management of peatland habitats. *Scottish Natural Heritage Commissioned Report No. 410*.

Dadey, K. A., Janecek, T. and Klaus, A. (1992) 'Dry bulk density: its use and determination', *Proceedings of the Ocean Drilling Program, Scientific Results*, 126, pp. 551–554.

Dainese, M. et al. (2017) 'Human disturbance and upward expansion of plants in a warming climate', *Nature Climate Change*, 7(July).

Danielson, R. E. and Sutherland, P. L. (1986) 'Porosity', in Methods of soil analysis, part 1, *Physical and mineralogical methods*, pp. 443–461.

Dargie, G. C., Lewis, S. L., Lawson, I. T., Mitchard, E. T. A., Page, S. E., Bocko, Y. E. and Ifo, S. A. (2017) Age, extent and carbon storage of the central Congo Basin peatland complex, *Nature*, 542(7639), 86–90.

Darroch, S. A. F., Locatelli, E. R., Mccoy, V. E., Clark, E. G., Anderson, R. P., Lidya, G. and Hull, P. M., (2016), Taphonomic Disparty in Foraminifera as a Paleo-Indicator for Seagrass, *Palaios*, 31, 242–258.

Davies, F. (2009) 'Pollen profile GB4, Gallanech Beg, United Kingdom', *European Pollen Database* (EPD).

Davies, G. M., Gray, A., Rein, G. and Legg, C. J., (2013), Peat consumption and carbon loss due to smouldering wildfire in a temperate peatland, *For. Ecol. Manage*., 308, 169–177.

Diaz, D. and Moore, F. (2017), Quantifying the economic risks of climate change, *Nature Climate Change*, 7(11), 774–782.

Dickens, A.F., Baldock, J.A., Smernik, R.J., Wakeham, S.G., Arnarson, T.S., Gélinas, Y., Hedges, J.I., (2006). Solid-state 13 C NMR analysis of size and density fractions of marine sediments: Insight into organic carbon sources and preservation mechanisms. *Geochimica et Cosmochimica Acta* 70, 666-686.

Diesing, M., Chris, P. and Claire, J.,(2017), Predicting the standing stock of organic carbon in surface sediments of the North – West European continental shelf, *Biogeochemistry*.

Dinsmore, K. J., Wallin, M. B., Johnson, M. S., Billett, M. F., Bishop, K., Pumpanen, J. and Ojala, A., (2013), Contrasting CO_2 concentration discharge dynamics in headwater streams : A multi-catchment comparison, *Journal of Geophysical Research*,118, 445–461.

Dix, J. K. and Duck, R. W., (2000), A high-resolution seismic stratigraphy from a Scottish sea loch and its implications for Loch Lomond Stadial deglaciation, *Journal of Quaternary Science*, 15, 645–656.

Dodds WK, Cole J (2007) Expanding the concept of trophic state in aquatic ecosystems: It's not just the autotrophs. *Aquatic Science* 69:427–439.

Donato DC, Kauffman JB, Murdiuarso D, (2011). Mangroves among the most carbon-rich forests in the tropics. *Nature Geoscience* 4:293–97

Draper, F. C., Roucoux, K. H., Lawson, I. T., Mitchard, E. T. a, Honorio Coronado, E. N., Lähteenoja, O., Torres Montenegro, L., Valderrama Sandoval, E., Zaráte, R. and Baker, T. R.(2014)The distribution and amount of carbon in the largest peatland complex in Amazonia, *Environmental Research Letters*, 9(12),

Drenzek NJ, et al. (2009) A new look at old carbon in active margin sediments. *Geology* 37:239–242.

Drenzek, N.J., Montluçon, D.B., Yunker, M.B., Macdonald, R.W., Eglinton, T.I., (2007). Constraints on the origin of sedimentary organic carbon in the Beaufort Sea from coupled molecular 13C and 14C measurements. *Marine Chemistry* 103, 146-162.

Duarte CM, Marbà N, Gacia E (2010). Seagrass community metabolism: assessing the carbon sink capacity of seagrass meadows. *Global Biogeochemical Cycles* 24: GB4032.

Duarte, C. M. (2017) 'Reviews and syntheses: Hidden Forests, the role of vegetated coastal habitats on the ocean carbon budget', *Biogeosciences*, 1981(August), pp. 1–17. doi: 10.5194/bg-2016-339.

Duarte, C. M. and Krause-Jensen, D. (2017) 'Export from Seagrass Meadows Contributes to Marine Carbon Sequestration', *Frontiers in Marine Science*, 4(January), pp. 1–7. doi: 10.3389/fmars.2017.00013.

Duarte, C. M., Dennison, W. C., Orth, R. J. W. and Carruthers, T. J. B.,(2008), The Charisma of Coastal Ecosystems : Addressing the Imbalance, *Perspect. Esturine Coast. Sci*., 233–238,

Duarte, C. M., Middelburg, J. J. and Caraco, N. (2005) 'Major role of marine vegetation on the oceanic carbon cycle', *Biogeosciences*, 2, pp. 1–8. doi: 10.5194/bgd-1-659-2004.

Duck, R.W. & McManus, J., (1990). Relationships between catchment characteristics, land use and sediment yield in the Midland Valley of Scotland. In: Boardman, J., Foster, 120 I.D.L. & Dearing, J.A. (eds), *Soil Erosion on Agricultural Land*. Wiley, Chichester, 285-299.

Duffield, C. *et al.* (2017) 'Spatial and temporal organic carbon burial along a fjord to coast transect: A case study from Western Norway', *The Holocene*.

Dye, J. Kirby, M. Gascoigne, M. Lawson, J. Kirby, J. and Read, J. (2001), The Sunart Oakwoods, a report on their History and Archaeology. *The Sunart Oakwoods Research Group*, (2001)

Edwards, A. and Sharples, F., (1986), Scottish Sea Lochs: A Catalogue. Scottish Marine Biological Association/Nature Conservancy Council, Oban.

Edwards, K.J and Whittington, G., (2010), Lateglacial palaeoenvironmental investigations at Wester Cartmore Farm, Fife and their significance for patterns of vegetation and climate change in east-central Scotland. *Review of Palaeobotany and Palynology* 159: 14-34.

Eglinton, G., and R. J. Hamilton. (1967). Leaf epicuticular waxes. *Science* 156: 1322–1335.

Faganeli, J., Malej, A., Pezdic, J., and Malacic, V., (1980), C:N:P ratios and stable C isotopic ratios as indicators of sources of organic matter in the Gulf of Trieste (northern Adriatic): *Oceanologica Acta*, v. 11, no. 4, p. 377–382.

Farquhar, G. D., M. C. Ball, S. Voncaemmerer, and Z. Roksandic. (1982). Effect of salinity and humidity on δ13C value of halophytes: Evidence for diffusional isotope fractionation determined by the ratio of inter-cellular atmospheric partial pressure of CO2 under different environmental conditions. Oecologia 52: 121–124.

Faust, J. C. et al. (2016) 'Norwegian fjord sediments reveal NAO related winter temperature and precipitation changes of the past 2800 years', *Earth and Planetary Science Letters*. Elsevier B.V., 435, pp. 84–93.

Faust, J.C., Knies, J., Slagstad, T., Vogt, C., Milzer, G., and Giraudeau, J., (2014), Geochemical composition of Trondheimsfjord surface sediments: Sources and spatial

variability of marine and terrigenous components, *Continental Shelf Research*, v. 88, p. 61–71.

Feng, X., Feakins, S.J., Liu, Z., Ponton, C., Wang, R.Z., Karkabi, E., Galy, V., Berelson, W.M., Nottingham, A.T., Meir, P., (2016). Source to sink: Evolution of lignin composition in the Madre de Dios River system with connection to the Amazon basin and offshore. *Journal of Geophysical Research: Biogeosciences* 121, 1316-1338.

Feng, X., Gustafsson, Ö., Holmes, R.M., Vonk, J.E., Dongen, B.E., Semiletov, I.P., Dudarev, O.V., Yunker, M.B., Macdonald, R.W., Wacker, L., (2015a). Multimolecular tracers of terrestrial carbon transfer across the pan-Arctic: 14C characteristics of sedimentary carbon components and their environmental controls. *Global Biogeochemical Cycles* 29, 1855-1873. 58

Feng, X., Gustafsson, Ö., Holmes, R.M., Vonk, J.E., van Dongen, B.E., Semiletov, I.P., Dudarev, O.V., Yunker, M.B., Macdonald, R.W., Montlucon, D.B., (2015b). Multi-molecular tracers of terrestrial carbon transfer across the pan-Arctic: comparison of hydrolyzable components with plant wax lipids and lignin phenols. *Biogeosciences* 12, 4841-4860.

Feng, X., Vonk, J.E., van Dongen, B.E., Gustafsson, Ö., Semiletov, I.P., Dudarev, O.V., Wang, Z., Montluçon, D.B., Wacker, L., Eglinton, T.I., (2013). Differential mobilization of terrestrial carbon pools in Eurasian Arctic river basins. *Proceedings of the National Academy of Sciences* 110, 14168-14173.

Fernandes, R., Millard, A.R., Brabec, M., Nadeau, M.J., and Grootes, P., (2014), Food reconstruction using isotopic transferred signals (FRUITS): A bayesian model for diet reconstruction: *PLoS ONE*, v. 9, no. 2, p. 1–9.

Ficken, K. J., B. Li, D. L. Swain, and G. Eglinton. (2000). An *n*-alkane proxy for the sedimentary input of submerged/floating freshwater aquatic macrophytes. *Organic Geochemistry* 31: 745–749.

Ficken, K. J., Barber, K. E. and Eglinton, G., (1998),Lipid biomarker, δ13C and plant macrofossil stratigraphy of a Scottish montane peat bog over the last two millennia, *Organic Geochmistry,* 28(3).

Forestry Commission., (2015), Carbon in living woodland trees in Britain: A National Forestry Inventory Report.

Forwick, M., Vorren, T. O., Hald, M., Korsun, S., Roh, Y., Vogt, C. and Yoo, K.-C., (2010), Spatial and temporal influence of glaciers and rivers on the sedimentary environment in Sassenfjorden and Tempelfjorden, Spitsbergen, Geol. Soc. London, Spec. Publ., 344(1), 163–193.

Fourqurean, J. W. *et al.* (2012) 'Seagrass ecosystems as a globally significant carbon stock', *Nature Geoscience*. Nature Publishing Group, 5(7).

Frankignoulle, M., Canon, C. and Gattuso, J.-P. (1994) 'Marine Calcification as a Source of Carbon Dioxide: Positive Feedback of Increasing Atmospheric CO2', *Limnology and Oceanography*, 39(2), pp. 458–462.

Frankignoulle, M., Pichon, M. and Gattuso, J. P. (1995) 'Aquatic calcification as a source of carbon dioxide'*, in Proceedings of the NATO ARW on Carbon Sequestration in the Biosphere*, pp. 265–271.

Freeman, K. H., J. M. Hayes, J.-M. Trendel, and P. Albrecht. (1990). Evidence from carbon isotope measurements for diverse origins of sedimentary hydrocarbons. *Nature* 343: 254–256.

Freeman, K. H., S. G. Wakeham, and J. M. Hayes. (1994). Predictive isotopic biogeochemistry: Hydrocarbons from anoxic marine basins. *Organic Geochemistry* 21: 629–644.

Friedrich, J., Janssen, F., Aleynik, D., Bange, H. W., Boltacheva, N., Çagatay, M. N., Dale, A. W., Etiope, G., Erdem, Z., Geraga, M., Gilli, A., Gomoiu, M. T., Hall, P. O. J., Hansson, D., He, Y., Holtappels, M., Kirf, M. K., Kononets, M., Konovalov, S., Lichtschlag, A., Livingstone, D. M., Marinaro, G., Mazlumyan, S., Naeher, S., North, R. P., Papatheodorou, G., Pfannkuche, O., Prien, R., Rehder, G., Schubert, C. J., Soltwedel, T., Sommer, S., Stahl, H., Stanev, E. V., Teaca, A., Tengberg, A., Waldmann, C., Wehrli, B., and Wenzhöfer, F., (2014), Investigating hypoxia in aquatic environments: Diverse approaches to addressing a complex phenomenon, *Biogeosciences*, 11, 1215–1259, doi:10.5194/bg-11- 1215-2014.

Froyd, C. and Bennett, K. (2006), Long-term ecology of native pinewood communities in East Glen Affric, Scotland. *Forestry* 79(3), 279-291.

Fyfe, R. M. et al. (2013) 'The Holocene vegetation cover of Britain and Ireland: Overcoming problems of scale and discerning patterns of openness', *Quaternary Science Reviews*. Elsevier Ltd, 73, pp. 132–148..

Gaines, S.M., G. Eglinton, and J. Rüllkolter. (2009). *Echoes of life—What fossil molecules reveal about earth history*. Oxford University Press, New York.

Galy, V., Beyssac, O., France-Lanord, C., Eglinton, T., (2008). Recycling of graphite during Himalayan erosion: A geological stabilization of carbon in the crust. *Science* 322, 943-945

Galy, V., France-Lanord, C., Beyssac, O., Faure, P., Kudrass, H., Palhol, F., (2007). Efficient organic carbon burial in the Bengal fan sustained by the Himalayan erosional system. *Nature* 450, 407-410.

Galy, V., Peucker-ehrenbrink, B. and Eglinton, T. (2015) 'Global carbon export from the terrestrial biosphere controlled by erosion', *Nature*.

Gillibrand, P. A., Cage, A. G. and Austin, W. E. N. (2005) 'A preliminary investigation of basin water response to climate forcing in a Scottish fjord: evaluating the influence of the NAO', *Continental Shelf Research*, 25(5-6), pp. 571–587. .

Gillibrand, P.A., Cromey, C.J., Black, K.D., Inall, M.E., Gontarek, S.J., (2006) Identifying the risk of deoxygenation in Scottish sea lochs with isolated deep water, *Scottish Aquaculture Research Forum*, SARF 07 Report..

Giri, C., Ochieng, E., Tieszen, L., Zhu, Z., Singh, A., Loveland, T., Masek, J. and N, D.(2014), Status and distribution of mangrove forests of the world using earth observation satellite data, Glob. Ecol. Biogeogr., 20(2011), 154–159.

Glud, R. N., Berg, P., Stahl, H., Hume, A., Larsen, M., Eyre, B. D. and Cook, P. L. M., (2016) Benthic Carbon Mineralization and Nutrient Turnover in a Scottish Sea Loch : An Integrative In Situ Study, Aquat. *Geochemistry*.

Golledge, N. R., (2010), Glaciation of Scotland during the Younger Dryas stadial : a review, J. Quat. Sci., 25(4), 550–566.

Goni, M.A., Monacci, N., Gisewhite, R., Crockett, J., Nittrouer, C., Ogston, A., Alin, S.R., Aalto, R., (2008). Terrigenous organic matter in sediments from the Fly River delta-clinoform system (Papua New Guinea). *Journal of Geophysical Research: Earth Surface* 113, F01S10

Goñi, M.A., Ruttenberg, K.C., Eglinton, T.I., (1998a). A reassessment of the sources and importance of land-derived organic matter in surface sediments from the Gulf of Mexico. *Geochimica et Cosmochimica Acta* 62, 3055-3075.

Goñi, M.A., Yunker, M.B., Macdonald, R.W., Eglinton, T.I., (2000). Distribution and sources of organic biomarkers in arctic sediments from the Mackenzie River and Beaufort Shelf. *Marine Chemistry* 71, 23-51.

Gordon, E.S., and Goni, M.A., (2003), Sources and distribution of terrigenous organic matter delivered by the Atchafalaya River to sediments in the northern Gulf of Mexico: *Geochimica et Cosmochimica Acta*, v. 67, no. 13, p. 2359–2375.

Gordon, E.S., Goñi, M.A., (2004). Controls on the distribution and accumulation of terrigenous organic matter in sediments from the Mississippi and Atchafalaya river margin. *Marine Chemistry* 92, 331-352.

Gordon, E.S., Goñi, M.A., Roberts, Q.N., Kineke, G.C., Allison, M.A., (2001). Organic matter distribution and accumulation on the inner Louisiana shelf west of the Atchafalaya River. *Continental Shelf Research* 21, 1691-1721.

Grieve, I.C , Hipkin, J.A. and Davidson, D.A., (1994), Soil erosion sensitivity in upland Scotland Research, *Survey and Monitoring Report No 24*, SNH, Perth.

Grob, R. L. (1977). *Modern practice of gas chromatography*. Wiley, Hoboken, NJ.

Guthrie, R. (2015) 'The catastrophic nature of humans', Nature Geoscience. *Nature* Publishing Group, 8(6), pp. 421–422.

Haas, H. De, Weering, T. C. E. Van and Stigter, H. De., (2002), Organic carbon in shelf seas : sinks or sources, processes and products, *Continental Shelf Research* , 22, 691–717.

Hansell DA, Olson D, Dentener F, Zamora L (2009) Assessment of excess nitrate development in the subtropical North Atlantic. *Marine Chemistry*, 106:562–579.

Harris, D., W. R. Horwáth, and C. van Kessel (2001), Acid fumigation of soils to remove carbonates prior to total organic carbon or carbon-13 isotopic analysis, *Soil Sci. Soc. Am. J.*, 65(6), 1853–1856.

Hartley, S. E. and Mitchell, R. J. (2005) 'Manipulation of nutrients and grazing levels on heather moorland: Changes in Calluna dominance and consequences for community composition', *Journal of Ecology*, 93(5), pp. 990–1004.

Hastings, R., Goñi, M., Wheatcroft, R., Borgeld, J., (2012). A terrestrial organic matter depocenter on a high-energy margin: the Umpqua River system, Oregon. *Continental Shelf Research* 39, 78-91

Hedges JI (1992) Global biogeochemical cycles: progress and problems. *Marine Chemistry*, 39:67–93.

Hedges, J.I., Keil, R.G. and Benner, R, (1997), What happens to terrestrial organic matter in the ocean? *Organic Geochemistry.* 27, 195–212.

Heijden, L. H. Van Der and Kamenos, N. A. (2015),Reviews and syntheses : Calculating the global contribution of coralline algae to total carbon burial, *Biogeosciences* , 6429–6441.

Hen, G, Azkab, MH, Chmura, GL, Chen, S, Sastrosuwondo, P, Ma, Z, Dharmawan, IWE, Yin, X and Chen, B, (2017) 'Mangroves as a major source of soil carbon storage in adjacent seagrass meadows', *Scientific Reports*. Nature Publishing Group, (January), pp. 1–10.

Henrys, P.A.; Keith, A.; Wood, C.M. (2016),Model estimates of aboveground carbon for Great Britain. NERC Environmental Information Data Centre.

Henrys, P.A.; Keith, A.M.; Robinson, D.A.; Emmett, B.A. (2012), Model estimates of topsoil carbon [Countryside Survey]. NERC Environmental Information Data Centre.

Herfort, L., S. Schouten, J. P. Boon, M. Woltering, M. Baas, J.W.H. Weijers, and J. S. Sinninghe Damsté. (2006). Characterization of transport and deposition of terrestrial organic matter in the southern North Sea using the BIT index. Limnology and Oceanography 51: 2196–2205

Hill, R. et al. (2015) 'Can macroalgae contribute to blue carbon ? An Australian perspective', *Limnology and Oceanography*, 2, pp. 1689–1706.

Hill, R., Bellgrove, A., Macreadie, P. I., Petrou, K., Beardall, J., Steven, A. and Ralph, P. J., (2015), Can macroalgae contribute to blue carbon ? An Australian perspective, Limnol. Oceanogr., 2.

Hilton, R.G., Galy, A., Hovius, N. & Horng, M.J., (2011), Efficient transport of fossil organic carbon to the ocean by steep mountain rivers: An orogenic carbon sequestration mechanism. Geology 39, 71–74.

Hinojosa, J.L, Christopher M. Moy, C.M, Claudine H. Stirling, C.H, Gary S. Wilson, G.S, and Eglinton, T.I., (2014), Carbon cycling and burial in New Zealand's fjords, , 4047–4063,

Hodgson, D. A., Graham, A. G. C., Grif, H. J., Roberts, S. J., Cofaigh, C. Ó., Bentley, M. J. and Evans, D. J. A., (2014), Glacial history of sub-Antarctic South Georgia based on the submarine geomorphology of its fjords , *Quat. Sci. Rev.*, 89, 129–147.

Hogg, O. T., Huvenne, V. A. I., Griffiths, H. J., Dorschel, B. and Linse, K., (2016), Landscape mapping at sub- Antarctic South Georgia provides a protocol for underpinning large-scale marine protected areas, *Sci. Rep*., (October), 1–15.

Hopmans, E. C. et al. (2004) 'A novel proxy for terrestrial organic matter in sediments based on branched and isoprenoid tetraether lipids', *Earth and Planetary Science Letters*, 224(1-2), pp. 107–116.

Houghton RA (2007) Balancing the global carbon budget. *Annual Review Earth Planet Science*, 35:313–347.

Howard, D. L. (1980). *Polycyclic triterpenes of anaerobic photosynthetic bacterium, Rhodomicrobium vannielii*. Thesis, University of California at Los Angeles, Los Angeles, CA.

Howard, P.J.A., Loveland, P.J., Bradley, R.I., Dry, F.T., Howard, D.M. and Howard, D.C., (1995), The carbon content of soil and its geographical distribution in Great Britain. *Soil Use and Management,* 11, 9–15.

Howe, J. A., Austin, W.E.N., Forwick, M., Paetzel, M., Harland, R., and Cage, A. G., (2010), Fjord systems and archives: a review, *Geological Society, London, Special Publications*, v. 344, no. 1, p. 5–15.

Howe, J. A., Shimmield, T., Austin, W. E. N. and Longva, O., (2002), Post-glacial depositional environments in a mid-high latitude glacially-overdeepened sea loch , inner Loch Etive , western Scotland, *Marine Geology*, 185, 417–433.

Hunt, J. H. (1996). *Petroleum geochemistry and geology*, 2nd ed. Freeman, New York.

Hwang, J., Druffel, E.R., Komada, T., (2005). Transport of organic carbon from the California coast to the slope region: A study of Δ14C and δ13C signatures of organic compound classes. *Global Biogeochemical Cycles* 19, GB2018

Hyndes, G. A., Nagelkerken, I., Mcleod, R. J., Connolly, R. M., Lavery, S. and Vanderklift, M. A.(2015), Mechanisms and ecological role of carbon transfer within coastal seascapes, Biol. Rev., 89(March), 232–254.

Hyndes, GA, Nagelkerken, I, Mcleod, RJ, Connolly, RM, Lavery, S and Vanderklift, MA , (2015) 'Mechanisms and ecological role of carbon transfer within coastal seascapes', 89(March), pp. 232–254.

Inall, M. et al. (2009) 'On the oceanographic variability of the North-West European Shelf to the West of Scotland', *Journal of Marine Systems*, 77(3), pp. 210–226.

IPCC, (2013) Climate Change 2013: The Physical Science Basis. Cambridge, UK: Cambridge University Press

Jackson, R.B., Banner, J.L., Jobbagy, E.G., Pockman, W.T. and Wall, D.H., (2012), Ecosystem carbon loss with woody plant invasion of grasslands. *Nature* 418: 623-626, 2012.

Johnston, D.H and R. Cooper, M.R., (2010), Methods and Applications in Reservoir Geophysics, Investigations in geophysics, no. 15., Tulsa, OK : *Society of Exploration Geophysicists.*

Jones, N.,(2013), Troubling milestone for CO2, *Nature Geoscience*, 6(8), 589

Karlsson, E., Charkin, A., Dudarev, O., Semiletov, I., Vonk, J., Sánchez-García, L., Andersson, A., Gustafsson, Ö., (2011). Carbon isotopes and lipid biomarker investigation of sources, transport and degradation of terrestrial organic matter in the Buor-Khaya Bay, SE Laptev Sea. *Biogeosciences* 8, 1865-1879

Karlsson, E., Gelting, J., Tesi, T., Dongen, B., Andersson, A., Semiletov, I., Charkin, A., Dudarev, O., Gustafsson, Ö., (2016). Different sources and degradation state of dissolved, particulate, and sedimentary organic matter along the Eurasian Arctic coastal margin. *Global Biogeochemical Cycles* 30, 898-919.

Kastner, T.P., Goñi, M.A., (2003). Constancy in the vegetation of the Amazon Basin during the late Pleistocene: evidence from the organic matter composition of Amazon deep sea fan sediments. *Geology* 31, 291-294.

Keil, R.G., Mayer, L.M., Quay, P.D., Richey, J.E., Hedges, J.I., (1997). Loss of organic matter from riverine particles in deltas. *Geochimica et Cosmochimica acta* 61, 1507-1511.

Kennedy H, Beggins J, Duarte CM, et al. (2010). Seagrass sediments as a global carbon sink: isotopic constraints. *Global Biogeochemical Cycles* 24.

Kennedy, H., Alongi, D. M., Karim, A., Chen, G., Chmura, G. L., Crooks, S., Kairo, J. G., Liao, B. and Lin, G., (2013), Coastal Wetlands , IPCC Guidelines for National Greenhouse, Gas Inventories: Wetlands.

Kennedy, P., Kennedy, H., and Papadimitriou, S., (2005), The effect of acidification on the determination of organic carbon, total nitrogen and their stable isotopic composition in algae and marine sediment, *Rapid Communications in Mass Spectrometry*, 19, (8), pp. 1063–1068.

Khanna, N., Godbold, J. A., Austin, W. E. N. and Paterson, D. M., (2013), The impact of ocean acidification on the functional morphology of foraminifera, *PLoS One*, 8(12), 10–13.

Kirkels, F.M.S.A., Cammeraat, L.H., and Kuhn, N.J., (2014), The fate of soil organic carbon upon erosion, transport and deposition in agricultural landscapes - A review of different concepts: *Geomorphology*, v. 226, p. 94–105.

Kirwan, M. L., Temmerman, S., Skeehan, E. E., Guntenspergen, G. R. and Fagherazzi, S.(2016), Overestimation of marsh vulnerability to sea level rise, *Nature Climate Change*, 6(3), 253–260.

Knight, J. and Harrison, S. (2012) 'The impacts of climate change on terrestrial Earth surface systems', *Nature Climate Change*. Nature Publishing Group, 3(1), pp. 24–29.

Kniskern, T.A., Kuehl, S.A., Harris, C.K., Carter, L., (2010). Sediment accumulation patterns and fine-scale strata formation on the Waiapu River shelf, New Zealand. *Marine Geology* 270, 188-201.

Kniskern, T.A., Mitra, S., Orpin, A.R., Harris, C.K., Walsh, J., Corbett, D., (2014). Characterization of a flood-associated deposit on the Waipaoa River shelf using radioisotopes and terrigenous organic matter abundance and composition. *Continental Shelf Research* 86, 66-84.

Knox, J.W., Rickson, R.J., Weatherhead, E.K., Hess, T.M., Deeks, L.K., Truckell, I.J., Keay C.A., Brewer, T.R. and Daccache, A. (2015), Research to develop evidence base on soil erosion and water use in agriculture, *Final technical report*.

Köchy, M., Hiederer, R. and Freibauer, A., (2015), Global distribution of soil organic carbon – Part 1: Masses and frequency distributions of SOC stocks for the tropics, permafrost regions, wetlands, and the world, Soil, 1(1), 351–365

Köhl, M., Lasco, R., Cifuentes, M., Korhonen, K. T., Mundhenk, P., de Jesus Navar, J. and Stinson, G., (2015), Changes in forest production, biomass and carbon: Results from the 2015 UN FAO Global Forest Resource Assessment, *For. Ecol. Manage*., 352, 21–34.

Komada, T., Burdige, D.J., Magen, C., Li, H.-L., Chanton, J., (2016). Recycling of organicmatter in the sediments of Santa Monica Basin, California Borderland. *Aquatic Geochemistry* 22, 593-618.

Komada, T., Druffel, E.R., Hwang, J., (2005). Sedimentary rocks as sources of ancient organic carbon to the ocean: An investigation through Δ14C and δ13C signatures of organic compound classes. *Global Biogeochemical Cycles* 19, GB2017.

Koziorowska, K., Kuli, K. & Pempkowiak, J., (2017). Distribution and origin of inorganic and organic carbon in the sediments of Kongsfjorden , Northwest Spitsbergen , European Arctic. *Continental Shelf Research*, (August).

Koziorowska, K., Kuliński, K., and Pempkowiak, J., (2016), Sedimentary organic matter in two Spitsbergen fjords: Terrestrial and marine contributions based on carbon and nitrogen contents and stable isotopes composition: *Continental Shelf Research*, v. 113, p. 38–46.

Krause-Jensen, D. and Duarte, C. M. (2016) 'Substantial role of macroalgae in marine carbon sequestration', *Nature Geoscience*. Nature Publishing Group, 9(10), pp. 737–742.

Krause-jensen, D. and Duarte, C. M.(2016), Substantial role of macroalgae in marine carbon sequestration, Nat. Geosci., 9(10), 737–742.

Kristensen, E, Bouillon, S, Dittmar, T and Marchand , (2008) 'Organic carbon dynamics in mangrove ecosystems : A review', *Aquatic Botany*, 89, pp. 201–219.

Krumhansl, K. A. and Scheibling, R. E., (2012), Production and fate of kelp detritus, *Mar. Ecol. Prog. Ser*., 467, 281–302.

Kuehl, S.A., DeMaster, D.J., Nittrouer, C.A., (1986). Nature of sediment accumulation on the Amazon continental shelf. *Continental Shelf Research* 6, 209-225

Kuliński, K., Kędra, M., Legeżyńska, J., Gluchowska, M. and Zaborska, A., (2014), Particulate organic matter sinks and sources in high Arctic fjord, *J. Mar. Syst.,* 139, 27–37.

Kuparinen, A. et al. (2007) 'Modeling air-mediated dispersal of spores, pollen and seeds in forested areas', *Ecological Modelling*, 208(2-4), pp. 177–188.

Lambeck, K., (1993), Glacial rebound of the British Isles II. A high resolution high precsion model, *Geophys. J. Int*.,115, 960-990.

Langdon, P. G., Barber, K. E. and Hughes, P. D. M. (2003) 'A 7500-year peat-based palaeoclimatic reconstruction and evidence for an 1100-year cyclicity in bog surface wetness from Temple Hill Moss, Pentland Hills, southeast Scotland', *Quaternary Science Reviews*, 22(2-4), pp. 259–274.

Ledger, D.C., Lovell, J.P.B. & McDonald, A.T. (1974). Sediment yield studies in upland catchments in south-east Scotland. *Journal of Applied Ecology*, 11, 201-206.

Lee, R. F. and A. R. Loeblich III. (1971). Distribution of 21:6 hydrocarbon and its relationship to 22:6 fatty acid in algae. *Phytochemistry* 10: 593–602.

Leipe, T., Tauber, F., Vallius, H., Virtasalo, J., Uścinowicz, S., owalski, N., Hille, S., Lindgren, S., Myllyvirta, T., (2011). Particulate organic carbon (POC) in surface sediments of the Baltic Sea. *Geo-Marine Letters* 31, 175-188

Leith, F. I., Dinsmore, K. J., Wallin, M. B., Billett, M. F., Heal, K. V, Laudon, H. and Öquist, M. G., (2015), Carbon dioxide transport across the hillslope – riparian – stream continuum in a boreal headwater catchment, , *Biogeosciences*, 1881–1892.

Li, D., Yao, P., Bianchi, T.S., Zhang, T., Zhao, B., Pan, H., Wang, J., and Yu, Z., (2014), Organic carbon cycling in sediments of the Changjiang Estuary and adjacent shelf: Implication for the influence of Three Gorges Dam: *Journal of Marine Sy*stems, v. 139, p. 409–419.

Li, X., Bianchi, T.S., Allison, M.A., Chapman, P., Mitra, S., Zhang, Z., Yang, G., Yu, Z., (2012). Composition, abundance and age of total organic carbon in surface sediments from the inner shelf of the East China Sea. *Marine chemistry* 145, 37-52.

Libby, W. F. (1952). Chicago radiocarbon dates, 3. *Science* 116: 673–681

Liu, X. L. et al. (2016) 'Novel archaeal tetraether lipids with a cyclohexyl ring identified in Fayetteville Green Lake, NY, and other sulfidic lacustrine settings', *Rapid Communications in Mass Spectrometry*, 30(10), pp. 1197–1205.

Loh, P. S. et al. (2010) 'Sediment fluxes and carbon budgets in Loch Creran, western Scotland', *Geological Society, London, Special Publications*, 344(1), pp. 103–124.

Loh, P. S., Miller, A. E. J., Reeves, A. D., Harvey, S. M., Overnell, J, (2008), Assessing the biodegradability of terrestrially-derived organic matter in Scottish sea loch sediments, *Hydrol. Earth Syst. Sci*., 811–823, 2008.

Louchouarn, P., Lucotte, M., Canuel, R., Gagné, J.-P., Richard, L.-F., (1997). Sources and early diagenesis of lignin and bulk organic matter in the sediments of the Lower St. Lawrence Estuary and the Saguenay Fjord. *Marine Chemistry* 58, 3-26

Lunn, D., Spiegelhalter, D., Thomas, A., and Best, N., (2009), The BUGS project: Evolution, critique and future directions: *Statistics in medicine*, v. 28, no. June, p. 221–239.

Macklin, M. G. et al. (2000) 'Human–environment interactions during the Holocene: new data and interpretations from the Oban area, Argyll, Scotland', *The Holocene*, 10(1), pp. 109–121.

MacNaughton, S. J., T. L. Jenkins, M. H. Wimpee, M. R. Cormier, and D. C. White. (1997). Rapid extraction of lipid biomarkers from pure culture and environmental samples using pressurized accelerated hot solvent extraction. *Journal of Microbiological Methods* 31: 19–27.

Macreadie, P. I., Nielsen, D. A., Kelleway, J. J., Atwood, T. B., Seymour, J. R., Petrou, K., Connolly, R. M., Thomson, A. C. G., Trevathan-tackett, S. M. and Ralph, P. J.(2017), Can we manage coastal ecosystems to sequester more blue carbon ?, *Frontiers Ecology*.

Macreadie, P. I., Ollivier, Q. R., Kelleway, J. J., Serrano, O., Carnell, P. E., Ewers Lewis, C. J., Atwood, T. B., Sanderman, J., Baldock, J., Connolly, R. M., Duarte, C. M., Lavery, P. S., Steven, A. and Lovelock, C. E.,(2017), Carbon sequestration by Australian tidal marshes, *Sci. Rep.*, 7, 1–10.

Mastrandrea, M.D., Field,C.B., Stocker, T.F., Edenhofer, O., Ebi, K.L. , Frame, D.J. Held, H., Kriegler, E., Mach, K.J., Matschoss, P.R., Plattner, G.K, Yohe, G.W., and Zwiers, F.W., (2010), Guidance Note for Lead Authors of the IPCC Fifth Assessment Report on Consistent Treatment of Uncertainties. Intergovernmental Panel on Climate Change (IPCC).

Mayewski, P. A. et al. (2004) 'Holocene climate variability', *Quaternary Research*, 62(3), pp. 243–255.

Mazarrasa, I, Marbà, N, Lovelock, CE, Serrano, O, Lavery, PS, Fourqurean, JW, Kennedy, H, Mateo, MA, Krause-Jensen, D, Steven, ADL and Duarte, CM, (2015) 'Seagrass meadows as a globally significant carbonate reservoir', *Biogeosciences*, 12(16), pp. 4993–5003.

McCave, I. N., Manighetti, B. and Robinson, S. G. (1995) 'Sortable silt and fine sediment size/composition slicing: Parameters for palaeocurrent speed and palaeoceanography', *Paleoceanography*, 10(3), pp. 593–610.

McEvedy, C. and Jones, R. (1978). Atlas of world population history, Penguin Books, Harmondsworth, UK, 19–119.

McIntyre, K. L. and Howe, J. A.(2010), Scottish west coast fjords since the last glaciation: a review. *Geological Society, London, Special Publications*, 344, 305-329, 2010.

McLeod, E, Chmura, GL, Bouillon, S, Salm, M, Duarte, CM, Lovelock, CE, Schlesinger, WH and Silliman, BR, (2011) 'A blueprint for blue carbon: Toward an improved understanding of the role of vegetated coastal habitats in sequestering CO2', *Frontiers in Ecology and the Environment*, 9(10), pp. 552–560.

McManus, J. and Duck, R.W., (1985). Sediment yields estimated from reservoir siltation in the Ochil Hills, *Scotland. Earth Surface Processes and Landforms*, 10, 193-200

Meeker, L. D. and Mayewski, P. a. (2002) 'A 1400-year high-resolution record of atmospheric circulation over the North Atlantic and Asia', *The Holocene*, 12(3), pp. 257–266.

Metcalfe, L. D., A. A. Schmitz, and J. R. Pelka. (1966). Rapid preparation of fatty acid esters from lipids for gas chromatographic analysis. *Analytical Chemistry* 38: 514–515.

Meybeck M (1982) Carbon, nitrogen, and phosphorus transport by world rivers. *American Journal of Science*,282:401–450.

Meyers, P. A. (1997). Organic geochemical proxies of paleoceanographic, paleolimnologic, and paieoclimatic processes. *Organic Geochemistry* 27: 213–250.

Meyers, P. A., and R. Ishiwatari. (1993). Lacustrine organic geochemistry: An overview of indicators of organic matter sources and diagenesis in lake sediments. *Organic Geochemistry* 20: 867–900.

Meyers, P.A., (1994). Preservation of elemental and isotopic source identification of sedimentary organic matter. *Chemical Geology*, 114, 289–302

Middelburg, J. J., (2017), Reviews and Synthesis: To the bottom of carbon processing at the seafloor, *Biogeosciences Discuss*.

Middelburg, J. J., Vlug, T., Jaco, F. and van der Nat, W. (1993). Organic matter mineralization in marine systems, *Glob. Planet. Change*, 8, 47–58.

Middelburg, J.J., and Levin, L.A., (2009), Coastal hypoxia and sediment biogeochemistry:, *Biogeosciences*, p. 1273–1293.

Miller, A.J., Kuehl, S.A., (2010). Shelf sedimentation on a tectonically active margin: a modern sediment budget for Poverty continental shelf, New Zealand. *Marine Geology* 270, 175- 187.

Mills, K. et al. (2016) 'Deciphering long - term records of natural variability and human impact as recorded in lake sediments : a palaeolimnological puzzle', *Wiley Interdisciplinary Reviews.*

Miltner, A., Emeis, K.-C., (2000). Origin and transport of terrestrial organic matter from the Oder lagoon to the Arkona Basin, Southern Baltic Sea. *Organic Geochemistry* 31, 57-66

Miltner, A., Emeis, K.C., (2001). Terrestrial organic matter in surface sediments of the Baltic Sea, Northwest Europe, as determined by CuO oxidation. *Geochimica et Cosmochimica Acta* 65, 1285-1299.

Mokeddem, Z., Baltzer, A.., Goubert, E and Clet-Pellerin, M., A ., (2010), Multiproxy palaeoenvironmental reconstruction of Loch Sunart (NW Scotland) since the Last Glacial Maximum, Geological Society, *London, Special Publications*, 344, (1), pp. 341–353.

Mokeddem, Z., Goubert, E., Lartaud, F. and Labourdette, N., (2015), The " Turritella Layer ": A Potential Proxy of a Drastic Holocene Environmental Change on the North – East Atlantic Coast, *Sediment Fluxes in Coastal Systems* , 3–21.

Mollenhauer, G., Eglinton, T.I., (2007). Diagenetic and sedimentological controls on the composition of organic matter preserved in California Borderland Basin sediments. *Limnology and Oceanography* 52, 558-576

Morris, D.J., O'Connell, M.T., and Macko, S.A., (2015), Assessing the importance of terrestrial organic carbon in the CHUKCHI and Beaufort seas: *Estuarine, Coastal and Shelf Science*, v. 164, p. 28–38.

Morton, D., Rowland, C., Wood, C., Meek, L., Marston, C., Smith, G., Wadsworth, R., Simpson, I.C., (2011), Final Report for LCM2007 - the new UK Land Cover Map. Countryside Survey Technical Report No. 11/07 NERC/Centre for Ecology & Hydrology 112pp. (CEH Project Number: C03259).

Muller, A., (2001). Geochemical expressions of anoxic conditions in Nordasvannet, a land-locked fjord in western Norway. *Appl. Geochem*. 16, 363–374.

Muri, G., S. G. Wakeham, T. K. Pease, and J. Faganeli. (2004). Evaluation of lipid biomarkers as indicators of changes in organic matter delivery to sediments from Lake Planina, a remote mountain lake in NW Slovenia. *Organic Geochemistry* 35: 1083–1093.

Nellemann C., Corcoran E., Duarte C.M., Valdés L., DeYoung C., Fonseca L., Grimsditch G. ., (2009), Blue Carbon: A Rapid Response Assessment, United Nations Environment Programme, GRID-Arendal.

Nieuwenhuize, J., Maas., Y. E. . and Middleburg, J. (1994) 'Rapid analysis of organic carbon and nitrogen in particulate materials', *Marine Chemistry*, 45(3), pp. 217–244.

Nordhaus, W. D., (2017), Revisiting the social cost of carbon, *Proc. Natl. Acad. Sci*., 2016, 201609244.

Nordhaus, W., (2014), Estimates of the Social Cost of Carbon: Concepts and Results from the DICE-2013R Model and Alternative Approaches, *J. Assoc. Environ. Resour. Econ*., 1(1/2), 273–312.

Nørgaard-Pedersen, N., Austin, W. E. N., Howe, J. A. and Shimmield, T., (2006), The Holocene record of Loch Etive, western Scotland: Influence of catchment and relative sea level changes, *Mar. Geol.,* 228(1-4), 55–71.

Nuwer, J.M., and Keil, R.G., (2005), Sedimentary organic matter geochemistry of Clayoquot Sound , Vancouver Island , British Columbia: *Limnology and Oceanography*,v. 50, no. 4, p. 1119–1128.

O'Neil, J. R. (1969) 'Oxygen Isotope Fractionation in Divalent Metal Carbonates', The *Journal of Chemical Physics*, 51(12), p. 5547.

Oppo, D. ., McManus, J. .and Cullen, J. L. (2003) 'Deepwater variability in the Holocne epoch', *Nature*, 422(March), p. 277.

Ortega, P. et al. (2015) 'A model-tested North Atlantic Oscillation reconstruction for the past millennium', *Nature*, 523(7558), pp. 71–74.

Overland, J. E. et al. (2016) 'Nonlinear response of mid-latitude weather to the changing Arctic', Nature Climate Change. *Nature Publishing Group*, 6(11), pp. 992–999.

Painter, S.C., Hartman, S.E., Kivimae, C., Salt, L.A., Clargo, N.M., Bozec, Y., Daniels, C.J., Jones, S.C., Hemsley, V.S., Munns, L.R., and Allen, S.R., (2016), Carbon exchange

between a shelf sea and the ocean: The Hebrides Shelf, west of Scotland: *Journal of Geophysical Research: Oceans*, v. 121, p. 4522–4544.

Panagos, P. et al. (2015) 'Estimating the soil erosion cover-management factor at the European scale', *Land Use Policy*. Elsevier Ltd, 48, pp. 38–50..

Panagos, P., Borrelli, P., Poesen, J., Ballabio, C., Lugato, E., Meusburger, K., Montanarella, L., Alewell, .C., (2015). The new assessment of soil loss by water erosion in Europe. *Environmental Science & Policy.* 54: 438-447.

Payne, R, Turrell, W, Moore, D, & Adams, R., (1989), Loch Sunart Surveys 1987, 1988.

Pedersen, J. B. T., Kroon, a., Jakobsen, B. H., Mernild, S. H., Andersen, T. J. and Andresen, C. S., (2013), Fluctuations of sediment accumulation rates in front of an Arctic delta in Greenland, *The Holocene*, 23(6), 860–868.

Peters, K. H., C. C.Walters, and J.M.Moldowan. (2005). *The biomarker guide*. Pp. 198–251. Cambridge University Press, Cambridge, UK.

Poerschmann, J., and R. Carlson. (2006). New fractionation scheme for lipid classes based on "in-cell fractionation" using sequential pressurized liquid extraction. *Journal of Chromatography A* 1127: 18–25.

Polson, D. and Curtis, A., (2010), Dynamics of uncertainty in geological interpretation, *J. Geol. Soc. London*., 167(1), 5–10.

Press, W.H., Flannery, B.P., Teukolsky, S.A., and Vetterling, W.T., (1988), Numerical Recipes in C, Cambridge University Press.

Randsalu-Wendrup, L. et al. (2016) 'Paleolimnological records of regime shifts in lakes in response to climate change and anthropogenic activities', J*ournal of Paleolimnology*. Springer Netherlands, 56(1), pp. 1–14.

Redfield A. C., Ketchum B. H., and Richards F. A. (1963) The influence of organisms on the composition of seawater. In The Sea, Vol. 2 (ed. M. N. Hill), pp. 26–77. John Wiley, New York.

Reimer, P. (2013) 'IntCal13 and Marine13 Radiocarbon Age Calibration Curves 0–50,000 Years cal BP', *Radiocarbon*, 55(4), pp. 1869–1887.

Reimer, P. J. , Bard, E. , Bayliss, A. , Beck, J. W. , Blackwell, P. G. , Bronk Ramsey, C. , Buck, C. E. , Cheng, H. , Edwards, R. L. , Friedrich, M. , Grootes, P. M. , Guilderson, T. P. , Haflidason, H. , Hajdas, I. , Hatté, C. , Heaton, T. J. , Hoffmann, D. L. , Hogg, A. G. ,

Hughen, K. A. , Kaiser, K. F. & 10 others 2013 In : Radiocarbon. 55, 4, p. 1869-1887 19 p.Reimer, P. J. , Bard, E. , Bayliss, A. , Beck, J. W. , Blackwell, P. G. , Bronk Ramsey, C. , Buck, C. E. , Cheng, H. , Edwards, R. L. , Friedrich, M. , Grootes, P. M. , Guilderson, T. P. , Haflidason, H. , Hajdas, I. , Hatté, C. , Heaton, T. J. , Hoffmann, D. L. , Hogg, A. G. , Hughen, K. A. , Kaiser, K. F. & 10 others (2013), INTCAL13 and MARINE13 radiocarbon age calibration curves 0-50,000 years cal BP, *Radiocarbon*. 55, 4, p. 1869-1887.

Risatti, J. B., S. J. Rowland, D. A. Yon, and J. R.Maxwell. (1984). Stereochemical, studies of acyclic isoprenoids, XII: Lipids of methanogenic bacteria and possible contributions to sediments. *Organic Geochemistry*. 6: 93–103.

Röhr, M. E., Boström, C., Canal-Verges, P. and Holmer, M., (2016), Blue carbon stocks in Baltic Sea eelgrass (Zostera marina) meadows, *Biogeosciences*, 13(22), 6139–6153.

Rothwell, R.G, Croudace, I.W. (2015), Micro-XRF Studies of Sediment Cores: A Perspective on Capability and Application in the Environmental Sciences, In: Croudace, I.W.; Rothwell, R.G., (eds.) Micro-XRF Studies of Sediment Cores: Applications of a non-destructive tool for the environmental sciences. Dordrecht, The Netherlands, Springer, 173-185, 688pp

Ruddiman, W. F.(2013) 'The Anthropocene', *Annual Review of Earth and Planetary Sciences*, 41, pp. 45–68..

Russell, M., Robinson, C.D., Webster, L., Walsham, P., Phillips, L., Dalgarno, E., Rose, M., Watson, D., Scurfield, J., Avery, D.J., Devalla, S., Gubbins, M., Davies, I.M., and Moffat, C.F., (2010), Persistent organic pollutants and trace metals in sediments close to Scottish marine fish farm, *Scottish marine and freshwater science volume 1 no 16*.

Rydval, M. et al. (2017) 'Spatial reconstruction of Scottish summer temperatures from tree rings', *International Journal of Climatology*, 37(3), pp. 1540–1556.

Sampere, T.P., Bianchi, T.S., Allison, M.A., (2011a). Historical changes in terrestrially derived organic carbon inputs to Louisiana continental margin sediments over the past 150 years. *Journal of Geophysical Research: Biogeosciences* 116, G01016.

Sampere, T.P., Bianchi, T.S., Allison, M.A., McKee, B.A., (2011b). Burial and degradation of organic carbon in Louisiana shelf/slope sediments. *Estuarine, Coastal and Shelf Science* 95, 232-244.

Sampere, T.P., Bianchi, T.S., Wakeham, S.G., Allison, M.A., (2008). Sources of organic matter in surface sediments of the Louisiana Continental margin: effects of major depositional/transport pathways and Hurricane Ivan*. Continental Shelf Research* 28, 2472-2487.

Sansum, P., Stewart, M. and Watson, F. (2005) A Preliminary History of the Clyde Valley Woodlands.

Scharlemann, J. P. W., Tanner, E. V. J., Hiederer, R., Kapos, V., Pw, J., Tanner, E. V. J., Hiederer, R. and Kapos, V.(2017), Global soil carbon : understanding and managing the largest terrestrial carbon pool Global soil carbon : understanding and managing the largest terrestrial carbon pool, *Carbon Management*, 3004.

Schmidt, M.W.I., and Gleixner, G., (2005), Carbon and nitrogen isotope composition of bulk soils, particle-size fractions and organic material after treatment with hydrofluoric acid, *European Journal of Soil Science,* v. 56, no. 3, p. 407–416.

Scottish Government. (2015). http://www.gov.scot/Publications/2015/06/1939; Accessed 25/11/2015.

Scourse, J. D., Haapaniemi, A. I., Colmenero-hidalgo, E., Peck, V. L., Hall, I. R., Austin, W. E. N., Knutz, P. C. and Zahn, R., (2009), Growth , dynamics and deglaciation of the last British – Irish ice sheet : the deep-sea ice-rafted detritus record, *Quat. Sci. Rev*., 28(27-28).

Seddon, A. W. et al. (2016) 'Sensitivity of global terrestrial ecosystems to climate variability', *Nature*. Nature Publishing Group, 531(7593), pp. 229–232.

Sepúlveda, J., Pantoja, S., and Hughen, K.A., (2011), Sources and distribution of organic matter in northern Patagonia fjords, Chile (~44-47°S): A multi-tracer approach for carbon cycling assessment: *Continental Shelf Research*, v. 31, no. 3-4, p. 315–329.

Shennan, I. et al. (2005) 'A 16000-year record of near-field relative sea-level changes, northwest Scotland, United Kingdom'*, Quaternary International*, 133-134, pp. 95–106..

Showers, W.J., Angle, D.G., 1986. Stable isotopic characterization of organic carbon accumulation on the Amazon continental shelf. *Continental Shelf Research* 6, 227-244.

Sikes, E.L., Uhle, M.E., Nodder, S.D., Howard, M.E., (2009). Sources of organic matter in a coastal marine environment: evidence from n-alkanes and their δ13C distributions in the Hauraki Gulf, New Zealand. *Marine Chemistry* 113, 149-163

Silva, N., Vargas, C.A., and Prego, R., (2011), Land – ocean distribution of allochthonous organic matter in surface and Ayse in interior seas (Chilean Northern Patagonia) sediments of the Chiloe: *Continental Shelf Research*, v. 31, no. 3-4, p. 330–339.

Silva, R. A., West, J. J., Lamarque, J., Shindell, D. T., Collins, W. J., Faluvegi, G., Folberth, G. A., Horowitz, L. W., Nagashima, T., Naik, V., Rumbold, S. T., Sudo, K., Takemura, T. and Bergmann, D.:(2017), Future global mortality from changes in air pollution attributable to climate change, *Nature Climate Change*, 7(September), 647–652,

Simpkin,P.G. and Davis, A. (1983), For seismic profiling in very shallow water, a novel receiver. In Sea Technology.

Smeaton, C. and Austin, W.E.N. (2017).Sources, sinks, and subsidies: Terrestrial carbon storage in midlatitude fjords.*Journal of Geophysical Research: Biogeosciences*, 122.

Smeaton, C., Austin, W.E.N., Davies, A.L., Baltzer, A., Abell, R.E., and Howe, J.A.,(2016), Substantial stores of sedimentary carbon held in mid-latitude fjords: *Biogeosciences*, v. 13, no. 20, p. 5771–5787.

Smedes, F., and T. K. Askland. (1999). Revisiting the development of the Bligh and Dyer total lipid determination method. *Marine Pollution Bulletin* 38: 193–201.

Smith, R. W., Bianchi, T. S. and Savage, C. (2010) 'Comparison of lignin phenols and branched/isoprenoid tetraethers (BIT index) as indices of terrestrial organic matter in Doubtful Sound, Fiordland, New Zealand', *Organic Geochemistry*, 41(3), pp. 281–290.

Smith, R.W., Bianchi, T.S., Allison, M., Savage, C., Galy, V., (2015). High rates of organic carbon burial in fjord sediments globally. *Nature Geoscience*, 450-453

Smittenberg, R.H., Hopmans, E.C., Schouten, S., Hayes, J.M., Eglinton, T.I., Sinninghe Damste, J.S., (2004). Compound-specific radiocarbon dating of the varved Holocene sedimentary record of Saanich Inlet, Canada. *Paleoceanography* 19, PA2012.

Smoak, JM, Breithaupt, JL, Smith, TJ and Sanders, CJ , (2013) Sediment accretion and organic carbon burial relative to sea-level rise and storm events in two mangrove forests in Everglades National Park', *Catena*. Elsevier B.V., 104, pp. 58–66.

Smout, T. C. (1993) Scotland since prehistory: Natural change and human impact.

Soil Survey of Scotland Staff. (1970-1987). Soil maps of Scotland (partial coverage) at a scale of 1:25 000. *Macaulay Institute for Soil Research*, Aberdeen.

Solomon, S., Plattner, G., Knutti, R. and Friedlingstein, P. (2009), Irreversible climate change due to carbon dioxide emissions*, Proc. Natl. Acad. Sci*., 106(6), 1704–1709.

Spencer, T., Schuerch, M., Nicholls, R.J., Hinkel, J., Lincke, D., Vafeidis, A.T., Reef, R., McFadden, L. and Brown, S., (2016). Global coastal wetland change under sea-level rise and related stresses: The DIVA Wetland Change Model. *Global and Planetary Change*, v. 139, p.15-30

Stoker, M, and Bradwell,T., (2009), Neotectonic deformation in a Scottish fjord, Loch Broom, NW Scotland, *Scottish Journal of Geology*, 45 (2), pp. 107-116.

Stoker, M., Wilson, C.R., Howe J.A., Bradwell, T., and Long, D., (2010), Paraglacial slope instability in Scottish fjords: Examples from Little Loch Broom, NW Scotland, *Geological Society Special Publications*, 344, pp. 225-242.

St-Onge, G., and Hillaire-marcel, C., (2001), Isotopic constraints of sedimentary inputs and organic carbon burial rates in the Saguenay Fjord,Quebec, *Marine Geology*, v. 176.

Struck, U., Emeis, K.-C., Voss, M., Christiansen, C., Kunzendorf, H., (2000). Records of southern and central Baltic Sea eutrophication in δ 13 C and δ 15 N of sedimentary organic matter. *Marine Geology* 164, 157-171.

Suess, H. E .(1968). Climatic changes, solar activity and the cosmic ray production rate of radiocarbon. *Meterological Monographs* 8: 146–150.

Suess, H. E. (1958). Radioactivity of the atmosphere and hydrosphere. *Annual Review of Nuclear Science* 8: 243–256.

Sugita, S. (2007) 'Theory of quantitative reconstruction of vegetation I: pollen from large sites REVEALS regional vegetation composition', *The Holocene*, 17, pp. 229–241.

Sun, G. and Mu, M. (2017) 'Responses of Terrestrial Ecosystem to Climate Change: Results from Approach of Conditional Nonlinear Optimal Perturbation of Parameters', in Park, S. K. and Xu, L. (eds) *Data Assimilation for Atmospheric, Oceanic and Hydrologic Applications* (Vol. III). Cham: Springer International Publishing, pp. 527–547.

Sun, M.-Y., S. G. Wakeham, and C. Lee. (1997). Rates and mechanisms of fatty acid degradation in oxic and anoxic coastal marine sediments of Long Island Sound, New York, USA. *Geochimica et Cosmochimica Acta* 61: 341–355.

Sun, S., Schefuß, E., Mulitza, S., Chiessi, C.M., Sawakuchi, A.O., Baker, P., Mollenhauer, G., (2017). Origin and processing of terrestrial particulate organic carbon in the Amazon system: lignin phenols in river, shelf and fan sediments. *Biogeosciences*, 14, 2495-2512

Syvitski, J. P. M., Burrell, D. C., and Skei, J. M., (1987), Fjords, Processes and Products, Springer-Verlag New York, 1987.

Syvitski, J.P.M., and Shaw, J., (1995), Sedimentology and Geomorphology of Fjords: *Geomorphology and Sedimentology of Estuaries*, v. 53, p. 113–178.

Szmytkiewicz, A. and Zalewska, T. (2014) 'Sediment deposition and accumulation rates determined by sediment trap and 210Pb isotope methods in the outer puck bay (Baltic Sea)', *Oceanologia*. Elsevier Masson SAS, 56(1),

Tao, S., Eglinton, T.I., Montlucon, D.B., McIntyre, C. Zhao M., (2015). Pre-aged soil organic carbon as a major component of the Yellow River suspended load: Regional significance and global relevance. *Earth and Planetary Science Letters* 414, 77-86

Tesi, T., Semiletov, I., Hugelius, G., Dudarev, O., Kuhry, P., Gustafsson, Ö., (2014). Composition and fate of terrigenous organic matter along the Arctic land–ocean continuum in East Siberia: Insights from biomarkers and carbon isotopes. *Geochimica et Cosmochimica Acta* 133, 235-256.

Theuerkauf, M. et al. (2016) 'A matter of dispersal: REVEALSinR introduces state-of-the-art dispersal models to quantitative vegetation reconstruction', Vegetation History and *Archaeobotany*. Springer Berlin Heidelberg, 25(6), pp. 541–553.

Thornalley, D. J. R., Elderfield, H. and McCave, I. N. (2009) 'Holocene oscillations in temperature and salinity of the surface subpolar North Atlantic', *Nature*. Nature Publishing Group, 457(7230), pp. 711–714.

Thornton, S.F., and McManus, J., (1994), Application of Organic Carbon and Nitrogen Stable Isotope and C/N Ratios as Source Indicators of Organic Matter Provenance in Estuarine Systems: Evidence from the Tay Estuary, Scotland: Estuarine, *Coastal and Shelf Science*, v. 38, no. 3, p. 219–233.

Tipping R, Davies A, Reid E and Tisdall E. Late Quaternary landscape evolution of Glen Affric and Kintail. In: Tipping R (ed.). The Quaternary of Glen Affric and Kintail: Field Guide. Quaternary Research Association field guides, London: Quaternary Research Association, pp. 9-28, (2003).

Tipping, R. (2013) Towards an Environmental History of Argyll & Bute: A Review of Current Data, Their Strengths and Weaknesses and Suggestions for Future Work.

Tornabene, T. G., T. A. Langworthy, G. Holzer, and J. Oró. (1979). Squalenes, phytanes and other isoprenoids as major neutral lipids of methanogenic and thermoacidophilic "archaebacteria." *Journal of Molecular Evolution* 13: 73–83.

Trouet, V. et al. (2009) 'Persistent positive North Atlantic oscillation mode dominated the Medieval Climate Anomaly.', *Science*, 324(5923), pp. 78–80.

Ullman, R., Bilbao-bastida, V. and Grimsditch, G.(2012), Ocean & Coastal Management Including Blue Carbon in climate market mechanisms, Ocean Coast. Manag., 2–5,

Van Der Heijden, L. H. and Kamenos, N. A., (2015), Reviews and syntheses: Calculating the global contribution of coralline algae to total carbon burial, *Biogeosciences*, 12(21), 6429–6441.

Vanguelova, E. I., Nisbet, T. R., Moffat, A. J., Broadmeadow, S., Sanders, T. G. M. and Morison, J. I. L., (2013), A new evaluation of carbon stocks in British forest soils, *Soil Use Manag*., 29(2), 169–181.

Verardo, D. J., Froelich., P. . and McIntyre, A. (1990) 'Determination of organic carbon and nitrogen in marine sediments using the Carlo Erba NA-1500 analyzer', *Deep Sea Research Part A*. Oceanographic Research Papers, 37(1), pp. 157–165.

Viso, A.-C., D. Pesando, P. Bernard, and J.-C. Marty. (1993). Lipid components of the Mediterranean seagrass *Posidonia oceanica*. *Phytochemistry* 34: 381–387.

Volkman, J. K. (2005). Sterols and other triterpenoids: Source specificity and evolution of biosynthetic pathways. *Organic Geochemistry* 36: 139–159.

Volkman, J. K., and J. R. Maxwell. (1986). Acyclic isoprenoids as biological markers. Pp. 1–42 *in* R. B. Johns, ed., *Biological markers in the sedimentary record*, Elsevier, New York.

Volkman, J. K., S. M. Barrett, S. I. Blackburn, M. P. Mansour, E. L. Sikes, and F. Gelin. (1998). Microalgal biomarkers: A review of recent research developments. *Organic Geochemistry* 29: 1163–1179.

Vonk, J., Sánchez-García, L., van Dongen, B., Alling, V., Kosmach, D., Charkin, A., Semiletov, I., Dudarev, O., Shakhova, N., Roos, P., (2012). Activation of old carbon by erosion of coastal and subsea permafrost in Arctic Siberia. *Nature* 489, 137-140

Wakeham, S. G., A. P. McNichol, J. E. Kostka, and T. K. Pease. (2006). Natural-abundance radiocarbon as a tracer of assimilation of petroleum carbon by bacteria in salt marsh sediments. *Geochimica et Cosmochimica Acta* 70: 1761–1771.

Wakeham, S.G., Canuel, E.A., Lerberg, E.J., Mason, P., Sampere, T.P., Bianchi, T.S., (2009). Partitioning of organic matter in continental margin sediments among density fractions. *Marine Chemistry* 115, 211-225.

Wakeham, S.G., McNichol, A.P., (2014). Transfer of organic carbon through marine water columns to sediments–insights from stable and radiocarbon isotopes of lipid biomarkers. *Biogeosciences* 11, 6895-6914.

Wang, J., Yao, P., Bianchi, T. S., Li, D., Zhao, B., Cui, X., Pan, H., Zhang, T. and Yu, Z.,(2016), The effect of particle density on the sources , distribution , and degradation of sedimentary organic carbon in the Changjiang Estuary and adjacent shelf, *Chem. Geol*., 402, 52–67.

Wang, J., Yao, P., Bianchi, T.S., Li, D., Zhao, B., Cui, X., Pan, H., Zhang, T., Yu, Z., (2015). The effect of particle density on the sources, distribution, and degradation of sedimentary organic carbon in the Changjiang Estuary and adjacent shelf. *Chemical Geology* 402, 52- 67.

Wang, X., Cammeraat, E. L. H., Romeijn, P. and Kalbitz, K., (2014), Soil Organic Carbon Redistribution by Water Erosion – The Role of CO2 Emissions for the Carbon Budget, *PLoS ONE,* 9(5).

Wang, X., Li, A., (2007). Preservation of black carbon in the shelf sediments of the East China Sea.*Chinese Science Bulletin* 52, 3155-3161.

Wang, ZA, Kroeger, KD, Ganju, NK, Gonneea, ME and Chu, SN, (2016) 'Intertidal salt marshes as an important source of inorganic carbon to the coastal ocean', *Limnology and Oceanography*, 61(5), pp. 1916–1931. doi: 10.1002/lno.10347

Watanabe, K., and Kuwae, T., (2015), How organic carbon derived from multiple sources contributes to carbon sequestration processes in a shallow coastal system? *Global Change Biology*, v. 21, no. 7, p. 2612–2623.

Waterson, E.J., Canuel, E.A., (2008). Sources of sedimentary organic matter in the Mississippi River and adjacent Gulf of Mexico as revealed by lipid biomarker and δ13CTOC analyses. *Organic Geochemistry* 39, 422-439.

Waycott, M., Duarte, C. M., Carruthers, T. J. B., Orth, R. J., Dennison, W. C., Olyarnik, S., Calladine, A., Fourqurean, J. W., Heck, K. L., Hughes, A. R., Kendrick, G. a, Kenworthy, W. J., Short, F. T. and Williams, S. L.,(2009), Accelerating loss of seagrasses across the globe threatens coastal ecosystems, Proc. Natl. Acad. Sci.,106(30), 12377–81.

Webster, L., Fryer, R. J., Megginson, C., Dalgarno, E. J., Mcintosh, A. D., Moffat, C. F., Road, V. and Ab, U.K., (2004), The polycyclic aromatic hydrocarbon and geochemical biomarker composition of sediments from sea lochs on the west coast of Scotland, *J Environ Monit* , 219–228.

Weijers, J.W.H., S. Schouten, O. C. Spaargaren, and J.S.S. Damsté. (2006). Occurrence and distribution of tetraether membrane lipids in soils: Implications for the use of the TEX86 proxy and the bit index. Organic Geochemistry 37: 1680–1693.

Weltje, G. J. and Tjallingii, R. (2008) 'Calibration of XRF core scanners for quantitative geochemical logging of sediment cores: Theory and application', *Earth and Planetary Science Letters*, 274(3-4), pp. 423–438.

White, H.K., (2006) Isotopic constraints on the sources and associations of organic compounds in marine sediments. PhD Dissertation, Woods Hole Oceanographic Institution.

Williams, E.K., Rosenheim, B.E., Allison, M., McNichol, A.P., Xu, L., (2015). Quantification of refractory organic material in Amazon mudbanks of the French Guiana Coast. *Marine Geology* 363, 93-101.

Williams, J. W. et al. (2002) 'Rapid and widespread vegetation responses to past climate change in the North Atlantic region', *Geology,* 30(11), pp. 971–974.

Wilson, B. T., Woodall, C. W. and Griffith, D. M.(2013), Imputing forest carbon stock estimates from inventory plots to a nationally continuous coverage, *Carbon Balance and Management* , 1–15, 2013.

Wilson, L. J., Austin, W. E. N. and Jansen, E., (2001), The last British Ice Sheet : growth, maximum extent and deglaciation, *Polar Research*, 243–250.

Woulds, C., Bouillon, S., Cowie, G. L., Drake, E., Middelburg, J. J. and Witte, U., (2016), Patterns of carbon processing at the seafloor: The role of faunal and microbial communities in moderating carbon flows, *Biogeosciences*, 13(15), 4343–4357.

Woulds, C., Cowie, G. L., Levin, L. A., Andersson, J. H., Middelburg, J. J., Vandewiele, S., Lamont, P. A., Larkin, K. E., Gooday, A. J., Schumacher, S., Whitcraft, C. and Jeffreys, R. M., (2007), Oxygen as a control on seafloor biological communities and their roles in sedimentary carbon cycling, *Limnology and Oceanography*, 52(4), 1

Wu, Y., Eglinton, T., Yang, L., Deng, B., Montluçon, D., Zhang, J., (2013). Spatial variability in the abundance, composition, and age of organic matter in surficial sediments of the East China Sea. *Journal of Geophysical Research: Biogeosciences* 118, 1495-1507

Wylie, L., Sutton-grier, A. E. and Moore, A.(2016), Keys to successful blue carbon projects : Lessons learned from global case studies, *Marine Policy*, 65, 76–84.

Wylie, L., Sutton-grier, A. E. and Moore, A.(2016), Keys to successful blue carbon projects : Lessons learned from global case studies, Mar. Policy, 65, 76–84.

Yang, H., Rose, N. and Battarbee, R. (2001) 'Dating of recent catchment peats using spheroidal carbonaceous particle (SCP) concentration profiles with particular reference to Lochnagar, Scotland', *The Holocene*, 11(5).

Yao, P., Yu, Z., Bianchi, T.S., Guo, Z., Zhao, M., Knappy, C.S., Keely, B.J., Zhao, B., Zhang, T., Pan, H., (2015). A multiproxy analysis of sedimentary organic carbon in the Changjiang Estuary and adjacent shelf. *Journal of Geophysical Research: Biogeosciences* 120, 1407- 1429.

Yano, Y., A. Nakayama, and K. Yoshida. (1997). Distribution of polyunsaturated fatty acids in bacteria present in intestines of deep-sea fish and shallow-sea poikilothermic animals. Applied and Environmental Microbiology 63: 2572–2577

Yu, Z, Loisel, J., Brosseau, D.P., Beilman, D.W., & Hunt, S.J., (2010), Global peatland dynamics since the Last Glacial Maximum. *Geophysical Research Letters,* 37.

Yunker, M.B., Belicka, L.L., Harvey, H.R., Macdonald, R.W., (2005). Tracing the inputs and fate of marine and terrigenous organic matter in Arctic Ocean sediments: A multivariate analysis of lipid biomarkers. *Deep Sea Research Part II: Topical Studies in Oceanography* 52, 3478-3508.

Zillén, L. and Conley, D. J. (2010) 'Hypoxia and cyanobacteria blooms - Are they really natural features of the late Holocene history of the Baltic Sea?', *Biogeosciences,* 7(8), pp. 2567–2580.

Zimmerman, A., Canuel, E., (2001). Bulk organic matter and lipid biomarker composition of Chesapeake Bay surficial sediments as indicators of environmental processes. Estuarine, *Coastal and Shelf Science* 53, 319-341.

Rogge, W. F., P. M. Medeiros, and B.R.T. Simoneit. (2007). Organic marker compounds in surface soils of crop fields from the San Joaquin Valley fugitive dust characterization study. Atmospheric Environment 41: 8183–8204.

Appendix A

Chapter 2 – Material and Methods

Supplementary Material

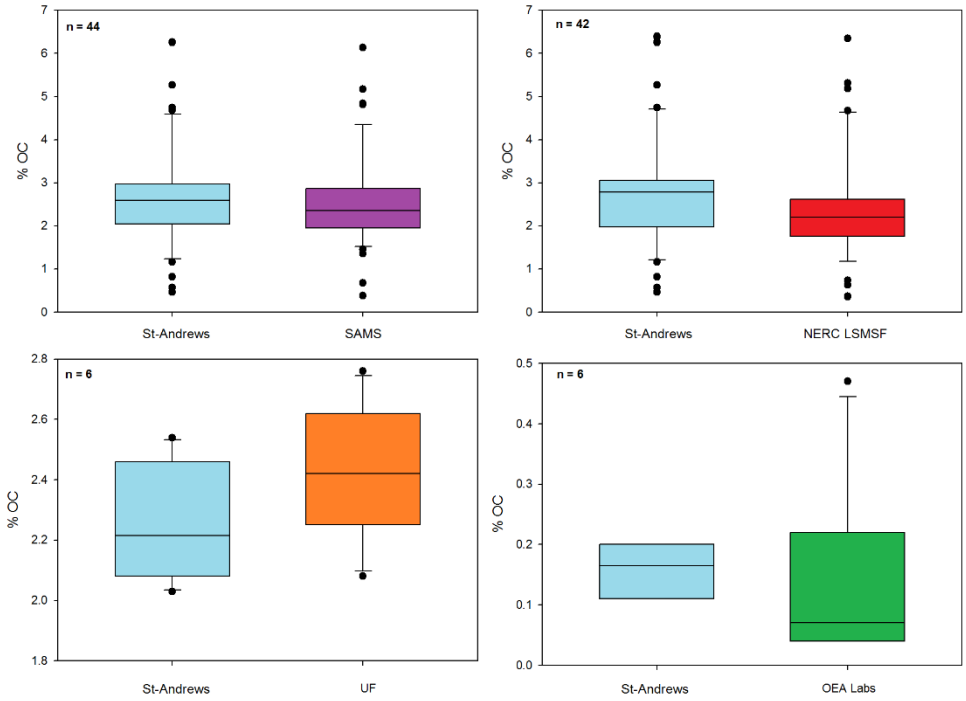

Figure A.1 Inter-laboratory comparison of OC content in marine sediment samples

Analysis of variance (SAMS):

Source	DF	Sum of squares	Mean squares	F	Pr > F
Model	1	50.500	50.500	360.549	**< 0.0001**
Error	42	5.883	0.140		
Corrected Total	43	56.383			

Computed against model Y=Mean(Y)

Analysis of variance (NERC LSMSF):

Source	DF	Sum of squares	Mean squares	F	Pr > F
Model	1	62.945	62.945	244.929	**< 0.0001**
Error	39	10.023	0.257		
Corrected Total	40	72.968			

Computed against model Y=Mean(Y)

Analysis of variance (UF):

Source	DF	Sum of squares	Mean squares	F	Pr > F
Model	1	0.273	0.273	21.119	**0.010**
Error	4	0.052	0.013		
Corrected Total	5	0.324			

Computed against model Y=Mean(Y)

Analysis of variance (OEA Labs):

Source	DF	Sum of squares	Mean squares	F	Pr > F
Model	1	0.005	0.005	7.275	0.054
Error	4	0.003	0.001		
Corrected Total	5	0.008			

Computed against model Y=Mean(Y)

Table A.1 Statistical comparison (ANOVA) of the variance between organic carbon (OC) measurements of marine sediment samples made at St-Andrews to the other labs.

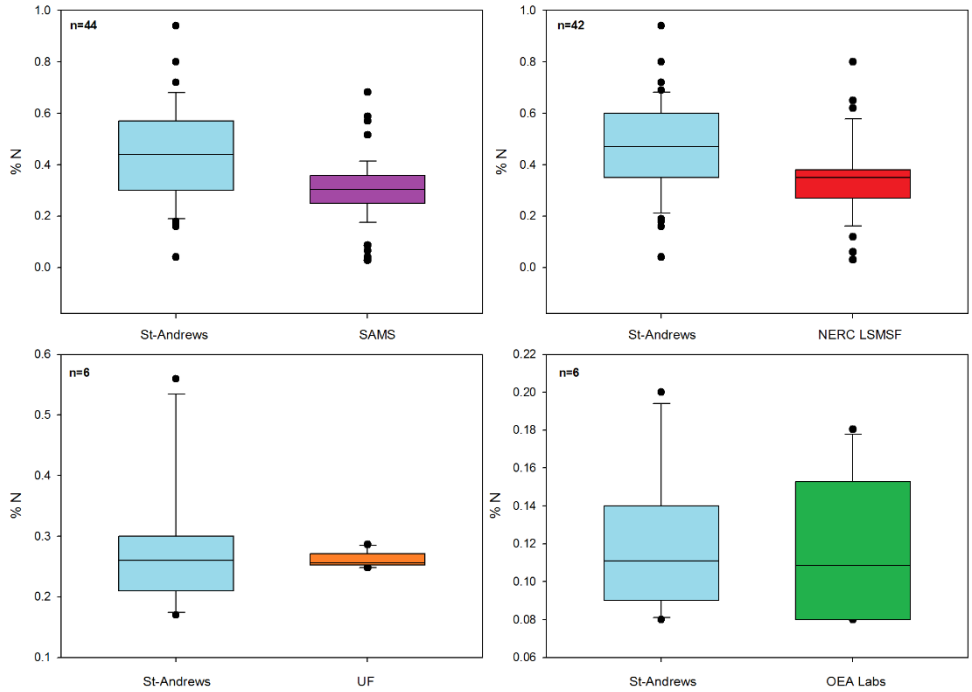

Figure A.2 Inter-laboratory comparison of N content in marine sediment samples.

Analysis of variance (SAMS):

Source	DF	Sum of squares	Mean squares	F	Pr > F
Model	1	0.351	0.351	39.719	**< 0.0001**
Error	42	0.371	0.009		
Corrected Total	43	0.722			

Computed against model Y=Mean(Y)

Analysis of variance (NERC LSMSF):

Source	DF	Sum of squares	Mean squares	F	Pr > F
Model	1	0.533	0.533	53.601	**< 0.0001**
Error	40	0.398	0.010		
Corrected Total	41	0.930			

Computed against model Y=Mean(Y)

Analysis of variance (UF):

Source	DF	Sum of squares	Mean squares	F	Pr > F
Model	1	0.000	0.000	1.260	0.324
Error	4	0.001	0.000		
Corrected Total	5	0.001			

Computed against model Y=Mean(Y)

Analysis of variance (OEA Labs):

Source	DF	Sum of squares	Mean squares	F	Pr > F
Model	1	0.098	0.098	184.216	**0.000**
Error	4	0.002	0.001		
Corrected Total	5	0.101			

Computed against model Y=Mean(Y)

Table A.2 Statistical comparison (ANOVA) of the variance between nitrogen (N) measurements of marine sediment samples made at St-Andrews to the other labs.

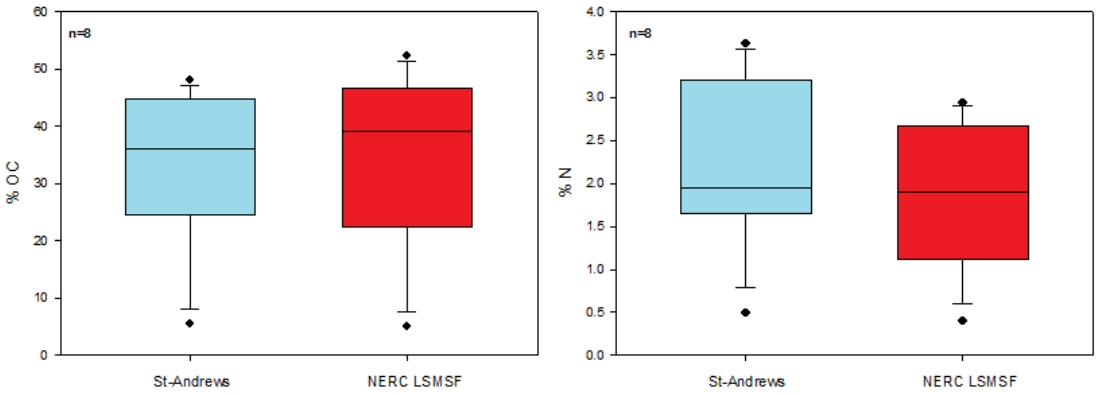

Figure A.3 Inter-laboratory comparison of OC and N content in terrestrial samples.

Analysis of variance (NERC LSMSF):

Source	DF	Sum of squares	Mean squares	F	Pr > F
Model	1	1925.034	1925.034	211.320	**< 0.0001**
Error	6	54.658	9.110		
Corrected Total	7	1979.691			

Computed against model Y=Mean(Y)

Analysis of variance (NERC LSMSF):

Source	DF	Sum of squares	Mean squares	F	Pr > F
Model	1	5.438	5.438	106.946	**< 0.0001**
Error	6	0.305	0.051		
Corrected Total	7	5.743			

Computed against model Y=Mean(Y)

Table A.3 Statistical comparison (ANOVA) of the variance between organic carbon (OC) and nitrogen (N) measurements of terrestrial samples made at St-Andrews to the other labs.

Appendix B

Chapter 3 - A Sedimentary Carbon Inventory for a Scottish Fjord: An Integrated Geochemical and Geophysical Approach

Supplementary Material

(Core Logs)

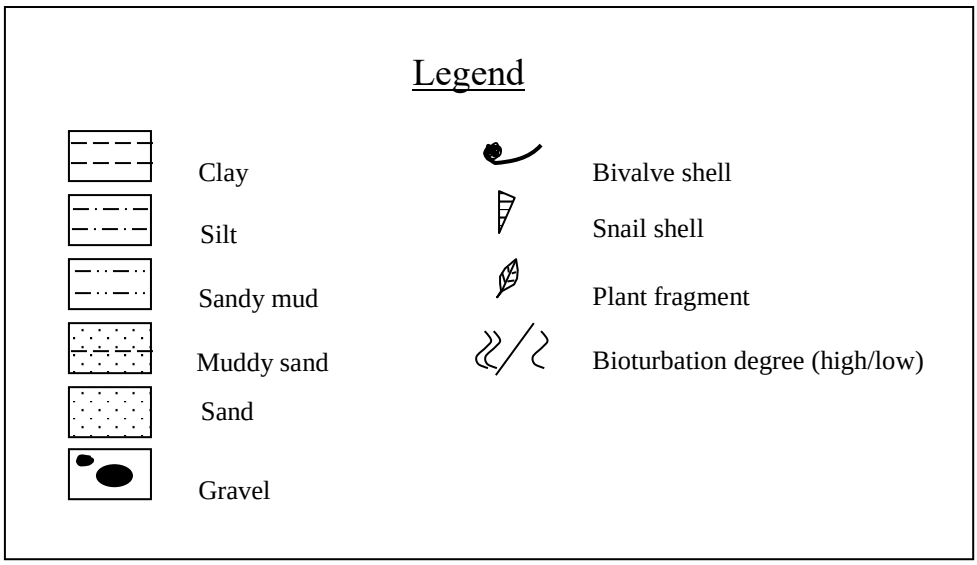
Legend
Clay
Silt
Sandy mud
Muddy sand
Sand
Gravel
Bivalve shell
Snail shell
Plant fragment
Bioturbation degree (high/low)

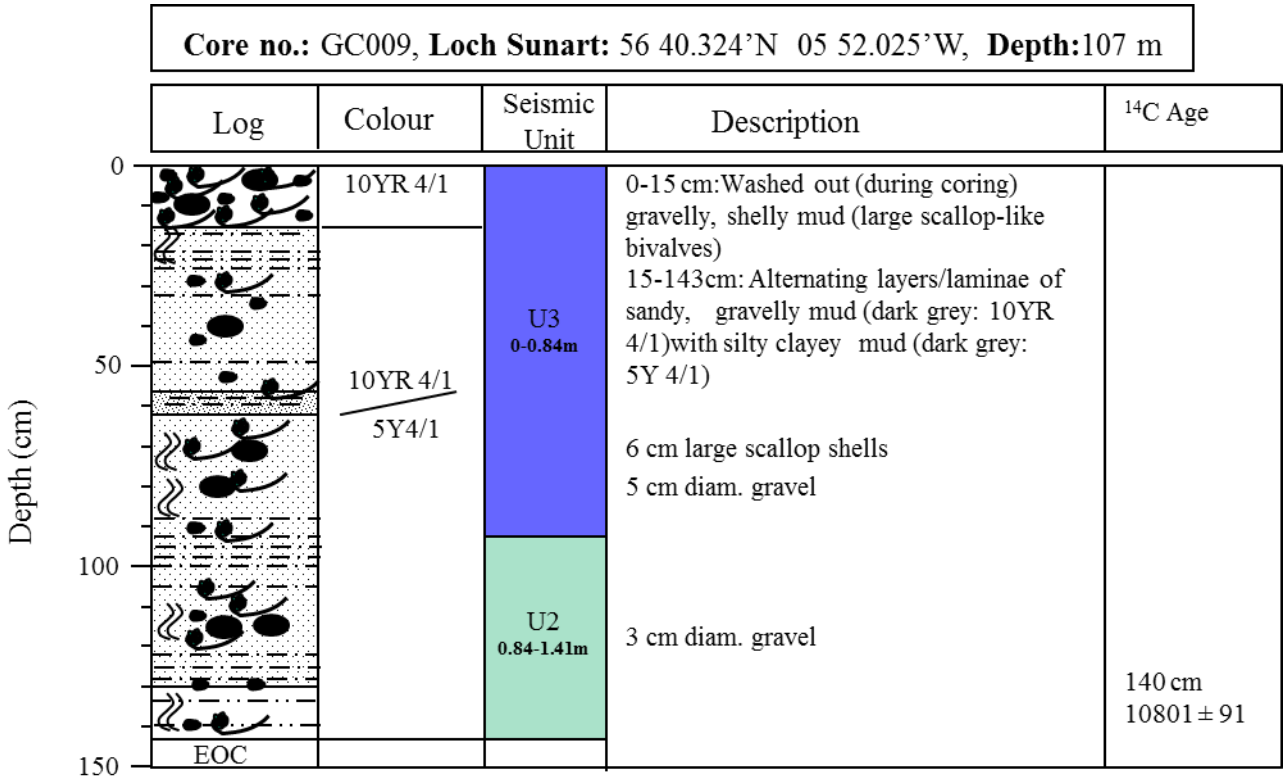
Core no.: GC009, Loch Sunart: 56 40.324'N 05 52.025'W, Depth:107 m
Log
Colour
Seismic Unit
Description
14C Age
Depth (cm)
0
50
100
150
EOC
10YR 4/1
10YR 4/1
5Y4/1
U3
0-0.84m
U2
0.84-1.41m
0-15 cm:Washed out (during coring) gravelly, shelly mud (large scallop-like bivalves)
15-143cm: Alternating layers/laminae of sandy, gravelly mud (dark grey: 10YR 4/1)with silty clayey mud (dark grey: 5Y 4/1)
6 cm large scallop shells
5 cm diam. gravel
3 cm diam. gravel
140 cm
10801 ± 91

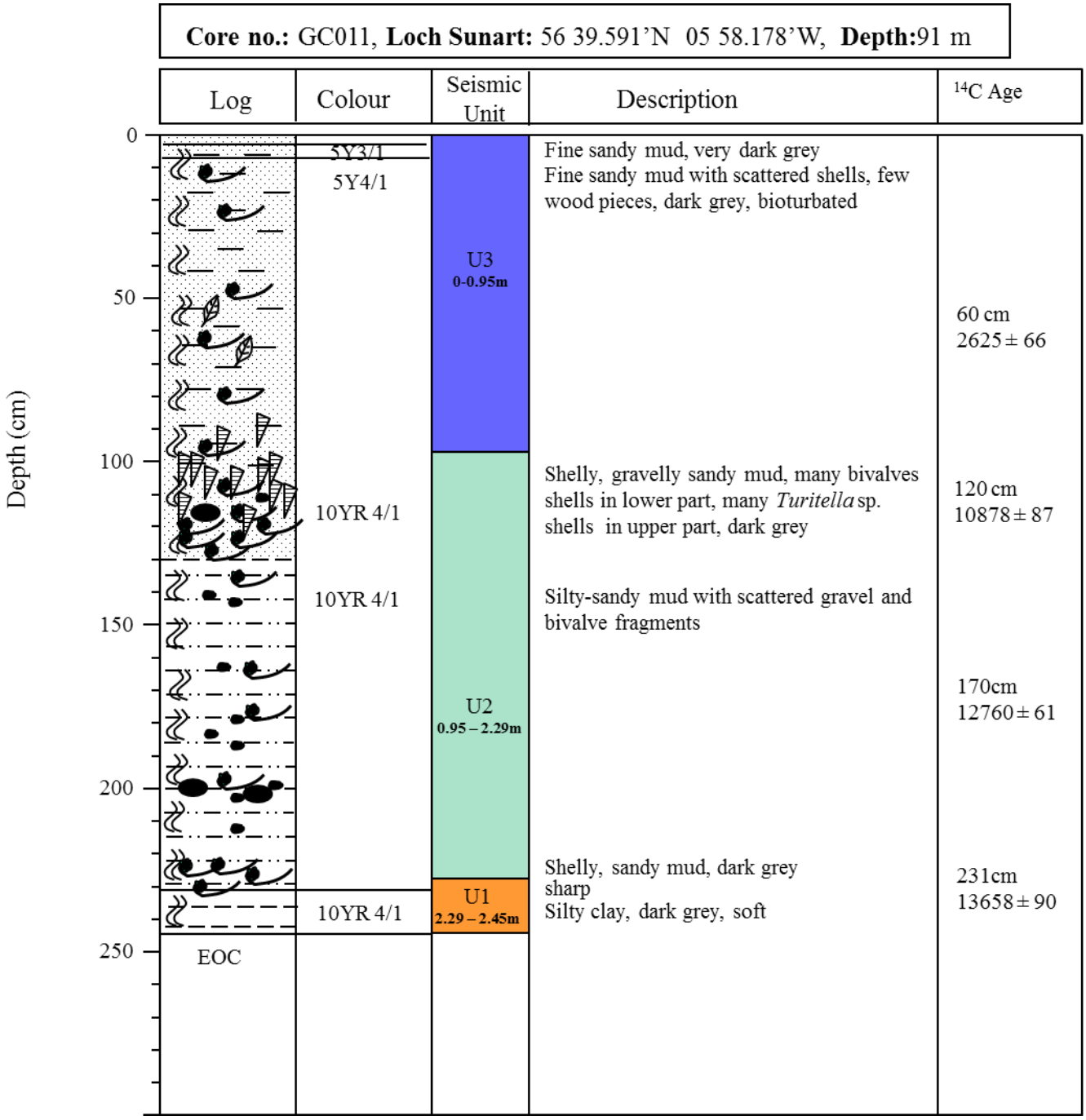
Core no.: GC011, Loch Sunart: 56 39.591'N 05 58.178'W, Depth:91 m
Log
Colour
Seismic Unit
Description
14C Age
Depth (cm)
0
50
100
150
200
250
5Y3/1
5Y4/1
10YR 4/1
10YR 4/1
10YR 4/1
EOC
U3
0-0.95m
U2
0.95 – 2.29m
U1
2.29 – 2.45m
Fine sandy mud, very dark grey
Fine sandy mud with scattered shells, few wood pieces, dark grey, bioturbated
Shelly, gravelly sandy mud, many bivalves shells in lower part, many Turitella sp. shells in upper part, dark grey
Silty-sandy mud with scattered gravel and bivalve fragments
Shelly, sandy mud, dark grey
sharp
Silty clay, dark grey, soft
60 cm
2625 ± 66
120 cm
10878 ± 87
170cm
12760 ± 61
231cm
13658 ± 90

Core no.:GC013, **Loch Sunart:** 56 40.879'N 05 37.771'W, **Depth:**87 m

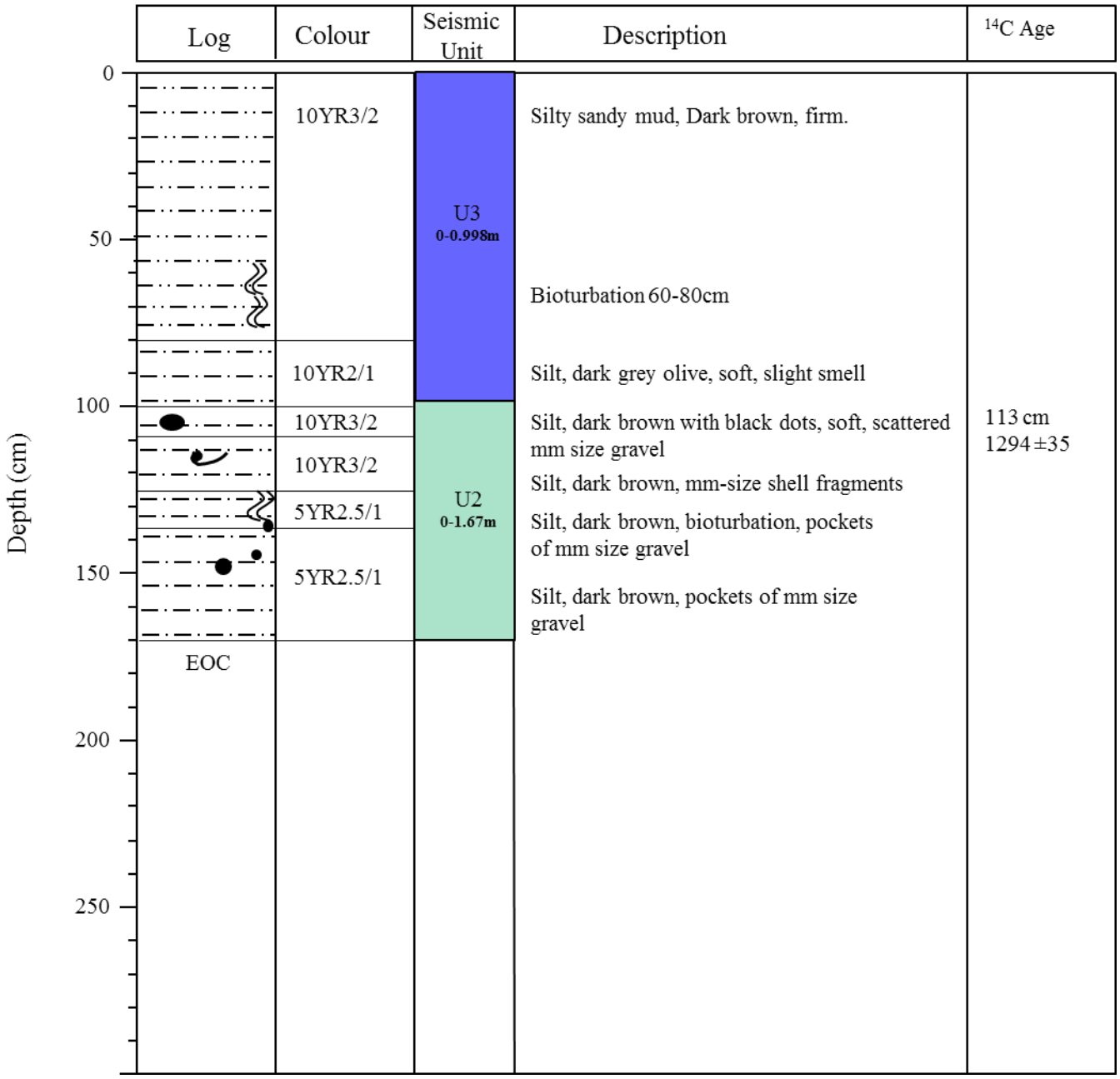

Core no.: GC023, **Loch Sunart:** 56 40.324'N 05 50.328'W, **Depth:**110m

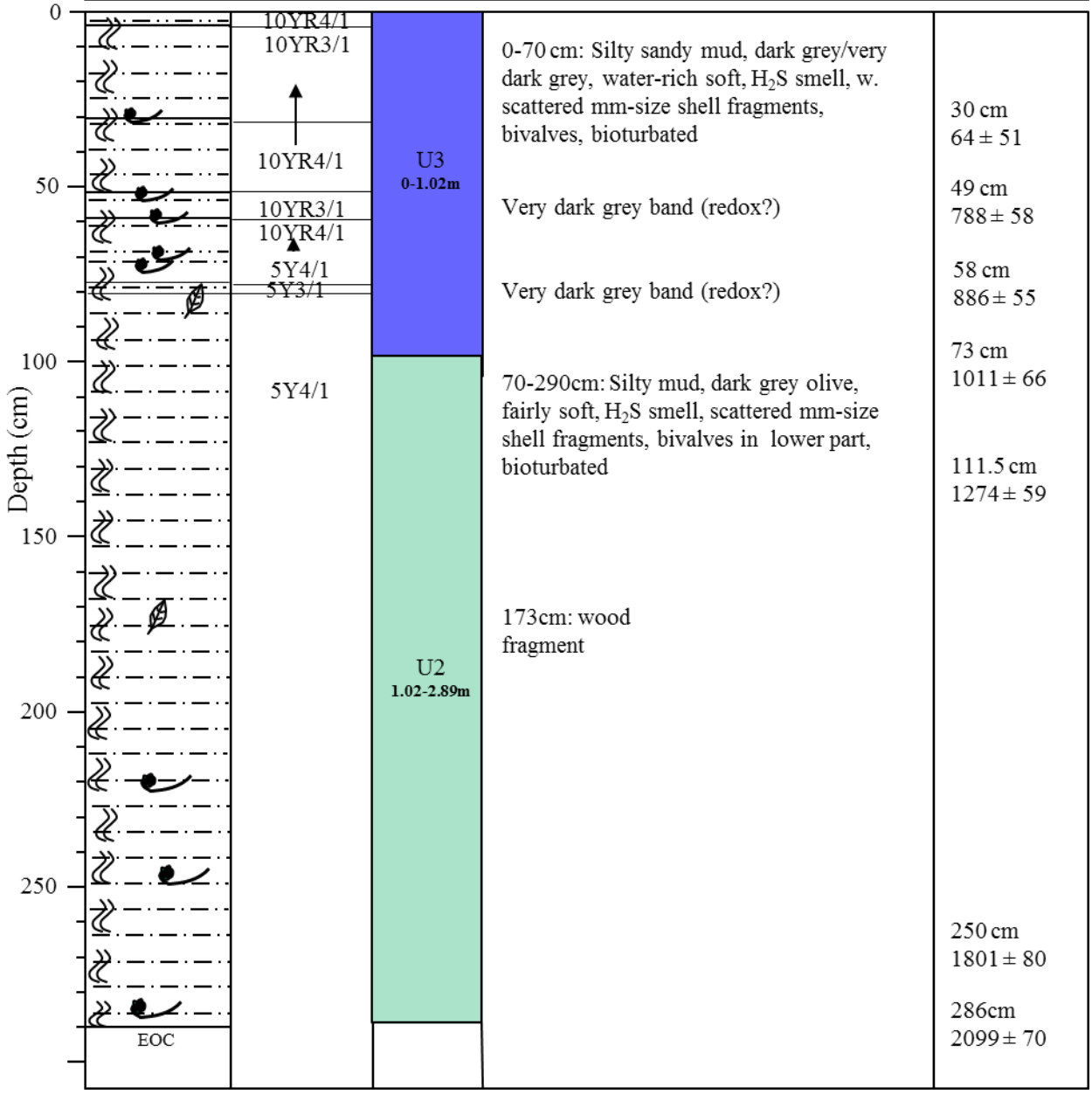

Core no.: GC081, **Loch Sunart:** 56 40 139' N 05 51 797' W, **Depth:** 58 m

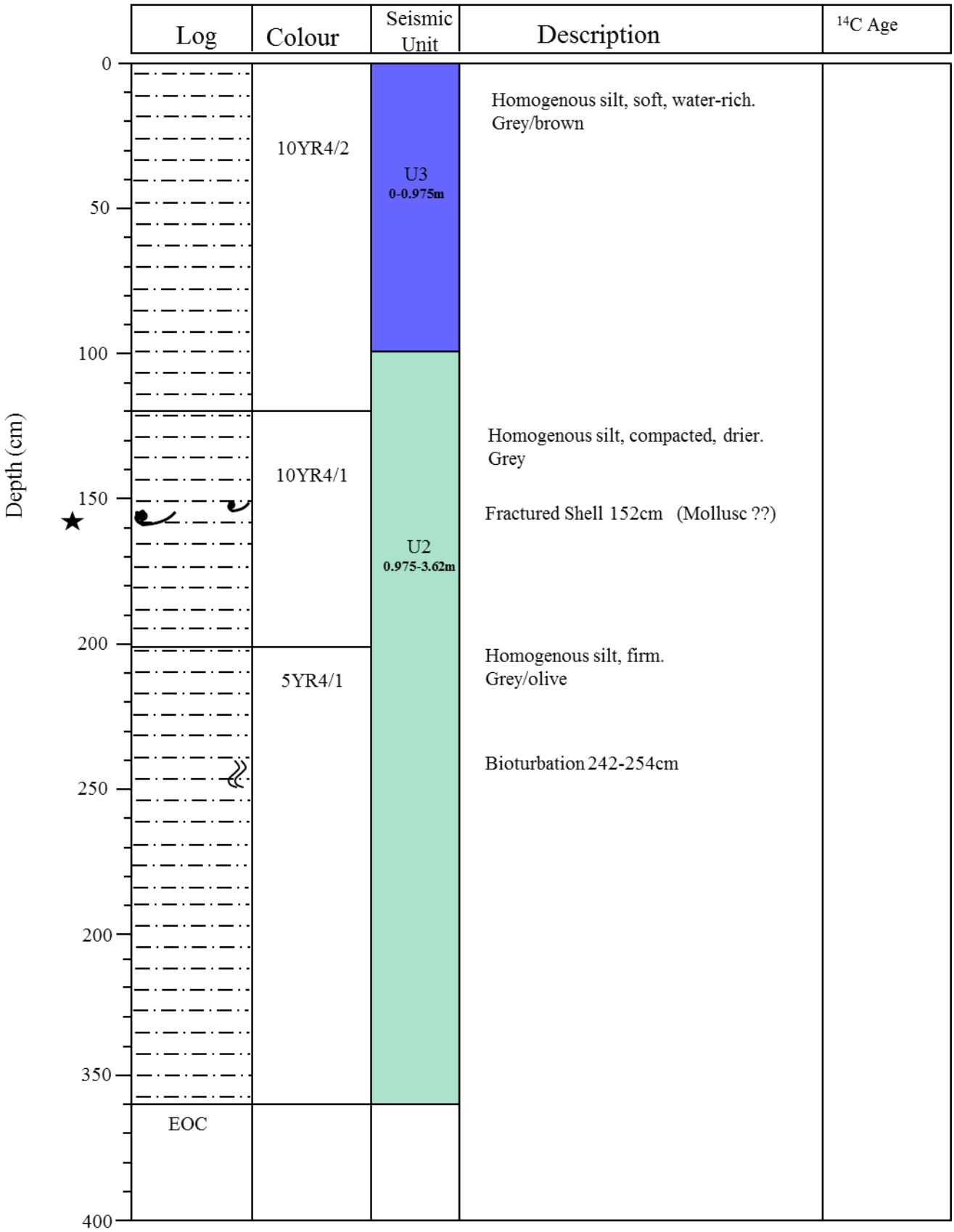

Core no.: GC-01, **Loch Sunart:** 56° 41.809'N 5° 42.299'W, **Depth:**42 m

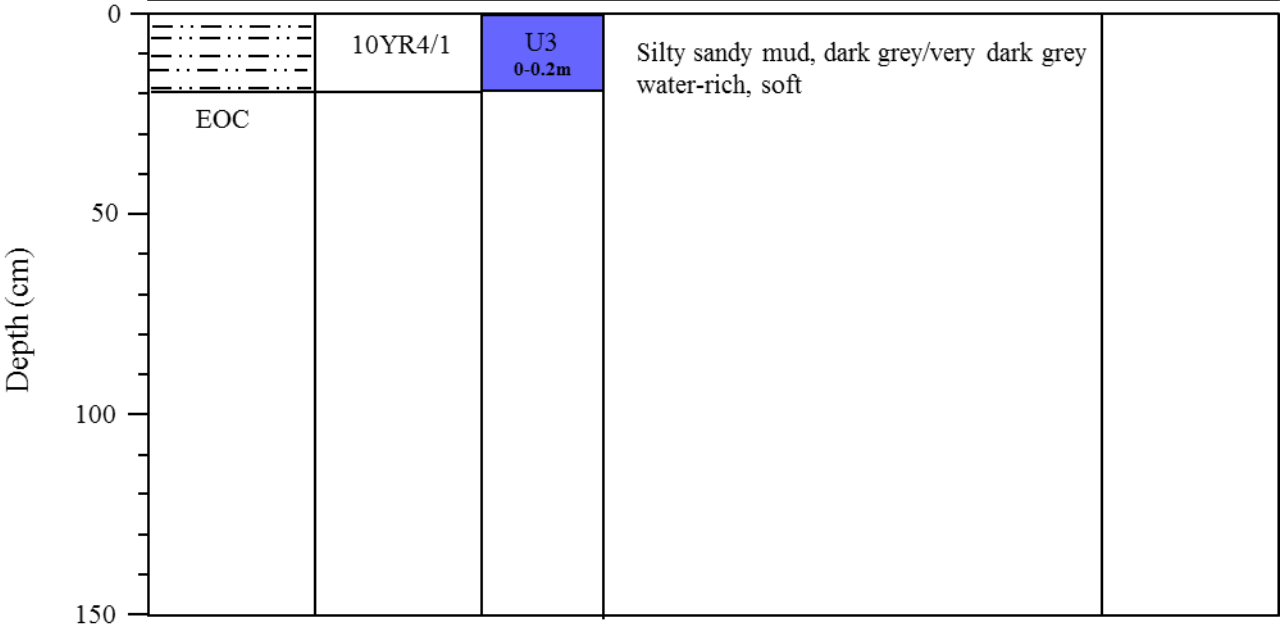

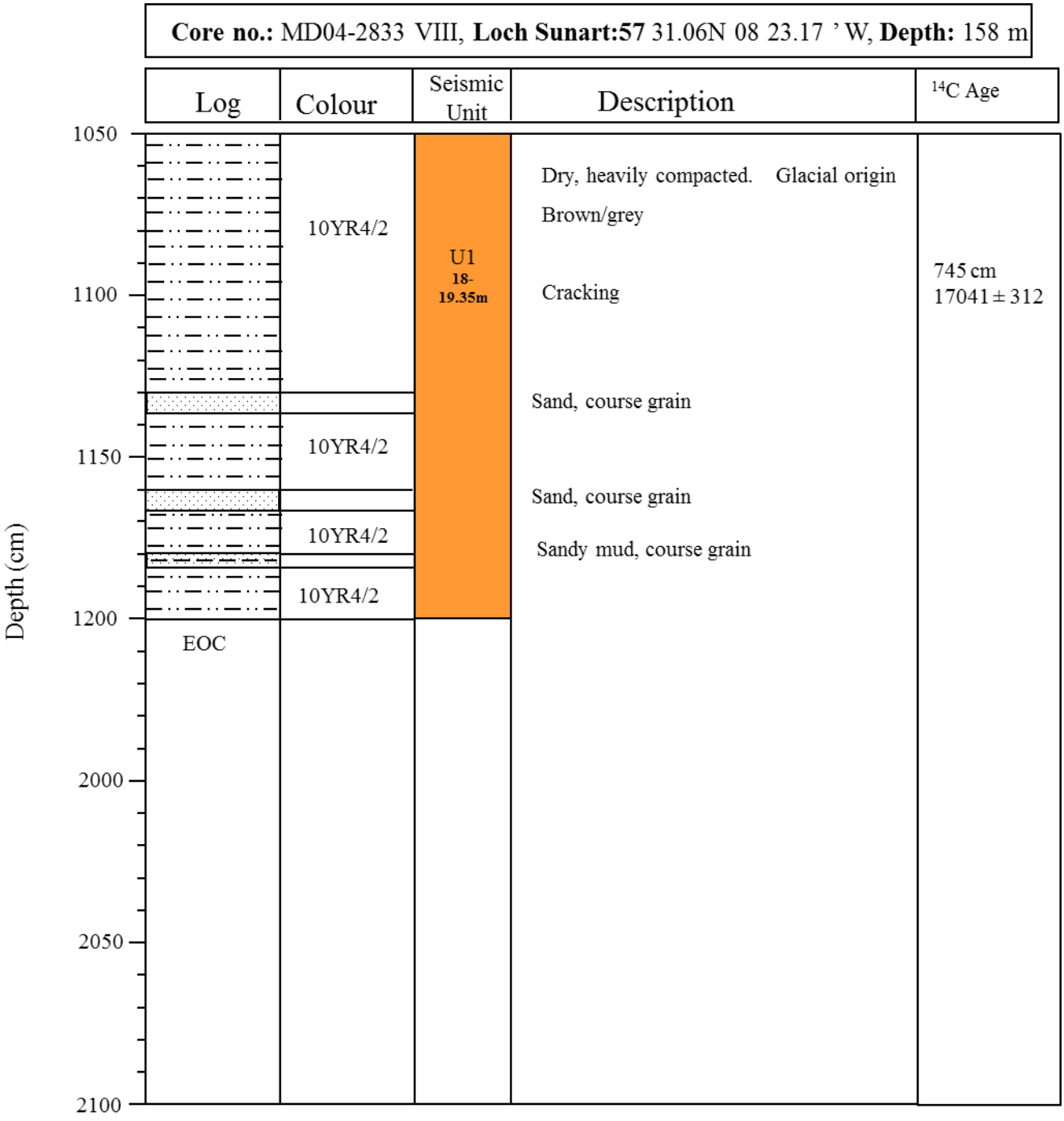
Core no.: MD04-2833 VIII, Loch Sunart:57 31.06N 08 23.17 ' W, Depth: 158 m
Log
Colour
Seismic Unit
Description
14C Age
Depth (cm)
1050
1100
1150
1200
2000
2050
2100
10YR4/2
10YR4/2
10YR4/2
10YR4/2
U1
18-
19.35m
Dry, heavily compacted. Glacial origin
Brown/grey
Cracking
Sand, course grain
Sand, course grain
Sandy mud, course grain
745 cm
17041 ± 312
EOC

Appendix C

Chapter 4 - Source to Sink: Tracing the Origin of Organic Carbon in a Mid-Latitude Fjord

Supplementary Material

Sample ID	Loch	Latitude (Decimal degrees)	Longitude (Decimal degrees)	Depth (m)
LS 1	Sunart	56.6867	-5.6683	18
LS 2	Sunart	56.6849	-5.6833	12
LS 3	Sunart	56.6851	-5.5464	2.0
LS 4	Sunart	56.6854	-5.5466	
LS 5	Sunart	56.6850	-5.5463	
LS 6	Sunart	56.6848	-5.5811	25.7
LS 7	Sunart	56.6877	-5.5806	6
LS 8	Sunart	56.6873	-5.5835	14
LS 9	Sunart	56.6853	-5.6129	42
LS 10	Sunart	56.6842	-5.6216	58.5
LS 11	Sunart	56.6846	-5.6202	55.8
LS 12	Sunart	56.6791	-5.6114	16.7
LS 13	Sunart	56.6783	-5.6109	16.3
LS 14	Sunart	56.6807	-5.6120	24
LS 15	Sunart	56.6821	-5.6128	42.6
LS 16	Sunart	56.6776	-5.6283	26.6
LS 17	Sunart	56.6771	-5.6281	2.5
LS 18	Sunart	56.6787	-5.6287	43.5
LS 19	Sunart	56.6822	-5.6748	10.1
LS 20	Sunart	56.6824	-5.6775	10
LS 22	Sunart	56.6855	-5.6750	15
LS 24	Sunart	56.6843	-5.6840	11.6
LS 25	Sunart	56.6848	-5.6836	
LS 26	Sunart	56.6854	-5.7015	39.2
LS 27	Sunart	56.6891	-5.6894	23.5
LS 28	Sunart	56.6924	-5.6998	14.1
LS 29	Sunart	56.6972	-5.7047	34.4
LS 30	Sunart	56.6990	-5.7126	70
LS 34	Sunart	56.7020	-5.7261	31.2
LS 35	Sunart	56.0000	-5.0000	10
LS 37	Sunart	56.7050	-5.7372	46.1
LS 38	Sunart	56.7055	-5.7496	98.6
LS 39	Sunart	56.6960	-5.7066	36.0
LS 40	Sunart	56.6710	-5.8552	28.5
LS 42	Sunart	56.6824	-5.9885	21.4
LS 43	Sunart	56.6804	-6.0117	36.1
LS 47	Sunart	56.6540	-5.9419	6.5
LS 48	Sunart	56.6569	-5.9150	3.4
LS 49	Sunart	56.6563	-5.9249	17.2
LS 53	Sunart	56.6756	-5.9157	18
LS 62	Sunart	56.6833	-5.8128	54.7
LS 63	Sunart	56.6829	-5.8096	68
LS 65	Sunart	56.6764	-5.8070	40.3
LS 66	Sunart	56.6871	-5.7847	38.9
LS 72	Sunart	56.6988	-5.7753	70
LS 73	Sunart	56.6825	-5.6338	92.6
LS 80	Sunart	56.6963	-5.7649	46
LS 82	Sunart	56.7070	-5.7725	25.5
LS 90	Sunart	56.6740	-5.8130	59.0
LS 91	Sunart	56.6669	-5.8296	18

LS 92	Sunart	56.6651	-5.8338	
LS 93	Sunart	56.6619	-5.8403	
LS 94	Sunart	56.6683	-5.8500	
LS 95	Sunart	56.6716	-5.8541	
LS 96	Sunart	56.6573	-5.9855	74.0
LS 97	Sunart	56.6532	-5.9756	74.0
LS 98	Sunart	56.6562	-5.9657	78.0
LS 99	Sunart	56.6600	-5.9715	65.0
LS 100	Sunart	56.6663	-5.9695	47.0
LS 101	Sunart	56.6660	-5.9593	70.0
LS 103	Sunart	56.6753	-5.9366	14.0
LS 104	Sunart	56.6728	-5.9228	16.0
LS 105	Sunart	56.6665	-5.9096	8.0
LS 106	Sunart	56.6673	-5.8944	6.0
LS 107	Sunart	56.6739	-5.8774	6.0
LS 108	Sunart	56.6993	-5.7730	8.2
LS 109	Sunart	56.6755	-5.8202	
LS 110	Sunart	56.7023	-5.7571	
LS 111	Sunart	56.7082	-5.7347	
LS 112	Sunart	56.7027	-5.7185	
LT1	Teacuis	56.6331	-5.8437	14.0
LT2	Teacuis	56.6311	-5.8401	16.0
LT3	Teacuis	56.6274	-5.8336	8.0
LT4	Teacuis	56.6258	-5.8311	6.0
LT5	Teacuis	56.6258	-5.8318	6.0
LT6	Teacuis	56.6283	-5.8343	8.2
LT7	Teacuis	56.6298	-5.8366	8.0
LT8	Teacuis	56.6311	-5.8386	11.1
LT9	Teacuis	56.6325	-5.8414	12.4
LT10	Teacuis	56.6324	-5.8470	19.1
LT11	Teacuis	56.6334	-5.8501	20.8
LT 22	Teacuis	56.6435	-5.8907	8.7
LT 23	Teacuis	56.6442	-5.8865	16.0
LT 24	Teacuis	56.6473	-5.8820	21.8
LT 25	Teacuis	56.6433	-5.8813	11.3
LS 67 LT	Teacuis /Sunart	56.6278	-5.8348	6.6
LS 70 LT	Teacuis/Sunart	56.6474	-5.8831	25.6
LS 71 LT	Teacuis /Sunart	56.6477	-5.8874	12

Table C.1 Detailed information on the location and depth at which each of the grab samples were taken.

Catchment Soil Erosion Estimations

Average Soil Erosion C Loss through Fluvial Erosion Calculation

Catchment Soil Loss (t yr^{-1}) = Average Soil Erosion Rate (t km^{-2} yr^{-1}) x Catchment Area (km^2)

Catchment C loss (t yr^{-1}) = Catchment soil loss (t yr^{-1}) x Carbon concentration (%)

Site Specific Soil C Loss through Fluvial Erosion Calculation

Land Cover Soil Loss (t yr^{-1}) **=** Land Cover Specific Soil Erosion Rate (t km^{-2} yr^{-1}) x Land Cover Area (km^2)

Land Cover C Loss (t yr^{-1}) = Land Cover Soil Loss (t yr^{-1}) x Land cover Carbon Concentration (%)

Catchment C Loss = Land Cover C Loss 1 + Land Cover C Loss 2 +…….

Data

Catchment Area: 299 km^2

Average Soil Erosion: 269 t km^{-2} yr^{-1} [*Panagos et al.* 2015]

Land Cover	Soil Erosion Rate ($t\ km^{-2}\ yr^{-1}$)	Reference
Woodland		
Woodland	7	*Panagos et al.* [2015]
Disturbed Forest	10	*Borrelli et al.* [2016]
Disturbed Forest	6	*Borrelli et al.* [2016]
Undisturbed Forest	5.4	*Borrelli et al.* [2016]
Undisturbed Forest	4	*Borrelli et al.* [2016]
Upland Heath		
No Management (Average)	200	*Grieve et al.* [1994]
Forested	1300	*Grieve et al.* [1994]
Sheep Grazing	3400	*Grieve et al.* [1994]
Burning (Low)	600	*Grieve et al.* [1994]
Burning (High)	2600	*Grieve et al.* [1994]
Improved Grassland		
Improved Grassland	269	*Panagos et al.* [2015]
Pasture	202	*Panagos et al.* [2015]
Grassland		
Grassland	235.50	*Panagos et al.* [2015]
Pasture	202	*Panagos et al.* [2015]
Ley Grassland	114	*Knox et al.* [2015]
Bog		
North Esk	25	*Ledger et al.* [1974]
Hopes Reserviour	26	*Ledger et al.* [1974]
Glenfarg	26	*McManus and Duck.* [1985]
Glenfarg	31	*McManus and Duck*. [1985]
Earlburn	68	*Duck and McManus.* [1990]
North Third Reservoir	205	*Duck and McManus.* [1990]
Carron Valley	142	*Duck and McManus.* [1990]

Table C.3 Land cover specific soil erosion rates from the literature.

Land Cover	Proportion of Catchment (%)	Area (km^2)	Minimum C (%)	Maximum C (%)
Woodland	25.13	75.14	13.18	31.03
Upland Heath	18.2	54.42	3.37	5.05
Improved Grassland	4.54	13.57	5.05	17.35
Grassland	44.59	133.32	5.05	17.35
Bog	7.54	22.54	28.51	44.22
Arable	0	0.00	-	-

Table C.4 Catchment land cover [*Morton et al.* 2011] with associated carbon concentrations.

Method	Minimum (tonnes yr^{-1})	Mean (tonnes yr^{-1})	Maximum (tonnes yr^{-1})
Average C Loss	2710.52	19139.56	35566.60
Site Specific C Loss		7534.68 ± 2249	

Table C.5 Calculated quantities of C lost from the catchment.

Fluvial Export Calculations

Calculation (Based on *Loh et al.* [2010])

Fluvial Soil Export (g d^{-1}) = River Discharge (m^3 d^{-1}) x Particle concentration (g m^{-3}) (1)

Fluvial C loss (g d^{-1}) = Fluvial Soil Export (g d^{-1}) x Carbon concertation (%) (2)

Annual C Loss (g) = Fluvial C loss (g d^{-1}) x 365 (3)

Annual C Loss (tonnes) = Annual C Loss (g) x 1000000 (4)

Data

River Discharge: 1434240 m^3 d^{-1} [*Payne et al.* 1989]

Particle Concentration: 113.76 g m^{-3} [*Loh et al.* 2010]

OC (Mean): 23.80 %

OC (Min): 3.37 %

OC (Max): 44.22 %

Results

	Fluvial C Loss (tonnes yr^{-1})
Minimum	2006.94
Mean	14170.70
Maximum	26334.40

Table C.6. Annual catchment OC loss through fluvial export.

Appendix D

Chapter 5 - A National Assessment of Mid-Latitude Fjord Sedimentary C Stocks

Supplementary Material

Fjord	ID	%TC	%OC	%IC	Location (Lat & long)
Gare Loch	GS 412	5.62	5.26	0.36	56.07633, -4.83017
Gare Loch	GS 414	4.38	3.83	0.55	56.0215, -4.79067
Loch Striven	GS 454	4.15	3.66	0.49	56.00417, -5.12333
Loch Striven	GS 456	3.91	2.31	1.60	55.96017, -5.08667
Loch Striven	GS 458	4.83	3.61	1.22	55.92067, -5.06217
Loch Riddon	GS 465	3.32	2.70	0.62	55.9535, -5.18933
Loch Portree	M 135	7.63	2.14	5.49	57.40967, -6.16117
Loch Long	GS 396	4.85	4.48	0.37	56.2015, -4.74567
Loch Long	GS 398	3.11	2.73	0.38	56.16433, -4.78917
Loch Long	GS 401	0.66	0.34	0.32	56.1025, -4.84883
Loch Goil	GS 402	7.10	4.54	2.56	56.16583, -4.90567
Loch Goil	GS 404	4.18	4.13	0.05	56.12267, -4.89483
Loch Fyne	GS 507	6.42	5.76	0.66	56.2655, -4.9305
Loch Fyne	GS 510	2.58	2.48	0.10	56.24166, -5.05233
Loch Fyne	GS 512	6.18	3.64	2.54	56.19017, -5.08733
Loch Fyne	GS 519	1.41	0.67	0.74	56.08083, -5.26933
Loch Fynne	GS 524	1.05	0.21	0.84	55.98833, -5.355
Loch Linnhe	56/06/134	0.23	0.14	0.09	56.685, -5.29333
Dale Voe	60-02/109	10.50	3.15	7.35	60.20667, -1.161767
Clift Sound	MD15-01	8.99	8.00	0.99	60.11943, -1.27727
Clift Sound	MD15-02	9.87	2.80	7.07	60.09987, -1.28453
Clift Sound	MD15-03	10.99	3.48	7.51	60.07995, -1.2975
Clift Sound	MD15-04	8.3	3.58	4.72	60.06635, -1.30778
Clift Sound	MD15-05	11.73	6.62	5.11	60.04765, -1.31588
Sand Sound	MD15-06	5.83	3.39	2.44	60.24485, -1.40295
Sand Sound	MD15-07	5.04	4.51	0.53	60.24477, -1.40418
Sand Sound	MD15-08	9.95	8.28	1.67	60.24477, -1.37952
Sand Sound	MD15-09	4.31	3.78	0.53	60.24178, -1.35835
Sand Sound	MD15-10	10.37	4.80	5.57	60.22822, -1.37052
Olna Firth	MD15-11	10.56	8.51	3.02	60.36277, -1.29588
Olna Firth	MD15-12	10.66	7.54	2.15	60.36425, -1.32315
Aith Voe	MD15-13	10.14	5.44	4.70	60.28945, -1.37488
Aith Voe	MD15-14	4.83	4.48	0.35	60.3055, -1.374
Busta Voe	MD15-15	40.71	38.38	2.33	60.39075, -1.36122
Busta Voe	MD15-16	33.96	7.68	26.28	60.38063, -1.35888
Busta Voe	MD15-17	24.15	3.76	20.39	60.3694, -1.37052
Vaila Sound	MD15-18	8.49	4.79	3.70	60.21943, -1.56408
Vaila Sound	MD15-19	7.42	3.51	3.91	60.213, -1.5624
Vaila Sound	MD15-20	8.14	4.07	4.07	60.21428, -1.58217
Vaila Sound	MD15-21	8.41	2.89	5.52	60.20567, -1.56747
Loch Ewe	GC009	7.20	0.48	6.72	57.90651, -5.687034
Loch Ewe	GS 1	3.59	2.34	1.25	57.84771, -5.626583
Loch Ewe	GS 2	5.49	2.26	3.23	57.84733, -5.628317
Loch Ewe	GS 3	5.53	2.91	2.62	57.84826, -5.625000
Loch Ewe	GS 4	5.28	2.09	3.19	57.84573, -5.646567
Loch Ewe	GS 5	2.64	1.55	1.09	57.83378, -5.651133
Loch Ewe	GS 6	3.82	1.28	2.54	57.81690, -5.635667
Loch Ewe	GS 7	6.13	5.29	0.84	57.79668, -5.629767
Loch Ewe	GS 8	5.72	5.18	0.54	57.78778, -5.634933
Loch Ewe	GS 9	4.44	3.68	0.76	57.78648, -5.634133

Table D.1 Location and carbon content of the spot samples collected as part of effort to constraint the upscaled estimates.

Fjord	Survey Line ID	Cruise ID	Method	URL
Loch Fyne	95931 -95939	1969/3	Sparker	http://mapapps2.bgs.ac.uk/geoindex_offshore/home.html
Loch Linnhe	45445928 - 45445938	2011/4	Surface Towed Boomer	
Loch Hourn	97823 - 97845	1973/WH/13	Pinger	
Loch Nevis	97823 - 97845	1973/WH/13	Pinger	
Loch Long	56634343 - 56634379	2015/1	Surface Towed Boomer	

Table D.2 Seismic transects used to estimate basic sedimentary C stocks for use to constrain the upscaling efforts. .

Acoustic Facies	Description	Sediment Unit	Sedimentary Process
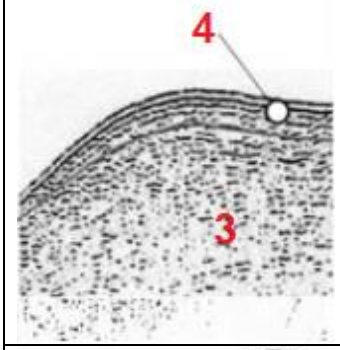	Thin deposit stratified	Postglacial	Lower supply Slow deposition
	Thick deposit transparent/semi-transparent		High supply Rapid deposition High water content
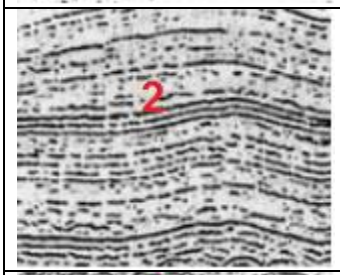	Lower texture Stratified reflectors Denser texture	Glacial (Younger Dryas)	Varying Supply Glaciomarine
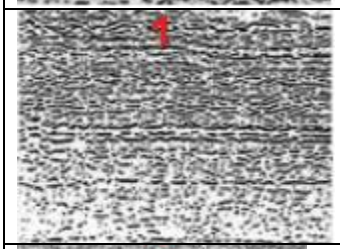	Short discontinuous reflections Hyperbola (Boulders)	Glacial	Moraine Type Glacial
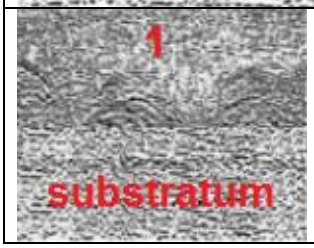	Short discontinuous reflections	Bedrock	

Table D.3 Reference guide used to interpolate the seismic profiles extracted from Baltzer et al. (2010) and further adapted with data from Howe et al. (2002), Stoker et al. (2009, 2010).

Fjord	Organic Carbon (Mt)				Inorganic Carbon (Mt)				Confidence Level
	Mean	σ	Min	Max	Mean	σ	Min	Max	
A'CHOIRE	0.16	0.04	0.14	0.18	0.22	0.07	0.13	0.46	Medium
A'CHUMHAINN	0.36	0.13	0.32	0.40	0.42	0.14	0.33	0.64	Medium
AILORT	0.72	0.21	0.68	0.76	0.76	0.28	0.71	0.90	Medium
AINORT	0.47	0.02	0.33	0.61	0.49	0.23	0.43	0.61	Medium
AIRDBHAIR	0.05	0.01	0.04	0.05	0.13	0.02	0.05	0.39	Low
AITH VOE	0.64	0.51	0.44	0.84	0.67	0.40	0.46	0.96	Medium
ALINE	0.21	0.08	0.17	0.25	0.28	0.08	0.17	0.53	Medium
ALSH	3.10	0.96	3.03	3.16	2.99	1.26	2.61	3.16	Medium
BALTA HARBOUR	0.23	0.18	0.17	0.30	0.30	0.14	0.17	0.57	Low
BASTA VOE	0.64	0.49	0.45	0.83	0.68	0.38	0.47	0.95	Low
BAY	1.73	0.53	1.72	1.75	1.72	0.71	1.60	1.79	Medium
BHROLLUM	0.30	0.10	0.29	0.31	0.37	0.12	0.30	0.58	Medium
BOISDALE	0.99	0.36	0.88	1.09	1.01	0.40	0.92	1.13	Medium
BROOM	2.41	0.47	3.35	1.47	2.69	0.44	3.57	1.81	Very High
BUIE	1.83	0.46	1.58	2.07	1.65	0.84	1.48	2.07	High
BURRA FIRTH	0.40	0.30	0.29	0.52	0.46	0.24	0.30	0.73	Medium
BUSTA VOE	0.49	0.40	0.34	0.64	0.54	0.31	0.36	0.82	Medium
A' CHAIM BHAIN	1.93	0.52	1.72	2.14	1.88	0.71	1.79	2.14	Low
CAMPBELTOWN	0.53	0.37	0.40	0.67	0.58	0.30	0.41	0.84	Low
CAOLISPORT	2.23	1.96	1.38	3.09	2.11	1.48	1.44	3.09	Medium
CARLOWAY	0.10	0.04	0.09	0.11	0.18	0.04	0.09	0.44	Low
CARRON	3.83	0.66	3.13	4.52	3.37	1.76	2.59	4.52	Medium
CAT FIRTH	0.38	0.30	0.26	0.49	0.44	0.23	0.28	0.71	Low
CLAIDH	0.52	0.16	0.50	0.54	0.57	0.21	0.52	0.74	Medium
COLLA FIRTH	0.16	0.13	0.11	0.20	0.23	0.10	0.11	0.50	Medium
CRAIGNISH	2.80	1.95	1.98	3.61	2.65	1.55	2.07	3.61	Medium
CRERAN	2.56	0.73	4.02	1.1	0.89	0.42	1.73	0.35	Very High
DALES VOE NORTH MAINLAND	0.42	0.34	0.30	0.55	0.48	0.26	0.31	0.75	High
DALES VOE SOUTH MAINLAND	0.47	0.37	0.33	0.61	0.52	0.29	0.34	0.80	Low
DON	0.05	0.02	0.04	0.06	0.14	0.02	0.05	0.40	Medium
DUGHAILL	0.23	0.07	0.22	0.23	0.30	0.09	0.23	0.53	Low
DUICH	1.87	0.21	1.48	2.27	1.70	0.86	1.41	2.27	High
DUNVEGAN	2.81	0.83	2.72	2.89	2.72	1.12	2.42	2.89	Medium
EISHORT	0.27	0.08	0.25	0.28	0.34	0.10	0.26	0.56	Medium
EPORT	0.43	0.13	0.40	0.46	0.49	0.17	0.41	0.68	Low
ERIBOLL	3.66	1.05	3.43	3.89	3.50	1.41	3.12	3.89	Medium
ERISORT	0.86	0.25	0.78	0.94	0.89	0.33	0.82	1.03	Low
ETIVE	11.51	0.37	12.25	10.77	6.2	0.27	6.74	5.66	Very High
EWE	8.26	1.51	7.83	8.68	7.17	3.43	5.92	8.68	High
EYNORT	0.19	0.06	0.18	0.20	0.27	0.08	0.18	0.50	Low
FEOCHAN	0.37	0.15	0.30	0.45	0.43	0.15	0.31	0.68	Medium
FYNE	40.04	1.80	34.33	45.75	34.39	12.92	24.61	45.75	High
GAIRLOCH	2.20	0.22	1.71	2.70	1.98	1.02	1.57	2.70	Medium
GARELOCH	1.58	0.81	1.28	1.88	1.55	0.73	1.33	1.88	High
GLUSS VOE	0.17	0.13	0.12	0.22	0.24	0.10	0.13	0.51	Low

GOIL	1.51	0.45	1.41	1.60	1.38	0.68	1.15	1.60	High
GRESHORNISH	0.42	0.13	0.41	0.42	0.48	0.17	0.44	0.65	High
GRIMSHADER	0.07	0.02	0.07	0.07	0.16	0.03	0.07	0.41	Low
GRUINART	0.52	0.28	0.42	0.62	0.57	0.25	0.44	0.80	Low
GRUTING VOE	0.98	0.87	0.63	1.33	0.98	0.66	0.65	1.33	Low
HOLY LOCH	0.64	0.17	0.62	0.67	0.64	0.28	0.48	0.80	Medium
HOURN	5.64	0.24	4.68	6.59	4.92	2.48	3.69	6.59	High
INCHARD	0.47	0.14	0.44	0.51	0.53	0.18	0.46	0.72	Medium
INDAAL	4.09	3.15	2.67	5.50	3.80	2.43	2.78	5.50	Low
INVER	0.51	0.14	0.45	0.57	0.57	0.19	0.47	0.77	Medium
KENTRA BAY	0.07	0.02	0.07	0.07	0.15	0.03	0.07	0.41	Medium
KISHORN	0.59	0.19	0.58	0.60	0.64	0.25	0.62	0.77	High
LAX FIRTH	0.28	0.22	0.20	0.37	0.35	0.17	0.21	0.62	Low
LAXFORD	1.39	0.05	1.16	1.62	1.28	0.61	1.16	1.62	Medium
LEURBOST	0.15	0.05	0.14	0.16	0.23	0.06	0.15	0.47	Low
LEVEN	1.40	0.10	1.33	1.47	1.29	0.55	1.05	1.47	Medium
LINNHE (Upper) & EIL	10.78	3.46	9.69	11.87	8.86	2.47	5.08	11.87	High
LINNHE(lower)	38.96	4.98	36.97	42.87	20.42	4.01	18.34	23.11	Medium
LITTLE LOCH BROOM	1.57	0.59	0.275	0.39	1.42	0.75	2.92	1.21	Very High
LONG ALSH	0.25	0.04	0.20	0.29	0.30	0.11	0.21	0.51	Medium
LONG CLYDE	6.29	1.71	6.00	6.57	5.48	2.75	4.62	6.57	High
MELFORT	1.41	0.93	1.02	1.80	1.38	0.75	1.07	1.80	Medium
MID YELL	0.26	0.20	0.19	0.34	0.33	0.16	0.20	0.60	Low
MOIDART NORTH CHANNEL	0.10	0.03	0.10	0.10	0.18	0.04	0.10	0.43	Medium
MOIDART SOUTH CHANNEL	0.28	0.03	0.25	0.31	0.33	0.12	0.22	0.54	Medium
NA CILLE	0.14	0.12	0.10	0.19	0.22	0.09	0.10	0.49	Low
NA KEAL	5.28	0.71	4.57	5.99	4.61	2.30	3.60	5.99	Low
NA LATHAICH	0.32	0.13	0.29	0.36	0.39	0.14	0.30	0.61	Medium
NAN CEALL	0.28	0.09	0.28	0.29	0.35	0.11	0.29	0.57	Medium
NEDD	0.07	0.02	0.07	0.07	0.15	0.03	0.07	0.41	Low
NEVIS	4.77	0.25	3.92	5.61	4.18	2.11	3.14	5.61	High
ODHAIRN	0.10	0.03	0.10	0.11	0.19	0.04	0.10	0.44	Low
OLNA VOE	0.54	0.44	0.37	0.71	0.59	0.34	0.39	0.87	Medium
PORTREE	0.32	0.02	0.24	0.41	0.37	0.15	0.29	0.53	High
RESORT	0.36	0.13	0.32	0.41	0.43	0.14	0.33	0.65	Medium
RIDDON	0.24	0.14	0.18	0.30	0.31	0.11	0.18	0.57	High
RONAS VOE	0.97	0.78	0.67	1.28	0.98	0.60	0.70	1.28	Low
RYAN	5.97	2.97	4.44	7.49	5.56	2.62	4.63	7.49	Low
SANDSOUND VOE	1.04	0.93	0.67	1.41	1.04	0.70	0.70	1.41	Medium
SCRIDAIN	4.46	0.63	3.97	4.95	3.91	1.91	3.18	4.95	Medium
SEAFORTH	2.48	0.68	2.23	2.74	2.40	0.92	2.30	2.74	High
SHELL	0.73	0.23	0.67	0.78	0.77	0.28	0.70	0.92	High
SKIPORT	0.24	0.08	0.23	0.26	0.32	0.10	0.24	0.54	Low
SLAPIN	0.25	0.02	0.19	0.31	0.31	0.12	0.22	0.50	Medium
SLIGACHAN	0.25	0.02	0.18	0.31	0.30	0.12	0.22	0.49	Medium
SNIZORT BEG	1.09	0.35	1.00	1.18	1.11	0.43	1.05	1.20	High
SPELVE	1.53	0.36	1.34	1.72	1.40	0.69	1.23	1.72	High

STORNOWAY	0.27	0.09	0.25	0.29	0.34	0.11	0.26	0.57	Low
STRIVEN	1.81	1.07	1.36	2.27	1.75	0.89	1.41	2.27	High
STROMNESS VOE	0.15	0.14	0.10	0.21	0.23	0.11	0.10	0.51	Low
SULLOM VOE	2.79	2.10	1.99	3.59	2.64	1.65	2.08	3.59	Low
SUNART	9.4	0.2	9.8	9	10.1	0.17	10.44	9.76	Very High
SWEEN	3.01	2.33	2.01	4.01	2.83	1.80	2.09	4.01	Medium
SWINING VOE	0.28	0.23	0.20	0.37	0.35	0.17	0.21	0.62	Low
TAMANAVAY	0.22	0.08	0.20	0.25	0.30	0.09	0.21	0.53	Medium
TARBERT	1.31	0.63	1.05	1.58	1.30	0.58	1.09	1.58	Low
TEACUIS	0.26	0.09	0.24	0.29	0.34	0.11	0.25	0.56	Medium
TORRIDON	11.12	2.35	8.55	13.69	9.62	5.39	6.43	13.69	High
URA FIRTH	0.29	0.23	0.20	0.37	0.35	0.18	0.21	0.63	Low
USKAVAGH	0.24	0.08	0.23	0.26	0.32	0.10	0.24	0.54	Low
VIDLIN VOE	0.41	0.33	0.29	0.53	0.46	0.25	0.30	0.74	Medium
WEISDALE VOE	0.78	0.71	0.51	1.06	0.80	0.53	0.53	1.11	Low
WEST LOCH TARBERT	1.42	0.52	1.27	1.58	1.41	0.58	1.32	1.58	Medium
HARRIS WEST LOCH TARBERT KINTYRE	2.41	2.12	1.49	3.34	2.28	1.59	1.55	3.34	Medium
WHALE FIRTH	0.49	0.37	0.34	0.63	0.53	0.29	0.36	0.81	Low
WHITENESS VOE	0.51	0.46	0.33	0.69	0.55	0.35	0.34	0.85	Low

Table D.4 Estimated postglacial sedimentary C stocks for individual fjords broken down into OC and IC. Additionally; the assigned confidence level for each estimate is listed.

Fjord	Organic Carbon (Mt)				Inorganic Carbon (Mt)				Confidence Level
	Mean	σ	Min	Max	Mean	σ	Min	Max	
A'CHOIRE	0.0396	0.009	0.0216	0.0576	0.09	0.018	0.054	0.1296	Low
A'CHUMHAINN	0.058	0.029	0.058	0.087	0.145	0.029	0.116	0.174	Low
AILORT	0.124	0.062	0.124	0.186	0.31	0.062	0.248	0.372	Low
AINORT	0.1364	0.031	0.0744	0.1984	0.31	0.062	0.186	0.4464	Low
AIRDBHAIR	0.008	0.004	0.008	0.012	0.02	0.004	0.016	0.024	Very Low
AITH VOE	0.08	0.04	0.08	0.12	0.2	0.04	0.16	0.24	Low
ALINE	0.03	0.015	0.03	0.045	0.075	0.015	0.06	0.09	Low
ALSH	0.55	0.275	0.55	0.825	1.375	0.275	1.1	1.65	Low
BALTA HARBOUR	0.03	0.015	0.03	0.045	0.075	0.015	0.06	0.09	Very Low
BASTA VOE	0.082	0.041	0.082	0.123	0.205	0.041	0.164	0.246	Very Low
BAY	0.312	0.156	0.312	0.468	0.78	0.156	0.624	0.936	Low
BHROLLUM	0.052	0.026	0.052	0.078	0.13	0.026	0.104	0.156	Low
BOISDALE	0.16	0.08	0.16	0.24	0.4	0.08	0.32	0.48	Low
BROOM	0.51	0.18	0.15	0.87	1.21	0.25	0.71	1.71	High
BUIE	0.4664	0.106	0.2544	0.6784	1.06	0.212	0.636	1.5264	Medium
BURRA FIRTH	0.052	0.026	0.052	0.078	0.13	0.026	0.104	0.156	Low
BUSTA VOE	0.062	0.031	0.062	0.093	0.155	0.031	0.124	0.186	Low
A' CHAIM BHAIN	0.312	0.156	0.312	0.468	0.78	0.156	0.624	0.936	Very Low
CAMPBELTOWN	0.072	0.036	0.072	0.108	0.18	0.036	0.144	0.216	Very Low
CAOLISPORT	0.25	0.125	0.25	0.375	0.625	0.125	0.5	0.75	Low
CARLOWAY	0.016	0.008	0.016	0.024	0.04	0.008	0.032	0.048	Very Low
CARRON	1.0164	0.231	0.5544	1.4784	2.31	0.462	1.386	3.3264	Low
CAT FIRTH	0.048	0.024	0.048	0.072	0.12	0.024	0.096	0.144	Very Low
CLAIDH	0.09	0.045	0.09	0.135	0.225	0.045	0.18	0.27	Low
COLLA FIRTH	0.02	0.01	0.02	0.03	0.05	0.01	0.04	0.06	Low
CRAIGNISH	0.36	0.18	0.36	0.54	0.9	0.18	0.72	1.08	Low
CRERAN	0.3857	0.133	0.266	0.532	0.931	1.197	0.532	3.192	High
DALES VOE NORTH MAINLAND	0.054	0.027	0.054	0.081	0.135	0.027	0.108	0.162	Low
DALES VOE SOUTH MAINLAND	0.06	0.03	0.06	0.09	0.15	0.03	0.12	0.18	Very Low
DON	0.008	0.004	0.008	0.012	0.02	0.004	0.016	0.024	Low
DUGHAILL	0.04	0.02	0.04	0.06	0.1	0.02	0.08	0.12	Very Low
DUICH	0.5104	0.116	0.2784	0.7424	1.16	0.232	0.696	1.6704	Low
DUNVEGAN	0.494	0.247	0.494	0.741	1.235	0.247	0.988	1.482	Low
EISHORT	0.046	0.023	0.046	0.069	0.115	0.023	0.092	0.138	Low
EPORT	0.072	0.036	0.072	0.108	0.18	0.036	0.144	0.216	Very Low
ERIBOLL	0.622	0.311	0.622	0.933	1.555	0.311	1.244	1.866	Low
ERISORT	0.142	0.071	0.142	0.213	0.355	0.071	0.284	0.426	Very Low
ETIVE	1.01	0.13	0.75	1.27	2.39	0.23	1.93	2.85	High
EWE	1.9536	0.444	1.0656	2.8416	4.44	0.888	2.664	6.3936	Low
EYNORT	0.032	0.016	0.032	0.048	0.08	0.016	0.064	0.096	Very Low
FEOCHAN	0.054	0.027	0.054	0.081	0.135	0.027	0.108	0.162	Low
FYNE	7.722	1.755	4.212	11.232	17.55	3.51	10.53	25.272	Medium
GAIRLOCH	0.6072	0.138	0.3312	0.8832	1.38	0.276	0.828	1.9872	Low
GARELOCH	0.232	0.116	0.232	0.348	0.58	0.116	0.464	0.696	Low
GLUSS VOE	0.022	0.011	0.022	0.033	0.055	0.011	0.044	0.066	Very Low

GOIL	0.3608	0.082	0.1968	0.5248	0.82	0.164	0.492	1.1808	Low
GRESHORNISH	0.076	0.038	0.076	0.114	0.19	0.038	0.152	0.228	Low
GRIMSHADER	0.012	0.006	0.012	0.018	0.03	0.006	0.024	0.036	Very Low
GRUINART	0.076	0.038	0.076	0.114	0.19	0.038	0.152	0.228	Very Low
GRUTING VOE	0.114	0.057	0.114	0.171	0.285	0.057	0.228	0.342	Very Low
HOLY LOCH	0.1496	0.034	0.0816	0.2176	0.34	0.068	0.204	0.4896	Medium
HOURN	1.4828	0.337	0.8088	2.1568	3.37	0.674	2.022	4.8528	Medium
INCHARD	0.08	0.04	0.08	0.12	0.2	0.04	0.16	0.24	Low
INDAAL	0.484	0.242	0.484	0.726	1.21	0.242	0.968	1.452	Very Low
INVER	0.082	0.041	0.082	0.123	0.205	0.041	0.164	0.246	Low
KENTRA BAY	0.012	0.006	0.012	0.018	0.03	0.006	0.024	0.036	Low
KISHORN	0.108	0.054	0.108	0.162	0.27	0.054	0.216	0.324	Low
LAX FIRTH	0.036	0.018	0.036	0.054	0.09	0.018	0.072	0.108	Very Low
LAXFORD	0.3652	0.083	0.1992	0.5312	0.83	0.166	0.498	1.1952	Low
LEURBOST	0.026	0.013	0.026	0.039	0.065	0.013	0.052	0.078	Very Low
LEVEN	0.33	0.075	0.18	0.48	0.75	0.15	0.45	1.08	Low
LINNHE (Upper) & EIL	0.5706	0.317	0.634	1.2046	7.608	0.634	0.634	8.876	Low
LINNHE(lower)	2.30	0.23	1.78	3.82523	30.60184	2.1	27.98	32.48	Medium
LITTLE LOCH BROOM	1.86	0.14	1.58	2.14	2.12	0.38	1.36	2.88	High
LONG ALSH	0.066	0.015	0.036	0.096	0.15	0.03	0.09	0.216	Low
LONG CLYDE	1.4784	0.336	0.8064	2.1504	3.36	0.672	2.016	4.8384	Medium
MELFORT	0.186	0.093	0.186	0.279	0.465	0.093	0.372	0.558	Low
MID YELL	0.034	0.017	0.034	0.051	0.085	0.017	0.068	0.102	Very Low
MOIDART NORTH CHANNEL	0.018	0.009	0.018	0.027	0.045	0.009	0.036	0.054	Low
MOIDART SOUTH CHANNEL	0.0704	0.016	0.0384	0.1024	0.16	0.032	0.096	0.2304	Low
NA CILLE	0.018	0.009	0.018	0.027	0.045	0.009	0.036	0.054	Very Low
NA KEAL	1.3464	0.306	0.7344	1.9584	3.06	0.612	1.836	4.4064	Very Low
NA LATHAICH	0.052	0.026	0.052	0.078	0.13	0.026	0.104	0.156	Low
NAN CEALL	0.05	0.025	0.05	0.075	0.125	0.025	0.1	0.15	Low
NEDD	0.012	0.006	0.012	0.018	0.03	0.006	0.024	0.036	Very Low
NEVIS	1.2628	0.287	0.6888	1.8368	2.87	0.574	1.722	4.1328	Medium
ODHAIRN	0.018	0.009	0.018	0.027	0.045	0.009	0.036	0.054	Very Low
OLNA VOE	0.068	0.034	0.068	0.102	0.17	0.034	0.136	0.204	Low
PORTREE	0.0924	0.021	0.0504	0.1344	0.21	0.042	0.126	0.3024	Low
RESORT	0.058	0.029	0.058	0.087	0.145	0.029	0.116	0.174	Low
RIDDON	0.032	0.016	0.032	0.048	0.08	0.016	0.064	0.096	Low
RONAS VOE	0.122	0.061	0.122	0.183	0.305	0.061	0.244	0.366	Very Low
RYAN	0.806	0.403	0.806	1.209	2.015	0.403	1.612	2.418	Very Low
SANDSOUND VOE	0.122	0.061	0.122	0.183	0.305	0.061	0.244	0.366	Low
SCRIDAIN	1.1132	0.253	0.6072	1.6192	2.53	0.506	1.518	3.6432	Low
SEAFORTH	0.404	0.202	0.404	0.606	1.01	0.202	0.808	1.212	Low
SHELL	0.122	0.061	0.122	0.183	0.305	0.061	0.244	0.366	Low
SKIPORT	0.042	0.021	0.042	0.063	0.105	0.021	0.084	0.126	Very Low
SLAPIN	0.0704	0.016	0.0384	0.1024	0.16	0.032	0.096	0.2304	Low
SLIGACHAN	0.0704	0.016	0.0384	0.1024	0.16	0.032	0.096	0.2304	Low
SNIZORT BEG	0.182	0.091	0.182	0.273	0.455	0.091	0.364	0.546	Low

SPELVE	0.3872	0.088	0.2112	0.5632	0.88	0.176	0.528	1.2672	Medium
STORNOWAY	0.046	0.023	0.046	0.069	0.115	0.023	0.092	0.138	Very Low
STRIVEN	0.246	0.123	0.246	0.369	0.615	0.123	0.492	0.738	Low
STROMNESS VOE	0.018	0.009	0.018	0.027	0.045	0.009	0.036	0.054	Very Low
SULLOM VOE	0.362	0.181	0.362	0.543	0.905	0.181	0.724	1.086	Very Low
SUNART	2.07	0.27	1.53	2.61	4.93	0.55	3.83	6.03	Very High
SWEEN	0.364	0.182	0.364	0.546	0.91	0.182	0.728	1.092	Low
SWINING VOE	0.036	0.018	0.036	0.054	0.09	0.018	0.072	0.108	Very Low
TAMANAVAY	0.036	0.018	0.036	0.054	0.09	0.018	0.072	0.108	Low
TARBERT	0.19	0.095	0.19	0.285	0.475	0.095	0.38	0.57	Very Low
TEACUIS	0.044	0.022	0.044	0.066	0.11	0.022	0.088	0.132	Low
TORRIDON	3.08	0.7	1.68	4.48	7	1.4	4.2	10.08	Low
URA FIRTH	0.036	0.018	0.036	0.054	0.09	0.018	0.072	0.108	Very Low
USKAVAGH	0.042	0.021	0.042	0.063	0.105	0.021	0.084	0.126	Very Low
VIDLIN VOE	0.052	0.026	0.052	0.078	0.13	0.026	0.104	0.156	Low
WEISDALE VOE	0.092	0.046	0.092	0.138	0.23	0.046	0.184	0.276	Very Low
WEST LOCH TARBERT HARRIS	0.23	0.115	0.23	0.345	0.575	0.115	0.46	0.69	Low
WEST LOCH TARBERT KINTYRE	0.27	0.135	0.27	0.405	0.675	0.135	0.54	0.81	Low
WHALE FIRTH	0.062	0.031	0.062	0.093	0.155	0.031	0.124	0.186	Very Low
WHITENESS VOE	0.06	0.03	0.06	0.09	0.15	0.03	0.12	0.18	Very Low

Table D.5 Estimated glacial sedimentary C stocks for individual fjords broken down into OC and IC. Additionally; the assigned confidence level for each estimate is listed**.**

Fjord	Organic Carbon (t yr^{-1})				Inorganic Carbon (t yr^{-1})			
	Mean	σ	Min	Max	Mean	σ	Min	Max
A'CHOIRE	13.57	3.76	11.84	15.31	19.46	6.33	10.97	39.73
A'CHUMHAINN	31.31	11.25	27.79	34.83	36.91	12.60	28.97	56.06
AILORT	62.86	18.42	59.42	66.30	66.52	24.58	61.93	78.42
AINORT	40.68	2.14	28.63	52.73	42.71	19.81	37.80	52.73
AIRDBHAIR	3.97	1.29	3.83	4.10	11.54	1.63	4.00	34.24
AITH VOE	55.66	44.51	38.33	73.00	58.61	34.35	39.95	83.17
ALINE	17.89	6.78	14.37	21.40	24.32	6.97	14.98	46.52
ALSH	269.23	83.05	263.54	274.92	259.93	109.56	226.60	274.92
BALTA HARBOUR	20.28	15.74	14.37	26.19	26.37	12.26	14.98	49.93
BASTA VOE	55.73	42.67	39.29	72.17	58.75	33.29	40.95	82.58
BAY	150.78	45.67	149.50	152.06	149.17	61.60	139.33	155.81
BHROLLUM	25.92	8.32	24.92	26.92	32.06	10.54	25.97	50.44
BOISDALE	85.70	31.52	76.67	94.73	87.48	34.97	79.91	98.61
BROOM	209.57	40.87	291.30	127.83	233.91	38.26	310.43	157.39
BUIE	158.77	39.62	137.25	180.30	143.90	73.17	128.81	180.30
BURRA FIRTH	35.02	26.01	24.92	45.12	39.84	20.44	25.97	63.37
BUSTA VOE	42.85	34.85	29.71	55.98	46.93	26.86	30.96	71.09
A' CHAIM BHAIN	167.89	45.52	149.50	186.27	163.80	61.55	155.81	186.27
CAMPBELTOWN	46.42	32.57	34.50	58.33	50.39	26.10	35.96	72.76
CAOLISPORT	194.07	170.68	119.79	268.35	183.73	128.29	124.85	268.35
CARLOWAY	8.81	3.60	7.67	9.94	16.00	3.71	7.99	38.39
CARRON	332.68	57.73	272.45	392.91	292.97	152.79	224.84	392.91
CAT FIRTH	32.86	26.03	23.00	42.71	37.84	20.17	23.97	61.66
CLAIDH	45.07	14.29	43.12	47.01	49.95	18.20	44.95	64.71
COLLA FIRTH	13.64	10.90	9.58	17.71	20.29	8.44	9.99	43.90
CRAIGNISH	243.34	169.24	172.50	314.18	230.23	134.54	179.79	314.18
CRERAN	222.61	63.48	349.57	95.65	77.39	36.52	150.43	30.43
DALES VOE NORTH MAINLAND	36.88	29.39	25.87	47.88	41.51	22.76	26.97	65.33
DALES VOE SOUTH MAINLAND	41.04	32.58	28.75	53.32	45.31	25.24	29.96	69.20
DON	4.43	1.96	3.83	5.04	11.94	1.93	4.00	34.90
DUGHAILL	19.79	6.48	19.17	20.41	26.34	8.14	19.98	45.82
DUICH	162.89	18.21	128.48	197.31	147.45	75.03	122.58	197.31
DUNVEGAN	244.13	72.46	236.70	251.55	236.24	97.59	210.00	251.55
EISHORT	23.25	6.83	22.04	24.46	29.54	9.12	22.97	48.70
EPORT	37.12	11.67	34.50	39.73	42.43	14.65	35.96	59.54
ERIBOLL	318.12	91.12	298.04	338.21	304.61	122.84	271.55	338.21
ERISORT	75.02	22.03	68.04	82.00	77.63	28.51	70.92	89.57
ETIVE	1000.87	32.17	1065.22	936.52	539.13	23.48	586.09	492.17
EWE	718.13	131.18	681.06	755.21	623.18	297.85	515.08	755.21
EYNORT	16.30	5.31	15.33	17.27	23.04	6.57	15.98	43.59
FEOCHAN	32.53	13.09	25.87	39.19	37.80	12.98	26.97	59.16
FYNE	3481.81	156.73	2985.12	3978.51	2990.21	1123.74	2139.94	3978.51
GAIRLOCH	191.62	19.22	148.51	234.73	172.08	88.98	136.81	234.73
GARELOCH	137.26	70.02	111.16	163.35	134.43	63.17	115.86	163.35
GLUSS VOE	14.67	11.18	10.54	18.80	21.25	8.76	10.99	44.68
GOIL	130.91	39.49	122.34	139.48	120.01	59.30	99.99	139.48
GRESHORNISH	36.12	11.26	35.82	36.42	41.74	15.06	37.95	56.77

GRIMSHADER	6.06	2.03	5.75	6.36	13.49	2.48	5.99	35.84
GRUINART	45.31	24.48	36.42	54.20	49.60	21.57	37.95	69.82
GRUTING VOE	85.04	75.60	54.62	115.46	85.09	57.01	56.93	115.46
HOLY LOCH	55.80	14.49	53.78	57.83	55.65	23.98	41.46	69.52
HOURN	490.30	21.14	407.39	573.21	428.05	215.25	320.69	573.21
INCHARD	41.22	12.17	38.33	44.12	46.26	15.97	39.95	62.66
INDAAL	355.22	274.04	231.91	478.53	330.84	210.92	241.71	478.53
INVER	44.52	11.88	39.29	49.75	49.16	16.14	40.95	66.66
KENTRA BAY	5.93	1.82	5.75	6.12	13.38	2.39	5.99	35.67
KISHORN	51.08	16.65	50.42	51.75	55.81	21.64	53.94	67.14
LAX FIRTH	24.64	19.52	17.25	32.03	30.33	15.13	17.98	54.08
LAXFORD	121.00	4.20	100.82	141.18	111.53	52.97	101.21	141.18
LEURBOST	13.19	4.35	12.46	13.92	20.14	5.35	12.98	41.21
LEVEN	121.56	8.30	115.56	127.57	112.00	48.15	91.45	127.57
LINNHE (Upper) & EIL	937.40	301.08	842.27	1032.52	770.22	215.12	441.37	1032.52
LINNHE(lower)	3387.88	433.04	3214.78	3727.83	1775.65	348.70	1594.78	2009.57
LITTLE LOCH BROOM	136.52	51.30	23.91	33.91	123.48	65.22	253.91	105.22
LONG ALSH	21.66	3.05	17.81	25.51	26.40	9.80	18.29	43.97
LONG CLYDE	546.62	149.11	521.73	571.51	476.21	238.85	401.90	571.51
MELFORT	122.83	80.73	89.12	156.53	120.26	65.29	92.89	156.53
MID YELL	23.03	17.79	16.29	29.77	28.88	13.86	16.98	52.47
MOIDART NORTH CHANNEL	8.78	2.78	8.62	8.93	16.05	3.61	8.99	37.67
MOIDART SOUTH CHANNEL	24.55	2.33	21.89	27.21	28.87	10.33	19.51	46.87
NA CILLE	12.55	10.49	8.62	16.47	19.28	8.04	8.99	43.02
NA KEAL	458.79	61.77	397.09	520.48	401.02	199.85	313.38	520.48
NA LATHAICH	28.03	11.15	24.92	31.15	33.87	11.79	25.97	53.45
NAN CEALL	24.60	7.63	23.96	25.23	30.85	9.99	24.97	49.24
NEDD	5.97	1.92	5.75	6.19	13.41	2.43	5.99	35.72
NEVIS	414.50	21.33	340.84	488.16	363.09	183.49	273.42	488.16
ODHAIRN	9.10	3.04	8.62	9.58	16.33	3.71	8.99	38.13
OLNA VOE	47.21	37.96	32.58	61.83	50.91	29.28	33.96	75.24
PORTREE	28.10	1.80	20.49	35.72	31.92	13.44	25.61	45.88
RESORT	31.61	11.02	27.79	35.43	37.17	12.49	28.97	56.49
RIDDON	20.75	11.77	15.33	26.17	26.85	9.94	15.98	49.91
RONAS VOE	84.78	68.01	58.46	111.10	85.18	52.47	60.93	111.10
RYAN	518.76	258.57	386.20	651.32	483.50	228.11	402.52	651.32
SANDSOUND VOE	90.70	81.29	58.46	122.94	90.24	61.26	60.93	122.94
SCRIDAIN	387.64	55.12	344.94	430.33	340.02	165.89	276.33	430.33
SEAFORTH	215.78	59.28	193.58	237.97	208.42	79.82	200.35	237.97
SHELL	63.36	19.57	58.46	68.25	66.86	24.75	60.93	79.80
SKIPORT	21.22	7.10	20.12	22.31	27.64	8.67	20.98	47.17
SLAPIN	21.94	1.48	16.66	27.21	26.63	10.25	19.51	43.15
SLIGACHAN	21.40	1.53	15.59	27.21	26.18	10.25	19.51	42.39
SNIZORT BEG	94.83	30.03	87.21	102.44	96.16	37.26	90.89	104.09
SPELVE	133.09	31.35	116.49	149.68	121.89	60.33	107.30	149.68
STORNOWAY	23.72	7.45	22.04	25.41	29.95	9.36	22.97	49.37
STRIVEN	157.51	92.78	117.87	197.14	152.31	77.77	122.85	197.14
STROMNESS VOE	13.24	12.16	8.62	17.86	19.87	9.15	8.99	44.01
SULLOM VOE	242.63	182.49	173.46	311.80	229.71	143.15	180.79	311.80

SUNART	817.39	17.39	852.17	782.61	878.26	14.78	907.83	848.70
SWEEN	261.53	202.75	174.41	348.65	245.96	156.44	181.78	348.65
SWINING VOE	24.61	19.57	17.25	31.96	30.30	15.15	17.98	54.02
TAMANAVAY	19.28	7.12	17.25	21.31	25.75	7.88	17.98	46.46
TARBERT	114.34	55.19	91.04	137.63	113.16	50.54	94.89	137.63
TEACUIS	22.97	7.62	21.08	24.86	29.22	9.15	21.97	48.98
TORRIDON	966.88	204.46	743.12	1190.65	836.61	469.06	559.16	1190.65
URA FIRTH	24.86	20.26	17.25	32.48	30.52	15.61	17.98	54.39
USKAVAGH	21.27	7.05	20.12	22.42	27.69	8.65	20.98	47.25
VIDLIN VOE	35.51	28.30	24.92	46.10	40.26	21.92	25.97	64.07
WEISDALE VOE	68.15	61.60	44.08	92.23	69.77	46.40	45.95	96.83
WEST LOCH TARBERT HARRIS	123.70	45.03	110.21	137.20	122.76	50.13	114.86	137.20
WEST LOCH TARBERT KINTYRE	209.71	184.20	129.37	290.05	197.90	138.46	134.84	290.05
WHALE FIRTH	42.25	32.13	29.71	54.80	46.43	25.08	30.96	70.24
WHITENESS VOE	44.47	40.14	28.75	60.19	48.25	30.24	29.96	74.08

Table D.6. Estimated postglacial C burial rates (tonnes yr^{-1}) for each of the 11 fjords.